UNIVERSITY OF SOUTHAMPTON
FACULTY OF ENGINEERING, SCIENCE AND MATHEMATICS
SCHOOL OF CHEMISTRY

DNA RECOGNITION BY TRIPLE HELIX FORMATION

by David Anthony Rusling

A Thesis Submitted for the Degree of Doctor of Philosophy
March 2006

UNIVERSITY OF SOUTHAMPTON

ABSTRACT

FACULTY OF ENGINEERING, SCIENCE AND MATHEMATICS
SCHOOL OF CHEMISTRY

Doctor of Philosophy

DNA RECOGNITION BY TRIPLE HELIX FORMATION

by David Anthony Rusling

Triplex-forming oligonucleotides (TFOs) are gene-targeting agents with potential in such diverse areas as gene-based therapeutics, functional genomics and molecular biology. These molecules bind in the major groove of double-stranded DNA, forming specific hydrogen bonds with exposed groups on the duplex base pairs, generating a three-stranded structure. There are currently several major limitations to their use: (i) there are no stable means for recognising TA or CG base pairs (pyrimidine interruptions) using natural DNA bases; (ii) formation of the C^+.GC triplet requires conditions of low pH (< 6.0), necessary for protonation of the third strand cytosine; (iii) the binding of the third strand may not be strong, due to electrostatic repulsion between the three polyanionic DNA strands. The work described in this thesis uses DNase I footprinting and thermal melting experiments to examine the triplex-forming properties of several novel nucleoside analogues that might be used to overcome each of these restrictions.

The simplest strategy to alleviate the charge repulsion problem is to incorporate positively charged moieties into the TFO by either modifying the backbone, the sugar or the base. Triplexes containing three or more substitutions with the bis-amino modified thymidine analogue 2′-aminoethoxy,5-propargylamino-U (BAU) were shown to be stable at pH 7.0, even though they contain several C.GC base triplets. In contrast, the unmodified TFO produced a stable triplex only at pH 5.0 and in the presence of magnesium. These modified TFOs retain exquisite sequence specificity, with enhanced discrimination against YR base pairs (especially CG) and a requirement for binding in the parallel motif. Several similar analogues containing guanidines or dimethylamines at similar positions did not improve upon the stabilisation.

To overcome the pH dependency of triplex formation 2′-aminoethoxy derivatives of N7G and 6-oxo-C were examined for their ability to recognise GC base pairs at different pH values. Both derivatives produced less stable complexes than C at pH 5.0 but were of a similar stability at pH 6.0. A better approach was achieved by combining the analogue 3-methyl,2-aminopyridine (^{Me}P) with BAU. Oligonucleotides containing three substitutions of each analogue extended triplex formation to pH 7.5 with a nanomolar binding affinity. However, the affinity depended on the arrangement of substitutions; oligonucleotides in which these analogues were evenly distributed throughout the third strand bound much better than those in which they are clustered.

The recognition of pyrimidine bases within a target oligopurine tract was also investigated using modified nucleosides. Of these, a substituted pyrrolopyrimidone-2-one analogue (^{A}PP) selectively recognised CG with the highest affinity. Whilst, the 2′-aminoethoxy modified thiazolyl-aniline analogue S recognised TA with the highest affinity but also interacted with other base pairs, in particular, CG. To improve on of the stability of the G.TA triplet several deoxyguanosine derivatives were also studied. It was shown that the addition of either a propargylamino chain to the base or 2′-aminoethoxy group to the sugar resulted in enhancing the affinity of this base for GC and not TA.

By using triplex-forming oligonucleotides that contain four of such modified nucleosides it was possible to achieve recognition of each of the four base pairs by triple helix formation at physiological pH. Fluorescence melting and DNase I footprinting demonstrated successful triplex formation at a polypurine.polypyrimidine target site that contained two CG and two TA interruptions. The complexes were pH dependent but were still stable at pH 7.5. Three of the four analogues used retained considerable selectivity (BAU, ^{Me}P, ^{A}PP) and single base changes opposite these residues cause a large reduction in affinity. In contrast, S was less selective and tolerated CG base pairs as well as TA

Lastly, the formation of DNA triple helices at target sites that contain mismatches in the duplex target was investigated. The introduction of a duplex mismatch were shown to destabilise the C^+.GZ, T.AZ and G.TZ triplets, whilst other base combinations, based on non-standard triplets such as C.AZ, T.TZ, G.CZ and A.CZ were stabilised by the presence of a duplex mismatch.

PREFACE

The work presented in this thesis was undertaken in the School of Biological Sciences, University of Southampton between October 2002 and August 2005. Some of the results presented have been published as follows;

Rusling, D.A., Brown, T., and Fox, K.R. (2006) DNA triple-helix formation at target sites containing mismatches in the duplex. *Biophys Chem.* In press.

Rusling, D.A., Le Strat, L., Powers, V.E.C., Broughton-Head, V.J., Booth, J., Lack, O. Brown, T. and Fox, K.R. (2005) Combining nucleoside analogues to achieve recognition of oligopurine tracts by triplex-forming oligonucleotides at physiological pH. *FEBS Letts.* 579, 6616-6620.

Rusling, D.A., Powers, V.E.C., Ranasinghe, R.T., Wang, Y., Osbourne, S.D., Brown, T. and Fox, K.R. (2005) Four base recognition by triplex-forming oligonucleotides at physiological pH. *Nucleic Acids Res.* 33, 3025-3032.

Ranasinghe, R.T., Rusling, D.A., Powers, V.E.C., Fox, K.R., and Brown, T. (2005) Recognition of CG inversions in DNA triple helices by methylated 3*H*-pyrollo[2,3-*d*]pyrimidin-2(7*H*)-one nucleoside analogues. *Chem. Comm.* 2555-25557

Wang, Y., Rusling, D.A., Powers, V.E.C., Lack, O., Osbourne, S., Fox, K.R and Brown, T. (2005) Stable recognition of TA interruptions by triplex-forming oligonucleotides containing a novel nucleoside. *Biochemistry.* 44, 5884-5892.

Osbourne, S., Powers, V.E.C., Rusling, D.A., Lack, O., Fox, K.R., and Brown, T. (2004) Selectivity and affinity of triplex-forming oligonucleotides containing 2´-aminoethoxy-5-(3-aminoprop-1-ynyl)uridine for recognising AT base pairs in duplex DNA. *Nucleic Acids Res.* 32, 4439-4447.

ACKNOWLEDGEMENTS

I would like to express my sincere thanks to both Professors Keith Fox and Tom Brown for their help and guidance throughout the course of my PhD. I would also like to thank the post docs (Peter, Loic, Ged, Vicki and Steve), fellow PhD students (Nick, Rohan, Andrew and Phil ☺), project students (Bouthayna, Hannah and Magdy) and technicians (Dave) who I have learnt a great deal from and who have made my time in and out of the lab enjoyable. I am also very grateful for the continued support of both my family and Vic.

TABLE OF CONTENTS

LIST OF FIGURES

LIST OF TABLES

5.7 C_{50} values determined by DNase I footprinting for the interaction of TFOs 5´-TCTCTTXTTTCT, where X is either a natural base or analogue, with target duplexes containing the sequence 5´-AGAGAAZAAAGA/ 3´-TCTCTTYTTTCT, where YZ is AT, TA, GC or CG.

6.1 T_m values determined by fluorescence melting for triplexes formed by the modified oligonucleotide TFO-1 at different pHs using a temperature gradient of 0.2 °C min^{-1}.

6.2 C_{50} values determined by DNase I footprinting for the interaction of the modified oligonucleotide TFO-1 with target sites that differed by a single base pair, generating a triplex mismatch opposite one of the novel nucleotides.

7.1 T_m values determined by fluorescence melting for triplexes composed of different triplet combinations containing duplex mismatches using a temperature gradient of 0.2 °C min^{-1} and the quencher methyl red at pH 5.5.

7.2 T_m values determined by fluorescence melting for triplexes composed of different triplet combinations containing the analogues BAU and S opposite duplex mismatches using a temperature gradient of 0.2 °C min^{-1} and the quencher methyl red at pH 5.5

7.3 T_m values determined by fluorescence melting for triplexes containing 5-amino-dU in the purine strand of the duplex, flanked by T.AT.

7.4 T_m values determined by fluorescence melting for triplexes containing 5-amino-dU in the purine strand of the duplex, flanked by C^+.GC.

ABREVIATIONS

A	adenosine
bp	base pair
bps	base pairs
CD	circular dichroism
cps	counts per second
C	cytidine
dATP	deoxyadenosine triphosphate
DNA	deoxyribonucleic acid
DNase	deoxyribonuclease
ds	double-stranded
EDTA	ethylenediaminetetracetic acid
G	guanosine
kb	kilobases
IPTG	isopropylthio-β-*D*-galactoside
MCS	multiple cloning site
mRNA	messenger RNA
PAGE	polyacrylamide gel electophoresis
PNA	peptide nucleic acid
R	purine
RNA	ribonucleic acid
SDS	sodium dodecyl sulphate
TBE	tris, Borate, EDTA; 5 x buffer
TFO	triplex-forming oligonucleotide
Tris	tris-hydroxymethyl-aminomethane
T	thymidine
U	uridine
UV	ultraviolet
W-C	watson-Crick
X-Gal	5-bromo-4-chloro-3-indoyl-β-*D*-galactosidase
Y	pyrimidine

1 INTRODUCTION

1.1 Triple helix discovery

Oligonucleotides can bind in the major groove of double stranded DNA by forming hydrogen bonds with exposed groups on the base pairs, generating a triple-helical structure (Figure 1.1). This was first demonstrated nearly 50 years ago by Rich and co-workers by mixing the synthetic polyribonucleotides polyU and polyA in the ratio 2:1 (Felsenfeld *et al.*, 1957). Subsequent studies showed that polyC and polyG could also generate a similar structure under low pH conditions (Howard *et al.*, 1964) and since then a variety of DNA and RNA triple-stranded structures have been identified (Morgan & Wells, 1968; Riley *et al.*, 1966; Marck *et al.*, 1978; Lee *et al.*, 1979; Broitman *et al.*, 1987). *Inter*molecular triplexes are generated by the binding of a triplex-forming oligonucleotide (TFO) to a separate DNA duplex. *Intra*molecular triplexes are formed at homopurine-homopyrimidine mirror-repeat sequences when a single strand of the duplex unwinds and folds back on itself. The latter have been identified in plasmids under conditions of superhelical stress or low pH (Lyamichev *et al.*, 1985; Frank-Kamenetskii, 1987; Htun & Dahlberg, 1988) and it is possible that such structures form *in vivo* with implications for gene regulation (Rao, 1996; Rustighi *et al.*, 2002; Dey & Rath, 2005) and genome instability (Bidichandani *et al.*, 1998; Wang & Vasquez, 2003; Raghavan *et al.*, 2005).

The realisation that synthetic oligonucleotides could be exploited to recognise unique DNA sequences came about in the late 1980s. Proof of principle was first demonstrated using a Fe·EDTA-oligonucleotide conjugate to elicit a single specific double-strand break within a 628 bp DNA fragment and a yeast chromosome (Moser & Dervan, 1987; Strobel & Dervan, 1990). This was later extended to include triplex-induced photo-crosslinking (Le Doan *et al.*, 1987) and triplex-induced transcriptional repression *in vitro* of the *c-myc* gene (Cooney *et al.*, 1988). This strategy was later termed the antigene approach by Hélène and co-workers by analogy to the closely related antisense approach, where gene expression is controlled by oligonucleotides that hybridise to specific single-stranded mRNA targets (Hélène, 1990). Since then triplex-forming oligonucleotides have received extensive research interest with many recent reviews highlighting their potential in such diverse areas as gene-based therapeutics, functional

Figure 1.1 Structure of triple helical DNA (taken from http://www.ibmb.csic.es).

genomics and molecular biology (Rice *et al.,* 2001; Seidman & Glazer, 2003; Potaman, 2003). To date the most encouraging advances have shown that TFOs can be used to elicit site-specific mutagenesis and to inhibit tumour growth in mice (Vasquez *et al.*, 2000; Re *et al.*, 2004).

1.1.1 Triplex binding motifs

The binding of a third strand of DNA within the major groove is asymmetric, as in general oligonucleotides only recognise the purine-containing strand of the duplex. The binding can be either parallel or antiparallel to the target strand, depending on the base composition of the oligonucleotide.

Pyrimidine-rich oligonucleotides bind under low pH conditions in a parallel orientation to the purine strand of the target duplex, with T and protonated C forming two Hoogsteen hydrogen bonds with AT and GC base pairs respectively (Moser & Dervan, 1987; Le Doan *et al.,* 1987). This generates the base triplets T.AT and C^+.GC as shown in Figure 1.2A. (In this thesis the notation X.ZY refers to a triplet, in which the third strand base X interacts with the duplex ZY base pair, forming hydrogen bonds to base Z). These triplets are isomorphous, that is if the C-1′ atoms of their Watson-Crick base pairs are superimposed, the positions of the C-1′ atoms are almost identical (Thuong & Hélène, 1993). This minimizes backbone distortion of both the third strand and duplex between adjacent triplets. It is also possible to form a G.GC triplet within this motif, though this is not isomorphous with T.AT and C^+.GC (Figure 1.2A(iii)). The majority of this thesis will focus on triplex formation using this binding motif.

Purine-rich oligonucleotides bind in an antiparallel orientation to the purine strand of the target duplex, with A and G forming two reverse-Hoogsteen hydrogen bonds with AT and GC base pairs respectively, generating A.AT and G.GC triplets (Figure 1.2B) (Beal & Dervan, 1991; Durland *et al.*, 1991). In contrast to the parallel triplets, A.AT and G.GC triplets are not isomorphous, leading to structural distortions at junctions between each triplet. As a consequence of this and other factors, the antiparallel motif is often less stable than the parallel motif. T.AT triplets can also adopt an antiparallel orientation (Figure 1.2B(ii)).

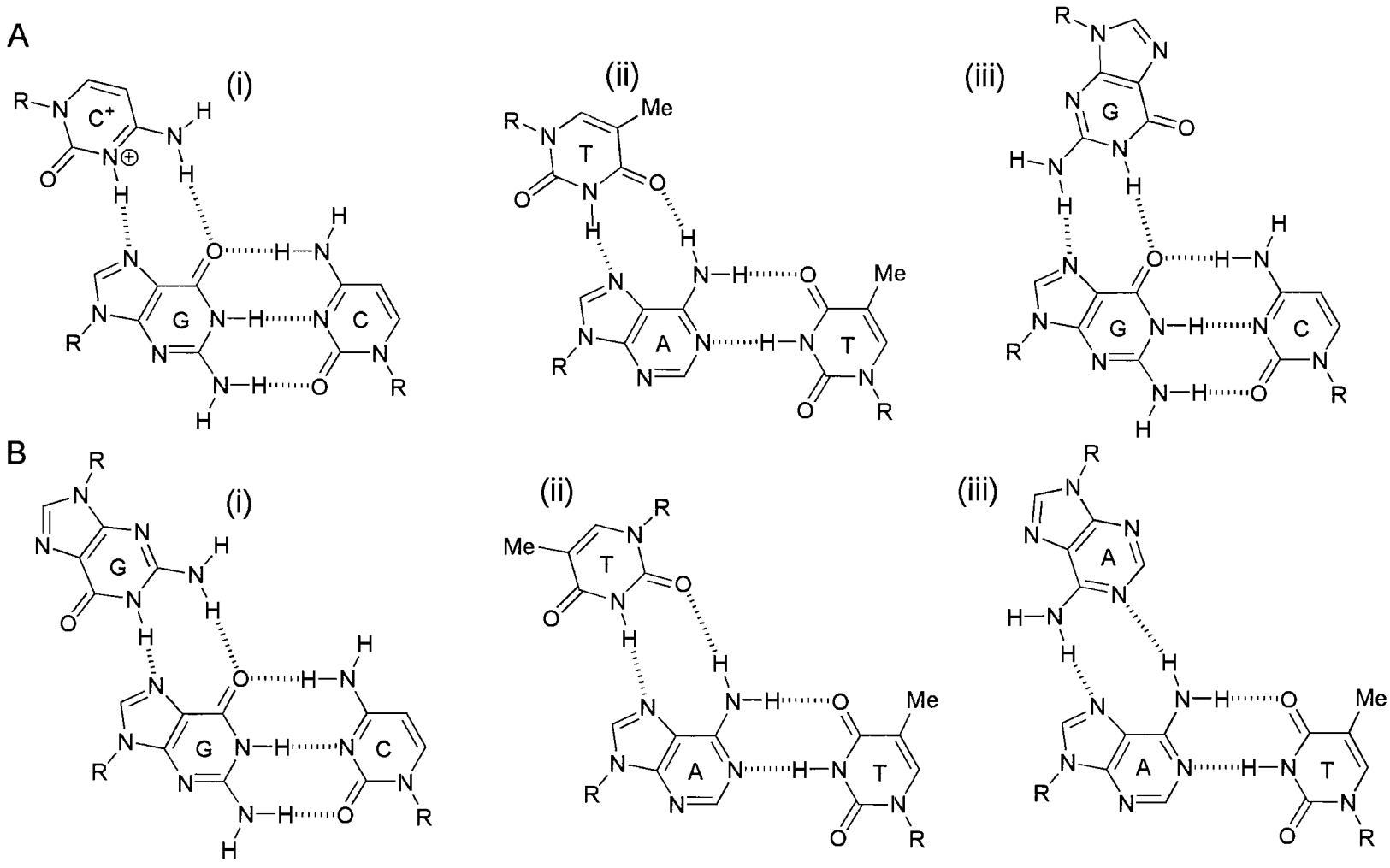

Figure 1.2 Chemical structures of the parallel and antiparallel DNA triplets. A) parallel; (i) C+.GC (ii) T.AT (iii) G.GC; B) antiparallel; (i) G.GC (ii) T.AT (iii) A.AT.

Since G.GC and T.AT triplets can be formed in both the parallel and antiparallel motifs GT-containing oligonucleotides can be designed to bind in either orientation parallel or antiparallel. The backbone distortion imposed by the non-isomorphous nature of these two triplets means the most stable orientation is dependent on the number of GpT and TpG steps (Thuong & Hélène, 1993). Energy minimization studies have suggested that a greater backbone distortion is exhibited for GT-oligonucleotides binding parallel rather than in an antiparallel orientation (Giovannangeli *et al.*, 1992; Sun & Hélène, 1993).

1.2 Triplex structure

The DNA duplex contains two grooves generated by the asymmetric disposition of the bases relative to the phosphate backbone. Only one of these, the major groove, is wide enough to accommodate a third strand of DNA. Recognition is predominantly by hydrogen bonds formed between the third strand and purine-strand of the duplex. These are longer than those formed between the bases of a W-C base pair and therefore exhibit a shorter lifetime (Cain & Glick, 1998; Rhee *et al.,* 1999).

Several studies have been carried out to determine how the binding of an oligonucleotide alters the structure of the underlying duplex. Early fiber diffraction studies identified mainly sugar-dependent differences; instead of the usual S-type conformation characteristic of B-DNA, the sugars were found to assume an N-type conformation, a characteristic much closer to A-DNA (Arnott *et al.,* 1973). It was suggested that the deeper major groove of A-DNA would be a better acceptor of a third strand than the shallow major groove of B-DNA (Arnott *et al.,* 1973). In recent years this view has changed. Several high-resolution NMR structures (Radhakrishnan *et al.*, 1994; Rajopal & Feignon, 1989; Macaya *et al.*, 1992; Asensio *et al.*, 1998/1999; Tarköy *et al.*, 1998) and one X-ray crystal structure (Rhee *et al.*, 1999) have been determined. These indicate only slight pertubations from the standard B-DNA structure. The current view is that the binding of an oligonucleotide leads to a slight unwinding of the duplex, resulting in the W-C bases becoming more perpendicular to the helix axis and a slight narrowing of the minor groove. This does not require any change to the sugar pucker within the duplex, with all sugars found predominantly as S-type.

The conformation of the third strand is of still some debate with some studies suggesting S-type (Bartley *et al.*, 1997; Asensio *et al.*, 1998; Radhakrisnan *et al.*, 1994), N-type (Rajopal & Feignon, 1989) and a mixture of N and S-type sugar puckers (Tarköy *et al.*, 1998; Asensio *et al.*, 1999; Rhee *et al.*, 1999). Generally, protonated C residues favor an N-type conformation whilst T residues favor S-type (Tarköy *et al.*, 1998; Asensio *et al.*, 1999; Rhee *et al.*, 1999). Protonated C residues also lead to an additional narrowing of the groove between the central purine strand and the third strand due to electrostatic interactions with the backbone (Asensio *et al.*, 1998; Rhee *et al.*, 1999). These findings suggest sequence-dependent differences in the overall third strand conformation.

1.2.1 Triplex-duplex junction

Enzymatic and chemical probing studies have suggested structural asymmetry between the 5′- and 3′- triplex-duplex junctions. For example, DNase I exhibits hypersensitivity at the 3′- junction (Chandler & Fox, 1996) whereas ellipticine derivatives preferentially intercalate at the 5′- junction (Perrouault *et al.*, 1990). Gel retardation and energy minimization have suggested an induced bending of the duplex towards the minor groove at the 5′-junction and towards the major groove at the 3′-junction (Chomilier *et al.*, 1993). This has been attributed to a greater stacking interaction at the 5′-junction, which in turn may be due to the right-handed nature of the helix (Asensio *et al.*, 1998; Alberti *et al.*, 2002). Further structural studies have identified only minor changes at these sites and any induced change in conformation is not propagated far beyond the overhanging junctions (Asensio *et al.*, 1998; Rhee *et al.*, 1999).

1.2.2 Triplexes composed of RNA strands

Several studies have looked at the properties of triplexes composed of different arrangements of RNA and DNA strands. It was found that the most stable are generally formed with central DNA rather than RNA purine strand. Conversely, RNA-TFOs have a greater affinity for their duplex targets than DNA-TFOs (Roberts & Crothers, 1992; Han & Dervan, 1994; Asensio *et al.*, 1999; Bernal-Méndez & Leumann, 2002). The latter has been attributed to the conformation of the sugar pucker, N-type conformations (RNA-like) leads to a lower distortion of the purine strand upon binding than S-type conformations (DNA-like) (Asensio *et al.*, 1999). The story is less clear for chimeric TFOs containing mixtures of RNA and DNA nucleotides. RNA TFOs that contain a few

deoxyribonucleotides are only marginally destabilising, again suggesting sugar-dependent sequence composition effects (Bernal-Méndez & Leumann, 2002).

1.3 Factors affecting triplex stability

The stability of a triple helix is generally lower than that of its underlying duplex and is typically seen as two separate transitions in a UV melting experiment (triplex-duplex and duplex-single strands). Triplex stability is affected by intrinsic factors such as base composition and oligonucleotide length as well as external influences such as temperature, pH and ionic conditions.

1.3.1 Mismatches

Triplex formation is stabilised by specific interactions and is sensitive to single base mismatches between third strand and duplex. A single base mismatch results in a typical free energy change of ~ 3 kcal mol^{-1} (Roberts & Crothers, 1991; Rougée *et al.,* 1992). The extent of this destabilisation is dependent on the nature and position of the mismatch. Central mismatches are more destabilising than terminal ones since they disrupt the cooperative interaction between neighbouring triplets (Mergny *et al.*, 1991; Rougée *et al.*, 1992). A thermodynamic study by Dervan and co-workers showed that T binds to AT better than any other base pair by $\geq$ 2.3 kcal mol^{-1}, whereas ^{Me}C binds to GC better than any other base pair by $\geq$ 1.4 kcal mol^{-1} (Best & Dervan, 1995). This suggests highly specific interactions with CT-containing oligonucleotides.

In an attempt to extend the triplex recognition code to include TA and CG base pairs (pyrimidine inversions) the least destabilising bases to be positioned opposite each of them has been determined. In the parallel binding motif it has been observed that G and T are the most stable against TA and CG respectively (Beal & Dervan, 1991; Yoon *et al.*, 1992; Chandler & Fox, 1993). In contrast, C and T are the most stable against TA and CG base pairs in the antiparallel motif (Beal & Dervan, 1991; Durland *et al.*, 1994; Chandler & Fox, 1996). The use of natural bases to recognise pyrimidine inversions will be dealt with in section 1.7.2.

Interestingly, mismatches found in the duplex strand of a triplex may enhance its stability (Sun *et al.*, 1991). Of the triplets examined, both T.AC and C.GA were

identified as being more stable than the canonical T.AT and C^+.GC triplets. It has been suggested that a mismatch may allow a greater structural flexibility of the duplex strand, leading to more favourable interactions with the third strand.

1.3.2 Length of third strand

Increasing the length of a third strand increases the stability of a triplex by increasing hydrogen bonding and base stacking interactions (Moser & Dervan, 1987). With purine-containing oligonucleotides this is not always observed and has been attributed to the non-isomorphous nature of the triplets formed and their effect on stacking and/or backbone distortion (Sun *et al.,* 1993) or the high propensity of G-rich oligonucleotides to form secondary structures such as G-quartets or G-duplexes (Noonberg *et al.*, 1995). Also, as triplex formation involves a structural change of the target duplex, it is likely to cost more free energy to convert a longer and more stable duplex than a shorter one (Yoon *et al*, 1992).

An increase in triplex length should theoretically lead to an increase in selectivity. In practice if the free-energy penalty of a single mismatch is small relative to the total free energy of formation of the complex, then the observed specificity of binding may be reduced (Plum *et al.,* 1995; Demidov & Frank-Kamenetskii, 2004). This is partly due to the mechanism of formation of nucleic acid complexes. The 1D-nucleation zipper mechanism can accommodate a mismatch more readily than the 3D-shape complementarity mechanism for the formation of a protein-small molecule complex (Demidov & Frank-Kamenetskii, 2004). Unless modifications to TFO chemistry can increase specificity there will be an optimal length of third strand employed before the third-strand selectivity is compromised.

Studies have shown that it is possible to form *intra*molecular (Wang & Patel, 1995) and *inter*molecular triplexes (Fox *et al.*, 2000) that contain nucleotide bulges (A or T) in the third strand. Fox *et al.* found that TFOs could bind to secondary target sites by forming single base bulges. Further studies have shown that single nucleotide bulges are generally more stable than dinucleotide, though triplexes can be formed with loops of up to nine thymidines (Fox *et al.*, 2000). This suggests that increasing the length of the triplex may also increase the affinity for secondary sites.

1.3.3 Temperature

Triplex formation occurs via a quasi-stable intermediate consisting of a few productive triplets and is therefore stabilised at low temperatures (Rougée *et al.,* 1992; Shindo *et al.*, 1993; Xodo *et al.,* 1995). However, G-rich oligonucleotides are predominantly stabilised at higher temperatures due to a destabilisation of any potential secondary structure formed that might compete with triplex formation (Svinarchuk *et al.*, 1994; Noonberg *et al.,* 1995).

1.3.4 Low pH requirement

Triplex formation in the parallel binding motif suffers from a requirement for low pH conditions necessary for protonation of cytosine at N3. This allows the protonated base to form two Hoogsteen hydrogen bonds between its 4-amino group and N3 proton and guanines 6-carbonyl and N7 atom respectively.

The pK_a of cytosine is around 4.5 for the free nucleoside but this is often elevated upon triplex formation, and is higher in the centre rather than the termini of a triplex (Asensio *et al.*, 1998; Leitner *et al*, 2000). Runs of contiguous cytosine residues are destabilising as they decrease the pK_a of cytosine, lead to protonation competition and/or to a lesser degree to electrostatic repulsion between residues (Lee *et al.*, 1984; Kiessling *et al.*, 1992; Völker & Klump, 1994; Asensio *et al*, 1998; Leitner *et al.,* 2000; Sugimoto *et al,* 2001). The most stable triplexes are therefore generated by TFOs containing alternating T.AT and C^+.GC triplets (Roberts & Crothers, 1996; Keppler & Fox, 1997; James *et al.*, 2003).

Several reports have suggested that C^+.GC is more stable than T.AT (Keppler & Fox, 1997; Asensio *et al.,* 1998; Soto *et al.*, 2002). This is attributed to electrostatic interactions of cytosines positive charge with the phosphate backbone, and/or favorable stacking interactions between the charge and the π-stack. More recently it has been shown that protonation affects not only the stability of a triplex but also that of the underlying duplex, this may have an important affect on the triplex lifetime (Sugimoto *et al.*, 2001; Wu *et al.*, 2002).

1.3.5 Ionic conditions

The formation of a triplex brings into close proximity three polyanionic strands, increasing the negative charge by 50 % relative to the duplex, leading to a high degree of charge repulsion. This can be partially screened by using high concentrations (up to 200 mM) of monovalent (Plum *et al.*, 1990) or low concentrations (up to 10 mM) of divalent metal cations (Moser & Dervan, 1987; Pilch *et al.,* 1990; Rougée *et al,* 1992). Triplexes are also stabilised by polyvalent cations such as polyamides and the extent of stabilisation is dependent on their charge and composition (Singleton & Dervan, 1993; Thomas & Thomas, 1993). Spermine is the most relevant of these as millimolar concentrations are present *in vivo*.

The parallel motif is most frequently stabilised using magnesium (Kohwi & Kohwi-Shigematsu, 1988) though recent studies have suggested copper may be a more suitable alternative requiring between 10-100 times lower concentration. It has been postulated that magnesium interacts non-specifically with the anionic oxygen atoms of the phosphodiester backbone (Völker & Klump, 1994) whereas copper co-ordinates the N7 of guanine in the duplex and the N3 of cytosine in the TFO, in a similar manner to protonated C (Horn *et al.*, 2004). The extent of stabilisation by cations is dependent on the base composition of the TFO and several reports have suggested that C^+.GC has a lower requirement for cations than T.AT (Latimer *et al.,* 1989; Keppler & Fox, 1997; James *et al.*, 2003; Coman & Russu, 2004).

The antiparallel motif suffers from a higher dependence for charge screening than parallel, predominantly due to the lack of protonated bases in the third strand. Stabilisation is greater for the transition metals, such as manganese, than the alkali earth metals, such as magnesium (Malkov *et al.*, 1993). Unlike the parallel motif, high concentrations of potassium can stabilise secondary structures such as G-quadruplexes or G-duplexes formed by purine-rich oligonucleotides. This ion therefore has an adverse affect on triplex formation (Cheng & Van Dyke, 1998).

1.3.6 Hydration effects

Bound water molecules have been identified in the grooves formed by a triple-helical structure (Radhadkrishnan & Patel, 1994). Fourier transform infrared and gravimetric

studies have estimated on average 17 ± 2 molecules of water per nucleotide within a triplex, compared to 21 ± 1 in the case of free duplex (Ouali *et al.*, 1997). The binding of a TFO induces the release of this water, producing significant volume and entropic changes (Spink & Chaires, 1999). Bound water may also act to partially screen the charge repulsion of the three strands but may limit the access of cations.
Polyethyleneglycol (PEG) has been shown to stabilise triplex formation. This crowding agent imitates the intracellular environment. Triplex association in crowded media is promoted because it increases the available volume and hence the entropy of the system (Goobes & Minsky, 2001).

1.4 Restrictions

The use of triplex-forming oligonucleotides as gene-targeting agents has received extensive research interest (Fox, 2000; Robles *et al.*, 2002; Buchini & Leumann, 2003). Unfortunately these molecules suffer from several intrinsic limitations (low binding affinity, pH dependence and target restrictions) as well as those pertaining to any oligonucleotide-based approach (biostability, cell permeability, access to target). The aim of this section is to summarise the major strategies that have been employed to overcome such limitations and where applicable highlight how modifications to TFO chemistry have improved their biophysical properties.

1.5 Strategies to increase triplex stability

The low stability of a triplex is determined by several intrinsic factors; (i) the level of distortion imposed to the duplex by binding of a third strand (ii) the degree of charge repulsion between the negative phosphate groups of the three strands (iii) the extent of hydrogen bonding and stacking interactions of the nucleotides.

1.5.1 Sugar modifications

Several studies have emphasised that TFOs composed of RNA nucleotides exhibit a higher affinity for dsDNA than those composed of DNA nucleotides (Roberts & Crothers, 1992; Shimizu *et al.*, 1992; Escudé *et al.*, 1992, Bernal-Mendeléz & Leumann, 2002). This has been attributed to a difference in sugar puckering; RNA nucleotides predominantly exhibit C3´-*endo* (N-type) whereas DNA nucleotides exhibit

C2′-*endo* (S-type) sugar puckers. NMR has confirmed that oligonucleotides containing N-type sugars require less distortion of the duplex purine strand upon triplex formation and thereby are less destabilising (Asensio *et al.*, 1999).

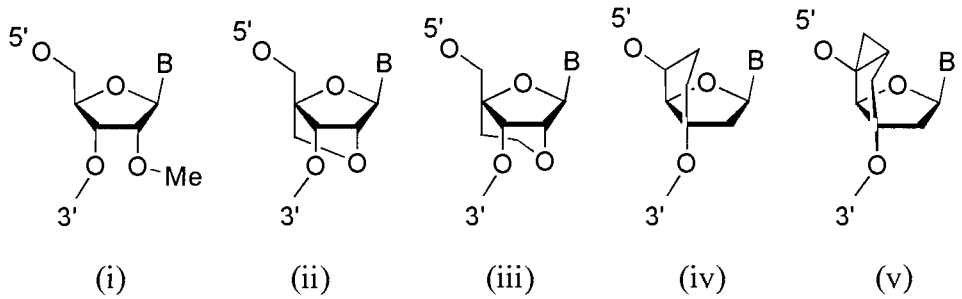

Figure 1.3 Chemical structures of modified sugars with restricted conformations. (i) 2'-OMe (ii) LNA (or BNA); (iii) ENA; (iv) bicyclo DNA; (v) tricyclo DNA.

The conformational equilibrium between N and S-type sugar puckering is dependent on several steric and stereoelectric effects (Imanishi & Obika, 2002; Plavec *et al.*, 1994). The addition of an electronegative group at the 2′-position of the sugar, as in RNA, strongly favors the N-type sugar pucker due to the gauche effect (Plavec *et al.*, 1994). It was therefore proposed that the 2′-*O*-methyl modification (Figure 1.3(i)), naturally present in RNA, maybe useful for its triplex-forming properties (Shimizu *et al.*, 1992; Escudé *et al.*, 1992). Thermal melting experiments on fully modified TFOs exhibited a higher thermal stability relative to the equivalent RNA or DNA oligonucleotides. NMR studies have confirmed that this increase in stability stems from a lower distortion imposed on the purine strand of the duplex and an enhanced rigidity of the triplex due to the presence of the methoxy group (Asensio *et al.*, 1999).

Other modifications can also be used to conformationally restrict the sugar to one type of pucker, this also leads to favorable entropic factors due to a reduction in the rotational freedom of the sugar phosphate backbone. The most characterized of these modifications is locked nucleic acid (LNA; Figure 1.3(ii)), where a 2′-*O*,4′-*C* methylene bridge is used to constrain the sugar to N-type. This modification was developed independently by both the Wengel and Imanishi groups for use in antisense or antigene applications, respectively (Singh *et al.*, 1998; Torigoe *et al.*, 2000). Despite some sequence constraints TFOs containing LNA every 2-3 bases are markedly more stable than their unmodified counterparts (Torigoe *et al.*, 2000; Sun *et al.*, 2004). Two further derivatives have also been developed. The first, ENA (Figure 1.3(iii)) contains an additional carbon spacer in the bridge and unlike LNA fully substituted ENA-TFOs are

not destabilising (Koizumi *et al.*, 2003). The second, 3′-amino-2′,4′-LNA, combines the LNA sugar modification with the N3′-P5′ modification (see below), this variant is no more stable than LNA by itself (Obika *et al.*, 2003).

The bicyclo and tricyclo furanose modifications developed by Leumann and co-workers represent further attempts to restrict the sugar conformation (Tarköy & Leumann, 1993; Steffens & Leumann, 1999). Bicyclo-DNA (Figure 1.3(iv)) contains a 3′-*O*,5′-*C* ethylene bridge that locks the sugar in an S-type conformation. The tricyclo derivative (Figure 1.3(v)) contains an additional cyclopropane unit locking the sugar in a N-type pucker. Studies with TFOs composed of tricyclothymidine showed a 2 °C increase in T_m for the addition of each modification at pH 7.0 (Renneberg & Leumann, 2004).

1.5.2 Addition of positive charges

The simplest strategy to alleviate the problem of charge repulsion between the three negative strands is to incorporate positively charged moieties into the TFO by either modifying the backbone, the sugar or the base.

1.5.2.1 Addition of positive charges to the backbone

A few studies have centered on the addition of positive charges to the phosphate residues within the backbone of pyrimidine TFOs. Studies by Bruice and co-workers have looked at replacement of these groups with positively charged guanidinium linkages (Figure 1.4(i)). A pentameric thymidyl oligomer of DNG with four positive charges exhibited an unprecedented high affinity for polyadenine, forming a 2:1 thymine adenine complex (Dempcy *et al.*, 1995, Blaskó et al., 1996). The synthesis of its ribose derivative has recently been reported but has yet to be studied for its triplex-forming properties (Park & Bruice, 2005). This derivative may combine the stabilising effect of both a positive charge and a favorable sugar conformation. Two further modifications that replace the phosphate residues with either cationic dimethylaminopropyl phosphoramidate linkages (PNHDMAP; Figure 1.4(ii)) or *N,N*-diethyl-ethylenediamine linkages (DEED; Figure 1.4(iii)) have also been synthesised (Chaturvedi, *et al.*, 1996; Dagle and Weeks, 1996; Michel *et al.*, 2005). Due to phosphorus chirality, oligonucleotides containing these modifications are a mixture of stereoisomers with 2^n species (n is the number of modifications). It was shown for the

PNHDMAP modification that TFOs containing α-anomers of the bases were more stabilising than β-anomers (Michel *et al.*, 2005). At pH 7.0, a triplex containing nine or more substitutions was more stable than the underlying duplex. Like unmodified TFOs containing pyrimidine α-anomers, these TFOs bind in a reversed antiparallel orientation (Thuong & Hélène, 1993; Michel *et al.*, 2005).

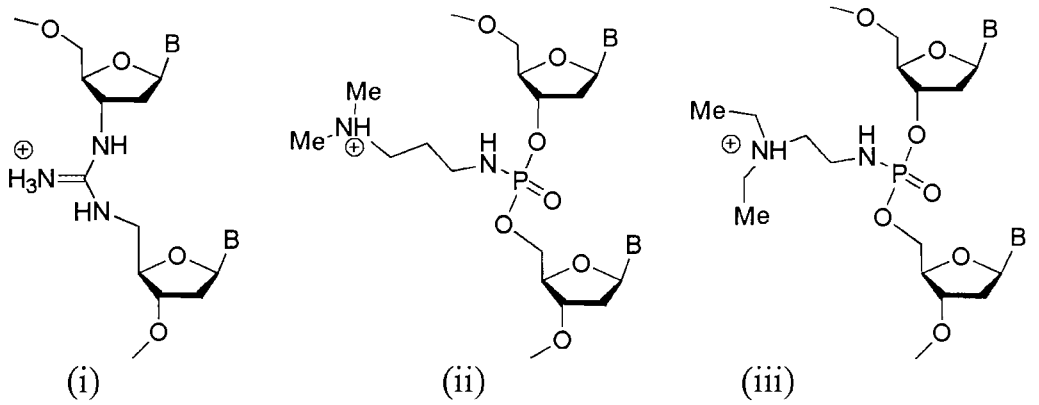

Figure 1.4 Chemical structures of backbone modifications that introduce a positive charge; (i) DNG, (ii) PNHDMAP, (iii) DEED.

1.5.2.2 Addition of positive charges to the sugar

Another strategy has centered on the addition of positively charged amino functions to various positions of the sugar unit. Different modifications have been attempted at either the 2′ (Figure 1.5(i)) (Cuenod *et al.*, 1998) or 4′-positions (Figure 1.5(ii)) (Atsumi *et al.*, 2002). In both cases the best results came from the addition of an aminoethoxy side chain with a T_m increase of 3.5 °C and 1 °C per modification at pH 7.0 for the 2′ and 4′ derivatives (Cuenod *et al.*, 1998; Atsumi *et al.*, 2002). The greater stabilisation in the case of the 2′-derivative was attributed via NMR to the formation of a salt bridge between the positive charge and a pro-R oxygen of the phosphodiester backbone of the purine strand and a favorable N-type sugar pucker (Blommers *et al.*, 1998). A further modification involves substitution of the furanose oxygen with nitrogen, generating pyrrolidine oligonucleotides (Figure 1.5(iii)). Again this positions a positive charge next to the pro-R non-bridging phosphate oxygen in the purine strand. In this instance the effect of the modification depends on the base that is attached to the modified sugar; pseudoisocytosine is stabilising giving a T_m increase of 2 °C per modification while uracil is destabilising (Mayer *et al.*, 2005). The addition of guanidine instead of amino functions to the sugar has also been attempted (Prakash *et*

al., 2004). This modification offers two further advantages. Firstly, it can be applied post oligonucleotide synthesis and secondly, the guanidine group is protonated over a greater range than the amine. This modification should give typically the same increase in stability as with an amine at neutral pH, but in principle should give greater triplex stabilisation at pH values above this.

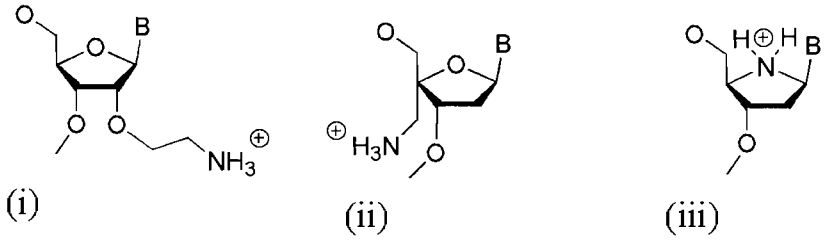

Figure 1.5 Chemical structure of sugar modifications that introduce a positive charge; (i) 2´-aminoethoxy, (ii) 4´-aminoethoxy, (iii) pyrrolidine.

1.5.2.3 Addition of positive charges to the base

As mentioned above, the C^+.GC triplet is more stable than T.AT due in part to a charge screening effect of the positive charge. With this in mind the base 5-propargylamino-dU (U^P; Figure 1.6(i)) was prepared in order to enhance the affinity of T for AT base pairs (Bijapur *et al.*, 1999). This analogue bears a positive charge attached to the 5-position of U rather than in the stacked ring system (as in protonated C). TFOs containing several substitutions of this analogue are markedly more stable than unmodified TFOs. The complexes formed are pH dependent which corroborates the requirement for protonation as the main stabilising factor (Bijapur *et al.*, 1999). Unlike protonated C, adjacent substitutions of U^P are not destabilising, suggesting that the concomitant removal of the charge from the π-stack and appendage to a position away from the base maybe a useful approach to stabilising triplexes. The alkynyl moiety of U^P also contributes to triplex stability by enhancing stacking interactions (see Section 1.5.4).

The covalent attachment of polyamide groups to different bases has also been attempted. The attachment of spermine at the 5-position of uracil (Nara *et al.*, 1995) and to the N4 position of methylcytosine (Barawker *et al.*, 1996) (Figure 1.6(iii) and (iv)) both increase triplex stability at physiological pH, though complexes exhibit a decreased selectivity.

Combining favorable base and sugar modifications has also been extremely successful. Bis-amino-U (BAU; Figure 1.6(ii)) combines the propargylamino modification at the 5-position of U with addition of an aminoethoxy group at the 2′-position of the sugar (Sollogoub *et al.*, 2002). Data at pH 7.0 show that U^P or ^{2AE}T modifications produce ΔT_m values of 27.1 and 12.5 °C, respectively. This compares with 42.4 °C for BAU, which is slightly greater than the sum of the other two (Sollogoub *et al.*, 2002). It has been suggested that the two positive charges act in different ways to enhance triplex stability: the 2′-aminoethoxy group interacts with a phosphate on the duplex purine strand, while the 5-propargylamino group interacts with a third strand phosphate.

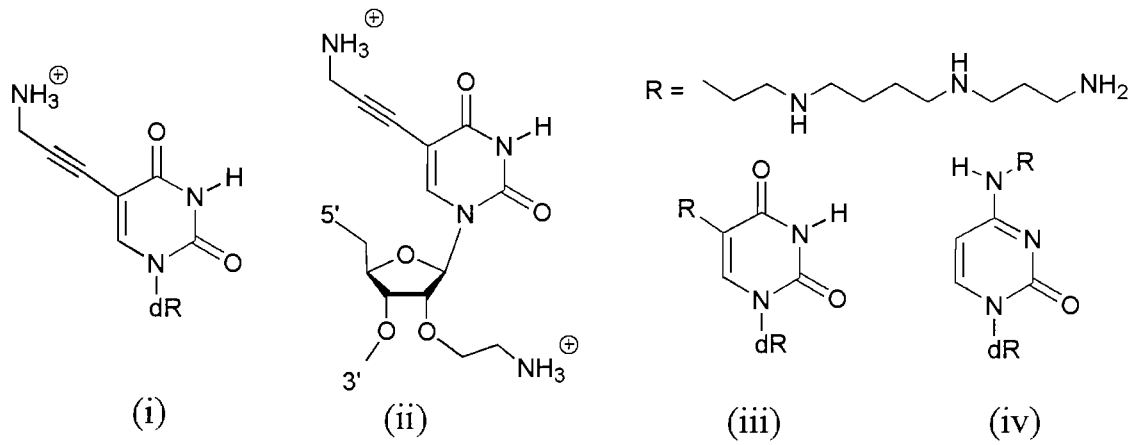

Figure 1.6 Chemical structures of base modifications that introduce a positive charge; (i) U^P, (ii) BAU, and spermine derivatives of T (iii) and C (iv).

1.5.3 Backbone modifications

An alternative method for decreasing the charge repulsion between the three polyanionic DNA strands is to use TFOs containing neutral backbones. Examples of these are shown in Figure 1.7. Replacement of the phosphate linkage with a 3′-5′-linked methyl phosphonate group (Figure 1.7(iii)) was the first to be assessed (Miller *et al.*, 1980). Triplex formation was first observed using short oligonucleotides containing alternating methylphosponate and phosphodiester linkers (Miller *et al.*, 1980). Subsequent studies with longer fully substituted TFOs showed that this modification was destabilising (Kibler-Herzog *et al.*,1990; Debart *et al.*, 1998). However, this may have been caused by the diastereoisomeric mixture of methylphosphonate residues produced during oligonucleotide synthesis. Other studies showed that α-methylphosphonate TFOs produce stable triplexes (Debart *et al.*, 1998).

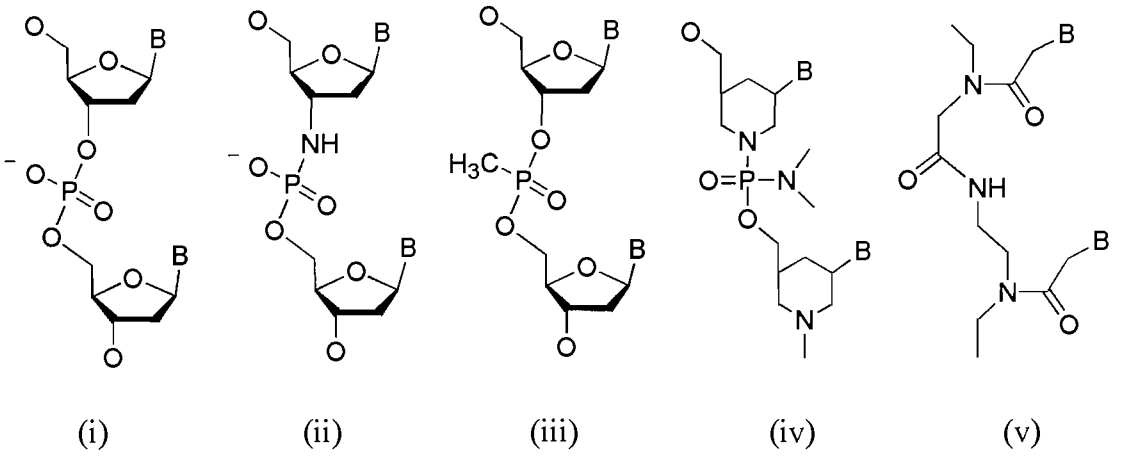

Figure 1.7 Chemical structures of modified backbones; (i) DNA; (ii) N3′-P5′; (iii) methyl phosphonate; (iv) morpholino; (v) PNA.

Morpholino oligonucleotides are another interesting class of analogues. This modification replaces the sugar with a six membered ring, while the phosphodiester linkage is replaced by a phosphorodiamidate linkage (Figure 1.7(iv)). TFOs containing this modification were less stable than the N3′-P5′ modification at high concentration of cations but were more stabilising at low ionic strength (Lacroix *et al.*, 2000; Basye *et al.*, 2001). This modification has recently been employed in α-oligonucleotides (Michel *et al.*, 2003).

The N3′-P5′ amidate modification (Figure 1.7(ii)), where O3′ of the internucleoside phosphate is replaced by NH (Gryaznov *et al.*, 1995), increases the binding constant at neutral pH by nearly two orders of magnitude (Torigoe *et al.*, 2001). Triplex binding is probably improved as this modification favours the N-type modification as discussed above. This modification has also been combined with the addition of a cationic copolymer. The combination of these two modifications synergistically stabilises triplex formation and increases association rates by four orders of magnitude (Torigoe *et al.*, 2005).

The most extensively employed class of uncharged backbone modifications is peptide nucleic acid (PNA; Figure 1.7(v)). PNA is composed of repeating (2-aminoethyl)glycine units to which nucleobases are linked by methylene bridges (Nielsen *et al.*, 1991; Nielsen, 2001). PNA usually interacts with duplex DNA via a mechanism of strand displacement and P-loop formation, requiring two molecules of

PNA (Nielsen *et al.,* 1994), generating a 2:1 PNA:DNA triplex. Two pyrimidine-containing PNA molecules form a local triplex with the purine-containing DNA strand leaving the pyrimidine DNA strand looped out as a single strand. The resulting triplex is more stable than the equivalent DNA triplex since there is much lower charge repulsion between the strands. In a few instances PNA can form a 1:2 PNA:DNA triplex, by simple binding of a PNA third strand to a DNA duplex, though this is usually restricted to cytosine-containing PNAs (Wittung *et al.,* 1997).

1.5.4 Increasing base stacking

Base stacking is an important factor that affects the stability and structure of both duplex and triplex DNA and stems from interactions between charges in the adjacent planar rings. Increasing the aromatic surface area might therefore be expected to increase triplex stability. Most such modifications have been based on thymine, by adding further aromatic rings across 4 – 5 or 5 – 6 positions, which minimizes disruption to the hydrogen-bonding groups (Staubli & Dervan, 1994; Michel *et al.*, 1996; Godde, 1998). Surprisingly none of these modifications are stabilising, though the non-natural pyrido[2,3-*d*] pyrimidine nucleoside F recognises AT base pairs with a similar affinity to T (Staubli & Dervan, 1994).

The addition of a hydrophobic substituent at the 5-position of a pyrimidine base increases hydrophobic interactions within the major groove. The simplest of these is the addition of a methyl group and probably explains why U.AT is more stable than T.AT and $^{Me}C^{+}$.GC is more stable than C^{+}.GC (Xodo, *et al.*, 1991; Leitner *et al.,* 2000). The addition of a propyne group further extends the hydrophobic surface and each propynyl dU substitution increases the T_m by about 2.5 °C relative to thymine at pH 6.0. Propynyl dC reduces triplex stability relative to C as it decreases the pK_a of the N3 atom of the heterocycle. (Froehler *et al.,*1992, Phipps *et al.*, 1998). A recent study on the properties of four different C5-amino modified deoxyuridines showed that the order of stability produced by 5-substitutions is alkyne > *E*-alkene > alkane > *Z*-alkene (Brazier *et al.*, 2005).

1.5.5 Triplex binding agents

Several external binding agents have been developed that preferentially bind to triplex over duplex DNA acting to stabilise these structures (Escude *et al.*, 2001). These compounds are usually composed of aromatic rings for stacking between the base triplets and may also incorporate a positive charge to partially alleviate the triplex charge repulsion.

1.5.5.1 BePI and derivatives

The first triplex binder to be developed was benzopyridoindole (BePI; Figure 1.8(i)), this polycyclic ligand intercalates between base triplets more readily than between base pairs (Mergny *et al.*, 1992). As this compound encompasses a positive charge it favours T.AT-rich sequences, minimizing the charge repulsion with C^+.GC triplets. Several derivatives have since been developed (Escudé *et al.*, 1995/98). The most recent and most stabilising is BQQ (Figure 1.8(ii)); 10 μM of this ligand was shown to stabilise a 14mer triplex by over 40 °C (Escudé *et al.*, 1998). More recently BQQ has been conjugated to the minor groove binder neomycin as neomycin by itself has recently been shown to stabilise triplexes by binding in the Watson-Hoogsteen groove (Arya *et al.*, 2001; Arya *et al.*, 2003). An increase in T_m of over 60 °C was seen with the addition of 4 μM of this conjugate to a triplex.

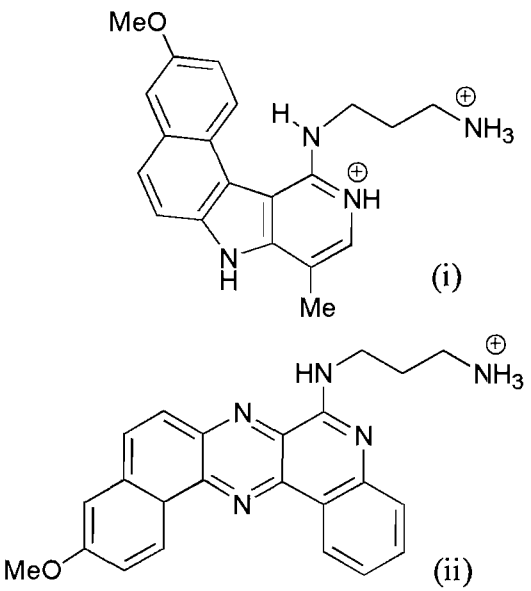

Figure 1.8 Chemical structures of the triplex stabilising agents BePI (i) and BQQ (ii).

1.5.5.2 Napthyquinoline and derivatives

Another group of triplex stabilising agents have been developed from quinolines, with the 2-napthyl derivative giving the highest degree of stabilisation (Figure 1.9(iii)) (Wilson *et al.*, 1993; Strekowski *et al.*, 2005). This compound encompasses unfused aromatic rings allowing a better stacking interaction between the base triplets. In a competition dialysis experiment this ligand bound to a poly T.AT triplex by a factor of at least 2.5 better than 13 other nucleic acid structures (Chaires *et al.*, 2003). This compound has also been synthesised as a dimer, allowing for bis-intercalation (Keppler *et al.*, 1999a). DNase I footprinting has shown that this compound is at least 30-fold more stabilising than its monomer; at concentrations as low as 0.1 μM it increased triplex stability by greater than 1000-fold.

1.5.5.3 Bi-substituted amidoanthraquinones

Another class of triplex ligands are the bi-substituted amidoanthraquinones (Figure 1.9(iv)). This class of molecules are less stabilising than those mentioned above but can bind to a broader range of sequences, attributed to a lack of positive charge (Keppler *et al.*, 1993b; Keppler *et al.*, 2003). The order of triplex affinity decreases in the order 2,7 > 1,8 = 1,5 > 2,6 and molecular modelling has suggested binding is by intercalation positioning the two side groups into the two grooves (Keppler *et al.*, 2003).

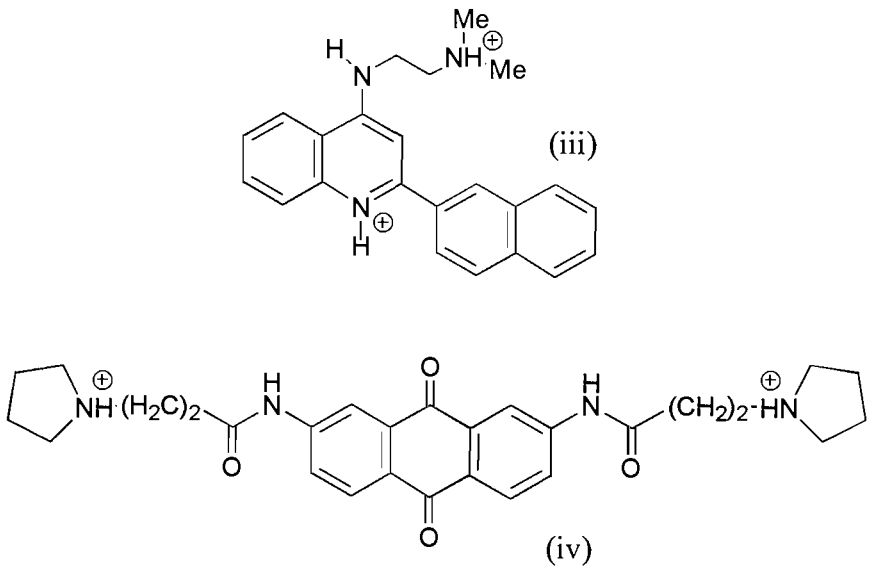

Figure 1.9 Chemical structure of the triplex stabilising agents napthylquinoline (iii) and 2,7 disubstituted amidoanthraquinone (iv).

1.5.6 Conjugation to other DNA binding agents

Triplex stability has also been enhanced by covalently attaching other DNA binding ligands to the TFO. In this way sequence selectivity is achieved through the oligonucleotide while the DNA binding ligand is used as a non-specific anchor to enhance the affinity. Examples of such additions include acridine (Asseline *et al.* 1991; Stonehouse & Fox, 1994), triplex binding ligands (Silver *et al.*,1997; Keppler, *et al.*,1999), minor groove binding ligands (Robles *et al.*, 1997) and daunomycin (Capobianco *et al.*, 2005). These additions have also been used to enhance the affinity of weaker triplexes that are formed at sites containing pyrimidine interruptions (Kukreti *et al.*, 1997). Triplex-forming oligonucleotides can be attached to psoralen, generating cross-links on UV irradiation (Takasugi, 1991).

1.6 Decreasing the pH dependence of TFOs

The requirement for low pH in the parallel binding motif, necessary for protonation of third strand cytosines, has led to the synthesis of a variety of cytosine mimics. These are either based on the pyrimidine ring system (protonated and non-protonated) or the purine ring system (non-protonated) and have been designed to incorporate the same array of hydrogen bond donors as cytosine. In some instances these have been used in combination with sugar or backbone modifications.

1.6.1 Pyrimidine base analogues

An intrinsic advantage of using a pyrimidine rather than purine analogue in the parallel binding motif is the triplet produced will be isomorphous with T.AT, resulting in less distortion of the TFO backbone. Two main types of pyrimidine analogues have been employed, those that retain the positive charge and those that mimick the same array of hydrogen bond donors as cytosine.

The simplest modification to the cytosine ring nucleus is the addition of a methyl group at the 5-position (^{Me}C; Figure 1.10(i)). Methylation of cytosine first implicated a means of gene regulation *in vivo* after studies showed that triplexes containing this modification could form at physiological pH (Lee *et al.*, 1984). Further studies extended its use to TFOs (Povsic & Dervan, 1989). The lower pH dependence and higher affinity

relative to cytosine was at first attributed to an increase in basicity, however a pK_a increase of only 0.1-0.2 pH units is too low to account for this increase alone. It has been suggested that the increase in stability might be entropic in origin, resulting from greater base stacking or hydrophobic interactions within the major groove (Xodo, *et al.*, 1991; Leitner *et al.*, 2000). Another suggestion was that better stacking increases the residence time of the non-protonated base and its lone hydrogen bond, reducing its tendency to unstack (Singleton & Dervan, 1992).

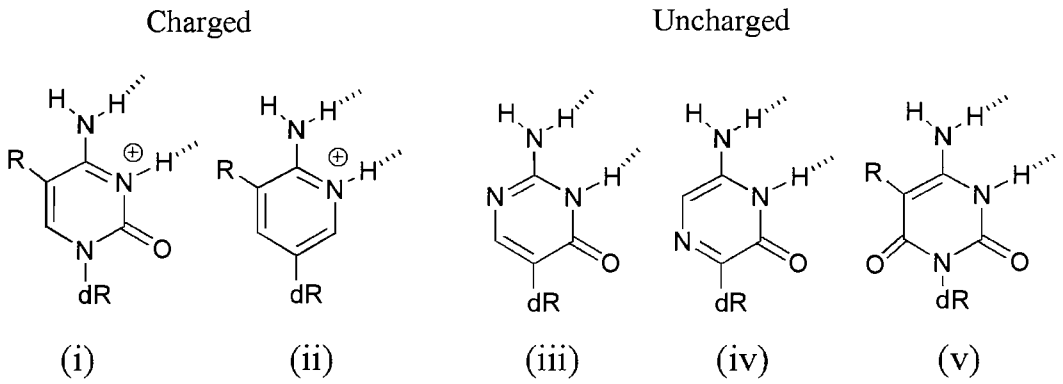

Figure 1.10 Pyrimidine base analogues for recognition of GC base pairs; (i) C (R = H) and ^{Me}C (R = CH_3), (ii) 2-aminopyridine (R = H) and 3-methyl-2-aminopyridine (R = CH_3), (iii) pseudoisocytosine (iv) PyDDA, (v) 6-oxo-C (R = H) and 5-methyl-6-oxo-C (R = CH_3). In each case dR indicates the deoxyribose sugar and the hydrogen bonds to the GC base pairs are shown.

Another charged cytosine analogue to be developed was based on the more basic pyridine *C*-nucleoside. A simple substitution of a carbon at N1 and removal of the 2-carbonyl gives 2-aminopyridine (P; Figure 1.10(ii)). This analogue was synthesised independently by two research groups (Bates *et al.*, 1996; Hildbrand *et al*, 1996). Both β and α-anomers were initially tested as the α-anomer is slightly more basic than the β-anomer (Bates *et al.*, 1996; Cassidy *et al.*, 1997). The β-anomer exhibited lower pH dependence than cytosine, attributed to a pK_a of 6.5 but the α-anomer did not bind presumably due to structural constraints. Unlike cytosine this analogue can be incorporated into TFOs at adjacent positions (Cassidy *et al.*, 1997). The 3-methyl (^{Me}P) and 2-*O*-methyl (^{OMe}P) derivatives were also synthesised and surprisingly neither showed any gain in stability (Hildbrand *et al.*, 1997).

Pseudoisocytosine ($^{\Psi}$C; Figure 1.10(iii)) was the first non-charged cytosine mimick to be developed. Its 2′-*O*-methyl derivative formed stable triplexes at pH 7.0 under

conditions where C and 2′-*O*-methyl C did not. As with 2-aminopyridine it exhibited no destabilising effects of contiguous substitutions (Ono *et al.*, 1991). This base isn't completely pH independent due to its tautomeric nature. At pH 7.0, the imino proton can occupy either N1 or N3 with only the later favouring triplex formation. Several derivatives of this base have appeared in the literature over the last few years and recently the complicated synthesis has been overcome (Maher & Leumann, 2003). The first, a deoxyribose derivative, exhibits a lower affinity for guanine presumably due to a less favourable S-type sugar conformation (Chin *et al.*, 2000). The second, a pyrrolidino derivative exhibited a 2.5-3 °C increase in T_m per modification, depending on the sequence contexts. This modification can also be used to target contiguous guanines (Maher & Leumann, 2003; Mayer *et al.*, 2005). Pseudoisocytosine has been more frequently employed for the pH independent recognition of a DNA by a PNA strand binding via Hoogsteen hydrogen bonds (Egholm *et al.*, 1995). Another analogue very similar to pseudoisocytosine is pyrazine (Figure 1.10(iv)), with N found at the 6-position not 1-position. It also exhibits stable triplex formation at pH 7.0 (Krosigk *et al.*, 1995).

6-Oxo cytosine (^{oxo}C; Figure 1.10(v)) and its 5-methyl derivatives are another group of cytosine mimics to be developed (Berressem & Engels, 1995; Xiang *et al.*, 1994). At low pH this analogue suffered from a much lower stability than cytosine but this was alleviated at high pH (Xiang *et al.*, 1994). Surprisingly, contiguous substitutions are destabilising (Xiang *et al.*, 1996). This was attributed to unfavorable stacking interactions and/or steric hindrance due to the 6-carbonyl group. This was overcome to some extent by attaching the base to the backbone via an acyclic linker, presumably giving greater flexibility (Xiang *et al*, 1998). 2′-*O*-Methyl and ribo derivatives have been synthesized and shown to be less stable (Berressem & Engels, 1995; Parsch & Engels, 2000).

1.6.2 Purine base analogues

The first purine analogues to be tested for pH independent recognition of guanine were 8-oxo-adenine (Miller *et al.*, 1992) and its N6-methyl derivative (Krawczyk *et al*, 1992). These bases are forced to adopt a syn orientation due to the presence of the 8-oxo-group, this presents both the 6-amino and N7 protons for recognition of guanine (Figure 1.11(i)). The 7,8-dihydro derivative has also been developed with similar results

(Jetter et al., 1993). These analogues are pH independent and exhibit the same relative stability as methyl C at low pH. They can also target contiguous guanine residues.

A different strategy has looked at the synthesis of N7-purine derivatives. The first to be synthesized was N7G (Hunziker *et al.*, 1995). This base essentially reverses the antiparallel G.GC triplet so that it can be incorporated within the parallel binding motif (Figure 1.11(ii)). This base offers good selectivity and pH insensitivity but suffers from sequence constraints since it is not isomorphous with the other triplets in the parallel motif. A single substitution is as stable as methyl C at pH 7.0 but is less stable at pH 5.0. When alternate third strand bases are substituted with this analogue the triplex is less stable by three orders of magnitude compared to contiguous substitutions. Similar characteristics were also exhibited by the further N7 analogues, P1 (Koh and Dervan, 1992; Singleton & Dervan, 1995) and N7-inosine (Figure 1.11(iii) and (iv)) (Marfut *et al*, 1996/1997). N7-inosine lacks the amino function of N7G but surprisingly shows stable recognition of guanine. This was attributed to an unconventional CH..O bond formed between the carbonyl group of inosine and the CH on guanine. It was postulated that this interaction gives a small, positive, direct electrostatic contribution to stability (Marfut *et al.*, 1998).

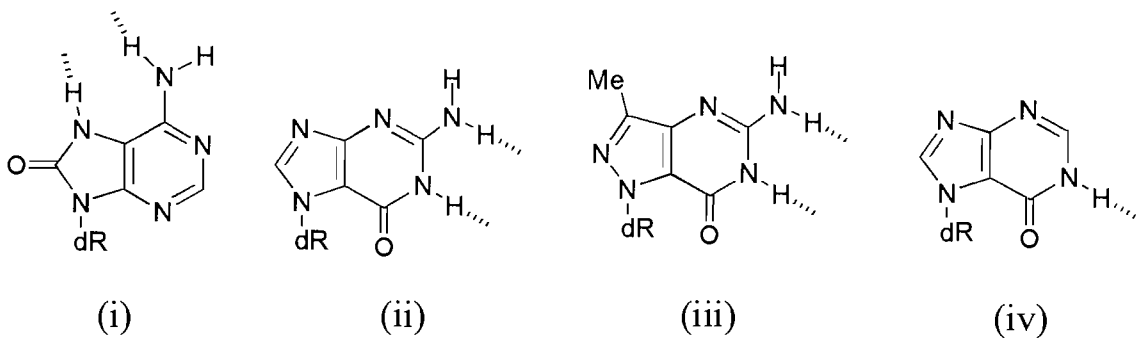

Figure 1.11 Purine base analogues for recognition of GC base pairs; (i) 8-oxoA, (ii) N7G, (iii) P1, (iv) N7I. In each case dR indicates the deoxyribose sugar and the hydrogen bonds to the GC base pairs are shown.

Several strategies have been employed to overcome the sequence constraints imposed by the lack of isomorphism of the triplets formed by these bases. An acyclic glycerol derivative was employed to attach N7G to the TFO backbone, though the increase in flexibility didn't alleviate this constraint (St. Clair *et al,* 1998). It may therefore be necessary to use a combination of such bases; N7-purines for binding contiguous GC

base pairs and pyrimidine analogues for binding to isolated guanines (Singleton & Dervan, 1995). An alternative is to develop an isomorphous N7 derivative, for example N7-adenine, for targeting A, though the propensity for purines to bind in an antiparallel orientation may create problem.

1.7 Recognition of pyrimidine interruptions

Triplex formation is restricted to homopurine.homopyrimidine target sites as the bases within a TFO can only recognise purine bases. Although there is an abundance of oligopurine target sites within the human genome (Manor *et al.*, 1988; Behe *et al.*, 1995; Goni *et al.*, 2005) this limits the use of triplexes and a method for targeting any DNA sequence is highly desirable. The recognition of pyrimidine bases, however, is hampered by several restrictions. Firstly, the Hoogsteen face of a pyrimidine base offers a single H-bond within the major groove. This therefore leads to triplets of low affinity and selectivity. Bases that recognise T may also recognise G as these contain an H-bond acceptor at similar positions; similarly the same is true for the recognition of C and interactions with A. Thymine presents a further problem, due to the presence of the 5-methyl group in the major groove, imposing a steric barrier to third strand binding. There have therefore been several strategies proposed to overcome each of these restrictions.

1.7.1 Null bases and abasic linkers

The binding of a third strand of DNA within the major groove is highly asymmetric, a TFO can only recognise the purine-containing strand of the duplex and not its partner on the opposing pyrimidine-containing strand. Providing the TFO is sufficiently long enough to compensate for lack of binding energy it may be possible to position a null base or universal base analogue opposite an inversion site. These are usually non-hydrogen bonding, hydrophobic, aromatic analogues that stabilise via stacking interactions (Loakes, 2001). Abasic linkers, such as 1,2-dideoxy-D-ribose (∅) have been tested for skipping the interruption but the binding affinity is low due to the loss of stacking interactions (Horne & Dervan, 1991). Neither of these approaches has yielded stable triple helical structures and both cause a loss of specificity at the skipped base as any base pair can be tolerated at this position.

1.7.2 Natural bases

Several studies have been carried out on TFOs to investigate the stability of all possible combinations of natural bases opposite each base pair (Griffin & Dervan, 1989; Yoon *et al.*, 1991; Mergny *et al.*, 1991). These studies have demonstrated that the least destabilising combinations for recognising TA and CG base pairs are G.TA and T.CG (C.CG) (Figure1.12). All three triplets are stabilised by a single hydrogen bond, resulting in complexes of lower affinity and selectivity than the canonical triplets; T prefers binding AT and G also binds GC with a slightly lower affinity.

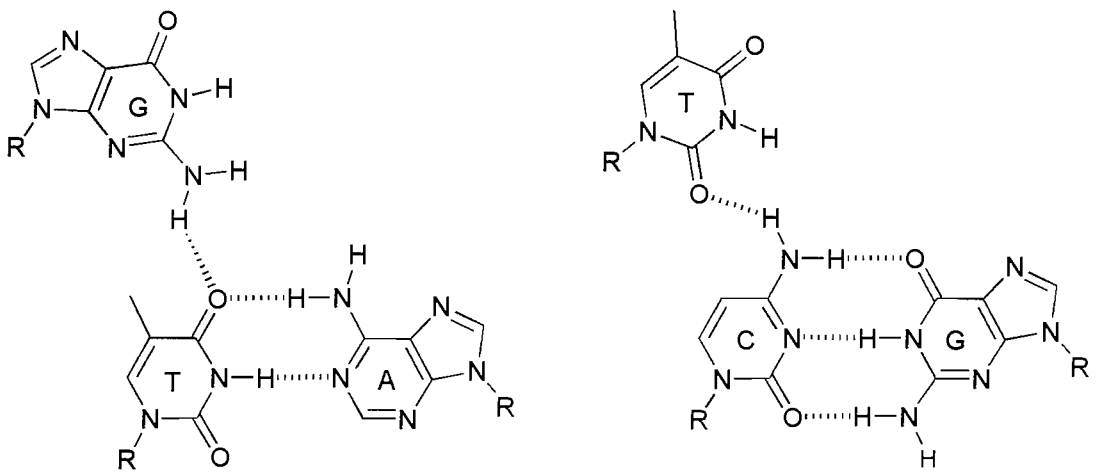

Figure 1.12 Structures of the G.TA and T.CG base triplets.

The G.TA triplet contains a single hydrogen bond between the exocyclic amino group of guanine and the 4-carbonyl group of thymine (Radhadkrisnan & Patel, 1991). This hydrogen bond arrangement has been confirmed by using several guanine analogues. Removal of the 2-amino group or the 6-oxo group, generating inosine or 2-aminopurine respectively, produces triplets which are less stable than guanine (Amosova *et al.*, 1999). The later was more surprising as the 6-oxo group is not thought to take part in binding, although 2-aminopurine also differs from guanine in lacking a hydrogen atom at N1. The stability of the G.TA triplet is affected by the sequence context and flanking T.AT triplets (especially on its 3′-side) produces more stable complexes than flanking C^+.GC. This is thought to be the consequence of the formation of an additional (weaker) hydrogen bond with T of an adjacent T.AT triplet (Radhadkrisnan & Patel, 1991). Stable complexes can be formed when this triplet is present every fourth position, so long as the triplex contains some C^+.GC triplets and T.AT is located on the 3′-side of each G.TA (Gowers *et al.*, 1999).

The parallel T.CG triplet was first proposed by Yoon *et al.* (1992) and has been shown to involve a single hydrogen bond between O2 of the third strand thymine and the C4-amino duplex proton on the duplex cytosine (Radhakrishnan & Patel, 1994). This hydrogen bonding pattern can also be generated with a third strand cytosine forming the C.CG triplet. Up to three consecutive T.CG or G.TA triplets can be tolerated in the centre of a triplex, if the interaction is stabilised by a triplex-binding ligand (Gowers & Fox, 1997).

1.7.3 Nucleoside analogues for recognising pyrimidine interruptions

1.7.3.1 Targeting C of a CG base pair

The most successful group of analogues designed for the recognition of cytosine within an oligopurine tract are based on thymine. This was initially demonstrated in the antiparallel motif using pyridine-2-one and pyridine-4-one (Figure 1.13(i) and (ii)), which utilise carbonyl groups for recognition of cytosines exocyclic amino group (Durland *et al.* 1994). By omitting either the 4-carbonyl or 3-NH groups of T, which are used in the recognition of adenine, the selectivity could be increased. 5-methyl-pyrimidine-2-one (^{4H}T; Figure 1.13(iii)) was the first such derivative to be synthesized (Prévot-Halter & Leumann, 1999); deletion of the C4-carbonyl of T removes hydrogen at N3 and abolishes the recognition of adenine. The 2-carbonyl of this derivative may also from an unconventional C-H...O bond at the 5-position of cytosine, an interaction that has previously been reported for the N7I.GC triplet (Marfut & Leumann, 1998). The ^{4H}T.CG triplet is as stable as T.CG but loses the recognition of adenine (Prévot-Halter & Leumann, 1999). Further derivatives have been synthesised to attempt to increase affinity and functionality. The first derivative encompassed an increased base-stacking surface, producing the monomer Q (Figure 1.13(iv)) (Prévot-Halter & Leumann, 2001). Unfortunately, triplets formed by this base are no more stable, and Q is less selective than ^{4H}T also recognising guanine. This was attributed to intercalation as no protonation events were observed. More recently the 2´-aminoethoxy derivative of this base has been synthesised, with an increase in T_m of 1.5 °C per modification. A further increase in affinity is seen in the context of fully modified 2´-aminoethoxy TFOs; this base can be used to recognise up to 5 pyrimidine inversions at pH 6.5 (33% pyrimidine content in the purine strand) (Buchini & Leumann, 2004).

Another analogue for cytosine recognition is 2-aminopyrimidine (d2APm; Figure 1.13(v)). This base has a pKa of 3.3 and is therefore unprotonated at physiological pH. It has a nitrogen atom (H-bond acceptor) that acts as a partner with the exocyclic amino group of cytosine. This base gives a 4 °C increase in T_m at pH 7.0 relative to cytosine (Chen & McLaughlin, 2000).

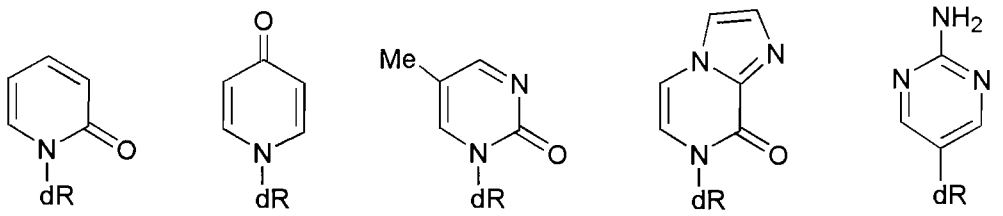

Figure 1.13 Base analogues for the recognition of CG base pairs; (i) pyridone-2-one, (ii) pyridone-4-one, (iii) ^{4H}T, (iv) Q, (v) d2APm.

It is possible to compensate for the loss in binding energy at a single pyrimidine inversion by combining suitable analogues with sugar and/or backbone modification known to increase stability. The LNA modification is one such example, which been extensively employed in this manner by the Imanishi group. CG recognition was first achieved using LNA bearing a 2-pyridone base (Figure 1.14(i)) (Obika *et al.*, 2001). A TFO containing a single substitution exhibited a T_m 9 °C higher than the same analogue attached to deoxyribose, which in turn exhibited the same T_m as thymine. As this modification exhibited enhanced AT recognition a further LNA derivative bearing 1-isoquinone was developed (Q^B; Figure 1.14(ii)). It was reasoned that the recognition of an AT base pair may be sterically hindered if this bicyclic analogue positions a hydrogen in close proximity to thymines 5-methyl group on the opposite side of the major groove (Hari *et al.*, 2003). AT recognition was decreased but at the same time so was CG recognition. A variety of analogues attached to LNA were also assessed for there ability to recognise pyrimidine inversions. (Figure 1.14(iii) to (v)). Oxazole recognised CG slightly better than TA, imidazole was not selective and 2-aminoimidazole recognised GC. However, all the triplets formed by these bases were of a lower stability than T.AT or C^+.GC (Hari *et al.*, 2005).

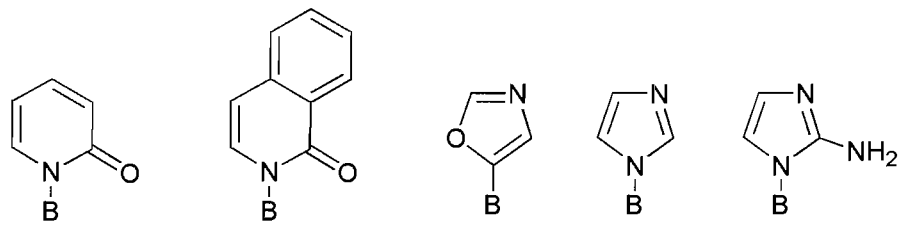

(i) (ii) (iii) (iv) (v)

Figure 1.14 LNA bearing analogues for the recognition of CG base pairs (i) P^B, (ii) Q^B (iii) O^B, (iv) I^B, (v) aI^B. In each case B is a BNA/LNA sugar.

1.7.3.2 Targeting T of a TA base pair

The presence of a methyl group at the 5-position of thymine presents a significant problem in the development of base analogues designed to interact with this base. One strategy that could be used to overcome this problem is the use of a linker that projects the analogue past the methyl group to bind to thymine 4-oxo group. To date this has only be attempted using 3-oxo-2,3-dihydropyridazine (E), this analogue has been attached to a PNA backbone via a β-alanine linker. This analogue shows a T_m increase of 5 °C relative to guanine in an identical position (Eldrup *et al.*, 1997). A derivative of this analogue, which has reduced flexibility in the linker, due to the presence of a double bond, has recently been described and is awaiting assessment (Olsen *et al.*, 2003).

1.7.4 Nucleoside analogues for recognising both partners of the base pair

Another strategy for recognising pyrimidine inversions uses analogues that are able to make contact with both bases of the target, recognising the entire base pair, rather than one of the bases.

1.7.4.1 Recognition of a CG base pair

4-(3-benzamidophenyl)imidazole (D_3; Figure 1.15(i)) was the first base designed to sterically match the edges of a CG base pair (Griffin *et al.*, 1992). It was anticipated that the imidazole moiety would form a single hydrogen bond to cytosine whilst additional stacking interactions would be possible due to the presence of two aromatic rings

positioned in the major groove. The rotational freedom present between these two rings could maximize these non-bonding interactions. Affinity cleavage showed that D_3 bound to CG and TA base pairs with greater affinity than GC and AT. However, later studies showed that this base formed triplets that are less stable when C^+.GC was present at the 3´-side (Kiessling *et al.*, 1992). A subsequent NMR study showed that the mode of binding was intercalation, effectively skipping the inversion site, with a preference for bind at YpA steps (i.e on 3´-side) (Koshlap *et al.*, 1993). Two similar carbocyclic ribofuranose analogues, L1 and L2 (Figure 1.15(ii) and (iii)) were also developed and both exhibited a preference for binding at pyrimidine inversions, these were also proposed to bind via an intercalative mechanism (Lehmann *et al.*, 1997).

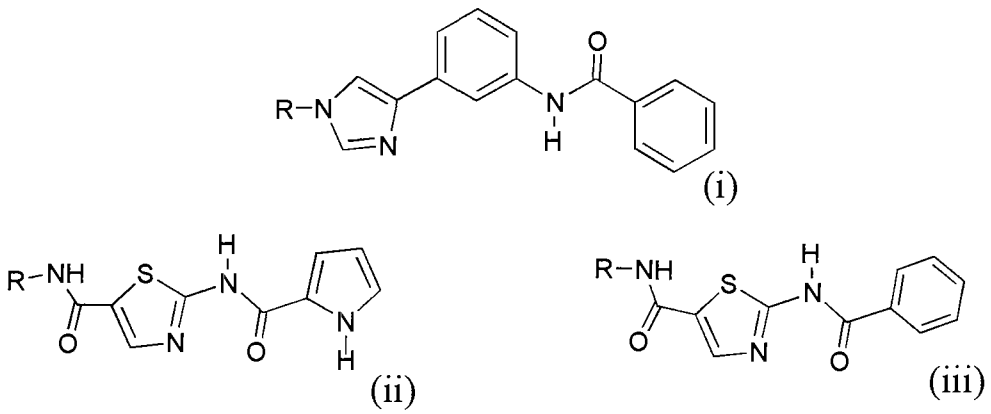

Figure 1.15 Nucleotide analogues that recognise YR base pairs by intercalation; (i) D_3 (ii) L1 (iii) L2.

N4 cytosine derivatives have been the most successful for recognition of both partners of the CG base pair (Figure 1.16). N^4-(3-acetamidopropyl)cytosine (Figure 1.16(i) positions a side chain across the major groove allowing the 3-amino group to form a hydrogen bond to the O6 carbonyl of guanine. UV melting showed this base to be more stable than the C.CG triplet but less stable than the canonical triplets (Huang *et al.*, 1993). A further derivative, N^4-(6-aminopyridinyl)cytosine (Figure 1.16(ii), contains a ring to constrain the rotational freedom of the side chain. This base recognised CG and AT, though a broad transition was observed during UV melting, suggesting two modes of binding; intercalation and hydrogen bonding (Huang & Miller, 1993; Huang *et al.*, 1996).

An interesting attempt to recognise both of the CG partners came from the synthesis of a ureidoisoindolin-1-one homo-N-nucleoside (Figure 1.16(iii)). This compound effectively formed a triplet with CG in chloroform, but showed no binding when

incorporated into a TFO, probably as it is not isomorphous with the other triplets (Mertz *et al.*, 2004).

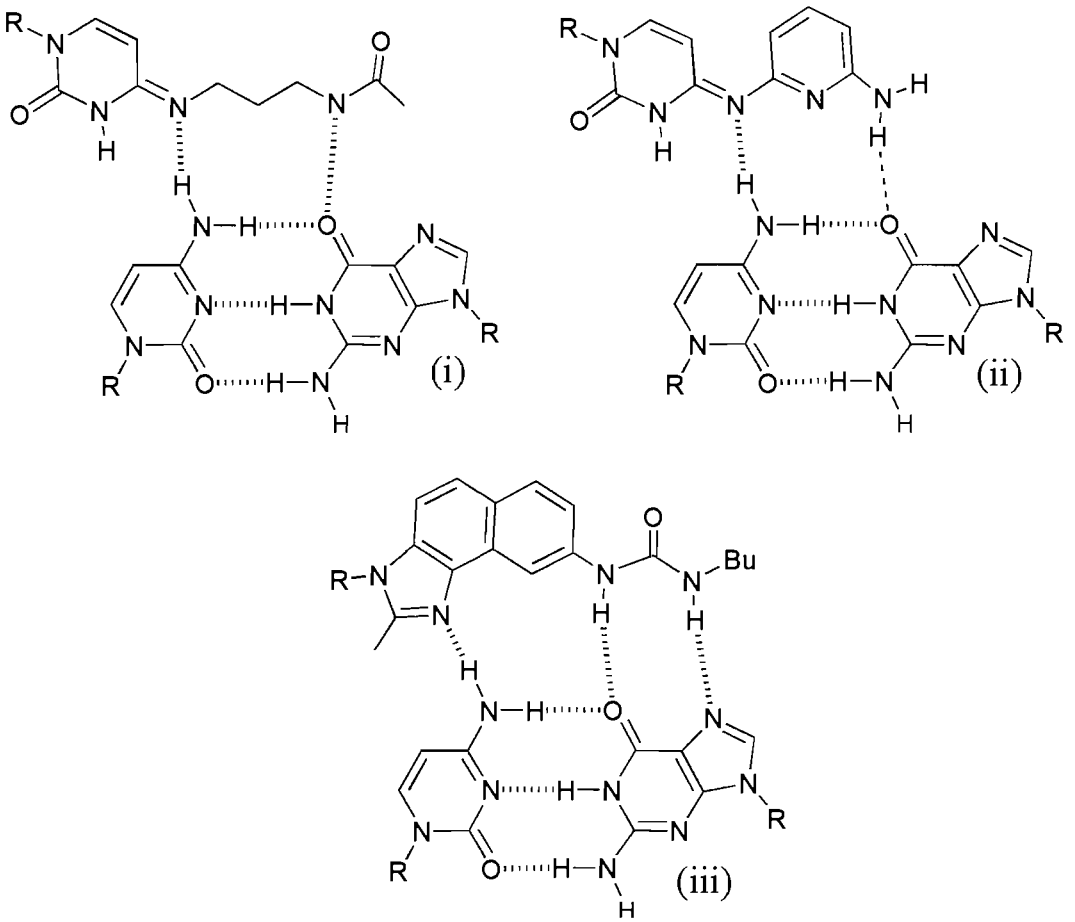

Figure 1.16 Nucleotide analogues for recognising both partners of a CG base pair; (i) AcPrC.CG, (ii) AmPy.CG, (iii) ureido napthimidazole.CG.

1.7.4.2 Recognition of a TA base pair

The most successful nucleoside analogue for the recognition of TA base pairs is N-(4-(3-acetamidephenyl)thiazoyl-2-yl-acetamide (S; Figure 1.17(i)). This nucleoside was based on the previously reported D_3 monomer for the selective recognition of a TA interruption (Guianvarc'h *et al.*, 2001). This base presents donor-acceptor-donor hydrogen bonding moieties for the formation of three hydrogen bonds with TA. The S.TA triplet was less stable when flanked with C^+.GC and the interaction was thought not to involve intercalation (Guianvarc'h *et al.*, 2003). Further derivatives of this nucleoside have since been prepared, including B^t (Figure 1.17(ii), which was designed in anticipation that increasing the rigidity of S would improve its triplex-binding properties (Guinvarc'h *et al.*, 2002, 2003). This analogue retains a similar H-bonding

pattern to S but is conformationally less flexible. Unfortunately this analogue exhibited a decrease in affinity and a loss of selectivity, suggesting that it favours an intercalating mode of binding.

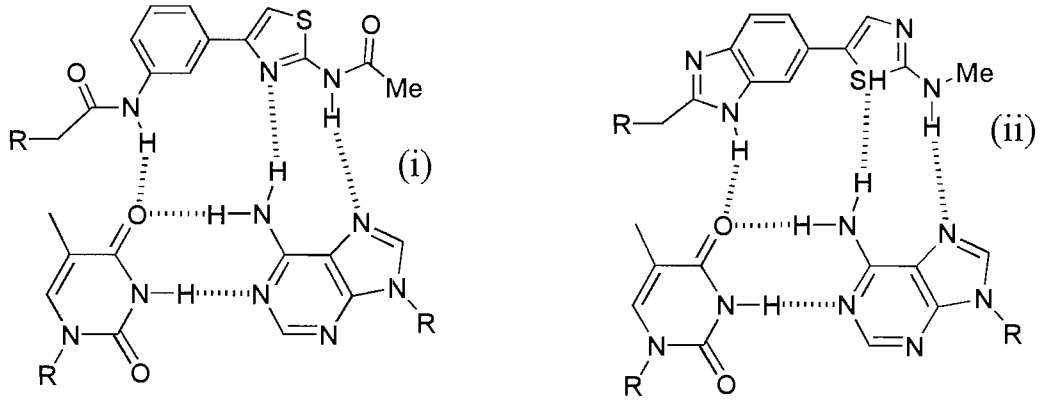

Figure 1.17 Nucleotides for recognising both partners of a TA base pair; (i.) S.TA, (ii) Bt.TA.

A different approach to the recognition of both partners of the base pair has arisen from the design and synthesis of a series of 2-aminoquinazolin-5-yl monomers (Figure 1.18). These molecules, designated TRIPsides, are designed to bind symmetrically within the major groove, forming Hoogsteen hydrogen bonds with both partners of base pair. In this strategy only the purine strand of the duplex is read, but because the backbone is located in the centre of the major groove, either strand can be recognised by choosing the appropriate TRIPside (Li *et al.*, 2003.). To date three of the four monomers antiCG, antiTA and antiGC (but not antiAT) have been synthesised and successfully employed at pH 7.0 for recognising a 19mer target site in which the purines switch from one strand to the other four times (Li *et al.*, 2004, 2005).

Recently a series of extended guanine analogues have been suggested for recognition of TA interruptions (Van Craynest *et al.*, 2004). These compounds use aminobenzimidazole as an analogue of G for recognition of T (mimicking the G.TA triplet). A thymine base is covalently attached to the benzimadazole ring via a linker to allow simultaneous recognition of the adenine by either Hoogsteen (N2) or reverse-Hoogsteen (N1) bonds. Synthesis of the free nucleosides has been reported but these have yet to be incorporated into triplex-forming oligonucleotides.

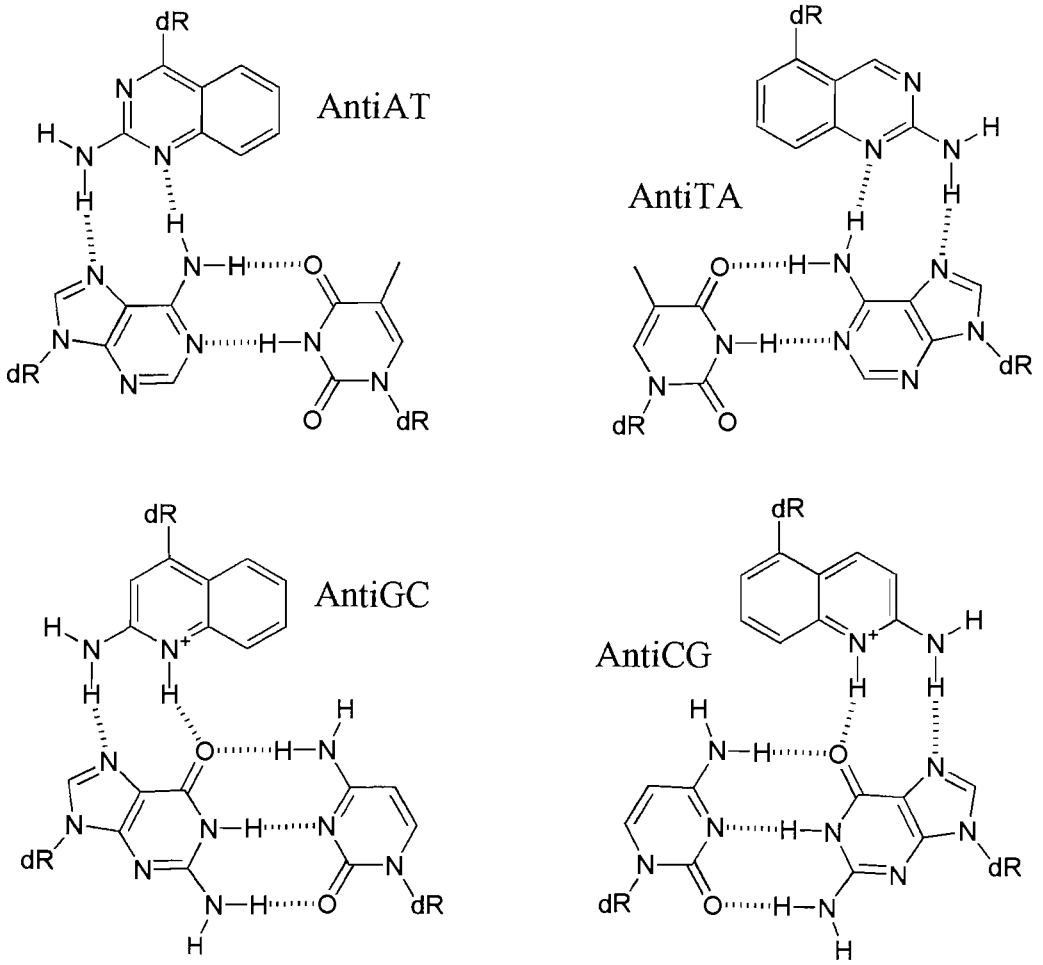

Figure 1.18 Structure of the four TRIPside nucleotides that have been proposed for recognising all four base pairs.

1.8 Purpose of this work

Although it is clear that a large number of nucleoside analogues have been prepared for overcoming the pH problem and for recognising pyrimidine interruptions, there are very few examples in which these have been combined to recognise mixed DNA sequences at physiological pH. In most cases only single pyrimidine interruptions, or single GC base pairs have been targeted, and the compatibility of these nucleosides remains questionable. The studies presented in this thesis examine the triplex-forming properties (selectivity, affinity, pH dependence) of several novel nucleosides analogues; initially as isolated substitutions and then in combination. The main techniques used to characterise these analogues are thermal melting (UV and fluorescence) and quantitative DNase I footprinting. All analogues, which can be seen in the appendix, were prepared and incorporated into oligonucleotides by the group of Prof. Brown, School of Chemistry, Southampton University.

2 MATERIALS AND METHODS

2.1 Methods for studying triplexes

A variety of biophysical techniques have been applied to the study of triplex structure and stability. The main techniques employed in this thesis are DNase I footprinting, thermal melting (UV and fluorescence) and circular dichroism.

2.1.1 Footprinting studies

Footprinting is a technique that can be used to study the sequence specific binding of drugs, proteins or oligonucleotides to a DNA target (Galas & Shmitz, 1978; Van Dyke *et al.*, 1982; François *et al.,* 1988). Briefly, a radiolabelled DNA fragment is incubated with ligand and subjected to partial digestion using a suitable DNA-cleavage agent. The sequence to which the ligand is bound is protected from digestion, and by separating the products of this reaction on a denaturing polyacrylamide gel, can be identified as a gap ('footprint') in an otherwise continuous ladder of bands (Fox, 1997). This is depicted in Figure 2.1. Furthermore footprinting can be used as a quantitative method for estimating ligand affinity, by varying the concentration of the ligand over a range that produces different target site occupancies (Rehfuss *et al.,* 1990). The footprint fades at lower ligand concentrations and this can be quantified by phosphorimaging. The C_{50} value, the concentration of ligand that reduces the band intensity by half, approximates to the dissociation constant of the ligand, so long as the DNA concentration is lower than the dissociation constant of the ligand-DNA interaction.

The choice of DNA-cleavage agent depends on both the fragment used and ligand being assessed. The most commonly used and choice for these studies is the endonuclease DNase I. Other inorganic agents such as methidiumpropyl-EDTA-Fe(II), dimethylsulfate and hydroxyl radicals are also frequently employed.

2.1.1.1 Deoxyribonuclease I

DNase I is a double-strand specific endonuclease that generates single strand nicks into the phosphodiester backbone by cleaving the O3´-P bond. The enzyme's optimal

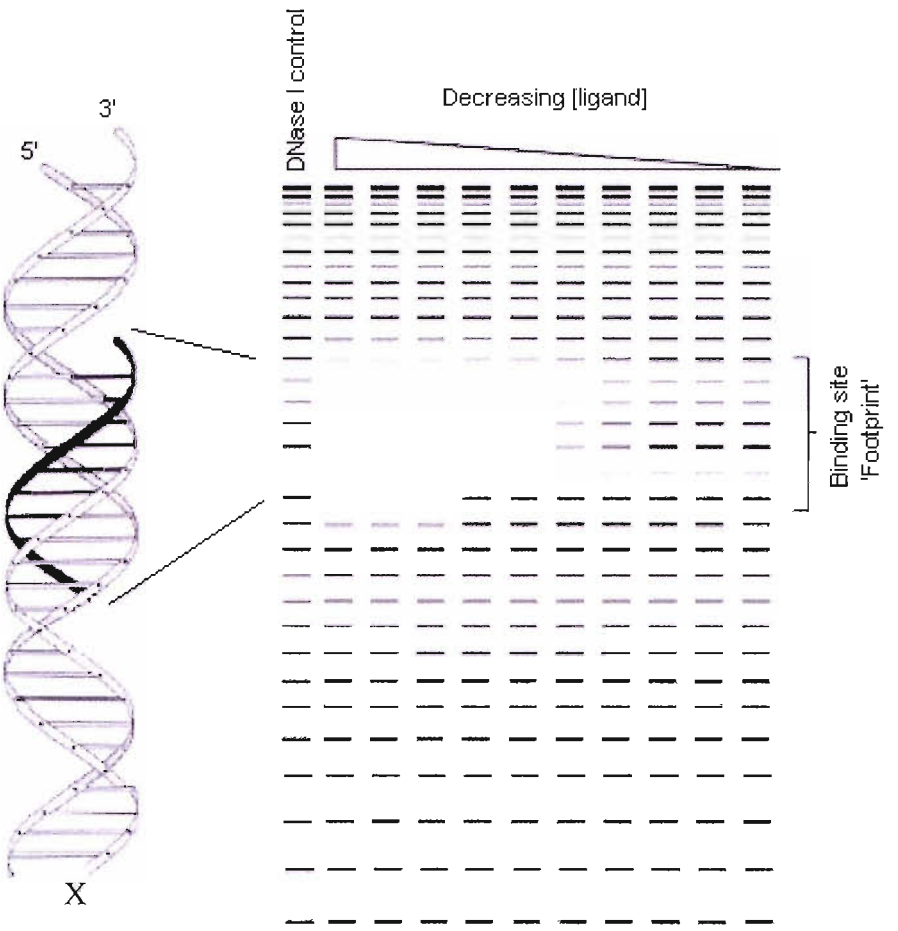

Figure 2.1 Schematic of the footprinting protection assay. The sequence to which a ligand is bound is protected from partial digestion by a suitable cleavage agent. When the products of digestion are separated on a denaturing polyacrylamide gel, the missing bands show the location of the ligand binding site. X marks the strand that is radiolabelled and hence visualised on the gel.

activity requires divalent metal cations such as magnesium, manganese or calcium (Price, 1975). Binding and catalysis occurs by insertion of an exposed loop into the minor groove and results in slight bending of the duplex towards the major groove (Hogan *et al.*, 1989; Suck *et al.*, 1994). GC-rich and $A_n.T_n$ sequences are poor substrates, presumably due to their high rigidity or narrower minor grooves respectively. The size of footprints generated by this enzyme are slightly overestimated due to its large size (M_r 30,400; 40 Å diameter), they are also staggered in the 3´-direction by 2-3 base pairs, across the two strands.

DNase I has been widely used as a cleavage agent for studying triplex formation (François *et al.*, 1988; Sollogoub *et al.*, 2002). As cleavage occurs from the minor groove, whereas the TFO binds in the major groove, triplex footprints must be the result of structural changes that are induced by the binding of the oligonucleotide and not from simple steric block. A further characteristic of triplex footprints is hypersensitivity at the triplex-duplex junction, most often observed at the 3´-side (see Section 1.2.1).

2.1.1.2 Other agents

The hydroxyl radical ($OH^{\cdot}$) is frequently employed as a DNA-cleavage agent. Once generated, usually via the Fenton reaction, hydroxyl radicals attack C4´ from the minor groove (Tullius, 1987). Its small size leads to little sequence preference and generates high-resolution footprinting patterns. As the primary cleavage point is still accessible from the minor groove of a triplex this probe is not employed for footprinting DNA triplexes.

An alternative agent is methidiumpropyl-EDTA-Fe(II) (MPE) (Hertzberg & Dervan, 1982). This ethidium derivative causes cleavage via a Fe^{2+} radical-generating group. This compound binds via intercalation and sequences that possess a smaller groove width, such as $A_n.T_n$, are not digested well (Van Dyke & Dervan, 1983). This agent offers a lower resolution compared to other footprinting agents and is not generally employed for footprinting triplexes as the methidium moiety is known to enhance triplex stability (Mergny *et al.*, 1991; Fox *et al.*, 2000).

Dimethyl sulphate (DMS) is another suitable agent for use in footprinting studies (Lawley & Brookes, 1963). Under limiting conditions this agent causes methylation of

guanine residues that are not protected by the bound ligand. Subsequent addition of piperidine leads to cleavage at methylated G residues. As this agent is specific for the N7 group of guanine, a site that is protected from cleavage by the formation of a Hoogsteen H-bond, it is suitable for footprinting triplexes (Young *et al.*, 1991) providing they contain GC base pairs.

2.1.2 Thermal melting studies

The thermodynamic stability of a nucleic structure can be determined by measuring the change of its absorbance of UV light at 260 nm as it is melted in a controlled fashion. As the complex dissociates, the substituent bases become unstacked and exposed to solvent, thereby causing an increase in absorbance. The melting of a triplex results in a biphasic melting profile with the first melt corresponding to the triplex to duplex transition and the second the duplex to single strand transition. The melting temperature, T_m, indicating the midpoint of each transition can be determined. This technique has been employed for measuring the stability of a variety of triplex structures, including those that contain novel nucleoside analogues (Sollogoub *et al.*, 2002, Buchini *et al.*, 2004).

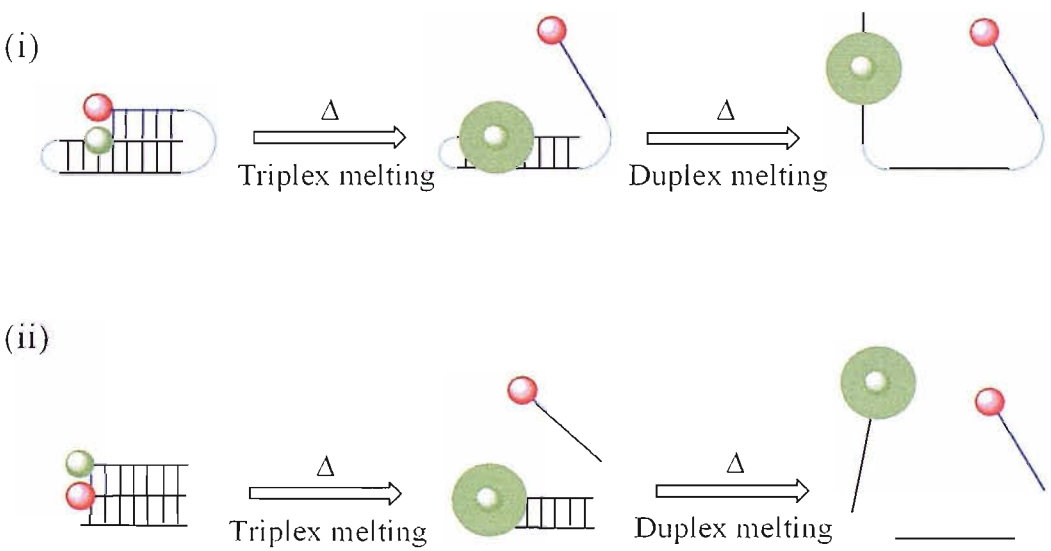

Figure 2.2 Schematic representation for the melting of a fluorescently-labelled intramolecular (i) and intermolecular (ii) triplex. The purine strand is labelled with a fluorophore (e.g. Fluorescein) and is shown in green, whereas the third strand is labelled with a quencher (e.g. methyl red) and is shown in red.

A similar method that measures the change in fluorescence yield of oligonucleotides containing suitably positioned molecular beacons (Antony *et al.*, 2001) and a Roche LightCycler has been developed (Darby *et al.*, 2002). *Intra*molecular triplexes have been studied in this way (Sollogoub *et al.*, 2000, Darby *et al.*, 2002). In this case the central purine strand of the duplex is labelled with a fluorophore (F, fluorescein) and the third strand with a quencher (Q, methyl red). Both are in close proximity upon triplex formation, and the fluorescence is quenched. When the complex is heated the third strand dissociates and a large increase in fluorescence is observed (Figure 2.2). In this way the dissociation of the third strand is observed directly, without interference from dissociation of the duplex. At the start of this project this technique had not been applied to the study of *inter*molecular triplexes.

2.1.3 Circular dichroism

Circular dichroism (CD) is a technique used to measure the conformation of ordered structures in solution. CD measures the differential absorption of right-handed and left-chromophore group. The CD spectra of triplex and duplex DNA are different and therefore this technique can be used to identify the formation of triplexes. These typically show an increased negative band below 220 nm, a characteristic that is associated with A-like DNA conformations (Gray *et al.*, 1978; Gray *et al.*, 1995).

2.2 Materials

2.2.1 Oligonucleotides

All oligonucleotides were synthesised by Prof. Brown (Department of Chemistry, Southampton University) on an Applied Biosystems ABI 394 automated DNA/RNA synthesizer on the 0.2 or 1 μM scale using the standard cycles of acid-catalysed detritylation, coupling, capping and iodine oxidation procedures. The deprotected oligonucleotides were purified by reversed-phase HPLC on a Brownlee Aquapore column (C8) using a gradient of acetonitrile in 0.1M ammonium acetate. Oligonucleotides were diluted in water and stored at –20 °C until required. Phosphoramidite monomers were purchased from Applied Biosystems or Link Technologies. The novel phosphoramidite monomers studied in this thesis were

prepared by Dr Oliver Lack, Dr Yang Wang, Rohan Ranasinghe, James Booth, Vicki Powers or Sadie Osbourne (under the supervision of Prof. Brown).

2.2.2 Chemicals and enzymes

T4 DNA ligase and all restriction enzymes were purchased from Promega (Southampton, UK) and stored at – 20 °C. *Pfu* DNA polymerase and AMV reverse transcriptase were purchased from Sigma-Aldrich (Poole, UK) and stored at – 20 °C. Redivue radioactive [α-^{32}P] ATP was purchased from Amersham Biosciences (Bucks, UK) at a concentration of 3,000 Ci per mmol and stored at 4 °C. Bovine DNase I was purchased from Sigma-Aldrich and stored at a concentration of 7200 U/ml in 150 mM NaCl and 1 mM $MgCl_2$. The napthylquinoline triplex binding ligand was a gift from Dr. L. Strekowski (Dept. of Chemistry, Georgia State University) and was stored at a concentration of 10 mM in dimethylsulphoxide. pUC18 was obtained from New England Biolabs (Herts, UK). The T7 dideoxy sequencing kit was purchased from USB corporation (Cleveland, OH, U.S.A). The QuickChange site-directed mutagenesis kit was purchased from Stratagene. The QIAprep plasmid preparation kit was obtained from Qiagen (Crawley, UK). Both Sequagel (40 % acrylamide;bisacrylamide 19:1 containing 8M urea) and Accugel (20 % acrylamide;bisacrylamide 19:1) were purchased from National Diagnostics (Hull, UK).

2.3 Protocols

2.3.1 Generation of DNA targets

Several DNA sequences were prepared for the footprinting studies presented within this thesis. The *tyr*T(43-59) DNA sequence was originally generated by cloning the 160 bp *tyr*T sequence into *Eco*RI and *Sma*I sites of pUC18 and then mutated so as to introduce a 17-base oligopurine tract between positions 43 and 59 (Brown *et al.*, 1998). Various TFOs and have been targeted to this sequence in the past (Keppler *et al.*, 1999; Sollogoub *et al.*, 2002). Derivatives of this sequence were generated by site-directed mutagenesis for use within this thesis. Several other sequences were also prepared by cloning synthetic oligonucleotides into the *Bam*H1 site of pUC18.

2.3.1.1 Site-directed mutagenesis

Three derivatives of the *tyr*T(43-59) DNA sequence were generated by site-directed mutagenesis using the QuickChange method as shown in Figure 2.4. The primers used are shown in Figure 2.3A. The derivatives TA1, GC1 and CG1 were generated by the mutation of a single AT base pair within the oligopurine tract (highlighted in bold), introducing each base pair in turn. The sequences that were produced are shown in Figure 2.3B.

A

Fragment	Primers
TA1	5′-GTGTTAGGAAGAGAA**T**AAAGAACTGGTTGCG-3′
	5′-CGCAACCAGTTCTTT**A**TTCTCTTCCTAACAC-3′
GC1	5′-GTGTTAGGAAGAGAA**G**AAAGAACTGGTTGCG-3′
	5′-GTGTTAGGAAGAGAA**G**AAAGAACTGGTTGCG-3′
CG1	5′-GTGTTAGGAAGAGAA**C**AAAGAACTGGTTGCG-3′
	5′-CGCAACCAGTTCTTT**G**TTCTCTTCCTAACAC-3′

B

5′-AATTCCGGTTACCTTTAATCCGTTACGGATGAAAATTACGCAACCAGTTCTTTTYTT
3′-----GGCCAATGGAAATTAGGCAATGCCTACTTTTAATGCGTTGGTCAAGAAAZAA

CTCTTCCTAACACTTTACAGCGGCGCGTCATTTGATATGAAGCGCCCCGCTTCC-3′
GAGAAGGATTGTGAAATGTCGCCGCGCAGTAAACTATACTTCGCGGGGCGAAGGGCTC-5′

Figure 2.3 Sequence of the oligonucleotide primers used in site-directed mutagenesis. A) Sequence of primers used for site-directed mutagenesis; B) Sequence of the *tyr*T(43-59) DNA fragment (ZY is AT) used in footprinting studies. TFOs were targeted against different portions of the 17-base oligopurine tract between positions 43-59 (underlined). The derivatives TA1, GC1 and CG1 where generated by introducing each base pair in turn at ZY. Footprinting fragments were generated by digesting each plasmid with *Eco*RI and *Ava*I and then radiolabelled at the 3′ end of the *Eco*RI site.

For the PCR reaction 125 ng of each primer, 1 µl of a 10 µM dNTP mix, 5 µl of 10x buffer and 1 µl of *pfu*DNA polymerase were added to 1 µl of the *tyr*(43-59) DNA template (diluted 1 in 10 from a typical plasmid preparation). The sample was made up to a total volume of 50 µl with dH_20. Samples were cycled in a Pelkin Elmer thermocycler using the following parameters;

Segment 1: Cycle 1: 94 °C for 5 minutes

Segment 2: Cycle 2: 94 °C for 30 seconds, 55 °C for 1 minute, and 68 °C for 3 minutes.

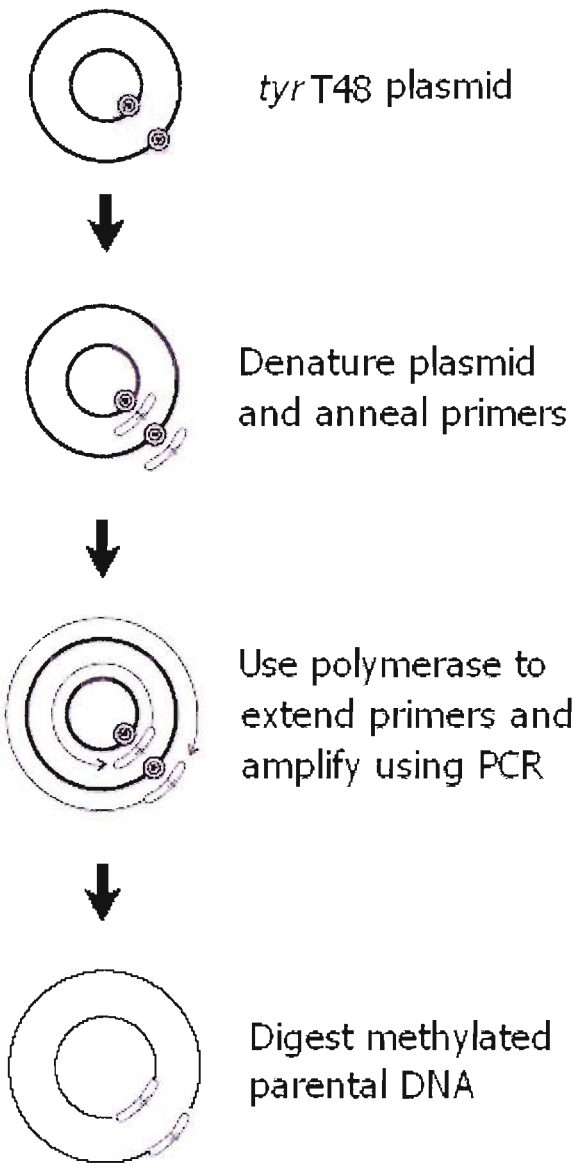

Figure 2.4 Quickchange site-directed mutagenesis. Three derivatives of the *tyr*T(43-59) DNA sequence were generated using this method. Initially, the plasmid was denatured and the oligonucleotides containing the required mutation annealed. *Pfu*Turbo polymerase was then used to extend the primers the length of the plasmid and subsequent rounds of PCR were employed to amplify the mutated sequence. The nonmutated parental DNA was then digested using *Dpn*1. The plasmid DNA was transformed and sequenced.

Segment 2 was cycled 16 times and the samples then cooled to 4 °C. 1 µl of *Dpn* restriction enzyme was then added to each sample to digest the parental DNA. The samples were then briefly spun for 1 minute in a microcentrifuge and left at 37 °C for greater than 4 hours. Plasmids were then transformed, the colonies grown and sequenced (see below).

2.3.1.2 BamHI cloning

Five further DNA sequences were generated by cloning synthetic oligonucleotides into the *Bam*HI site found in the MCS of pUC18. Each duplex insert can be seen in Figure 2.5A. Each of these contained a 19-base oligopurine tract interrupted by several pyrimidine bases. The sequences generated are shown in Figure 2.5B.

A

Fragment	Inserts
Con	5′-GATCAGACATAAGAGCATGAGAA-3′ 3′-TCTGTATTCTCGTACTCTTCTAG-5′
S.AT	5′-GATCAGACA**A**AAGAGCATGAGAA-3′ 3′-TCTGT**T**TTCTCGTACTCTTCTAG-5′
BAU.TA	5′-GATCAGACAT**T**AGAGCATGAGAA- 3′-TCTGTA**A**TCTCGTACTCTTCTAG-5′
^{Me}P.TA	5′-GATCAGACATAA**T**AGCATGAGAA-3′ 3′-TCTGTATT**A**TCGTACTCTTCTAG-5′
PP^{A}.TA	5′-GATCAGACATAAGAG**T**ATGAGAA-3′ 3′-TCTGTATTCTC**A**TACTCTTCTAG-5′

B

```
5′-AGCTTGCATGCCTGCAGGTCGACTCTAGAGGATCTTCTCAT8CT6T42TGTCTGAT
3′-----ACGTACGGACGTCCAGGTGAGATCTCCTAGAAGAGTA7GA5A31ACAGACTA

CCCCGGGTACCAGCTCG----3′
GGGCCCATGGTCGAGCTTAA-5′
```

Figure 2.5 Sequence of the oligonucleotide primers used in *Bam*H1 cloning. A) Sequence of the inserts used for *Bam*H1 cloning into pUC18; B) Sequence of the DNA fragment used in footprinting studies. TFOs were targeted against the 19-base oligopurine tract (underlined). The five fragments differ by single bp changes at different positions (1.2, 3.4, 5.6 and 7.8). The fragments were generated by digesting each plasmid with *Eco*RI and *Hind*III and then radiolabelled at the 3′ end of the *Eco*RI site.

50 µM of each duplex strand was mixed and annealed to its complementary duplex strand, heated to 95 °C and slowly cooled to 4 °C. 10 µl of each of each duplex insert, 2

µl DNA ligase, 2 µl multicore buffer and 4 µl of dH_2O were added to 2 µl alkaline phosphatase-treated pUC18 and left at room temperature for greater than three hours. The samples were then transformed and grown overnight on blue-white selection plates (200 ml agar, 20 mg carbenicillin, 1ml of 100 mM IPTG and 1 ml of 2% X-Gal). White colonies were picked and sequenced (see below).

2.3.2 Preparation of competent cells

E.coli TG2 cells were grown overnight at 37 °C in 2YT media (16 g tryptone, 10 g yeast extract, 5 g NaCl per litre). 500 µl of these cells were then transferred to 50 ml of media and allowed to grow till the suspension reached an O.D of 0.6-0.8 as measured at 600 nm. The cells were then pelleted by centrifugation at 5,000 rpm for 5 minutes at 4 °C. After removal of the supernatant the pellet was resuspended in transformation buffer (50 mM $CaCl_2$, 10 mM Tris-HCl pH 7.0.4) and placed on ice for 30 minutes. This suspension was again centrifuged as above and the supernatant discarded. The pellet was resuspended in 3 ml of the transformation buffer and stored at 4 °C ready for the transformation procedure.

2.3.3 Transformation

200 µl of competent cells were added to either 20 µl of ligated construct (cloning), or 20 µl of the mutated plasmid (mutagenesis). The mixture was placed on ice for 30 minutes, heatshocked at 45 °C for 1 minute and placed immediately back on ice. The transformed cells were plated on agar plates containing 100 µg/ml carbenicillin (mutagenesis) or 100 µg/ml carbenicillin, 0.5 mM IPTG, and 0.5 mM X-Gal (cloning) and left to grow overnight at 37 °C. Plates were stored at 4 °C until required.

2.3.4 Plasmid purification

Colonies were picked and grown overnight in 5 ml of 2YT media containing 100 µg/ml carbenicillin. Each culture was split between two 1.5 ml Eppendorf tubes and centrifuged at 7,000 rpm for 5 mins and the supernatant discarded. The plasmids were then purified using a Qiagen QIAprep kit. This involved resuspending the cells in 250 µl of buffer P1 (Qiagen), cells lysis by the addition of 250 µl buffer P2 (Qiagen) and

neutralization by the addition of 350 µl of buffer P3 (Qiagen). The solution was then centrifuged for 10 minutes at 13,000 rpm and the supernatant transferred to a QIAprep spin column. Three separate centrifugation steps were then applied, discarding the flow through each time. After the first and second the plasmid was washed with 0.5 ml of buffer PB (Qiagen) and 0.75 ml of buffer PE (Qiagen) respectively. After the third the column was placed in a 1.5 ml Eppendorf tube and 50 µl of buffer EB (Qiagen) was added. A final centrifugation step eluted the plasmid in the flow through, this was stored stored at – 20 °C until required.

2.3.5 Dideoxy sequencing

Plasmids were then sequenced using a T7 dideoxy sequencing kit (USB Corporation). 40 µl of plasmid obtained as above was denatured by the addition of 10 µl NaOH and left at room temperature for at least 10 minutes. The DNA was precipitated by the addition of 15 µl 3M sodium acetate and 300 µl ethanol, leaving the sample in dry ice for at least 10 minutes. The DNA was then centrifuged at 13,000 rpm for 10 minutes, the pellet washed in 70 % ethanol and dried in a SpeedVac. The pellet was then resuspended in 10 µl dH_20 and 2 µl of both annealing buffer (kit) and universal primer added. This sample was incubated at 37 °C for 20 minutes and then a further 10 minutes at room temperature. For each template, a polymerase mix consisting of 3 µl Label Mix A (kit), 1.5 µl dH_20, 0.5 µl α-^{32}P dATP and 2 µl of polymerase (1:4 ratio with polymerase dilution buffer) was made and kept on ice until required. 6 µl of this solution was added to the template and left for 5 minutes at room temperature. During this period tubes containing 2.5 µl of one of the 4 dideoxy mixes were incubated at 37 °C. 4.5 µl of the reaction mixture was added to each of these samples and left for 5 minutes at 37 °C. The reaction was then stopped by addition of 5 µl of the DNase STOP solution (kit). The samples were run on a 10 % (w/v) denaturing polyacrylamide gel at 1500 V for about 2 hrs and fixed in 10% (v/v) acetic acid. These were transferred to Whatman 3MM paper and dried under vacuum at 86 °C for 1 hour. The dried gels were subjected to phosphorimaging using a Molecular Dynamics Storm phosphorimager.

Plasmids containing the correctly cloned or mutated sequence were then transformed and plated (as above). These were used as stock plates for each plasmid and a streak of

colonies was grown when required for labelling and footprinting studies (see below). Plates were kept at 4 °C and could be used for up to one month.

2.3.6 DNA radiolabelling

10 µl of MultiCore buffer was added to 40 µl of purified plasmid containing either *Tyr*T(43-59), TA1, GC1 or CG1 fragments. 1.5 µl (20 units) of the restriction enzymes *Ava*I and *Eco*RI were then added and left to incubate at 37 °C for greater than 1 hour. After this time the fragments were 3´-end labelled using 1 µl of [α-^{32}P]dATP and 0.5 µl of AMV reverse transcriptase and left for a further 1 hour. A similar protocol was employed for labelling of the *Bam*HI cloned fragments but as their generation requires cutting with *Hind*III and *Eco*RI which both leave 3´ overhangs it was modified. In these cases, *Eco*RI was added first and the fragment labelled as above. Reverse transcriptase was then deactivated by heating the sample to 65 °C for 10 minutes and the fragment was then cut with *Hind*III.

All fragments were separated from the remainder of the plasmids on an 8 % non-denaturing polyacrylamide gel (40 cm by 0.3 mm) at 800 V for about 2.5 hrs. The wet gel was then exposed to X-ray film for 2.5 minutes and the band corresponding to the labelled fragment excised. The DNA was eluted by the addition of 300 µl of pH 7.5 10 mM Tris-HCl containing 10 mM EDTA, at 37 °C overnight. The DNA was precipitated by the addition of 40 µl 3M NaOAc and 600 µl ethanol, leaving the sample on dry ice for at least 10 minutes. The DNA was then centrifuged at 13,000 rpm for 10 minutes, the pellet washed in 70 % ethanol and dried in a SpeedVac. The pellet was redissolved in pH 7.5 10 mM Tris containing 0.1 mM EDTA to yield approximately 10 cps/µl as estimated using a hand held Geiger counter.

2.3.7 DNase I footprinting experiments

2.3.7.1 Footprinting incubations

1.5 µl of radiolabelled DNA was mixed with 3 µl of appropriately diluted oligonucleotide and left to equilibrate at 20 °C overnight. Experiments at pH 5.0 were performed in 50 mM sodium acetate, at pH 6.0 in 10 mM PIPES containing 50 mM

NaCl and at pH 7.0 and 7.5 in 10 mM Tris-HCl containing 50 mM NaCl. If binding was not evident $MgCl_2$ was also included in the buffer at various concentrations. The final oligonucleotide concentrations varied between 1 nM and 30 μM depending on the triplex study. A control for each experiment was also included, consisting of radiolabelled DNA and buffer.

2.3.7.2 DNase I digestion

DNase I digestion was carried out under limiting conditions by adding 2 μl of DNase I (typically 0.01 units/ml) dissolved in 20 mM NaCl containing 2 mM $MgCl_2$ and 2 mM $MnCl_2$. As the activity of this enzyme varies with temperature, pH, DNA concentration and ionic strength the exact concentration varied depending on the reaction conditions. The reaction was stopped after 1 min by adding 4 μl DNase I STOP solution (80% formamide, 10 mM EDTA, 10 mM NaOH, and 0.1% (w/v) bromophenol blue).

2.3.7.3 GA marker

A GA marker specific for purines was also prepared for each gel. This was prepared by mixing 1.5 μl radiolabelled DNA, 5 μl DNase STOP and 25 μl dH_2O and boiled for 1 hour with the cap open before rapidly cooling on ice and loading onto the gel.

2.3.7.4 Denaturing polyacrylamide gel electrophoresis

The products of digestion were separated on either 9% or 12% polyacrylamide gels containing 8M urea. Samples were heated to 100 °C for 3 min, before rapidly cooling on ice and loading onto the gel. Polyacrylamide gels (40 cm long, 0.3 mm thick) were run at 1500 V for about 2 hrs and then fixed in 10% (v/v) acetic acid. These were transferred to Whatman 3MM paper and dried under vacuum at 86 °C for 1 hour. The dried gels were subjected to phosphorimaging using a Molecular Dynamics Storm 860 phosphorimager.

2.3.7.5 Footprint quantification

The intensity of bands within each footprint was estimated using ImageQuant software. These intensities were then normalised relative to a band in the digest which is not part

of the triplex target site, and which was not affected by addition of the oligonucleotides. Footprinting plots (Dabrowiak & Goodisman, 1989) were constructed from these data by plotting the oligonucleotide concentration against relative intensity of bands within footprint. C_{50} values, indicating the TFO concentration that reduces the band intensity by 50 %, were calculated using Sigmaplot for windows by plotting equation 1.

Equation 1 $I/I_0 = C_{50}/(L + C_{50})$

Where I and I_0 are the relative intensity in presence and absence of an oligonucleotide, L is the oligonucleotide concentration and C_{50} is the TFO concentration that reduces the band intensity by 50 %.

This analysis relies on several important assumptions. Firstly, the cleavage reaction should be carried out under conditions that leave about 80 % of the DNA target undigested ('single hit kinetics'). Secondly, cleavage should be relatively independent of the sequence undergoing digestion. Thirdly, the concentration of duplex target should be lower than the concentration of TFO. This assures that the amount of oligonucleotide bound to its target duplex is dependent on its dissociation constant and is not limited by the stoichiometric amount of oligonucleotide to duplex. The amount of duplex DNA has been estimated to be about 1 nM in these studies and in most cases this is much lower than the TFO concentration employed. Under these conditions, the C_{50} value approximates to the dissociation constant, K_d.

2.3.8 Spectroscopic studies

2.3.8.1 UV melting studies

UV melting experiments on the intermolecular triplexes were carried out using a Varian Cary 400 Scan UV-Visible spectrophotometer. Absorbance was determined in Hellma® SUPRASIL synthetic quartz cuvettes with a 10 mm pathlength, monitoring at 260 nm. The oligonucleotides were prepared in 10 mM sodium phosphate pH 5.8 containing 200 mM NaCl and 1 mM EDTA. Samples were filtered into the cuvettes with Kinesis regenerated cellulose 13 mm, 0.45 μM syringe filters. Melting experiments were carried out in a total volume of 1.5 ml and contained 1 μM duplex and varying concentrations of TFO. The complexes were first denatured by heating to 95 °C at a rate of 10 °C min^{-1}

and left to equilibrate for 10 minutes. The complexes were then cooled to 30 °C at a rate of 0.1 °C min^{-1} and left to equilibrate for a further 5 minutes before heating to a temperature higher than the triplex melting temperature. Recordings were taken during both the heating and cooling steps to check for hysteresis. T_m values were determined from the first derivatives of the melting profiles using the software provided with the machine and usually differed by less than 1 °C.

2.3.8.2 Fluorescence melting studies

Fluorescence melting experiments on intermolecular triplexes were carried out using a Roche LightCycler. In these experiments each TFO is labelled at the 5′-end with a suitable quencher while the 5′-end of the purine strand of the duplex is labelled with a suitable fluorophore. The triplexes were prepared in either 50 mM sodium acetate buffer (pH 5.0, 5.5 or 6.0) or 50 mM sodium phosphate (pH 6.5, 7.0 or 7.5) containing 200 mM sodium chloride. Melting experiments were carried out in a total volume of 20 µl and contained 0.25 µM duplex and concentrations varying between 0.25 and 12 µM of TFO. The complexes were first denatured by rapidly heating to 95 °C and left to equilibrate for 10 minutes. The complexes were then cooled to between 22 and 30 °C at a suitably slow rate to eliminate hysteresis, generally 0.2 °C min^{-1}. After 5 minutes the complexes were heated to a temperature sufficiently higher than the triplex melting temperature at the same temperature gradient. Although the slowest rate of continuous temperature change in the LightCycler is 0.1 °C sec^{-1}, slower melting profiles were obtained by increasing the temperature in 1 °C steps, leaving the samples to equilibrate for a suitable amount of time. Recordings were taken during both the heating and cooling steps to check for hysteresis. T_m values were determined from the first derivatives of the melting profiles using the software provided with the machine and usually differed by less than 0.5 °C.

2.3.8.3 Circular dichroism

Circular dichroism on intermolecular triplexes was carried out using a JASCO J-710 spectropolarimeter. Spectra were collected between 320–210 nm, at 100 nm/min, 1 s response time, 1 nm bandwidth in Hellma® synthetic quartz cuvettes with a 5 mm pathlength. The oligonucleotides were prepared in 50 mM sodium acetate pH 6.0

containing 200 mM NaCl. Melting experiments were carried out in a total volume of 1.5 ml and contained 5 μM duplex and 5 μM TFO. The samples were filtered into the cuvettes using 0.2 μM syringe filters. The complexes were first denatured by heating to 95 °C and were slowly cooled to 4 °C. Recordings were taken at 25 °C and each spectrum was accumulated sixteen times, smoothed and the spectrum of the buffer was subtracted.

3 THE STABILITY OF *INTER*MOLECULAR TRIPLEX FORMATION AS DETERMINED BY FLUORESCENCE MELTING

3.1 Introduction

A novel approach for measuring the melting profiles of higher order nucleic structures using molecular beacons and a Roche Lightcycler has recently been developed and applied to the study of *intra*molecular triplexes (Darby *et al.*, 2002; Sollogoub *et al.*, 2002). In these experiments the central purine strand of a duplex is labelled with a fluorophore (F, fluorescein) and the third strand with a quencher (Q, methyl red). These are in close proximity upon triplex formation, and the fluorescence is quenched. When the complex is heated the third strand dissociates and a large increase in fluorescence is observed (Figure 2.2). In this manner, the dissociation of the third strand is observed directly, without interference from dissociation of the duplex. This technique should be especially useful for separating the melting transitions of triplexes that are as stable or more stable than their underlying duplexes, such as those containing modified nucleosides.

At the start of this work this approach had not been applied to the study of *inter*molecular triplexes. The difference in molecularity between *intra-* and *inter*molecular triplexes profoundly affects the experimental parameters required to accurately measure their melting profiles. For example, the formation of an *inter*molecular triplex is at least a bimolecular reaction (between the duplex and the third strand) dependent on the concentration of reactants, with several studies suggesting slow rates of formation (Craig *et al.*, 1971; Pörschke & Eigen, 1971; Rougée *et al.*, 1992; Alberti *et al.*, 2002). In contrast, *intra*molecular triplex formation is unimolecular and is therefore independent of reactant concentration and is expected to be much faster. It is also less susceptible to the formation of competing secondary structures, due to the structural constraints imposed by the loops positioned between each of the strands.

This chapter assesses the validity of this approach for measuring the stability of several unmodified *inter*molecular triplexes that are used for reference in later chapters. Several experimental parameters are assessed, such as the rate of temperature change and the choice of the reporter groups used. In addition, several factors that affect triplex

A

	5′-Q-TCTCTCTT**A**TCCTCCTCC
	5′-Q-TCTCTCTT**G**TCCTCCTCC
	5′-Q-TCTCTCTT**C**TCCTCCTCC
	5′-Q-TCTCTCTT**T**TCCTCCTCC
$TFO-T_{15}$	5′-Q-TCTCTCTT**T**TCCTCC
$TFO-T_{12}$	5′-Q-TCTCTCTT**T**T
Duplex	5′-F-AGAGAGAA**Z**AGGAGGAGG
	3′-TCTCTCTT**Y**TCCTCCTCC

B

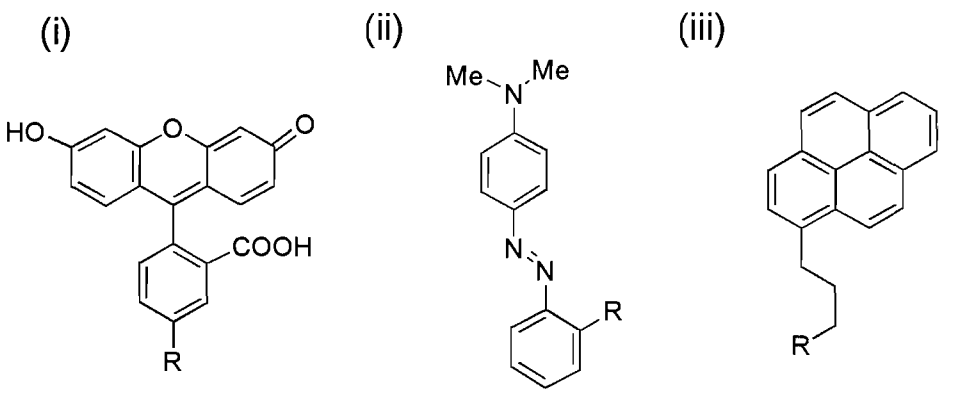

C

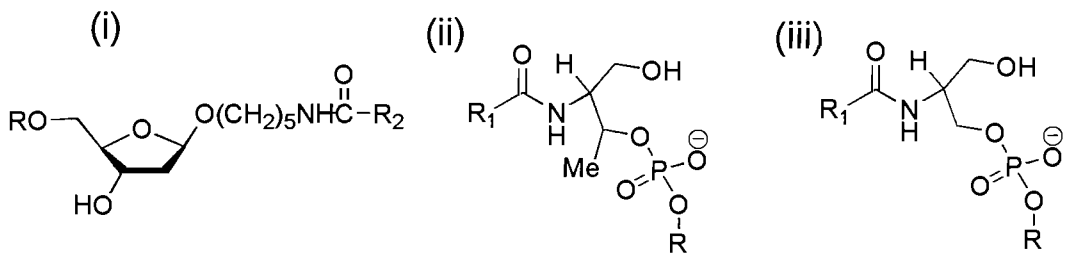

Figure 3.1 Oligonucleotides and molecular beacons used in fluorescence melting experiments. A) The duplexes are labelled with fluorescein (F) at the 5′-end of the purine strand and with methyl red serinol, methyl red threoninol or pyrene butyryl threoninol (Q) at the 5′-end of the TFO. For the single substitution studies; ZY is each base pair in turn (AT, TA, GC, CG) and X is A, G, C or T; B) Chemical structures of the fluorophores and quenchers used in this study; (i) fluorescein, (ii) methyl red, (iii) pyrene; C) These reporter groups were attached to the oligonucleotide directly to deoxyribose (i) or via a threoninol (i) or serinol (ii) linker.

Stability are examined, such as mismatches between the third strand and the duplex, the length of triplex and the effect of ionic and pH conditions.

3.2 Experimental design

The sequences of the oligonucleotides used in the fluorescence melting experiments are shown in Figure 3.1A. These were designed to generate 18mer parallel triplexes, asymmetric in nature, containing a single variable central triplet flanked on either side by T.AT triplets. The purine-containing strand of the duplex was labelled at the 5′end with fluorescein (F; Figure 3.1B(i)), whilst the third strand was labelled at the 5′ end with either methyl red or pyrene (Q; Figure 3.1B(ii) and (iii)). The quencher was placed on the third strand, so that it could be added in molar excess without increasing the fluorescence signal. Methyl red was attached to the TFO via either deoxyribose (Figure 3.1C(i)), a threoninol linker (Figure 3.1C(iii)) or a serinol linker (Figure 3.1C(ii)). Pyrene was attached via a threoninol linker. The excitation source used by the LightCyler is 488 nm and in this study the change in fluorescence emission was measured at 520 nm.

3.3 Results

Initially the melting profiles for parallel triplexes composed of standard T.AT and C^+.GC triplets were determined using different experimental parameters. Two 18mer triplexes that differed by a single central T.AT or C^+.GC triplet were studied (i.e. ZY is AT or GC). These were generated using the oligonucleotides shown in Figure 3.1A. Each assay was performed in a total volume of 20 µl and contained 0.25 µM duplex and 3µM third strand. This excess of third strand was used to facilitate triplex formation. All oligonucleotides were dissolved in 50 mM sodium acetate containing 200 mM sodium chloride at pH 5.5. Each reaction was performed in triplicate, and the T_m values usually differed by less than 0.5 °C.

3.3.1 Rate of temperature change

The slowest rate of continuous temperature change that can be performed by the LightCycler is 6 °C min^{-1} (0.1 °C sec^{-1}). Representative melting and annealing profiles for the triplexes obtained at this rate are shown in Figure 3.2 (top graphs).

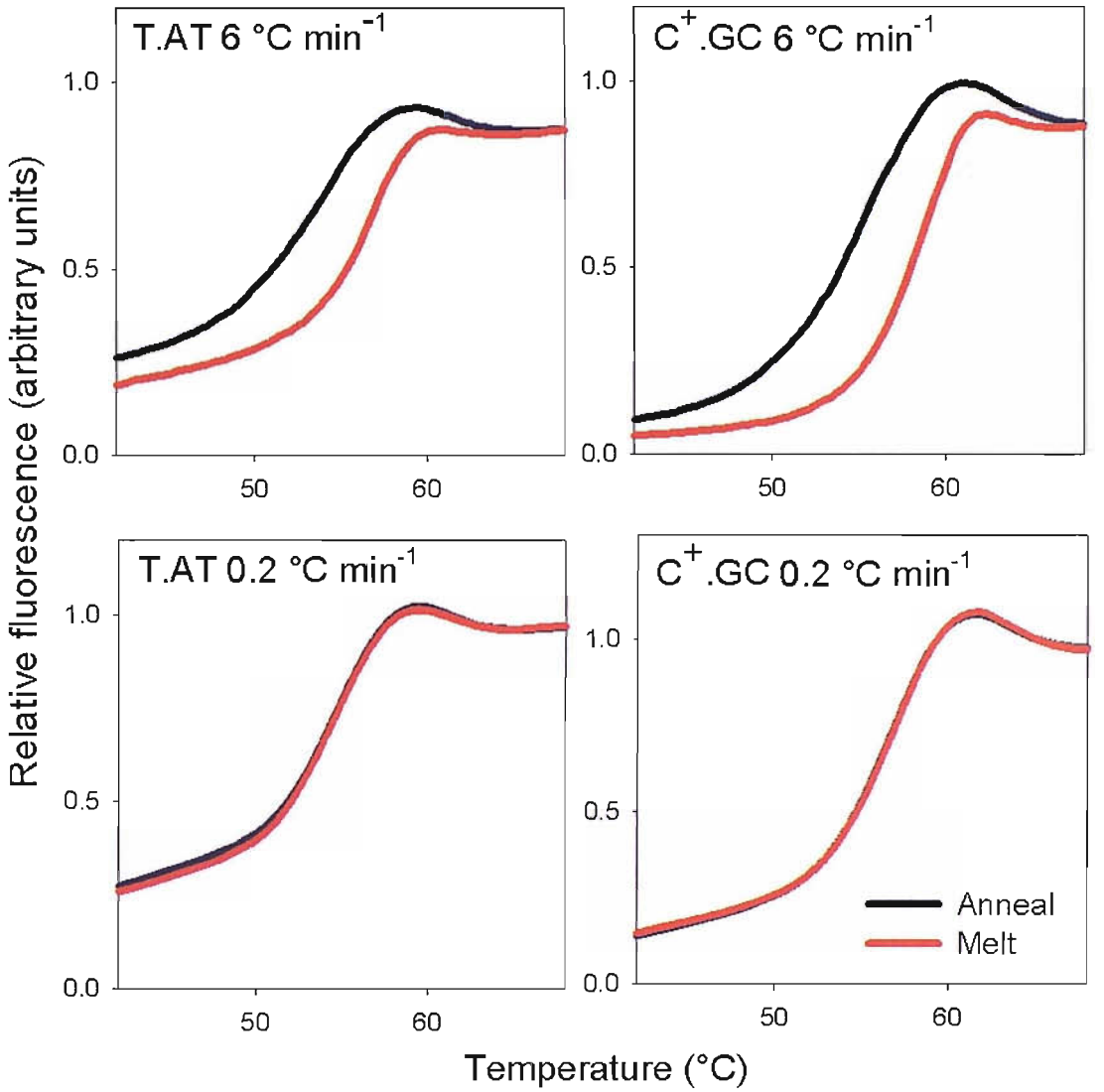

Figure 3.2 Representative fluorescence melting and annealing profiles for *inter*molecular parallel triplexes. Each triplex differs by a single central triplet (X.ZY). These were generated using a temperature gradient of 6 °C min^{-1} (top graphs) and 0.2 °C min^{-1} (lower graphs). The experiments were performed in 50 mM sodium acetate, pH 5.5 containing 200 mM NaCl. The y-axes show the normalised fluorescence (arbitrary units), while the x-axis shows the temperature (°C).

It can be seen that these profiles exhibit hysteresis (i.e. the melting and annealing curves are not superimposable). Melting temperatures (T_m) calculated from the heating profiles are overestimated, whilst T_ms calculated from the cooling profiles are underestimated. For example, the T_m values calculated from the heating and annealing profiles for the C^+.GC-containing triplex were 58.8 and 55.7 °C respectively, a difference of about 3 °C. This suggests that the rate of temperature change is too fast for this reaction. A slower rate was employed by programming the LightCycler to increase the temperature in small steps (1 °C), taking readings after a set equilibration time at each temperature. Representative melting and annealing profiles obtained at a rate of 0.2 °C min^{-1} are shown in Figure 3.2 (bottom graphs). Under these conditions the hysteresis is eliminated and the curves appear to be at thermodynamic equilibrium. The T_ms calculated from the first derivatives of these profiles were 54.3 and 56.6 °C for the T.AT and C^+.GC-containing triplexes respectively. These T_ms are approximately mid-way between the melting and annealing values obtained at the faster rate of temperature change (6 °C min^{-1}). Unless otherwise stated, this temperature gradient is used throughout the rest of this chapter. Factors affecting the extent of hysteresis are considered later in the chapter.

3.3.2 Triplex melting profiles

Further examination of these melting and annealing profiles reveals a secondary transition at high temperatures, seen as a small decrease in fluorescence. This was previously observed in the case of *intra*molecular triplex formation and postulated to be a result of melting of the underlying duplex (Darby *et al.*, 2002). To test this theory each duplex was melted and annealed in the absence of third strand. Melting profiles for these can be seen in Figure 3.3. The decrease in fluorescence is still evident in the absence of TFO, suggesting this is indeed a property of the underlying duplex. T_ms calculated from these transitions are 59 °C and 62 °C for the AT and GC-containing duplexes respectively. These values are the same as those estimated from the first derivatives of the transitions reported above. The difference in T_m between the two duplexes is expected, on account of the greater stability of the GC-containing duplex.

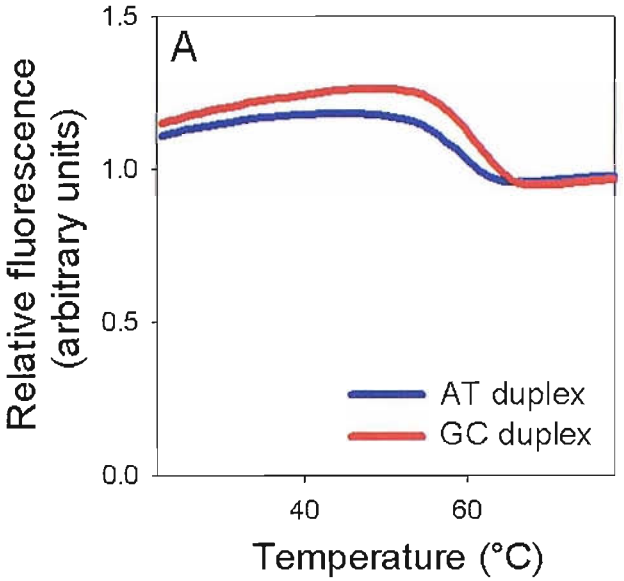

Figure 3.3 Representative fluorescence melting profiles for the interaction of the duplex oligonucleotides in the absence of third strand. The experiments were performed in 50 mM sodium acetate, pH 6.0 containing 200 mM NaCl.

3.3.3 Concentration dependence

Since intermolecular triplex formation is a bimolecular reaction an increase in the concentration of third strand should favour the association reaction, which should translate into an increase in T_m (Mergny & Lacroix, 2003). This concentration dependence was studied by adding various concentrations of the third strand (note that this cannot affect the total fluorescence signal as the quencher is located on the third strand). Figure 3.4 shows representative fluorescence melting profiles for the triplex containing the central T.AT triplet. This experiment was carried out in 50 mM sodium acetate pH 5.8 containing 200 mM sodium chloride. The third strand concentration was varied between 0.25 μM and 10 μM whereas the duplex concentration remained constant at 0.25 μM. The T_ms determined were 41.3, 42.7, 44.8, 45.6 and 47.3 °C for third strand concentrations of 0.25, 1, 3, 5 and 10 μM respectively. As expected this reveals that an increase in the concentration of third strand leads to an increase in the thermal stability of the triplex; a 40-fold increase in concentration translates to an increase in T_m of about 6 °C.

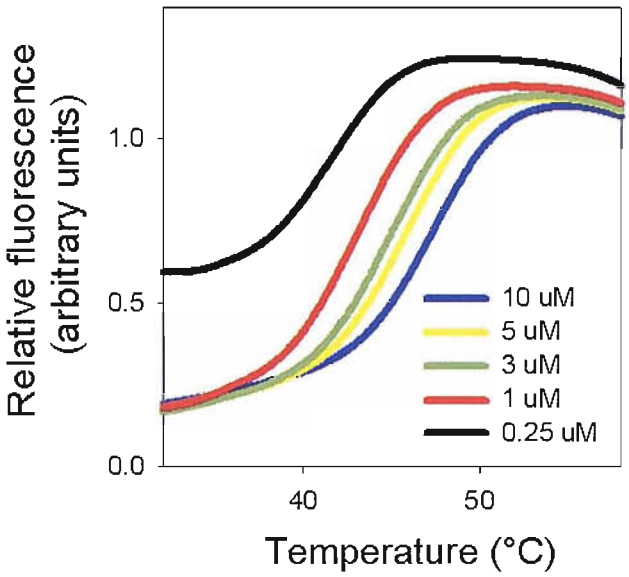

Figure 3.4 Representative fluorescence melting profiles for the interaction of different concentrations of the T-containing TFO with the AT-duplex target. The experiments were performed in 50 mM sodium acetate, pH 5.8 containing 200 mM NaCl.

Further examination of the melting profile for the triplex generated in the presence of 0.25 μM TFO reveals an initial relative fluorescence that is much higher than that seen with higher third strand concentrations. This is presumably because this concentration is below the K_d for complex formation so that a significant amount of free duplex is present, even at a temperature well below the T_m.

The concentration dependency of the T_m can be used to determine the enthalpy for the formation of this triplex by plotting $1/T_m$ against In[NA], where NA is the total nucleic acid concentration (duplex plus third strand) and the slope of the graph is equal to $R/\Delta H$. An example of this kind of plot is shown in Figure 3.5. Although this plot produces a straight line, it should be noted that this analysis assumes that the enthalpy (ΔH) is independent of temperature ($\Delta C_p = 0$). From the graph a ΔH value of -438 KJ Mol^{-1} was determined for the formation of this triplex. This value is similar to those previous reported for parallel triplexes of a similar size (Roberts and Crothers, 1996, Marky *et al.*, 2002; James *et al.*, 2003).

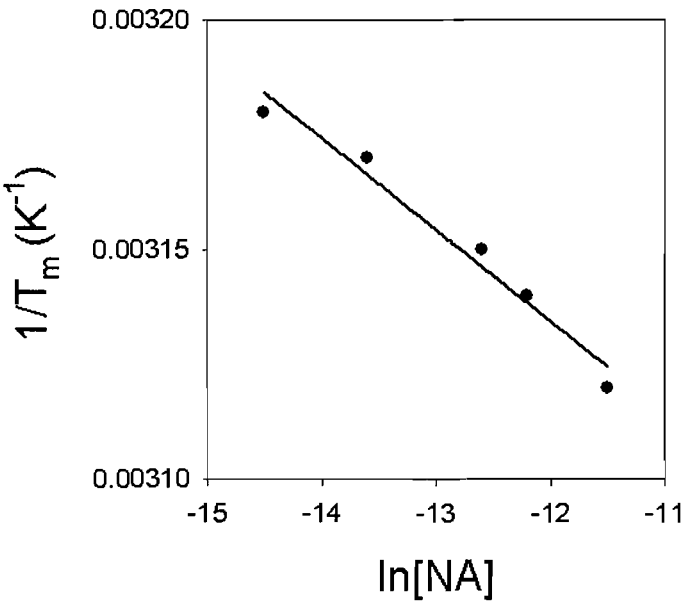

Figure 3.5. Van't Hoff plot showing the concentration dependency of the T_m for the T.AT-containing triplex. The experiments were performed in 50 mM sodium acetate, pH 5.8 containing 200 mM NaCl.

3.3.4 Effect of the quencher moieties

It is possible that triplex stability is influenced by the presence of the terminal fluorescent or quencher moieties (Moreira *et al.*, 2005). To test this, the stabilities of triplexes labelled with either methyl red or pyrene quenchers were determined. Methyl red was attached to the TFO either directly to deoxyribose, or via a serinol or threoninol linker. Pyrene was attached via a threoninol linker. The structures of these groups are shown in Figure 3.1B and C. Representative melting profiles for the interaction of TFOs containing each of these quenchers with their intended duplex target at pH 6.0 are shown in Figure 3.6. The T_ms obtained for these were 59.7, 54.3, 54.8 and 57.9 °C for the triplexes containing methyl red deoxyribose, methyl threoninol red, methyl red serinol or pyrene, respectively. These data show that triplex stability is, as expected, affected by the choice of quencher. The order of stabilisation was methyl red deoxyribose > pyrene > methyl red linker. The presence of a linker attaching methyl red to the oligonucleotide only moderately affected stability; a difference in T_m of less than 1 °C between serinol and threoninol linkers is observed. The effect of each quencher on the specificity of triplex formation is considered later in the chapter, however, it is clear that any comparison between different triplexes must use oligonucleotides that bear the same reporter group.

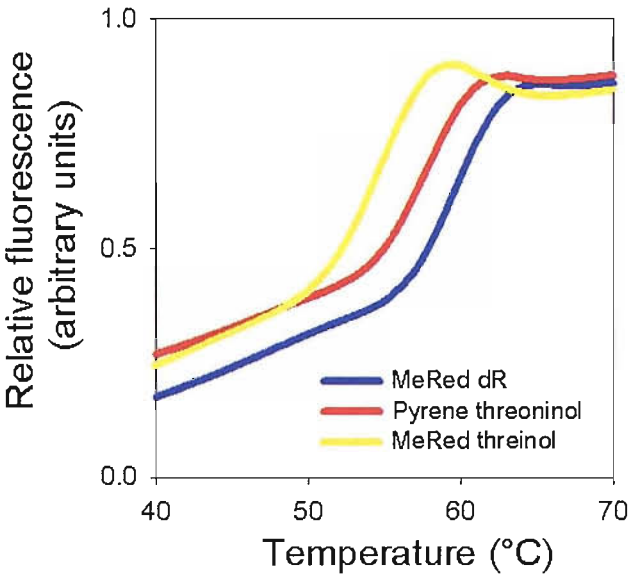

Figure 3.6 Representative fluorescence melting profiles showing the interaction of TFOs labelled with different quenchers with their intended duplex target. The experiments were performed in 50 mM sodium acetate, pH 5.5 containing 200 mM NaCl.

3.3.5 Fluorescence yield

Both the fluorescence yield of fluorescein and triplex stability is pH dependent. Figure 3.7 shows fluorescence melting profiles for the C^+.GC-containing triplex at different pH values, these curves were not normalised. It can be seen that at low pH the fluorescence yield was much less than at higher pH; about 6-fold lower at pH 5.0 relative to pH 6.0. However, this was still sufficient to allow the determination of accurate profiles. T_ms of 67.4 and 63.8 °C were determined at pH 5.0 for the C^+.GC and T.AT-containing triplexes, compared to 41.1 and 39.4 °C at pH 6.0. The difference in stability of the two triplexes is therefore greatest at lower pH and can be attributed to the pH dependency of the C^+.GC triplet. It was not possible to determine melting temperatures for the complexes at pH values greater than 6.0 as these were too low to measure accurately (The LightCycler can typically determine T_ms that are greater than 28 °C as it cannot cool below ambient temperature).

Interestingly, examination of the melting profile at pH 5.0 (blue line) reveals a small secondary transition at low temperatures, typically involving about a 10 % change in fluorescence relative to the full triplex melt. This can also be seen in the right hand

graph of Figure 3.7 (blue line), which is normalised. Several experiments were undertaken to account for this transition. Melting of the duplex, as above, did not show any transition at low temperatures, nor did melting of the fluorescein-labelled purine strand in the absence of its duplex complement (Figure 3.7; right hand graph; red line). However, melting of the fluorescein-labelled purine strand in the presence of 3 μM TFO (i.e. the triplex minus the duplex pyrimidine strand) did show an additional transition at pH 5.0 (Figure 3.7; yellow line). A comparison of the profiles obtained for the TFO and purine strand (yellow line) and the triplex (blue line) shows that both exhibit a transition at similar temperatures, with a T_m value of about 48 °C. It is therefore likely that the transition is due to the presence of a small amount of Hoogsteen duplex DNA formed between the third strand and duplex purine strand. It should be noted that this was only evident at pH 5.0 and the position of the transition varied depending on the nature of the triplex.

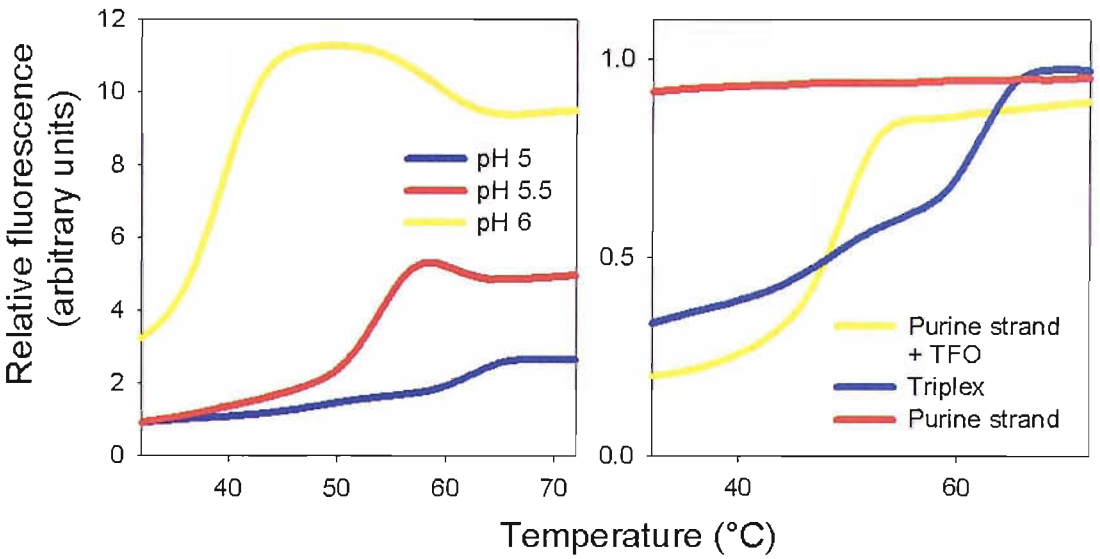

Figure 3.7 Representative fluorescence melting profiles showing the interaction of differerent oligonucleotides. A) Profiles determined for the C^+.GC-containing triplex at different pH values. B) Profiles determined for different combinations of the three strands. The experiments were performed in 50 mM sodium acetate, pH 5.5 containing 200 mM NaCl.

3.3.6 Factors affecting triplex stability

Several factors affecting triplex stability and selectivity, such as TFO length, base composition and pH were examined using this thermal melting technique.

3.3.6.1 Effect of mismatches in the third strand

In these experiments, TFOs containing each base in turn at the central position (X) were targeted against four duplexes that contained each of the four base pairs (ZY) at an equivalent position, generating triplexes that contained each possible X.ZY triplet. The sequences of the oligonucleotides used are shown in Figure 3.1A. Representative fluorescence melting curves for the 16 possible triplexes at pH 6.0 are shown in Figure 3.8. Each graph compares in turn the affinity of each base for each of the possible base pairs. The melting temperatures calculated from each of these, and from equivalent experiments performed at pH 5.0 and 5.5 are shown in Table 3.1. These experiments were undertaken in 50 mM sodium acetate buffer containing 200 mM sodium chloride. Each TFO was labelled with methyl red threoninol at the 3´-end.

		ZY			
X	pH	AT	TA	GC	CG
A	5.0	57.1 (57.5)	54.4 (54.6)	61.1 (61.4)	54.9 (55.2)
	5.5	43.7 (43.8)	39.6 (39.8)	47.3 (47.5)	39.5 (39.8)
	6.0	28.2 (28.1)	< 28.0	30.0 (30.1)	< 28.0
G	5.0	54.2 (54.5)	58.7 (46.7)	57.3 (57.3)	56.3 (56.4)
	5.5	38.2 (38.4)	46.7 (46.8)	43.1 (43.4)	41.2 (41.5)
	6.0	< 28.0	30.6 (30.7)	28.0 (27.9)	< 28.0
C	5.0	54.9 (55.3)	53.2 (53.4)	67.1 (65.3)	58.2 (57.6)
	5.5	39.1 (39.2)	38.0 (38.2)	56.2 (56.3)	42.5 (42.7)
	6.0	< 28.0	< 28.0	40.5 (40.6)	28.4 (28.2)
T	5.0	63.8 (62.5)	52.7 (53.1)	56.8 (57.3)	57.4 (57.5)
	5.5	54.0 (54.0)	38.1 (38.3)	42.9 (43.0)	43.3 (43.4)
	6.0	39.4 (39.4)	< 28.0	27.7 (27.7)	28.3 (28.3)

Table 3.1 T_m values determined by fluorescence melting for triplexes composed of different triplet combinations using a temperature gradient of 0.2 °C min^{-1} and the quencher methyl red threoninol. Values in parenthesis were calculated from the annealing phase. Each value is an average of three separate determinations which usually differed by less than 0.5 °C.

Examination of Table 3.1 reveals that the most stable triplets with natural bases in the third strand are formed with T against AT, C against GC, G against TA and A against GC. The T_m values of these complexes vary between 67.1 °C and 61.3 °C at pH 5.0 showing that C^+.GC is more stable than T.AT and that the triplets involving GC or TA base pairs (A.GC and G.TA) were less stable. Other triplets identified with an intermediate affinity were T.CG, C.CG, T.GC, G.GC and A.AT. The difference in affinity between triplets was more pronounced as the pH increased, with the exception

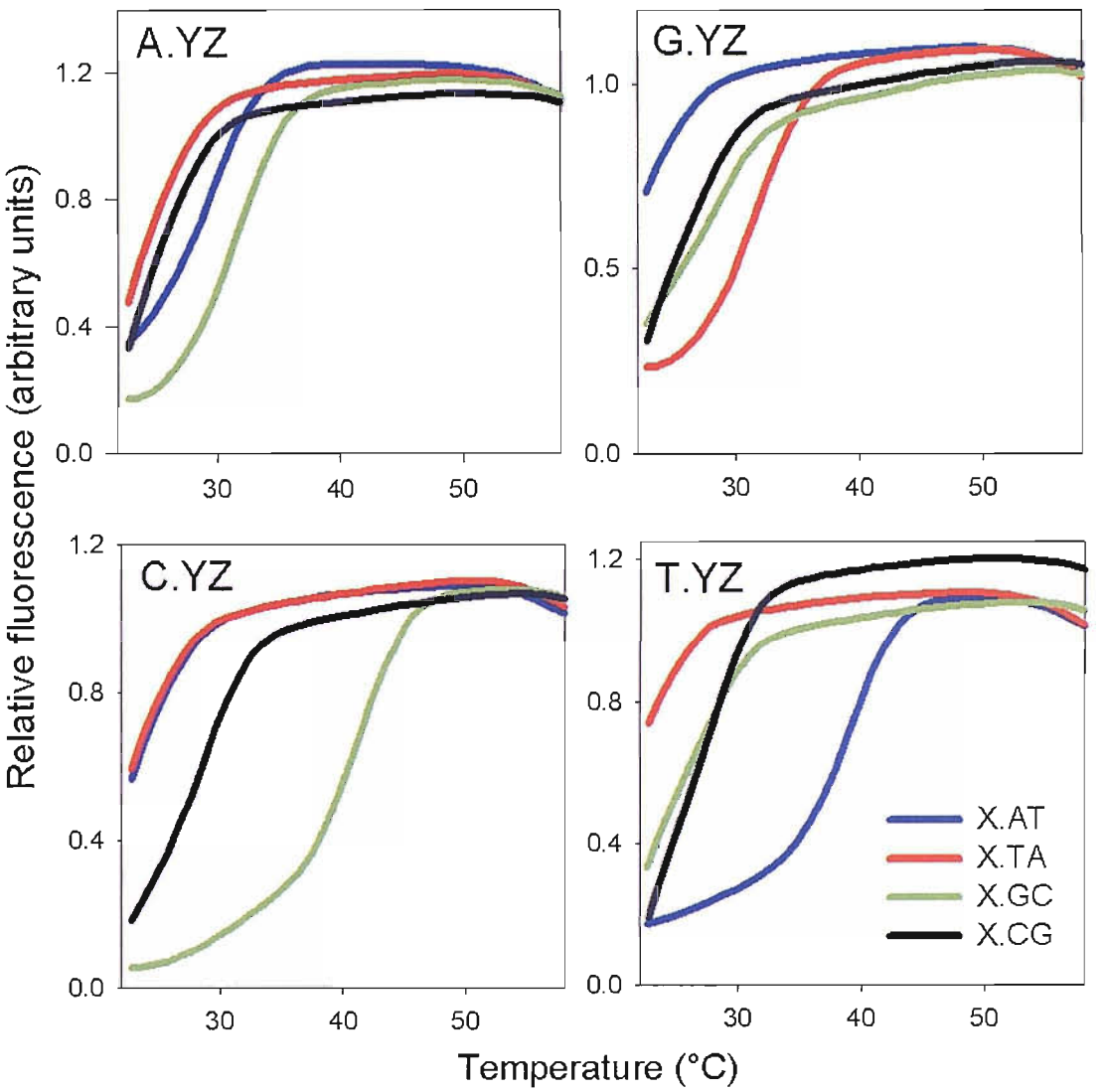

Figure 3.8 Representative fluorescence melting curves showing the interaction of TFOs with target sites containing a variable central base pair (AT, TA, GC or CG). Each TFO contains either A, G, C or T at the identical position, generating X.ZY triplets.The experiments were performed in 50 mM sodium acetate, pH 6.0 containing 200 mM NaCl. The y-axes show the normalised fluorescence (arbitrary units), while the x-axis shows the temperature (°C). The samples were heated at a rate of 0.2 °C min^{-1}.

of the C^+.GC and A.GC triplet, where the affinity became less pronounced at higher pH values, presumably due to a requirement for protonation.

It can also be seen that the four natural bases exhibit very different selectivities for the four possible Watson-Crick base pairs. C and T bind to GC and AT respectively much better than to any other base pair. At pH 6.0, the most stable and second most stable triplexes formed with either C or T differ in T_m by about 12 °C. In contrast, A and G show little discrimination between the different base pairs. The most stable and second most stable triplexes formed with these base differ in T_m by as little as 3 °C. This suggests that several of these combinations are effectively "null bases" in which the third-strand base makes little or no contribution to specificity.

The next step was to assess whether the choice of quencher, or the choice of linker attaching the quencher to the oligonucleotide affected the selectivity of the TFO. The above experiment was repeated using oligonucleotides labeled with pyrene or with methyl red attached via a serinol linker. The T_ms obtained from these are shown in Table 3.2 and 3.3. It can be seen from examination of Table 3.1 and 3.2 that the T_ms are virtually identical. In each instance the triplexes labeled with methyl red serinol exhibited T_ms that were typically about 0.5-1 °C higher than those containing methyl red threoninol. In this instance the choice of linker attaching the quencher to the TFO did not affect triplex stability or selectivity. In contrast, comparing Table 3.1 and 3.3 reveals that the stability of the triplexes containing pyrene were slightly greater than those containing methyl red; an increase in T_m of typically 1-2 °C at pH 5.0 and 4-6 °C at pH 6.0 was observed. However, in all cases the relative selectivity of the third strand was independent of the nature of the quencher.

		ZY			
X	pH	AT	TA	GC	CG
A	5.0	57.3 (57.6)	54.7 (54.8)	61.8 (61.9)	55.7 (55.5)
	5.5	44.4 (44.2)	40.7 (40.4)	48.4 (48.0)	40.7 (40.4)
	6.0	29.3 (29.4)	< 28.0	31.0 (31.2)	< 28.0
G	5.0	54.7 (54.4)	58.8 (58.9)	58.1 (58.1)	56.8 (56.6)
	5.5	39.0 (38.8)	47.3 (47.2)	44.1 (43.9)	41.9 (41.6)
	6.0	< 28.0	31.8 (32.3)	28.6 (28.4)	< 28.0
C	5.0	55.3 (55.2)	53.4 (53.7)	67.4 (65.9)	57.6 (57.7)
	5.5	39.8 (39.4)	38.7 (38.6)	56.6 (56.7)	43.7 (43.4)
	6.0	< 28.0	< 28.0	41.1 (41.2)	28.9 (28.7)
T	5.0	63.8 (63.7)	53.8 (53.9)	57.8 (57.8)	58.1 (58.2)
	5.5	54.3 (54.7)	39.2 (38.8)	43.7 (43.9)	44.5 (44.3)
	6.0	57.3 (57.6)	54.7 (54.8)	61.8 (61.9)	55.7 (55.5)

Table 3.2 T_m values determined by fluorescence melting for triplexes composed of different triplet combinations using a temperature gradient of 0.2 °C min^{-1} and the quencher methyl red serinol. Values in parenthesis were calculated from the annealing phase. Each value is an average of three separate determinations which usually differed by less than 0.5 °C.

		ZY			
X	pH	AT	TA	GC	CG
A	5.0	58.5 (58.8)	56.0 (56.1)	62.2 (62.5)	57.6 (57.9)
	5.5	48.0 (48.2)	44.4 (44.4)	51.4 (51.4)	44.5 (44.6)
	6.0	32.7 (32.8)	28.7 (28.8)	34.6 (35.1)	29.2 (28.9)
G	5.0	55.5 (55.9)	59.6 (59.9)	58.9 (59.1)	58.4 (58.5)
	5.5	42.3 (42.6)	50.5 (50.4)	47.4 (47.5)	45.6 (45.7)
	6.0	< 28.0	35.3 (35.7)	31.5 (31.6)	29.4 (29.4)
C	5.0	56.0 (56.3)	54.9 (55.0)	67.2 (66.8)	59.3 (59.2)
	5.5	42.7 (42.7)	41.4 (42.8)	59.0 (59.1)	46.7 (46.9)
	6.0	< 28.0	< 28.0	45.1 (45.2)	31.9 (31.9)
T	5.0	64.8 (64.8)	55.1 (55.3)	59.2 (59.3)	60.0 (60.2)
	5.5	57.4 (57.7)	42.6 (42.7)	47.5 (47.7)	48.1 (48.1)
	6.0	45.1 (45.3)	28.5 (28.3)	32.4 (32.7)	33.2 (33.3)

Table 3.3 T_m values determined by fluorescence melting for triplexes composed of different triplet combinations using a temperature gradient of 0.2 °C min^{-1} and the quencher pyrene. Values in parenthesis were calculated from the annealing phase. Each value is an average of three separate determinations which usually differed by less than 0.5 °C.

3.3.6.2 Effect of triplex length

To assess the effect of third strand length on the affinity and selectivity of triplex formation, the interaction of TFO-T_{15} and TFO-T_{10} with the four different duplexes was studied. The T_ms obtained for melting of these are shown in Table 3.4. The experiments were carried out under identical conditions to those described above. The TFOs were labelled with a pyrene quencher. Examination of Table 3.4 and Table 3.3 reveals that, as expected, decreasing the TFO length decreases the stability of the triplex. At pH 6.0, T_m values of 45.1, 42.5, and 34.1 °C were obtained for the interaction of the 18mer, 15mer and 10mer with their intended AT-duplex target, respectively. This is a difference of 11 °C between the longest and shortest TFO. At lower pH values this difference is increased, with a difference of 13 °C and 15 °C at pH 5.5 and 5.0, respectively. It can also be seen that the selectivity of the TFO increases as it becomes shorter, at pH 5.0 the 18mer exhibits a difference of 5 °C between the most stable and the second most stable triplex it forms, in contrast the 10mer exhibits a difference of 10 °C. This is surprising since the shorter TFO positions the mismatches near the triplex termini, and should be less destabilising.

		ZY			
X	pH	AT	TA	GC	CG
T_{15}	5.0	61.6 (61.9)	47.7 (47.7)	53.5 (53.4)	54.6 (54.4)
	5.5	55.6 (55.6)	37.4 (36.9)	43.1 (43.1)	43.6 (43.5)
	6.0	42.5 (42.6)	< 28.0	28.9 (28.5)	29.1 (29.0)
T_{10}	5.0	49.8 (50.2)	36.9 (36.6)	36.4 (37.2)	39.6 (39.2)
	5.5	44.2 (44.2)	< 35.0	< 35.0	< 35.0
	6.0	34.1 (34.4)	< 28.0	< 28.0	< 28.0

Table 3.4 T_m values determined by fluorescence melting for triplexes of different lengths and different triplet combinations using a temperature gradient of 0.2 °C min^{-1} and the quencher pyrene. Values in parenthesis were calculated from the annealing phase.

3.3.6.3 Factors effecting hysteresis

Finally, the effect of pH and base composition on hysteresis was examined by repeating the above study at a faster rate of heating (6 °C min^{-1}). The difference in T_ms (ΔT_m) between melting and annealing temperatures for the 16 possible triplexes are shown in Table 3.5. At pH 5.0., it can be seen that the greatest hysteresis was evident for the C^+.GC triplet (ΔT_m = 12.8 °C), followed by T.AT (ΔT_m = 10.6 °C), then G.TA (ΔT_m =

4.5 °C) and A.GC (ΔT_m = 3.9 °C). This follows the order of stability of these triplets. The remaining triplets exhibit very little or no hysteresis at this pH.

It can be seen that the extent of hysteresis was different at pH 5.5; a decrease was observed for the most stable triplets whilst an increase was seen for the remaining triplets. Increasing the pH further still also effected the degree of hysteresis. At pH 6.0, an increase in hysteresis was observed for all triplets that could be accurately measured (some T_ms were lower than the LightCycler could measure). It is therefore evident that the extent of hysteresis is dependent on a range of factors.

		ZY			
X	pH	AT	TA	GC	CG
A	5.0	1.6	0.7	3.9	0.3
	5.5	1.8	1.8	1.6	1.5
	6.0	< 28.0	< 28.0	3.4	< 28.0
G	5.0	0	4.5	0.9	0.4
	5.5	1.5	1.5	1.3	1.1
	6.0	< 28.0	3.2	> 3.6	> 1.6
C	5.0	0.4	0	12.8	0.4
	5.5	1.0	0.7	3.1	1.8
	6.0	< 28.0	< 28.0	4.6	1.8
T	5.0	10.6	0.7	3.9	0.3
	5.5	1.8	1.8	1.6	1.5
	6.0	2.4	< 28.0	3.4	< 28.0

Table 3.5 ΔT_m values determined from the difference in T_m between the melting and annealing profiles of the 16 triplexes under study using a temperature gradient of 6 °C min^{-1} and the quencher methyl red serinol. Each value is an average of three separate determinations which usually differed by less than 0.5 °C.

3.4 Discussion

The aim of the work described in this chapter was to demonstrate that the fluorescence melting technique could be employed for assessing the relative stability of *inter*molecular triplexes that contain appropriately positioned fluorophores and quenchers using a Roche LightCycler.

3.4.1 Rate of heating

The slowest rate of continuous temperature change with the LightCycler (6 °C min^{-1}) was too fast to allow for the slow rates of *inter*molecular triplex formation, leading to hysteresis between the melting and annealing curves. The standard temperature gradient usually employed in UV melting studies on triplexes is between 0.1-0.4 °C min^{-1} (Mergny & Lacroix, 2003). By programming the LightCycler to increase the temperature in 1 °C steps, leaving the sample to equilibrate for 5 minutes at each step, an apparent temperature gradient of 0.2 °C min^{-1} was obtained. This rate was sufficiently slow to eliminate hysteresis and produce true equilibrium curves for the triplexes under study. However, it should be noted that under different experimental conditions or for triplexes containing modified bases this might not be the case.

The extent of the hysteresis was dependent on a range of factors, such as TFO length, base composition and pH. Hysteresis arises because of slow steps in the association or dissociation reactions so that the reaction is not at thermodynamic equilibrium during the melting process. At low pH the triplexes containing the most stable triplets; C^+.GC, T.AT, G.TA and A.GC, exhibited much greater hysteresis than those containing a central mismatch. As mismatches in the centre of a triplex do not affect k_{on} but affect k_{off} in a manner that is dependent on the nature of the mismatch (Rougée *et al.*, 1992) it is likely that this hysteresis was predominately the result of the slow dissociation rate of these triplets, though this would require further experiments. The extent of hysteresis was also profoundly affected by pH, suggesting that protonation is another important factor determining the association and dissociation rates of triplex formation, though no clear relationship was identified.

Understanding the factors that contribute to hysteresis should allow the design of short melting experiments, thereby minimizing the time samples are exposed to high temperatures and decreasing the chance of degradation, photobleaching and evaporation. Melting and annealing profiles that exhibit hysteresis have also been used to generate kinetic data for the association and dissociation of *inter*molecular triplexes (Rougée *et al.*, 1992; Bernal-Méndez *et al.*, 2002).

3.4.2 Melting profiles

The melting profiles determined by this fluorescence melting technique are qualitatively very similar to those determined by UV melting except for the presence of some small secondary transitions. At high temperature a small decrease in fluorescence is observed. This can be attributed to the melting of the underlying duplex since melting of the duplex strands in the absence of TFO produced an identical transition. Also, this transition is no longer evident under conditions where the triplex is more stable than the underlying duplex (i.e. low pH) when only the triplex melting transition is seen. The reason for the decrease in fluorescence is not clear, but may be attributed to the different electronic properties of fluorescein when bound to the duplex and when free in solution. These differences maybe the result of stacking interactions with the bases of the duplex or an altered pK_a of fluorescein.

A further transition was observed at low pHs, at the start of the triplex melt, and is likely to be attributed to the formation of short-lived secondary structures. Melting of the TFO and just the purine-containing strand of the duplex exhibited a clear transition at similar temperatures. Under these conditions the two oligonucleotides could potentially form a parallel Hoogsteen duplex (see below), an antiparallel Hoogsteen duplex, a slipped or bulged structures or other secondary structures involving protonated C residues. The transition disappears at relatively low temperatures and therefore should not effect the triplex melt.

Parallel Hoogsteen duplexes

```
5'-Q-TCTCTCTTXTCCTCCTCC
5'-F-AGAGAGAAZAGGAGGAGG

                    TCCTCCTCC
5'-Q-TCTCTCTTX
5'-F-AGAGAGAAZAGGAGGAGG
```

3.4.3 Choice of reporter groups

It was anticipated that the type of quencher used in these studies could influence the affinity and selectivity of the third strand for its target duplex. The quenchers methyl red and pyrene were attached to TFOs via the same linker and their effect on triplex

stability assessed. The pyrene-containing triplexes exhibited higher melting temperatures than those containing methyl red, an effect that was greater at elevated pH. As pyrene is a good triplex intercalator (Xue *et al.,* 2002) the higher stability of the triplexes containing this quencher is not surprising. To examine whether these groups affect triplex stringency, TFOs containing each of these quenchers were targeted against different duplex targets. The TFOs exhibited the same selectivity irrespective of the quencher employed, furthermore this selectivity was the same as previously reported (see below). This highlights that although the addition of these groups does affect triplex stability, this should not affect the selectivity of triplexes that are the same length and differ by a single central triplet.

It was also anticipated that different linkers used to attach the quencher to the TFO could influence triplex formation. In these studies methyl red was attached directly to deoxyribose, or via a threoninol or serinol linker to the TFO backbone. The deoxyribose variant exhibited the greatest increase in stability, which is likely to be attributed to the presence of a further nucleotide within the TFO. The serinol and threoninol variants exhibited very similar melting temperatures, this was not surprising as the difference between the two is a single methyl group.

The attachment of fluorescein to the end of a duplex has previously been shown to lead to little or no stabilisation effects (Moreira *et al.*, 2005), though this was not investigated in this work. The fluorescence yield of fluorescein is pH dependent and could potentially be a problem for studying parallel triplexes, where low pH is required for these complexes to form. Despite a lower overall fluorescence, it was possible to obtain accurate melting curves at pH values as low as 5.0.

3.4.4 Factors effecting triplex stability

Several factors effecting triplex stability were examined, mainly to verify that the results produced by this approach are similar to those obtained by other techniques but also to use as reference for studies on modified triplexes presented in later chapters.

Several studies have been carried out on TFOs to investigate the stability of all combinations of natural bases opposite each base pair (Mergny *et al.*, 1991; Yoon *et al.*, 1992; Fossela *et al.* 1993; Chandler and Fox, 1993; Dervan; Best and Dervan, 1995).

These have shown that triplex formation is sensitive to single mismatches between the bases in the third strand and the duplex. In this study the thermal stability of triplexes containing all possible triplet combinations at a central position were also investigated. The most stable triplexes are formed with those that contain central T.AT and C^+.GC triplets, with several other combinations producing triplexes of intermediate stability, including G.TA, T.CG, C.CG, G.GC, A.GC and T.GC triplets. These results emphasise that the most suitable bases for recognising AT, GC, TA and CG base pairs are T, C, G and T or C, respectively. This third-strand binding code was exhibited at different pH values and with triplexes of different lengths, with a greater differentiation exhibited at higher pH and shorter third strand lengths. Again, these observations are consistent with those previously reported (Moser & Dervan, 1987; Howard *et al.*, 1964; Lee *et al.*, 1979). Taken together, these results demonstrate that this fluorescence melting technique provides an accurate means for measuring the thermal stability of different triplexes under a variety of experimental conditions.

4 ENHANCING TRIPLEX STABILITY USING OLIGONUCLEOTIDES CONTAINING NUCLEOSIDE ANALOGUES

4.1 Introduction

Parallel triplex formation is currently hampered by low stability under physiological pH and ionic conditions. This is predominantly the result of charge repulsion between the three adjacent polyanionic DNA strands and a requirement for protonation of cytosine at N3. This chapter considers several nucleoside analogues designed to overcome each of these restrictions.

The simplest strategy to alleviate the charge repulsion problem is to incorporate positively charged moieties into the TFO by either modifying the backbone, the sugar or the base. The first part of this chapter examines the triplex-forming properties of several 5- and 2′-substituted derivatives of deoxyuridine that are protonated under physiological conditions. 5-propargylamino-dU (U^P; Figure 4.1(iii)) and 2′-aminoethoxy,5-propargylamino-U (BAU; Figure 4.1(v)) have previously been shown to form more stable triplets with AT base pairs than T (Bijapur *et al*, 1999; Sollogoub *et al*, 2002). Both analogues contain positively charged amino functions suitably positioned to interact with the negative phosphodiester residues within the duplex purine-strand and/or the TFO. The analogues propargylguanidino-dU (U^{PG}; Figure 4.1(iv)) and the novel 2′-guanidinoethoxy ,5-propargylguanidino-U (BGU; Figure 4.1(vi)) are also investigated. These nucleosides contain guanidine functions in place of the amine groups of U^P and BAU. Guanidines are protonated over a greater pH range than amines and may stabilise triplex formation to a greater extent (Roig *et al.*, 2003; Prakesh *et al.*, 2004).

Alongside electrostatic interactions it is likely that these analogues participate in favourable hydrophobic and base stacking interactions within the major groove. It may also be possible for the amine or guanidine moieties to participate in hydrogen bonding. The analogue 5-dimethylaminopropargyl-dU (U^{DMP}; Figure 4.1(ii)) is a novel derivative of U^P that contains a dimethylamine in place of the amine, this group retains a positive charge but unlike U^P cannot participate in hydrogen bonding. 5-amino-dU (U^A; Figure 4.1(i)) also contains an amino group at the 5-position of dU, which is not likely to be protonated under physiological conditions and lacks the hydrophobic propyne moiety.

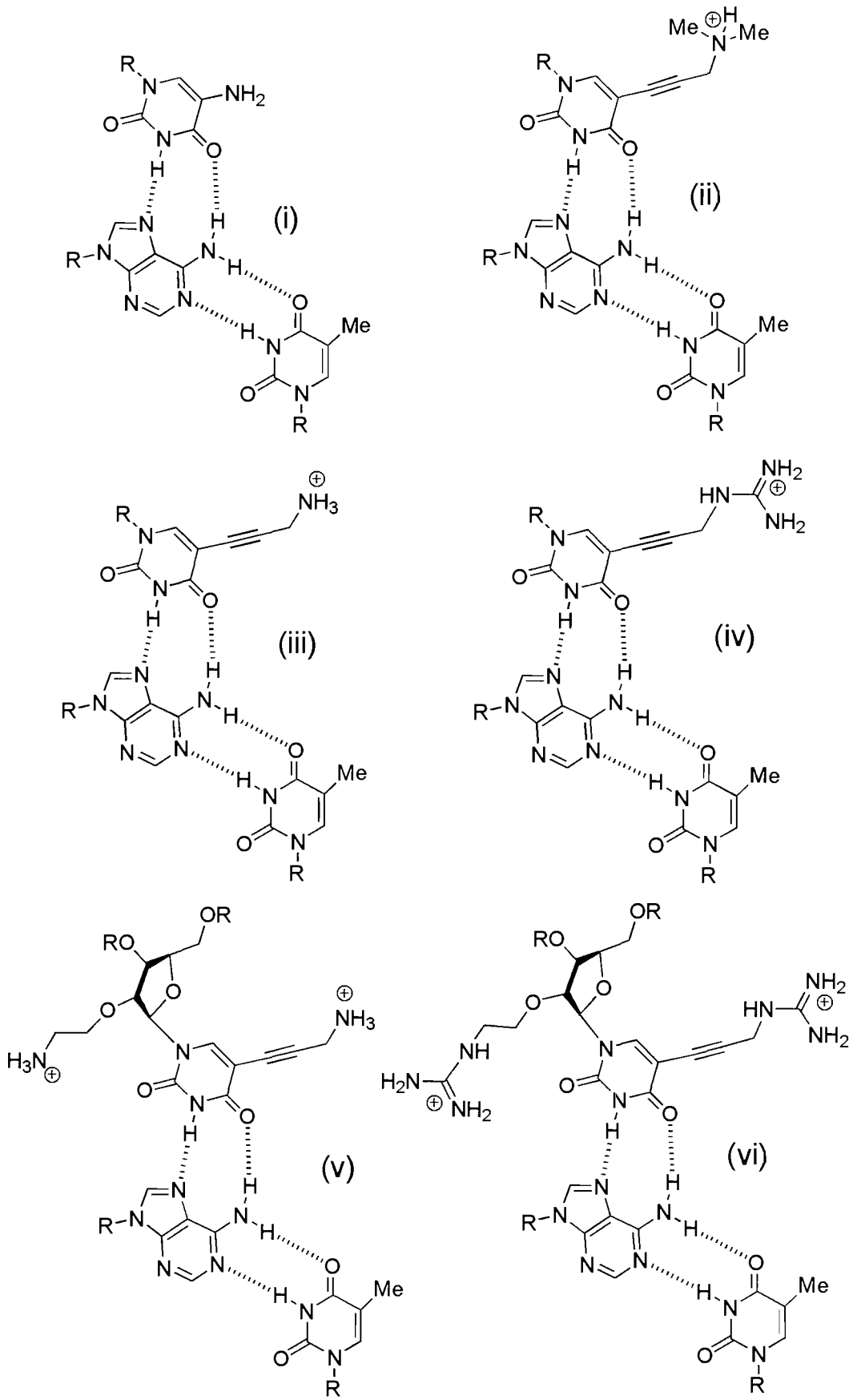

Figure 4.1 Chemical structures and proposed hydrogen bonding patterns of the nucleoside analogues designed to recognise AT base pairs; (i) U^{A}.AT (ii) U^{DMP}.AT (iii) U^{P}.AT (iv) U^{PG}.AT (v) BAU.AT and (vi) BGU.AT. The third strand sugar is included only when a modification is present.

The second part of this chapter looks at the triplex-forming properties of several nucleosides designed to alleviate the pH dependency of the C^+.GC triplet. 2-aminopyridine (P; Figure 4.2A) and 3-methyl,2-aminopyridine (^{Me}P; Figure 4.2C) are cytosine analogues based on the more basic pyridine *C*-nucleus and exhibit pK_a values two pH units higher than C (Bates *et al.*, 1996; Hildbrand *et al*, 1996; Cassidy *et al.*, 1997). 6-Oxo deoxycytidine is a cytosine mimick that contains suitable H-bond donors at positions 3 and 4 for pH independent recognition of GC (Xiang *et al.*, 1994). The 2´-*O*-methyl and ribo derivatives of this base have also been reported, though these produce less stable complexes (Berressem & Engels, 1995; Parsch *et al.*, 2000). The novel 2´-aminoethoxy derivative (^{AE}6-oxo-C; Figure 4.2B) of this base is examined in this study. N7G is generated by linking deoxyribose to the N7 position of guanine (instead of the usual N9), this orients it such that the groups involved in hydrogen bond formation mimic those seen in the C^+.GC triplet (Hunziker *et al.*, 1995). The 2´-aminoethoxy derivative (^{AE}N7G; Figure 4.2D) of this base is investigated.

The last part of this chapter focuses on achieving recognition of oligopurine sequences at physiological pH using TFOs containing multiple substitutions of U^P or BAU for recognition of AT and P or ^{Me}P for recognition of GC. It is known that the base sequence and composition of an unmodified parallel TFO affects its affinity for its duplex target (Keppler *et al.*, 1997; James *et al.*, 2003). Most notably, TFOs containing alternating C^+.GC and T.AT triplets generate the most stable triplets. TFOs containing different numbers and arrangements of these nucleoside analogues are studied by DNase I footprinting experiments.

4.2 Experimental design

4.2.1 Fluorescence melting experiments

The sequences of the oligonucleotides used in the thermal melting experiments are illustrated in Figure 4.3A. For these experiments the purine strand of the duplex (boxed) was labelled at the 5´-end with a fluorophore (F; fluorescein), while the third strand was labelled at the 5´-end with a quencher (Q; pyrene or methyl red). Melting temperatures (T_m) for these intermolecular triplexes were determined as described in Chapter 3 using an appropriate rate of temperature change. As the 18mer third strands contained several

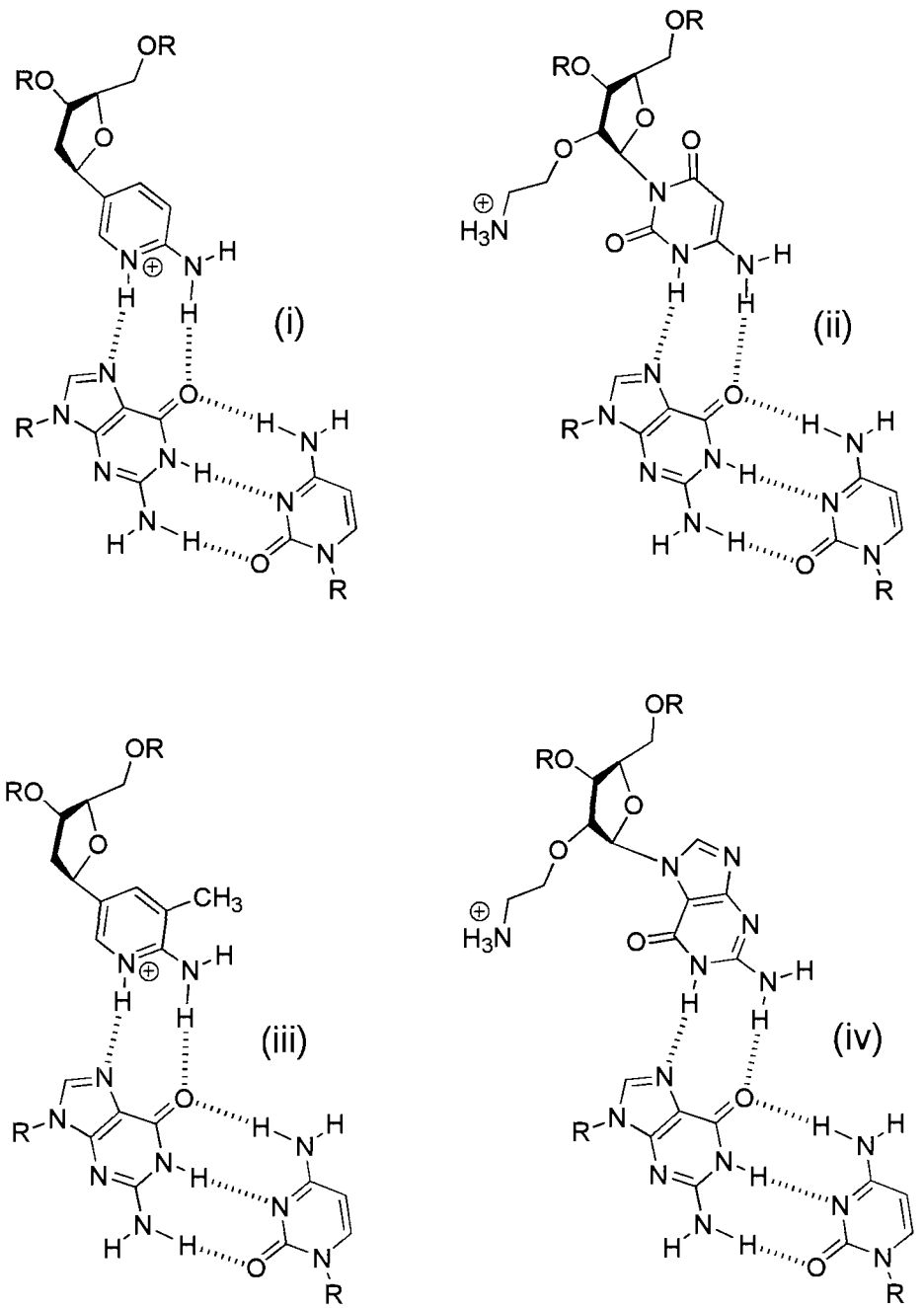

Figure 4.2 Chemical structures and proposed hydrogen bonding patterns of the nucleoside analogues designed to reduce the pH dependency of triplex formation; (i) P.GC (ii) ^{AE}6-oxo-C.GC (iii) ^{Me}P.GC and (iv) ^{AE}N7G.GC. The third strand sugar is included to show any sugar modifications.

A

(i)	TFO-X	5′-Q-TCTCTCTT**X**TCCTCCTCC
	Duplex	5′-F-AGAGAGAA**Z**AGGAGGAGG
		3′-TCTCTCTT**Y**TCCTCCTCC
(ii)	TFO-OC_{10}	5′-Q-TCTCT**O**TTTT
	TFO-OC_{15}	5′-Q-TCTCTCTTTT**O**CT**O**C
	TFO-OC_{18}	5′-Q-TCT**O**TCTTTT**O**CT**O**CTCC

B

	5′-TCCTTCTC
$1U^A$	5′-TCC**U**$^{\mathbf{A}}$TCTC
$3U^A$	5′-TCC**U**$^{\mathbf{A}}$**U**$^{\mathbf{A}}$C**U**$^{\mathbf{A}}$C
	5′-TTTTTTCTT
6BAU	5′-**BBBBBB**C**B**T
	5′-TCTCTTTTTTCT
3P	5′-T**P**T**P**TTTTTT**P**T
$2U^P$	5′-TCTCT**U**$^{\mathbf{P}}$T**U**$^{\mathbf{P}}$TTCT
$2P2U^P$	5′-T**P**T**P**T**U**$^{\mathbf{P}}$T**U**$^{\mathbf{P}}$TT**P**T
$1^{Me}P$	5′-TCT$^{\mathbf{Me}}$**P**TTTTTTCT
1BAU	5′-TCTCTTT**B**TTCT
^{Me}PBAU	5′-TCT$^{\mathbf{Me}}$**P**TTT**B**TTCT
2BAU	5′-TCTCT**B**T**B**TTCT
$2^{Me}P2BAU$	5′-TCT$^{\mathbf{Me}}$**P**T**B**T**B**TT$^{\mathbf{Me}}$**P**T
$3^{Me}P$	5′-T$^{\mathbf{Me}}$**P**T$^{\mathbf{Me}}$**P**TTTTTT$^{\mathbf{Me}}$**P**T
3BAU	5′-TCTCT**B**T**B**T**B**CT
$3^{Me}P3BAU$	5′-T$^{\mathbf{Me}}$**P**T$^{\mathbf{Me}}$**P**T**B**T**B**T**B**$^{\mathbf{Me}}$**P**$^{\mathbf{e}}$T
$3^{Me}P3BAU$	5′-T$^{\mathbf{Me}}$**PB**$^{\mathbf{Me}}$**PBB**TTTT$^{\mathbf{Me}}$**P**T
5BAU	5′-**B**C**B**C**B**T**B**TT**B**CT
GT_{par}	5′-TGTTTTTTGTGT
GT_{anti}	3′-TGTTTTTTGTGT
$GBAU_{par}$	5′-TG**B**T**B**T**B**TG**B**GT
$GBAU_{anti}$	3′-TG**B**T**B**T**B**TG**B**GT

Duplex target

5′..AGGAAGAGAA**Z**AAAGA..
3′..TCCTTCTCTT**Y**TTTCT..

Figure 4.3 Sequence of oligonucleotides used in Chapter 4; A) Oligonucleotides used in fluorescence melting experiments. The duplexes are labelled with fluorescein (F) at the 5′-end of the purine strand and with methyl red serinol or threoninol (Q) at the 5′-end of the TFO; (i) Single substitution studies; ZY is each base pair in turn (AT, TA, GC, CG) and X is each base or analogue; (ii) TFOs contain several substitutions of 6-oxo-C (**O**). B) Oligonucleotides used in footprinting experiments. Sequence of TFOs and their oligopurine target site within the *tyr*T(43-59) DNA fragment (boxed; ZY = AT). TFOs contain the nucleoside analogues 5-aminouracil ($\mathbf{U}^A$), 5-propargylamino dU (**U**), 2′-aminoethoxy,5-propargylamino-U (**B**), 2-aminopyridine (**P**) and 3-methyl,2-amino pyridine (^{Me}**P**). In the selectivity studies the oligonucleotide 5BAU positions B opposite ZY, when ZY is each base pair in turn (AT, TA, GC, CG).

cytosine residues triplex formation using these oligonucleotides was pH dependent and was restricted to low pH conditions (pH < 6.0). All melting experiments were undertaken in 50 mM sodium acetate buffer containing 200 mM sodium chloride at a pH between 5.0 and 6.0. No additional stabilising factors were employed in the assay, so as to maximize the intrinsic affinity of each analogue. In each assay the concentration of duplex was 0.25 μM and the concentration of third strand was 3 μM. The excess of third strand was used to facilitate triplex formation. T_m values were calculated from the first derivatives of the melting and annealing profiles. Each value was recorded in triplicate and usually differed by less than 0.5 °C.

The oligonucleotides shown in Figure 4.3A(i) were designed to position a single nucleoside analogue (X) within a TFO so as to form a central X.ZY triplet upon triplex formation, where ZY is each bp in turn (AT, TA, GC or CG). These sequences are identical to those studied in Chapter 3, except X is an analogue and not a natural base. The third strand oligonucleotides illustrated in Figure 4.3A(ii) were designed to target the same duplex as above, when ZY is AT. In these oligonucleotides several substitutions of C were replaced with the nucleoside analogue ^{AE}6-oxo-C.

4.2.2 DNase I footprinting experiments

The sequences of the third strand oligonucleotides and their duplex targets used in DNase 1 footprinting experiments are shown in Figure 4.3B. The oligonucleotides were designed to target different positions of the polypurine tract (boxed; ZY is AT) found within the 105 bp *tyr*T(43-59) DNA fragment. For the selectivity studies, position ZY was mutated by site-directed mutagenesis to TA, GC and CG. The full sequences of this fragment can be seen in Figure 2.4. Each fragment was radiolabelled at the 3´-end of the *Eco*RI site using reverse transcriptase and [α-^{32}P]dATP. The experiments were performed in an appropriate buffer and the complexes were left to equilibrate overnight at 20 °C. Quantitative analysis of the bands within each footprint allowed calculation of C_{50} values, indicating the TFO concentration that reduced the band intensity by 50%. The C_{50} values obtained for the interaction of each of the oligonucleotides examined within this chapter are summarised in Table 4.5.

4.3 Results

In these studies the selectivity and affinity of TFOs containing single or multiple substitutions of the above mentioned nucleoside analogues are assessed by quantitative DNase I footprinting and/or fluorescence melting. These are compared to TFOs containing natural bases.

4.3.1 Increasing the stability of triplex formation

4.3.1.1 Triplex formation with 5-amino-dU

To corroborate the stabilising affect of a hydrophobic group at the 5-position of dU, the base analogue 5-amino dU, which contains a hydrophilic amino group at this position, was compared for its triplex-forming properties with T. The interactions of the modified oligonucleotides 5′-TCCU^{A}TCTCT (1U^{A}) and 5′-TCC^{A}U^{A}UC^{A}UCT (3U^{A}) with the tyr*T*(43-59) DNA fragment were determined and compared with the interaction of the unmodified control oligonucleotide 5′-TCCTTCTCT. The sequence of the intended target site within tyr*T*(43-59) is 5′-AGGAAGAGA/3′-TCCTTCTCT. Since this target contains four GC base pairs triplex formation with oligonucleotides containing only natural bases was strongly pH dependent. These experiments were therefore performed in pH 5.0 50 mM sodium acetate containing 2.5 mM magnesium chloride. The complexes were left to equilibrate overnight at 20 °C.

Representative cleavage patterns for the interaction of each oligonucleotide with the 105 bp DNA fragment are shown in Figure 4.4. Clear footprints are evident for the interaction of all three TFOs at the intended target site at the 5′-end of the polypurine tract (boxed). The cleavage pattern remains unaltered for the rest of the fragment, indicating only specific binding of the TFOs. The bands within the gel are of different intensities as DNase I does not generate even cleavage patterns, in this case this is most notable for the GC-rich regions, such as within the polypurine tract (marked). The concentrations of TFOs used in each gel are identical and direct visual comparison between gels indicates the footprint produced by the control TFO persists to a lower concentration than either of the two modified TFOs. It is also evident that the footprint produced by the TFO containing one substitution of ^{A}U persists to a lower concentration than the TFO containing three. Quantitative analysis for the interaction of these TFOs

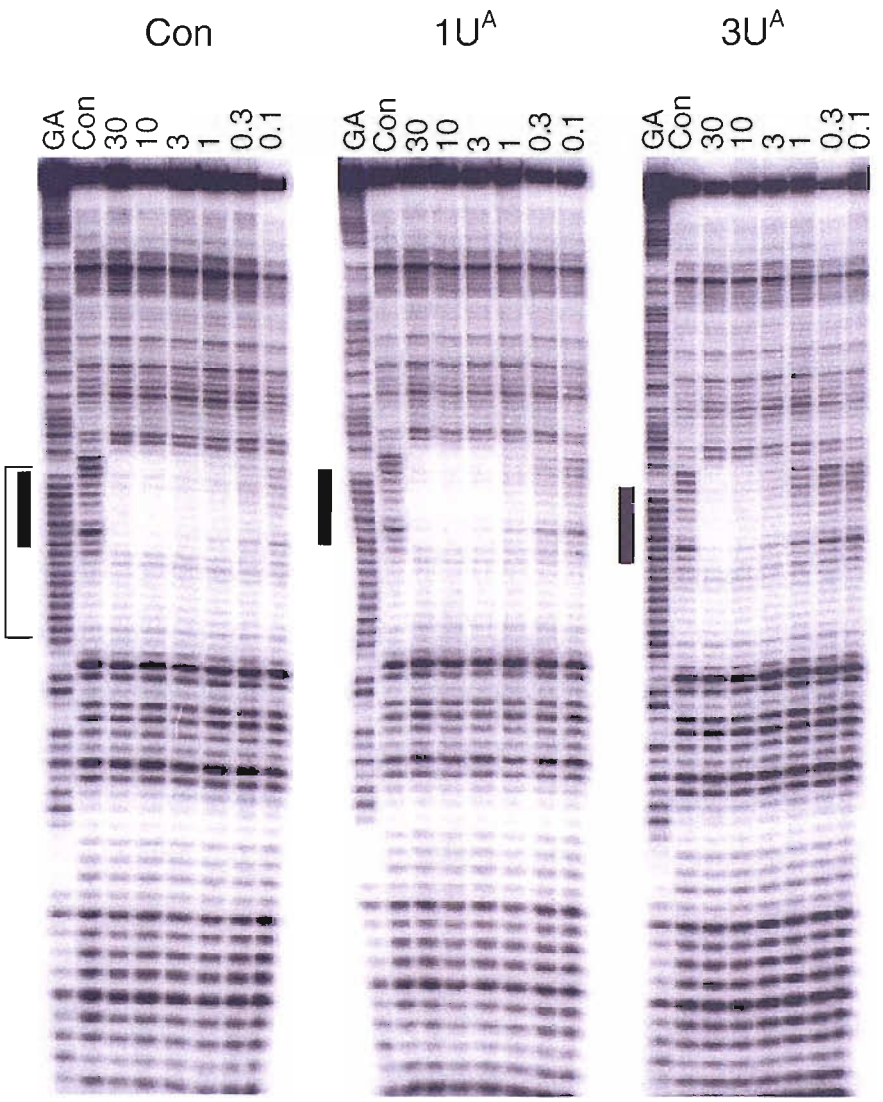

Figure 4.4 DNase I cleavage patterns of *tyr*T(43-59) in the presence of unmodified and 5-amino-dU substituted oligonucleotides at pH 5.0. The lanes labelled 'GA' are Maxam-Gilbert markers specific for purines while 'con' indicates DNase I cleavage in the absence of added oligonucleotide. The concentration (μM) of TFO is shown at the top of each gel lane. The experiments were performed in pH 5.0 50mM sodium acetate containing 2.5 mM magnesium chloride and the complexes were left to equilibrate overnight at 20 °C. The filled boxes show the position of the triplex target site within the 17 base oligopurine tract (also indicated).

yields C_{50} values of 24 ± 1 nM, 86 ± 15 nM and 150 ± 40 nM for the control, $1U^A$ and $3U^A$ oligonucleotides respectively. This corresponds to about a 3-fold decrease in affinity for replacement of a single T with U^A. These footprinting experiments demonstrate that triplexes composed of U^A.AT triplets are less stable than those composed of T.AT triplets. Therefore the replacement of a hydrophobic for a hydrophilic substituent at the 5-position of dU is destabilising.

4.1.1.2 Triplex formation with 5-propargyl deoxyuridine derivatives

The triplex-forming properties of nucleoside analogues containing different substituents at the 5-position and 2´-position of deoxyuridine were assessed by fluorescence melting. The sequence specificity and affinity of the analogues U^{DMP}, U^P, U^{PG}, BAU and BGU in triplex formation was assessed by determining the T_m of the fluorescently-labelled intermolecular triplexes shown in Figure 4.3A. The structures of these analogues are shown in Figure 4.1. T_ms were determined by fluorescence melting experiments as described in Chapter 3. In these experiments a single substitution of each analogue was incorporated at the centre of the 18mer TFO (indicated by X in Figure 4.3A) and targeted against four duplexes in which ZY was each base pair in turn. The stability of these complexes was compared with those formed by TFOs that contain each of the natural bases at this central position. All oligonucleotides were dissolved in 50 mM sodium acetate containing 200 mM sodium chloride at the appropriate pH.

A rate of temperature change of 6 °C min^{-1} was initially employed for heating and cooling the complexes at pH 5.0. The melting and annealing temperatures were obtained from the first derivatives of these profiles can be seen in Table 4.1. At this rate of temperature change the melting and annealing curves exhibited hysteresis, the extent of which was dependent on the nature of the central triplet. For each analogue the hysteresis was greatest against the intended AT base pair target rather than against a mismatch base pair. A comparison between the analogues shows that hysteresis was greatest for the triplexes containing the BAU.AT and BGU.AT triplets, with about a 20 °C difference between melting and annealing curves. This was followed by triplexes containing the U^{DMP}.AT, U^P.AT and U^{PG}.AT triplets, with a difference of about 16 °C. These compare with an 11 °C difference for the triplex containing the T.AT triplet. On reducing the rate of heating to 0.2 °C min^{-1}, this hysteresis disappears for almost all triplexes containing mismatched triplets but is still evident for those containing X.AT

triplets, especially for BAU.AT and BGU.AT. Melting and annealing temperatures for these can be seen in Table 4.2. The T_ms are approximately mid-way between the melting and annealing values obtained at the faster rate of temperature change. On reducing the rate to 0.067 °C min^{-1} the hysteresis was reduced even further and was evident only for BAU and BGU.AT triplets, with a difference of about 3 °C between melting and annealing temperatures. At this rate the annealing and melting profiles were obtained on separate samples as the long exposure to high temperatures led to sample degradation.

		ZY			
X	pH	AT	TA	GC	CG
U^P	5.0	72.8 (58.3)	55.2 (54.8)	61.8 (58.9)	59.5 (58.7)
U^{PG}	5.0	74.1 (58.1)	55.1 (54.6)	61.9 (59.0)	59.1 (58.4)
U^{DMP}	5.0	72.0 (56.7)	54.9 (53.3)	61.4 (57.4)	59.1 (57.3)
BAU	5.0	77.5 (58.4)	55.0 (55.7)	66.5 (55.9)	56.1 (57.2)
BGU	5.0	78.3 (57.4)	55.8 (54.6)	67.0 (59.1)	56.2 (56.0)

Table 4.1 T_m values determined by fluorescence melting for triplexes composed of triplets containing deoxyuridine derivatives using a temperature gradient of 6 °C min^{-1} and the quencher methyl red. Values in parenthesis were calculated from the annealing phase. Each value is an average of three separate determinations which usually differed by less than 0.5 °C.

It was also observed that hysteresis could be eliminated by increasing the pH, all triplexes formed at pH 5.5 and pH 6.0 did not show any hysteresis at a rate of temperature change of 0.2 °C min^{-1}. Melting and annealing temperatures obtained for these are also included in table 4.2. These T_ms can be compared directly with those obtained for the TFOs containing natural bases (Table 3.1).

This hysteresis arises because the melting curves are not in thermodynamic equilibrium and indicates the presence of slow steps in the association and/or dissociation reactions. These slow steps are clearly longer for the modified analogues compared to T, and these were the longest for the analogues containing two positive charges. Interestingly, the T_ms obtained from the annealing profiles for each X.AT triplet were very similar, whereas the T_ms obtained from the melting profiles varied depending on X. This suggests that the difference in stability of these triplets arises from a difference in dissociation rates.

X	pH	ZY			
		AT	TA	GC	CG
U^P	5.0	65.4 (64.0)	54.4 (54.5)	59.4 (59.5)	58.4 (58.4)
	5.5	55.6 (55.8)	39.9 (40.1)	46.5 (46.3)	44.5 (44.3)
	6.0	41.8 (42.0)	< 28.0	30.9 (31.0)	29.5 (29.6)
U^{PG}	5.0	66.5 (64.0)	54.8 (54.8)	60.3 (60.3)	58.7 (58.7)
	5.5	56.9 (56.9)	40.3 (40.4)	47.0 (47.2)	44.9 (44.8)
	6.0	43.7 (43.9)	< 28.0	32.3 (32.3)	29.9 (30.2)
U^{DMP}	5.0	67.8 (64.1)	54.6 (54.7)	60.2 (60.2)	58.5 (58.5)
	5.5	57.7 (57.8)	39.6 (39.8)	47.2 (47.0)	43.9 (43.9)
	6.0	43.8 (43.7)	< 28.0	30.7 (31.0)	28.4 (28.2)
BAU	5.0	70.8 (64.4)	55.9 (55.9)	62.8 (63.0)	56.7 (56.8)
	5.5	59.5 (59.2)	41.8 (41.3)	51.8 (51.6)	42.0 (41.9)
	6.0	47.5 (47.6)	< 28.0	36.5 (36.7)	< 28.0
BGU	5.0	72.1 (64.0)	55.2 (55.2)	62.8 (62.8)	55.8 (55.8)
	5.5	60.0 (59.8)	40.1 (40.3)	51.3 (51.2)	40.3 (40.5)
	6.0	47.4 (47.3)	< 28.0	35.0 (35.4)	< 28.0

Table 4.2 T_m values determined by fluorescence melting for triplexes composed of triplets containing deoxyuridine derivatives using a temperature gradient of 0.2 °C min^{-1} and the quencher methyl red. Values in parenthesis were calculated from the annealing phase. Each value is an average of three separate determinations which usually differed by less than 0.5 °C.

Representative melting profiles obtained for the triplexes formed at pH 6.0 are shown in Figure 4.5 and are true equilibrium curves obtained at a slow rate of heating (0.2 °C min^{-1}). Examination of the profiles obtained against the intended AT duplex target (top left) reveals that all analogues increased the stability of the triplexes relative to T (red line), this was greatest for the BAU and BGU analogues (blue lines). Comparison of the melting temperatures obtained from these profiles shows a T_m increase of between 2 and 8 °C relative to T at pH 6.0 with an order of stability of T < U^{DMP} < U^P = U^{PG} < BAU = BGU. This increase in stability was more evident at higher pH values. It can be seen that each X.AT triplet is now more stable than C^+.GC at all pHs, in contrast to T.AT which produces less stable complexes than C^+.GC. Also, the guanidylated derivatives of U^P and BAU are no more stable than their unmodified counterparts. Whilst a comparison of the stability of U^{DMP} and U^P, shows that the replacement of the amino group attached to the propargyl chain with a dimethylamino group is slightly destabilising.

Examination of Figure 4.5 and Table 4.2 reveals that as well as showing increased triplex stability at AT each analogue produced more stable complexes than T against

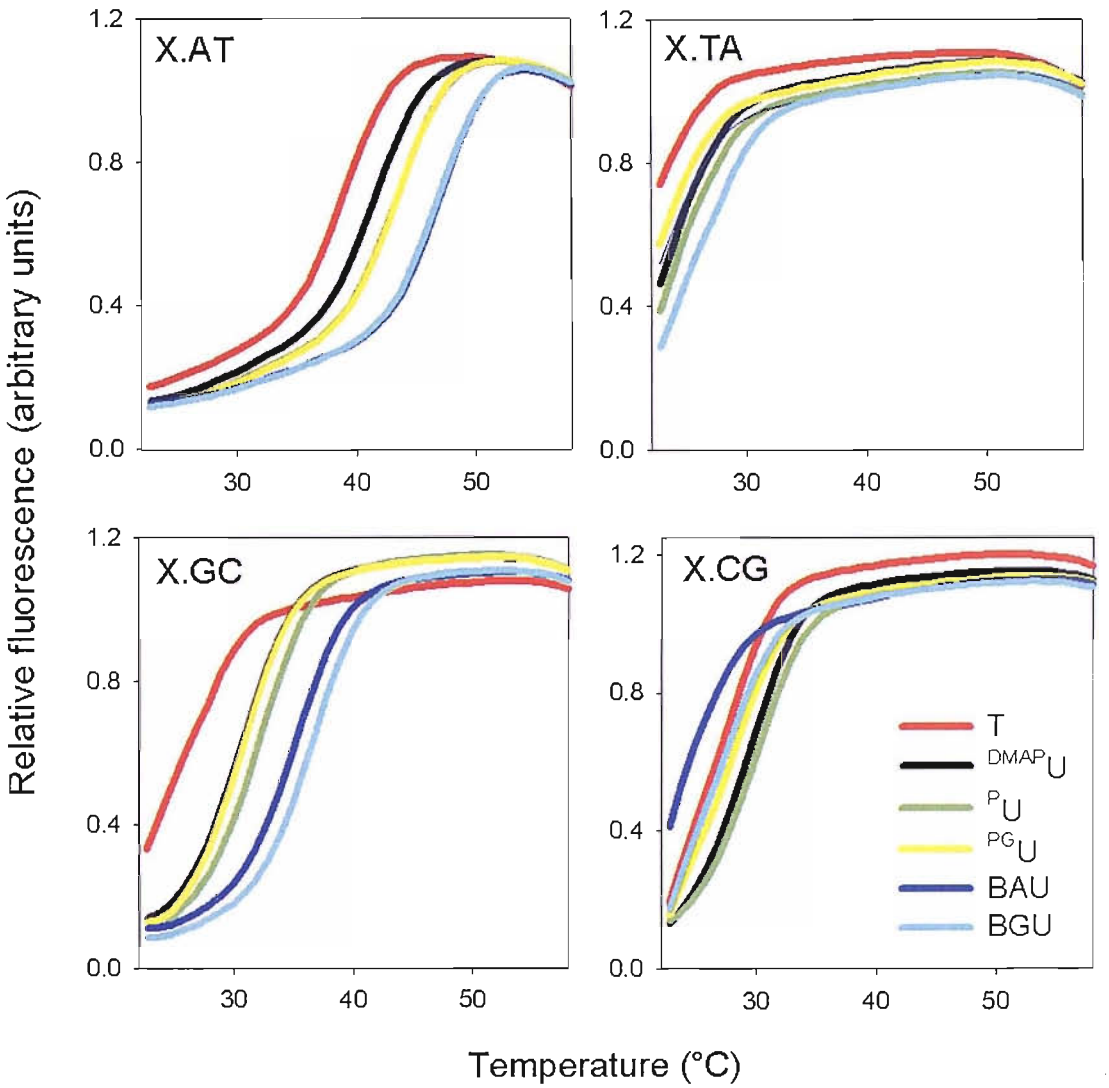

Figure 4.5 Fluorescence melting curves showing the interaction of TFOs containing 5-propargyl-dU derivatives with duplex targets containing a variable central base pair at pH 6.0. The experiments were performed in 50 mM sodium acetate containing 200 mM NaCl. The y-axes show the normalised fluorescence (arbitrary units), while the x-axes show the temperature (°C). The samples were heated at a rate of 0.2 °C/min.

GC base pairs. However, the ability of these analogues to discriminate between AT and GC is similar to that that of T, and the difference in T_m between X.GC and T.GC is similar to that between X.AT and T.AT. For example, the difference in T_m between U^P.AT and T.AT is 4.3 °C and the difference between U^P.GC and T.GC is 4.6 °C. In contrast, the difference between X.TA and T.TA is very small, whilst X.CG is as stable (X is U^{DMP}, U^P or U^{PG}) or actually less stable than T.CG (X is BAU or BGU). These results suggest that as well as producing very stable complexes at AT these nucleosides exhibit enhanced discrimination against TA and CG base pairs. This effect is greatest for the BAU and BGU analogues.

4.1.1.3 Triplex specificity of 2´-aminoethoxy,5-propargylamino-U at physiological pH

The fluorescence melting studies presented above were undertaken under low pH conditions, as the TFOs contained several C residues. The selectivity of BAU was therefore examined at physiological pH by DNase I footprinting. For these experiments, the interactions of 5´-BCBCBTBTTBCT (5BAU) with the four DNA fragments shown in Figure 4.2B were determined. Each fragment differed by a central base pair (ZY) within the 12 bp oligopurine target site. The TFO was designed to position a single BAU residue at an identical position (underlined). In this manner the selectivity of this analogue for each base pair in turn could be examined. The sequence of the duplex target site is 5´-AGAGAAZAAAGA/3´-TCTCTTTTTTCT and is found at the 3´-end of the polypurine tract within tyr*T*(43-59). Since this target contains three GC pairs triplex formation with oligonucleotides containing only natural bases is strongly pH dependent, while the nine AT base pairs result in a complex with relatively low affinity. The TFO therefore required four additional BAU substitutions to stabilise triplex formation at pH 7.0.

Experiments were undertaken under standard footprinting conditions in 10 mM tris containing 50 mM sodium chloride, leaving the complexes to equilibrate overnight at 20 °C. An unusual phenomenon was observed; under these conditions the target DNA was seen to either aggregate or precipitate out of solution. Shortening the incubation time to just 30 minutes reduced this effect. The gels obtained are shown in Figure 4.6. A clear footprint is evident with the target containing a central AT bp (left hand panel), whilst the rest of the cleavage pattern remains unaffected. Quantitative analysis of the bands within this footprint produced a C_{50} value of 0.4 ± 0.1 μM. A much weaker

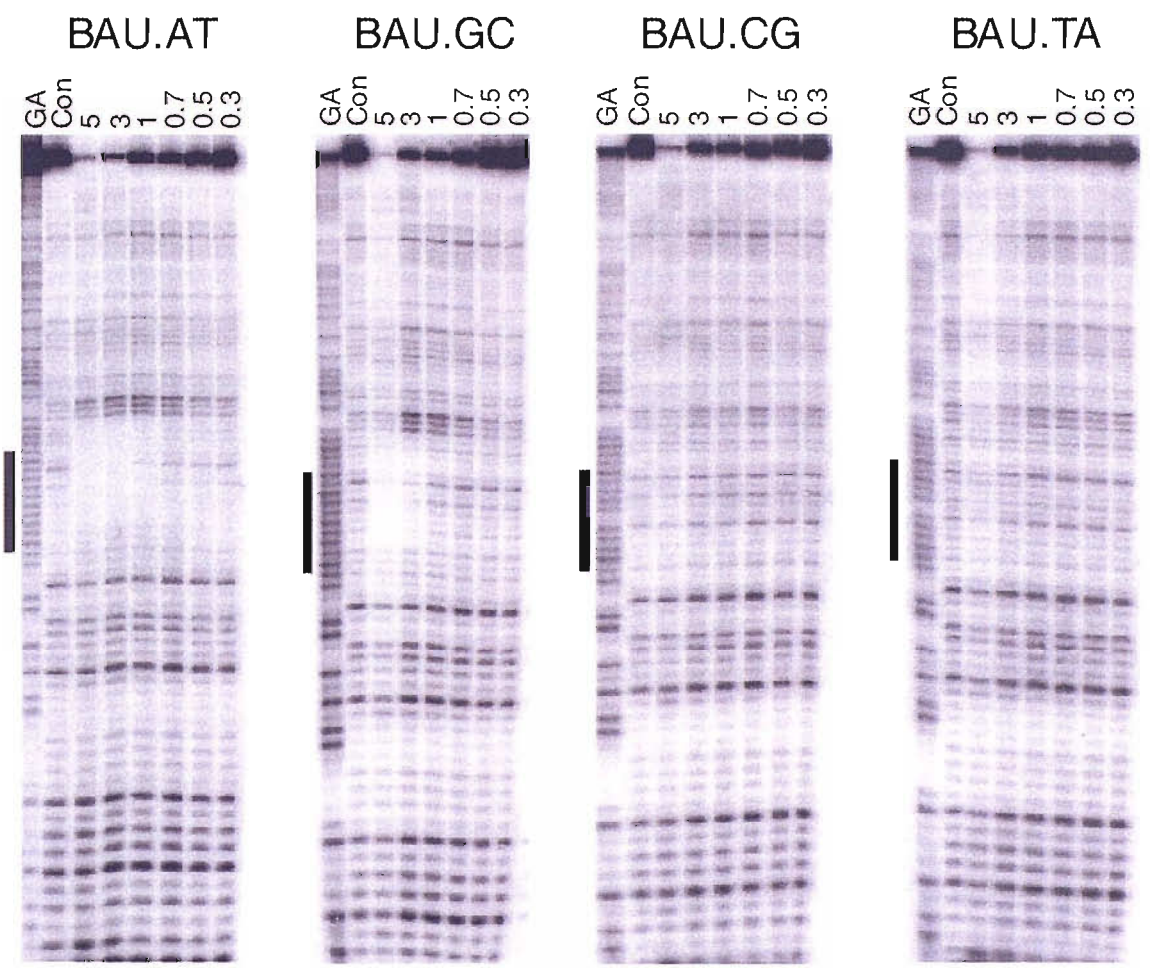

Figure 4.6 DNase I cleavage patterns of different *tyr*T(43-59) fragments in the presence of a TFO containing 2′-aminoethoxy,5-propargylamino-U at pH 7.0. Experiments used the oligonucleotide 5′-BCBCBTBTBTCT, where B is BAU, with DNA fragments derived from *tyr*T(43-59) containing each base pair in turn at the centre of the oligopurine tract. This generated the central triplets B.AT, B.TA, B.GC and B.CG (indicated). These experiments were performed in standard microcentrifuge tubes. The experiments were performed in 10 mM tris containing 50 mM sodium chloride at pH 7.0 and the complexes were left at 20 °C for 30 minutes to equilibrate. The oligonucleotide concentration (μM) is shown at the top of each gel lane. Tracks labelled 'GA' are Maxam-Gilbert markers specific for purines, while 'con' indicates DNase I cleavage in the absence of added oligonucleotide. The filled boxes show the position of the triplex target sites.

footprint is evident with the target generating a BAU.GC triplet (at concentration of 3 μM and above), while no interaction is seen with the TA or CG targets. The experiment was repeated with the unmodified oligonucleotide 5′-TCTCTTTTTTCT. As expected, this did not produce footprints at any of these target sequences at concentrations as high as 30 μM and the presence of 10 mM magnesium chloride.

At a later stage this experiment was repeated with hydrophobic microcentrifuge tubes, to assess whether this affected the target precipitation and/or the binding of the heavily modified TFO. This time no precipitation was evident after incubating overnight. The gels obtained are shown in Figure 4.7 and a comparison between the two sets of gels demonstrates a clear difference. The same selectivity is observed; a clear footprint is evident with the target containing a central AT and a weaker footprint was observed against GC, but both footprints persist to lower TFO concentrations. Quantitative analysis of the footprint at the AT target produced a C_{50} value of 5.5 ± 5 nM whereas the GC target produced a C_{50} value of 91 ± 15 nM. Again no interaction with TA or CG was observed at concentrations as high as 5 μM. This suggests at least a 20-fold difference in affinity between intended target and the least destabilising mismatch and clearly corroborates the results obtained from fluorescence melting; BAU produces very stable triplets with AT bp and enhanced discrimination against CG and TA bp.

The clear difference in affinity of this heavily modified TFO suggests that the positive charges present within the oligonucleotide may result in the TFO 'sticking' to the standard microcentrifuge tube. As this is likely to depend on the base composition of the TFO the results presented in the remainder of this chapter were obtained using hydrophobic microcentrifuge tubes.

4.3.2. Decreasing the pH dependency of triplex formation

4.3.2.1 Triplex formation with 3-methyl,2-aminopyridine

The specificity of 3-methyl,2-aminopyridine (^{Me}P) in triplex formation was assessed by determining the T_m of the fluorescently-labelled intermolecular triplexes shown in Figure 4.3A. A single ^{Me}P substitution was incorporated at the centre of the 18mer TFO (indicated by X in Figure 4.3A(i)) and this was targeted against four duplexes in which ZY was each base pair in turn. These experiments were carried out in 50 mM sodium

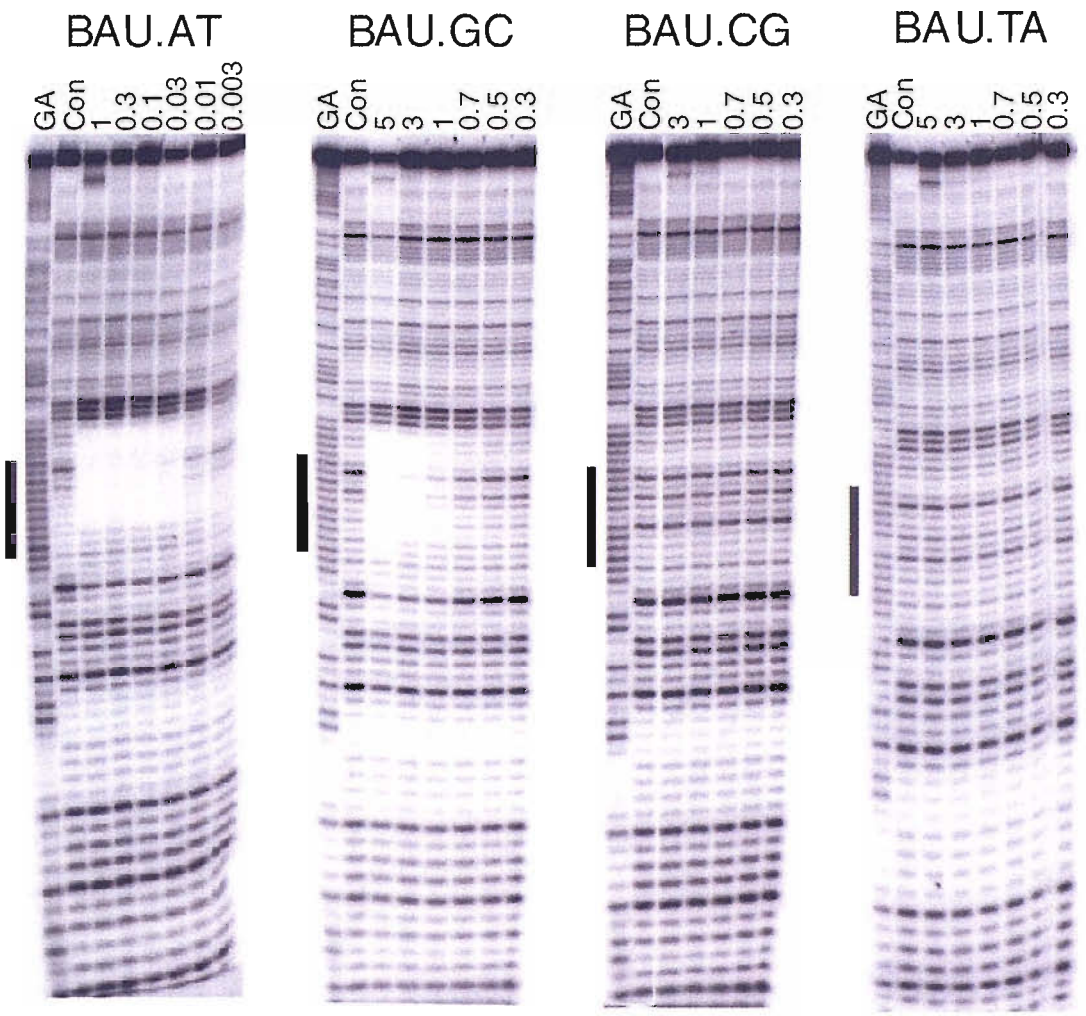

Figure 4.7 DNase I cleavage patterns of different *tyr*T(43-59) fragments in the presence of a TFO containing 2´-aminoethoxy,5-propargylamino-U at pH 7.0. Experiments used the oligonucleotide 5´-BCBCBTBTBTCT, where B is BAU, with DNA fragments derived from *tyr*T(43-59) containing each base pair in turn at the centre of the oligopurine tract. This generated the central triplets B.AT, B.TA, B.GC and B.CG. These experiments were performed in hydrophobic microcentrifuge tubes. The experiments were performed in 10 mM tris containing 50 mM sodium chloride at pH 7.0 and the complexes were left at 20 °C overnight to equilibrate. The oligonucleotide concentration (μM) is shown at the top of each gel lane. Tracks labelled 'GA' are Maxam-Gilbert markers specific for purines, while 'con' indicates DNase I cleavage in the absence of added oligonucleotide. The filled boxes show the position of the triplex target sites.

acetate containing 200 mM sodium chloride at the appropriate pH.

Representative melting profiles obtained for the triplexes formed by this analogue at pH 6.0 are shown in Figure 4.8 (left panel). The melting temperatures calculated from these and those obtained at pH 5.0 and 5.5 are shown in Table 4.3. These T_ms can be compared directly with those obtained for the TFOs containing natural bases (Table 3.1). The melting curves clearly show that ^{Me}P binds with the greatest affinity against a GC bp (green line) and examination of the T_ms reveals that the ^{Me}P.GC triplet is more stable than C.GC at all pH values. This is greater at higher pH, with a difference of 3.5 °C at pH 6.0. At pH 5.0, triplexes containing C$^+$.GC and ^{Me}P.GC are more stable than those containing T.AT, thought this difference decreases as the pH increases, emphasising the importance of protonation. It was not possible to investigate this analogue at a greater pH than 6.0 as the TFO also contained several unmodified cytosine residues that required protonation.

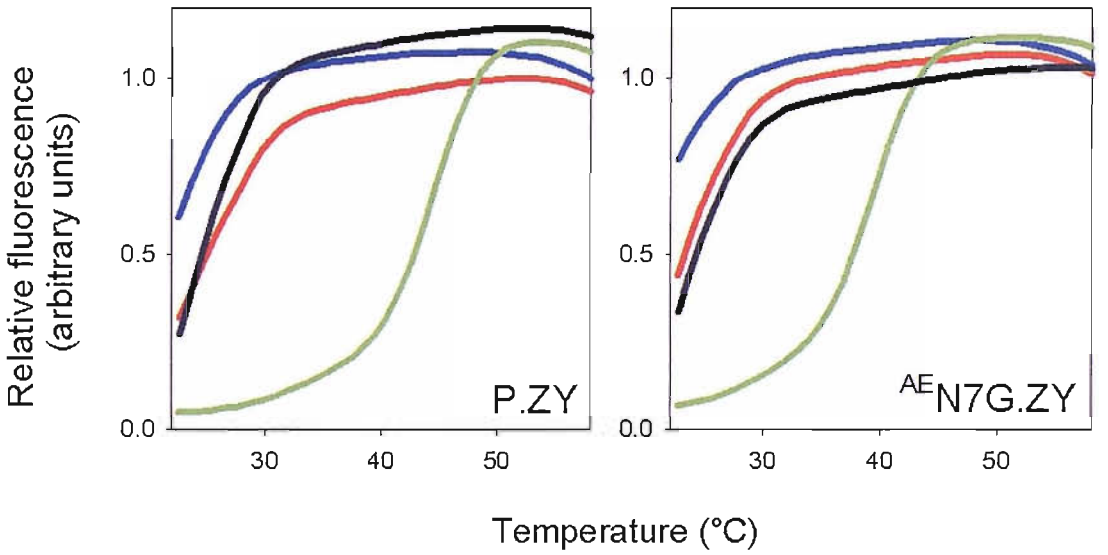

Table 4.8 Fluorescence melting curves showing the interaction of TFOs containing 3-methyl,2-amino pyridine or 2′-aminoethoxy,N7G with duplex targets containing a variable central base pair at pH 6.0. The experiments were performed in 50 mM sodium acetate, containing 200 mM NaCl. The y-axes show the normalised fluorescence (arbitrary units), while the x-axes shows the temperature (°C). The samples were heated at a rate of 0.2 °C min^{-1}.

Further examination of Table 4.3 shows that ^{Me}P also produced less stable complexes when positioned against CG and AT base pairs compared to C. For example, the difference in T_m at pH 5.0 between C.CG and ^{Me}P.CG is 2.5 °C and the difference between C.AT and ^{Me}P.AT is 1.5 °C. Furthermore, at pH 6.0 the difference between the

most stable triplet X.GC and second most stable triplet formed by this base, X.TA, is at least 16 °C, this compares to a 12 °C difference for C. In contrast, the ^{Me}P.TA triplet is slightly more stable than the C.TA triplet with a difference of about 3.5 °C at pH 5.0. ^{Me}P differs from C by the loss of the 2-carbonyl and is likely to be the reason for its altered selectivity relative to C.

		ZY			
X	pH	AT	TA	GC	CG
C	5.0	55.3 (55.2)	53.4 (53.7)	67.4 (65.9)	57.6 (57.7)
	5.5	39.8 (39.4)	38.7 (38.6)	56.6 (56.7)	43.7 (43.4)
	6.0	< 28.0	< 28.0	41.1 (41.2)	28.9 (28.7)
^{Me}P	5.0	53.8 (53.9)	56.6 (56.4)	67.9 (65.6)	55.0 (54.7)
	5.5	38.7 (38.8)	42.5 (42.4)	58.0 (58.3)	40.4 (40.4)
	6.0	< 28.0	< 28.0	44.6 (44.5)	< 28.0
^{AE}N7G	5.0	53.4 (53.7)	55.3 (55.4)	64.9 (64.1)	55.5 (55.7)
	5.5	38.0 (37.7)	40.9 (40.7)	54.5 (54.4)	40.4 (40.4)
	6.0	< 28.0	< 28.0	40.3 (40.4)	< 28.0

Table 4.3 T_m values determined by fluorescence melting for triplexes composed of triplets containing 3-methyl,2-amino pyridine or 2´-aminoethoxy,N7G using a temperature gradient of 0.2 °C min^{-1} and the quencher methyl red serinol. Values in parenthesis were calculated from the annealing phase. Each value is an average of three separate determinations which usually differed by less than 0.5 °C.

4.3.2.2 Triplex formation with 2´-aminoethoxy,N7G

The 2´-aminoethoxy derivative of the analogue N7G (^{AE}N7G) was examined in the same manner as above, this time X in the TFO shown in Figure 4.3A(i) was ^{AE}N7G. Representative melting profiles obtained for the triplexes formed by this analogue at pH 6.0 are shown in Figure 4.8 (right panel). The melting temperatures calculated from these and those obtained at pH 5.0 and 5.5 are shown in Table 4.3. Unlike the aminoethoxy and guanidinoethoxy uracil analogues studied earlier in the chapter, annealing and melting profiles obtained with this analogue showed no hysteresis at a temperature gradient of 0.2 °C min^{-1}. Examination of Table 4.4 reveals that at all pH values ^{AE}N7G exhibited slightly lower affinity for GC than C. The difference was less at pH 6.0, with a difference of T_m of 1 °C. As this base recognises GC in a pH independent fashion it is likely that it will bind more strongly to GC than C at higher pH values.

Examination of the T_ms obtained when positioning this base opposite the three remaining base pairs reveals a better selectivity than C, producing less stable complexes against CG and AT than C, which were 2 °C less stable than the equivalent C-containing triplets at pH 5.0. In contrast, a slight increase in affinity for TA relative to C.TA is evident, though this is not surprising since unmodified G is known to recognise TA. A comparison between ^{AE}N7G.TA and G.TA (Table 3.1) shows that that ^{AE}N7G recognises TA with a lower affinity in this arrangement.

4.3.3.3 Triplex formation with 2´-aminoethoxy 6-oxo-cytidine

The 2´-aminoethoxy 6-oxo-cytidine (^{AE}6-oxo-C) analogue was investigated in a different manner to above. In this study the affinity of several modified TFOs of different lengths were compared with equivalent TFOs containing natural bases. The oligonucleotides employed are shown in Figure 4.3A(ii), these were positioned opposite the duplex shown in Figure 4.3A(i) when ZY is AT. The modified TFOs employed were 10, 15 and 18 bases long and contained 1, 2 and 3 ^{2AE}6-oxo-C residues in place of C respectively.

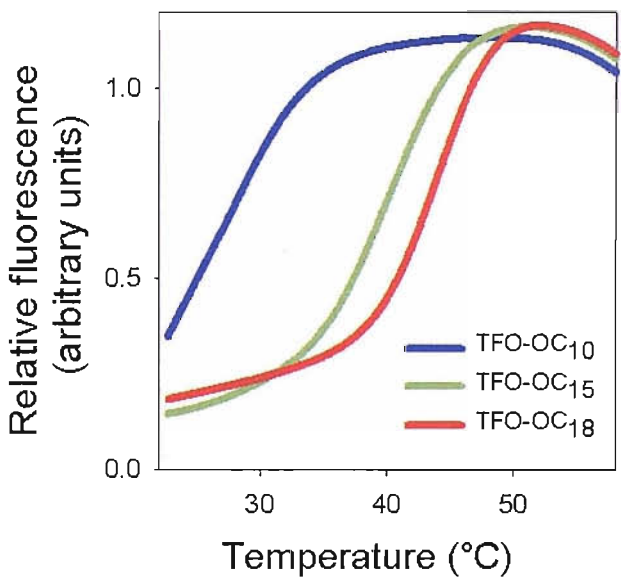

Figure 4.9 Fluorescence melting curves showing the interaction of TFOs of different lengths containing different numbers of 2´-aminoethoxy,6-oxo-C with the AT-containing duplex target at pH 6.0. The experiments were performed in 50 mM sodium acetate containing 200 mM NaCl. The y-axis show the normalised fluorescence (arbitrary units), while the x-axis shows the temperature (°C). The samples were heated at a rate of 0.2 °C min^{-1}.

Representative melting profiles for these modified triplexes at pH 6.0 are shown in Figure 4.9 and the melting temperatures obtained from them and those at pH 5.0 are shown in Table 4.5. These data can be compared with the data obtained for the unmodified triplexes shown in Chapter 3 (Table 3.3 and 3.4). Examination of the T_ms for both modified and unmodified triplexes reveals that in all cases the TFOs containing ^{AE}6-oxo-C were less stable than their unmodified counterparts. However, the extent of destabilisation was again dependent on the pH. For example, at pH 5.0 the differences in T_m between the modified and unmodified triplexes were 5, 4.3 and 11.6 °C for the 18, 15 and 10mer TFOs whereas at pH 6.0 this difference drops to 1.1, 1.7 and 5.6 °C for the same complexes. This suggests that in a similar manner to ^{AE}N7G, this analogue produces a complex of lower stability than C at pH 5.0 but should be more stabilising at pH 7.0 due to its pH independent mode of recognition.

X	pH	T_m
TFO-OC_{18}	5.0	59.9 (60.2)
	6.0	43.9 (44.0)
TFO-OC_{15}	5.0	57.3 (57.5)
	6.0	40.8 (40.9)
TFO-OC_{10}	5.0	38.2 (38.0)
	6.0	28.5 (28.4)

Table 4.4 T_m values determined by fluorescence melting for triplexes of different lengths containing different numbers of ^{AE}6-oxo-C using a temperature gradient of 0.2 °C min^{-1}. Values in parenthesis were calculated from the annealing phase. Each values is an average of three separate determinations which usually differed by less than 0.5 °C.

4.3.3 Combining nucleoside analogues to achieve triplex formation at pH 7.0

This section focuses on achieving recognition of oligopurine sequences at physiological pH using TFOs containing multiple substitutions of U^P, BAU, P or ^{Me}P, generating U^P.AT, BAU.AT, P.GC and ^{Me}P.GC triplets.

*4.3.3.1 TFOs containing non-*contiguous 2′-aminoethoxy,5-propargylamino-U *substitutions*

The pH dependency and affinity of TFOs containing different numbers of BAU substitutions was examined. The oligonucleotides 5′-TCTCTTTBTTCT (1BAU), 5′-TCTCTTTBTBCT (2BAU), 5′-TCTCTBTBTBCT (3BAU) and 5′-BCBCBTBTTBCT

(5BAU) contained 1, 2, 3 and 5 substitutions of BAU, respectively. Their affinity was compared with the control oligonucleotide 5′-TCTCTTTTTTCT and the oligonucleotide 5′-TCTCTU^{P}TU^{P}TTCT (2U^{P}) that contained 2 substitutions of U^{P}. Their interaction with the tyr*T*(43-59) DNA fragment was studied at pH values between 5.0 and 7.5. The sequence of the duplex target site is 5′-AGAGAAZAAAGA/3′-TCTCTTTTTTCT and is found at the 3′-end of the polypurine tract within tyr*T*(43-59). This is the same target as used in the BAU selectivity studies presented above. The experiments at pH 5.0 were carried out in 50 mM sodium acetate, at pH 6.0 in 10 mM pipes containing 50 mM sodium chloride and at pH 7.0 in 10 mM Tris containing 50 mM sodium chloride, leaving the complexes to equilibrate overnight at 20 °C. The cleavage patterns for the interaction of these oligonucleotides obtained are shown in Figure 4.10 and 4.11.

The cleavage pattern of the tyr*T*(43-59) fragment in the presence of the unmodified oligonucleotide at pH 5.0 is shown in Figure 4.10. This oligonucleotide shows no interaction with its intended target at concentrations as high as 30 μM (left panel), but binds well on addition of 2.5 mM magnesium chloride and a clear footprint is evident (right panel). Quantitative analysis of the bands within this footprint produced a C_{50} value of 58 ± 1 nM. Cleavage patterns of the fragment in the presence of the oligonucleotide where two of the third strand Ts are replaced with U^{P} are shown in Figure 4.10. Again the oligonucleotide shows no interaction with its target in the absence of magnesium (left panel), but binds well in the presence of magnesium (right panel). Quantitative analysis of the bands within this footprint produced a C_{50} value of 22 nM ± 2. Under these conditions the TFO containing U^{P} binds with about a 3-fold greater affinity than the unmodified TFO.

The cleavage patterns of the tyr*T*(43-59) fragment in the presence of the BAU-substituted oligonucleotides at pH 5.0 are shown in Figure 4.11. Examination of these gels reveals that in each case a footprint is evident at the intended target site (boxed), with no other differences in the cleavage patterns. Triplex formation with these BAU-containing oligonucleotides did not require the addition of magnesium. The affinity of these TFOs was dependent on the number of substituted BAU residues, therefore the oligonucleotide concentrations employed in each gel are different. Quantitative analysis of the bands within each footprint gave C_{50} values of 400 ± 200 nM, 29 ± 10 nM, 8.3 ± 2 nM and < 1 nM for the interaction of the TFOs containing 1, 2, 3 and 5 substitutions

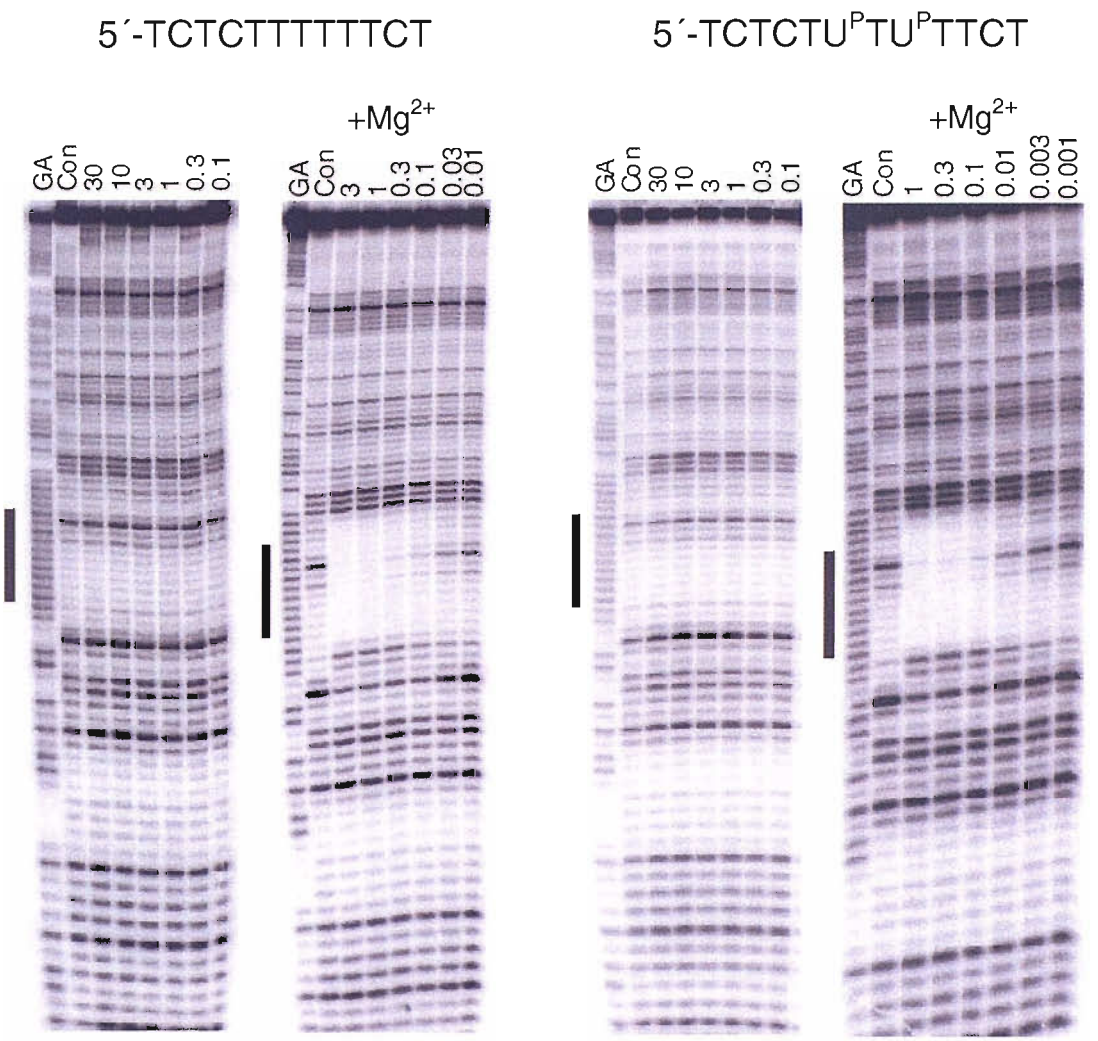

Figure 4.10 DNase I cleavage patterns of *tyr*T(43-59) in the presence of unmodified and 5-propargylamino-dU substituted oligonucleotides at pH 5.0. These experiments were performed in 50 mM sodium acetate in the presence and absence of 2.5 mM magnesium (indicated). The complexes were left overnight at 20 °C to equilibrate. The oligonucleotide concentration (μM) is shown at the top of each gel lane. Tracks labelled 'GA' are Maxam-Gilbert markers specific for purines, while 'con' indicates DNase I cleavage in the absence of added oligonucleotide. The filled boxes show the position of the triplex target sites.

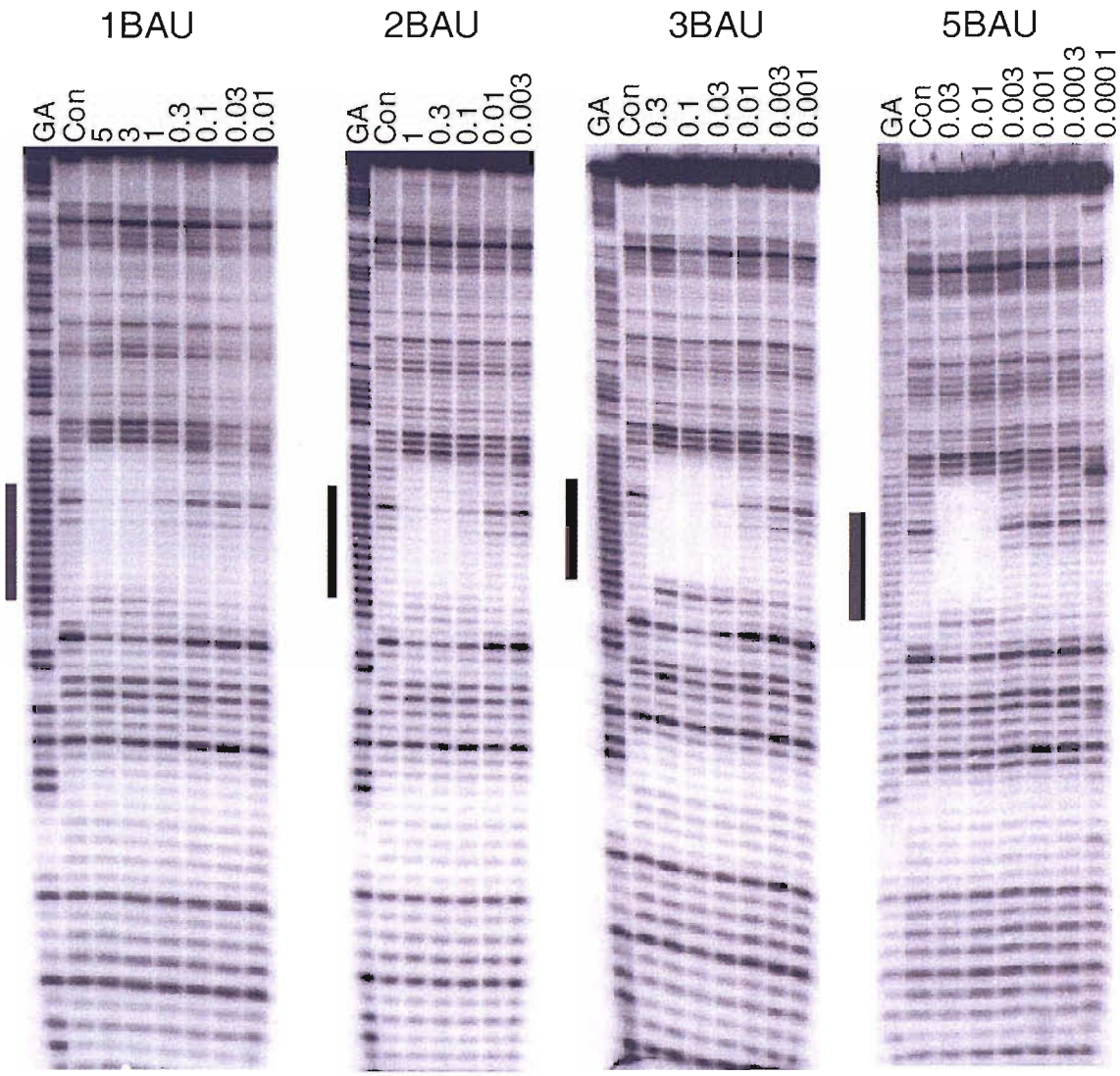

Figure 4.11 DNase I cleavage patterns of *tyr*T(43-59) in the presence of oligonucleotides containing 2´-aminoethoxy,5-propargylamino-U at pH 5.0. These experiments were performed in 50 mM sodium acetate in the absence of magnesium. The complexes were left overnight at 20 °C to equilibrate. The oligonucleotide concentration (μM) is shown at the top of each gel lane. Tracks labelled 'GA' are Maxam-Gilbert markers specific for purines, while 'con' indicates DNase I cleavage in the absence of added oligonucleotide. The filled boxes show the position of the triplex target sites.

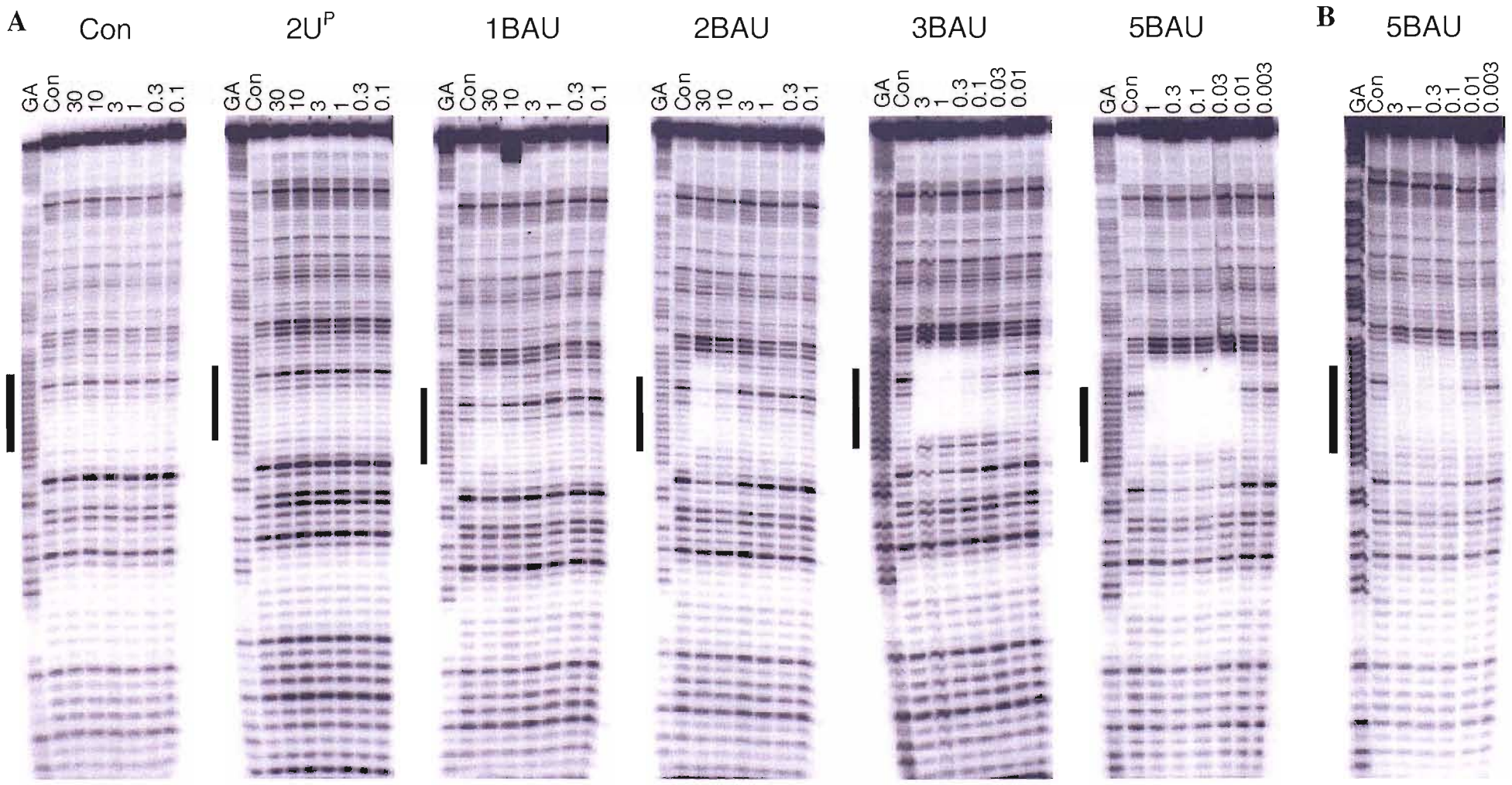

Figure 4.12 DNase I cleavage patterns of *tyr*T(43-59) in the presence of oligonucleotides containing 5-propargylamino-dU or 2´-aminoethoxy,5-propargylamino-U at pH 6.0. These experiments were performed in an appropriate buffer and the complexes were left overnight at 20 °C to equilibrate. The oligonucleotide concentration (μM) is shown at the top of each gel lane. Tracks labelled 'GA' are Maxam-Gilbert markers specific for purines, while 'con' indicates DNase I cleavage in the absence of added oligonucleotide. The filled boxes show the position of the triplex target sites.

of BAU respectively. These values show that for every additional substitution of BAU a further increase in TFO affinity is observed.

The experiment was repeated at pH 6.0, the cleavage patterns for the interaction of the oligonuceotides are shown in Figure 4.12. Examination of these gels reveals that the control oligonucleotide and U^P-containing oligonucleotide do not show any interaction with the target even in the presence of magnesium. The TFO containing a single BAU substitution (1BAU) also failed to produce a footprint at concentrations as high as 30 μM whilst the TFO containing 2 substitutions exhibited a weak interaction at high TFO concentrations (3 μM and above). In contrast, the oligonucleotides 3BAU and 5BAU exhibited footprints that persisted into the nM range. The C_{50} values for the interaction of these oligonucleotides were 6900 ± 1400 nM, 21 ± 2 nM and 1.5 ± 0.9 nM for the oligonucleotides containing 2, 3 and 5 substitutions respectively. It is therefore evident that TFOs containing 2 or more substitutions of BAU extend triplex formation to pH 6.0.

The experiment was repeated at pH 7.0 and pH 7.5 for the oligonucleotides that showed interactions at pH 6.0 At pH 7.0, binding was only evident for the TFO containing 5 substitutions (see Figure 4.7; BAU.AT) and was still evident even at pH 7.5 (Figure 4.11). The C_{50} values for the interaction of this TFO were 5.5 ± 1.3 nM and 80 ±11 nM at pH 7.0 and 7.5 respectively. This study suggests that TFOs containing several BAU substitutions can compensate for the low affinity of unprotonated C residues, extending triplex formation into the nM range at physiological pH.

4.3.3.2 TFOs containing contiguous 2´-aminoethoxy,5-propargylamino-U substitutions

Previous studies have shown that contiguous U^P bases are beneficial to triplex stability (Bijapur *et al.* 1999). This is in contrast to TFOs containing contiguous cytosine. This study looks at the interaction of the modified oligonucleotide 5´-BBBBBBCBT (6BAU) with the *tyr*T(43-59) DNA fragment at different pH values. This is compared with the unmodified oligonucleotide 5´-TTTTTTCTT. The sequence of the duplex target site is 5´-AAAAAAGAA/ 3´-TTTTTTCTT and is found at the 3´-end of the polypurine tract within *tyr*T(43-59). Each experiment was carried out in an appropriate buffer containing 50 mm sodium chloride, leaving the complexes to equilibrate overnight at 20 °C.

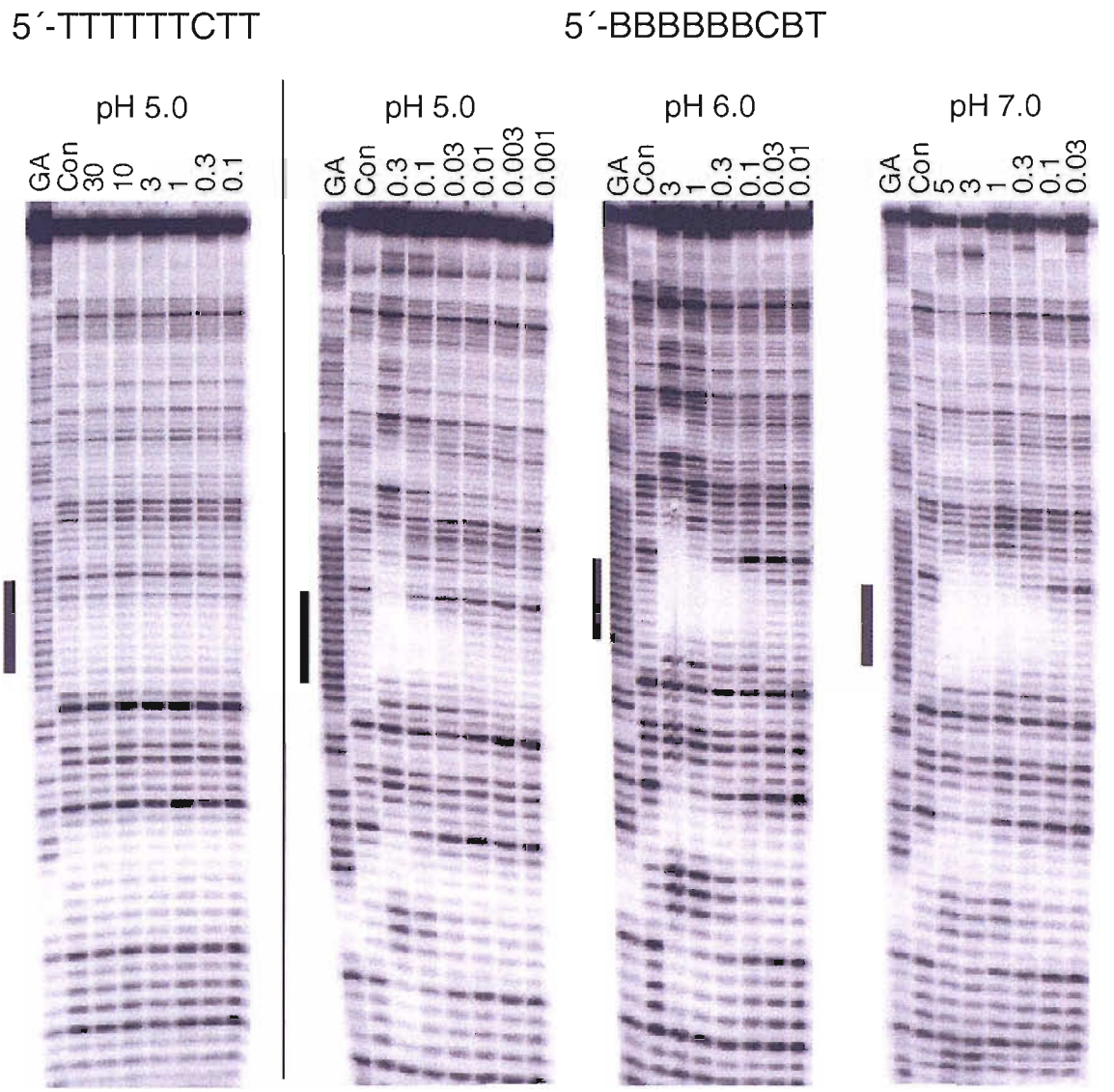

Figure 4.13 DNase I cleavage patterns of *tyr*T(43-59) in the presence of unmodified and 2´-aminoethoxy,5-propargylamino-U substituted oligonucleotides at varying pH values. These experiments were performed in an appropriate buffer at the pH indicated, the complexes were left overnight at 20 °C to equilibrate. The oligonucleotide concentration (μM) is shown at the top of each gel lane. Tracks labelled 'GA' are Maxam-Gilbert markers specific for purines, while 'con' indicates DNase I cleavage in the absence of added oligonucleotide. The filled boxes show the position of the triplex target sites.

The cleavage pattern for the *tyr*T(43-59) fragment in the presence of the control oligonucleotide at pH 5.0 are shown in Figure 4.13, the buffer contained 10 mM magnesium chloride. Examination of the gel reveals that as expected the cleavage pattern is unaltered, showing no interaction of this TFO at concentrations as high as 30 μM. This confirms the result of a previous study (Bijapur *et al.*, 1999).

The cleavage patterns for the *tyr*T(43-59) fragment in the presence of the BAU-containing oligonucleotide is shown in Figure 4.13, each gel was undertaken at a different pH and in each case the concentration of the TFO employed was sufficient to produce a footprint. Examination of the three gels shows that as well as a footprint at the intended target site (boxed) several secondary footprints are also evident. These disappear at low oligonucleotide concentrations, suggesting a much weaker interaction than with the intended target site. A larger footprint is also evident at higher oligonucleotide concentrations, this also suggests this TFO is binding non-specifically within the polypurine tract. The most prominent secondary footprint is seen about 10 bases below the 3´-end of the polypurine tract. Examination of the *tyr*T(43-59) sequence shown if Figure 2.3 indicates that this TFO is binding to the site 5´-GTAA. The reason for this is unclear.

Despite these secondary target sites it is seen that this oligonucleotide exhibits a very high affinity. Quantitative analysis of the bands within the target site give C_{50} values of 12 nM ± 5, 47 nM ± 13, 61 nM ± 11 and 400 nM ± 100 for the interaction of this oligonucleotide at pH 5.0, 6.0, 7.0 and 7.5. As this TFO contains only a single cytosine it is most likely that the decrease in affinity at pH 7.5 can be attributed to loss of protonation of the amino functions of the propargylamino chain and/or aminoethoxy group. It is also apparent that the affinity of the oligonucleotide isn't adversely affected by the contiguous positioning of the BAU substitutions but does affect the specificity of the TFO.

4.3.3.3 Triplex formation in the GT-motif with 2´-aminoethoxy,5-propargylamino-U

BAU was also examined to see whether it could stabilise triplexes that are formed in the GT motif, since the structures are known to be less stable than parallel (CT-containing) triplexes. These experiments used DNase I footprinting to examine the interaction of the 12mer oligonucleotides 3´-TGBGTBTBTBGT and 3´-TGTGTTTTTTGT which are

designed to form antiparallel G.GC, T.AT and BAU.AT triplets, with the tyrT(43-59) DNA fragment. No footprints were evident at oligonucleotide concentrations as high as 10 μM for both the modified and unmodified TFOs at pH 7.0 in the presence of 10 mM magnesium chloride. A similar negative results was observed using oligonucleotides with the reverse polarity, which could in theory form a parallel GT triplex. The interaction of the 12mer oligonucleotides 5′-TGBGTBTBTBGT and 5′-TGTGTTTTTTGT which are designed to form parallel G.GC, T.AT and BAU.AT triplets, with the tyrT(43-59) DNA fragment were examined. No footprints at oligonucleotide concentrations as high as 10 μM for both the modified and unmodified TFOs at pH 7.0 in the presence of 10 mM magnesium chloride.

A similar result was also obtained for oligonucleotides containing U^P (Darby, 2001) and suggests that stabilisation of parallel triplexes by BAU or U^P results from specific interactions with the amino substituents, and not from non-specific charge interactions.

4.3.3.4 TFOs containing 2-aminopyridine or 3-methyl,2-aminopyridine

The above study showed that the unmodified oligonucleotide 5′-TCTCTTTTTTCT binds well with its 11-base pair target site at pH 5.0 in the presence of magnesium but fails to give a footprint even at a concentration of 30 μM at pH 6.0 and 7.0. This is attributed to the presence of three C residues within the third strand. This study examines the effect of substituting one or all of the Cs within this oligonucleotide with the cytosine analogues P or ^{Me}P. The oligonucleotides 5′-TPTPTTTTTTPT (3P), 5′-TCT^{Me}PTTTTTTCT ($1^{Me}P$) and 5′-T^{Me}PT^{Me}PTTTTTT^{Me}PT ($3^{Me}P$) were examined for their interaction with the same target site at different pH values. Experiments were carried out in the same buffers as above, leaving the complexes to equilibrate overnight at 20 °C. These oligonucleotides failed to generate footprints at pH 5.0 at a concentration of 30 μM in the absence of magnesium, therefore 2.5 mM magnesium chloride was employed in each assay. The DNase I digestion patterns showing the interaction of these modified oligonucleotides at pH 5.0 and 6.0 are shown in Figure 4.14.

The left panels of Figure 4.14 shows representative footprinting patterns obtained at pH 5.0 for each of the three modified oligonucleotides. All three exhibit a single footprint at their intended target site, producing C_{50} values of 50 ± 8 nM, 170 ± 8 nM and 200 ± 100 nM for the interaction of the oligonucleotides $1^{Me}P$, 3P and $3^{Me}P$. From the above study

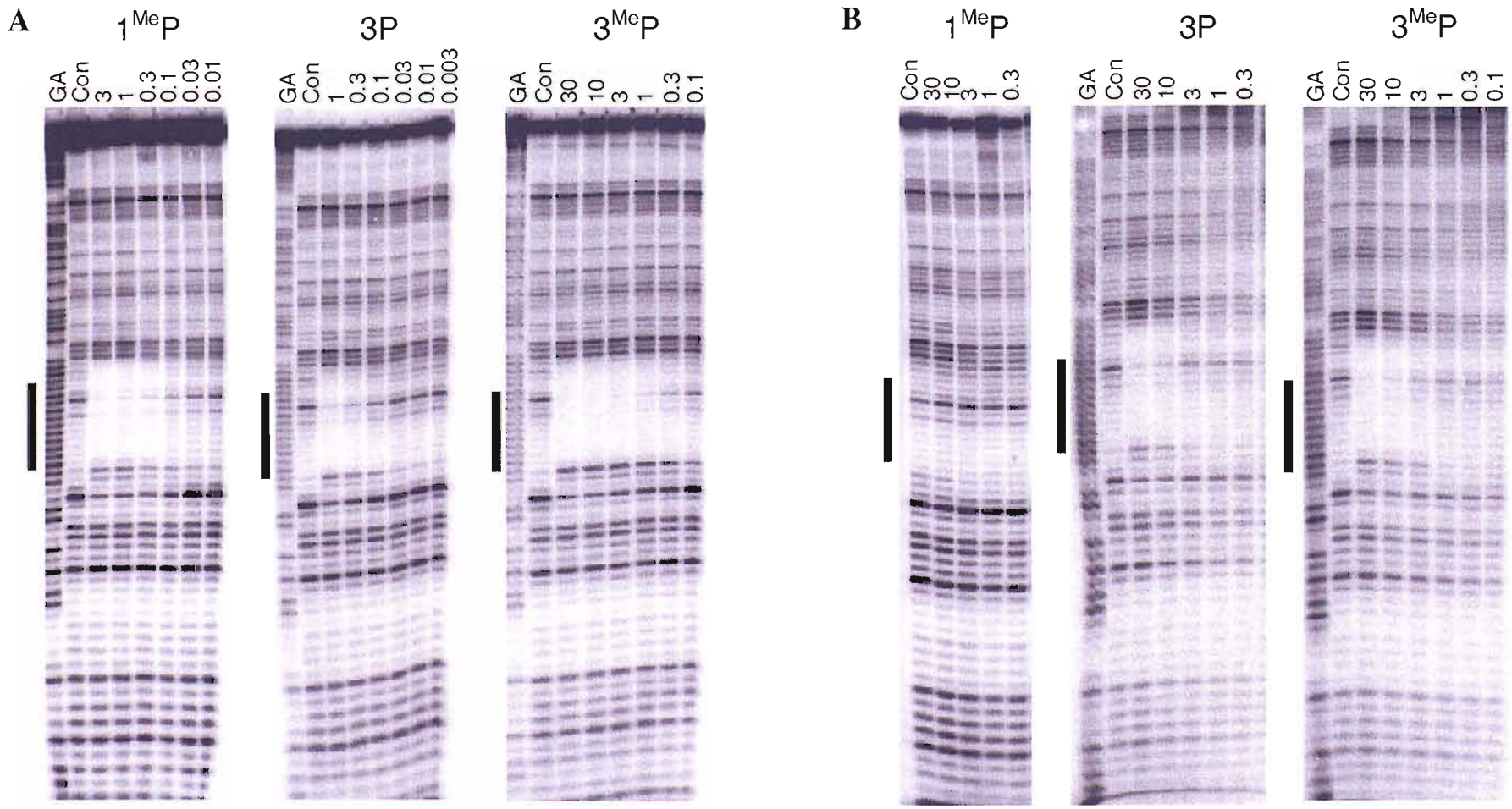

Figure 4.14 DNase I cleavage patterns of *tyr*T(43-59) in the presence of oligonucleotides containing 2-aminopyridine or 3-methyl,2-aminopyridine at pH 5.0 (A) and 6.0 (B). These experiments were performed in an appropriate buffer and the complexes were left overnight at 20 °C to equilibrate. The oligonucleotide concentration (μM) is shown at the top of each gel lane. Tracks labelled 'GA' are Maxam-Gilbert markers specific for purines, while 'con' indicates DNase I cleavage in the absence of added oligonucleotide. The filled boxes show the position of the triplex target site.

the unmodified oligonucleotide exhibited a C_{50} of 58 nM ± 1. The data show that replacement of a single C with ^{Me}P has little affect on the affinity, a similar result to that obtained by fluorescence melting. In contrast, the replacement of all three Cs with P or ^{Me}P leads to a slight reduction in affinity relative to the unmodified oligonucleotide.

The right panels of Figure 4.14 shows representative footprinting patterns obtained at pH 6.0 for each of the three modified oligonucleotides. It can be seen that replacement of a single C with ^{Me}P fails to increase the binding affinity of the TFO, as it fails to produce a clear footprint. In contrast the TFOs containing either three P or ^{Me}Psubstitutions exhibit a footprint in the μM range. Analysis of the bands within the footprints yields C_{50} values of 6.3 ± 1 μM and 6.9 ± 1.4 μM for the P- and ^{Me}P-containing TFO respectively. The data show that the substitution of each cytosine within the TFO with either P or ^{Me}P extends triplex formation to pH 6.0 in the presence of magnesium. The experiments was repeated at pH 7.0 however no footprints were observed.

4.3.3.5 TFOs containing 2′-aminoethoxy,5-propargylamino-U and 3-methyl,2-aminopyridine

The data presented above demonstrate that TFOs containing either 2 substitutions of BAU for T or 3 substitutions of P or ^{Me}P for C leads to stable triplex formation at pH 6.0. This study examines the triplex-forming ability of oligonucleotides containing substitutions for both T and C. The oligonucleotides 5′-TCTP^{Me}TTTBTTCT (1^{Me}P1B), 5′-TCT^{Me}PTBTBTT^{Me}PT (2^{Me}P2B) and 5′-T^{Me}PT^{Me}PTBTBTB^{Me}PT (3^{Me}P3B) contained one, two or three substitutions of both ^{Me}P and BAU at equivalent positions to the mono-substituted TFOs presented previously. Whereas the oligonucleotide 5′-T^{Me}PB^{Me}PBBTTTT^{Me}PT (3^{Me}P3B$_{clu}$) has the same base composition as 3^{Me}P3B, but in this instance the modifications are placed together towards the 5′-end of the oligonucleotide rather than being distributed throughout the third strand. These oligonucleotides are compared with the same unmodified oligonucleotide as in the last study and the oligonucleotide TCTPTU^{P}TU^{P}TTPT (2P2U^{P}) that contained two P and U^{P} residues. Their interaction with the *tyr*T(43-59) DNA fragment was examined by DNase I footprinting. Each experiment was carried out in an appropriate buffer containing 50 mM sodium chloride, leaving the complexes to equilibrate overnight at 20 °C. Figure 4.15A shows the interaction of the BAU- and ^{Me}P-containing oligonucleotides at pH 5.0 in the absence of magnesium. Examination of the gels (left panel) reveals that all

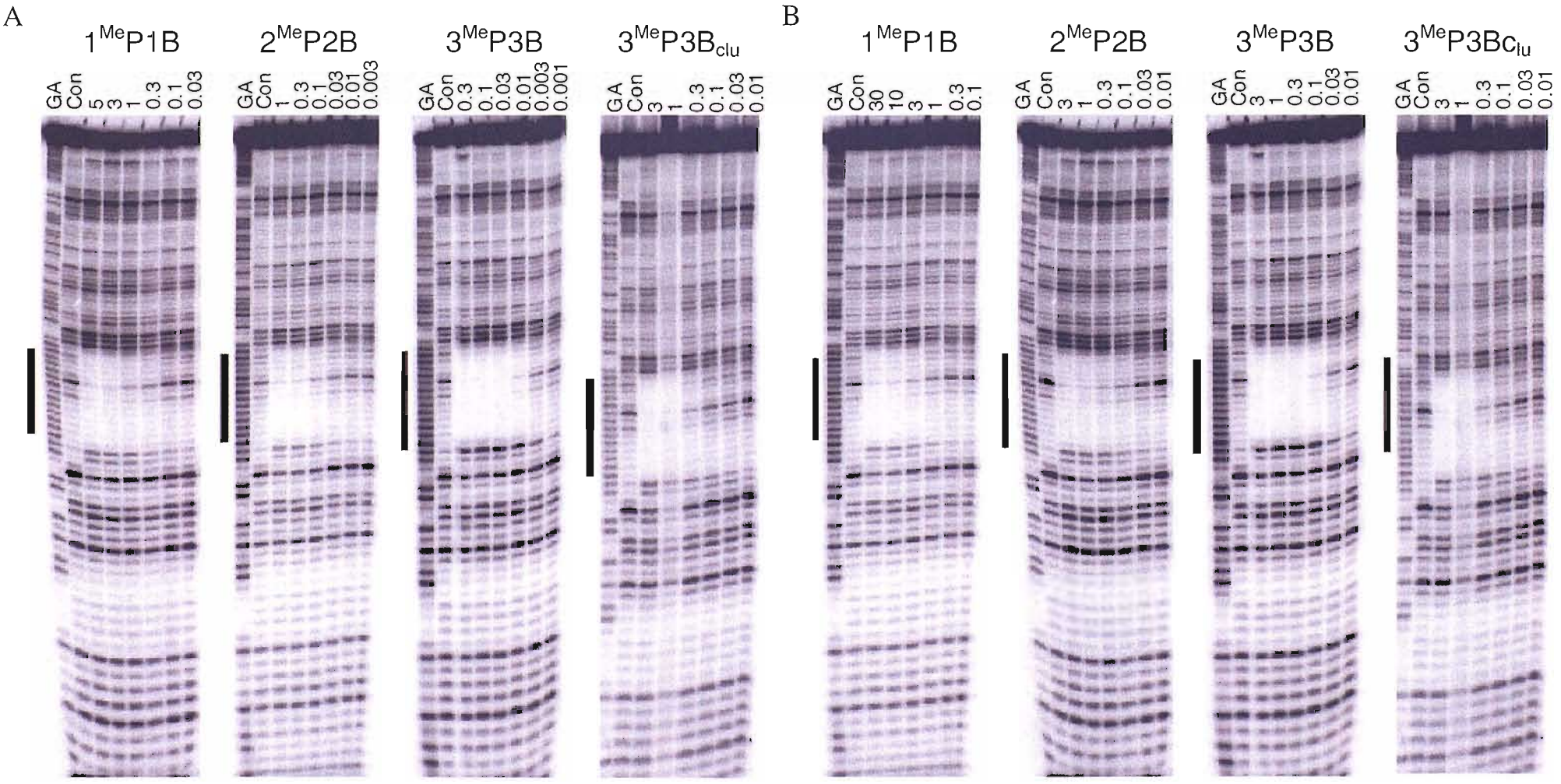

Figure 4.15 DNase I cleavage patterns of *tyr*T(43-59) in the presence of oligonucleotides containing 3-methyl,2-aminopyridine and 2´-aminoethoxy,5-propargylamino-U at pH 5.0 (A) and 6.0 (B). These experiments were performed in an appropriate buffer and the complexes were left overnight at 20 °C to equilibrate. The oligonucleotide concentration (μM) is shown at the top of each gel lane. Tracks labelled 'GA' are Maxam-Gilbert markers specific for purines, while 'con' indicates DNase I cleavage in the absence of added oligonucleotide

oligonucleotides produce clear footprints with their intended target sites and did not affect the remainder of the cleavage pattern. Quantification of the bands within these footprints yielded C_{50} values of 500 nM ± 300, 39 nM ± 8, 3 nM ±1 and 40 nM ± 7 for 1^{Me}P1B, 2^{Me}P2B, 3^{Me}P3BAU and $3^{Me}P3B_{clu}$. These values suggest that as the number of substitutions increases so does the affinity of the TFO, with one exception, the oligonucleotide $3P^{Me}3B_{clu}$ produces a complex that is 13-fold less stable than $3P^{Me}3B$ and about as stable as the TFO containing two substitutions of each analogue. All TFOs are at least as stable as the equivalent oligonucleotides containing BAU and C (not ^{Me}P).

The cleavage patterns for *tyr*T(43-59) in the presence of the same oligonucleotides at pH 6.0 are shown in Figure 4.15B. At this pH, both the unmodified oligonucleotide and the oligonucleotide $2P2U^{P}$ fail to generate footprints at oligonucleotide concentrations as high as 30 μM (not shown). Examination of the gels shows that the TFO containing a single substitution of BAU and ^{Me}P fails to produce a footprint whilst the remaining oligonucleotides produce clear footprints that generate C_{50} values of 200 ± 100 nM, 8 ± 5 nM and 400 ± 100 nM for 2^{Me}P2BAU, 3^{Me}P3BAU and $3^{Me}P3BAU_{clu}$ respectively. As expected these complexes are less stable than those produced at pH 5.0. These results again suggest the arrangement of substitutions is important as $3^{Me}P3B_{clu}$ exhibits a lower affinity than 3^{Me}P3B.

The cleavage patterns for *tyr*T(43-59) in the presence of the same oligonucleotides at pH 7.0 and 7.5 are shown in Figure 4.16A. The oligonucleotides containing 2 and 3 separated substitutions of BAU and ^{Me}P show clear footprints whilst the oligonucleotide containing 3 clustered substitutions of each base fails to produce a complex at oligonucleotide concentrations as high as 30 μM. The C_{50} values for the interaction of the TFOs 3^{Me}P3BAU and 3^{Me}P3BAU were 600 ± 100 nM and 35 ± 4 nM. As expected, these complexes are less stable than at low pH, but have submicromolar affinity at pH 7.0. Repeating the experiment at pH 7.5 with the oligonucleotide with two substitutions of each residue failed to produce a footprint, whilst the interaction of the oligonucleotide containing three residues (3^{Me}P3B) is shown in Figure 4.16B. This oligonucleotide produced a clear footprint with a C_{50} of 200 nM ± 100. These results demonstrate that BAU and ^{Me}P can act to cooperatively to enhance triplex stability and extend triplex formation to physiological pH when they are separated within a TFO.

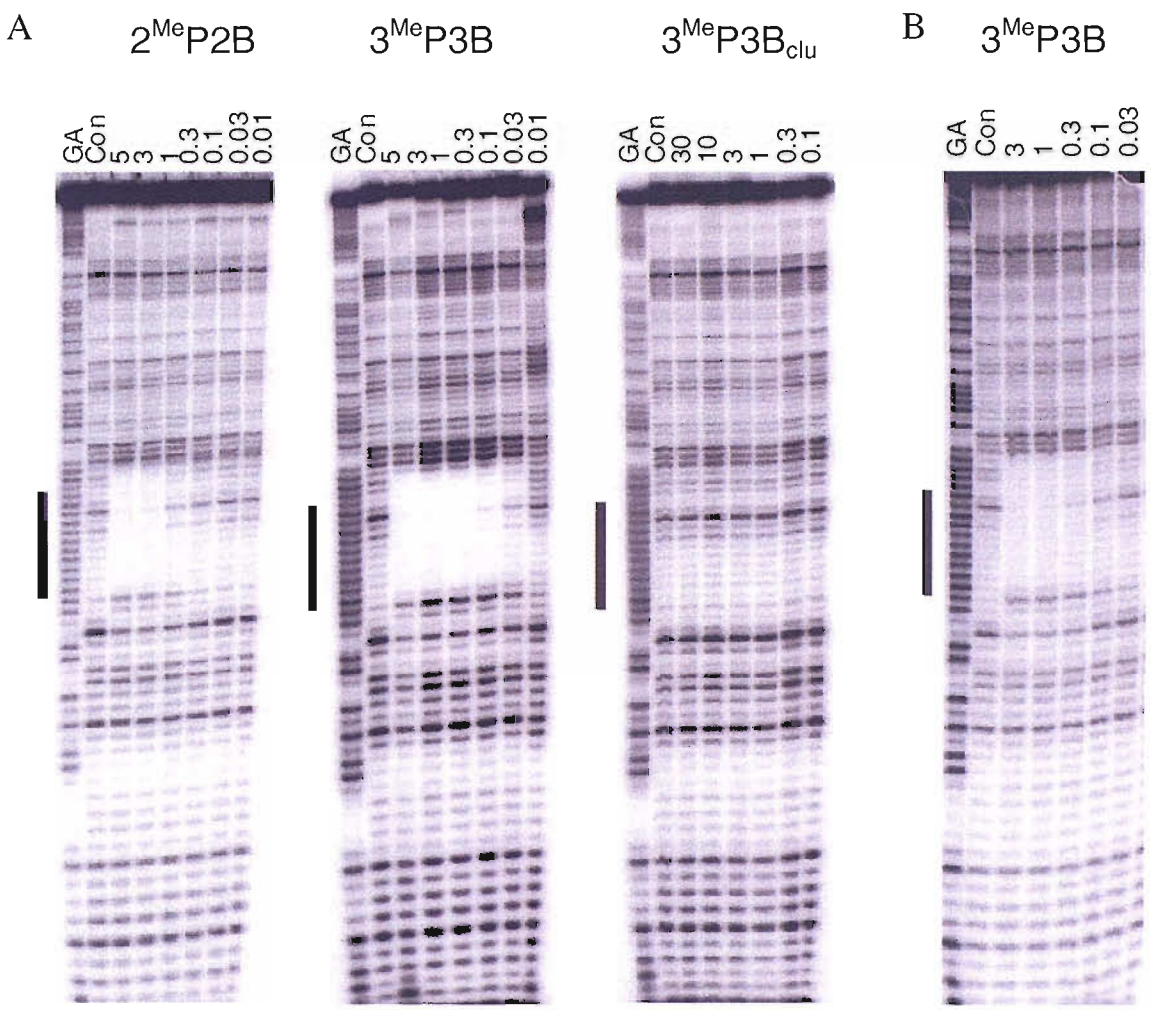

Figure 4.16 DNase I cleavage patterns of *tyr*T(43-59) in the presence of oligonucleotides containing 3-methyl,2-aminopyridine and 2′-aminoethoxy,5-propargylamino-U at pH 7.0 (A) and 7.5 (B). These experiments were performed in an appropriate buffer and the complexes were left overnight at 20 °C to equilibrate. The oligonucleotide concentration (μM) is shown at the top of each gel lane. Tracks labelled 'GA' are Maxam-Gilbert markers specific for purines, while 'con' indicates DNase I cleavage in the absence of added oligonucleotide. The filled boxes show the position of the triplex target sites.

TFO	sequence	pH 5.0	6.0	7.0	7.5
Con[a]	5′-TTTTTTCTT	n.d	n.d	-	-
6BAU	5′-**BBBBBB**CBT	12 nM ± 5	47 nM ± 13	61 nM ± 11	400 nM ± 100
Con[a]	5′-TCTCTTTTTTCT	58 nM ± 1	n.d	-	-
3P[a]	5′-T**P**T**P**TTTTTT**P**T	170 nM ± 8	6300 nM ±1000	n.d	-
$2U^{P}$[a]	5′-TCTCT**U**^{P}T**U**^{P}TTCT	22 nM ± 2	n.d		-
$2U^{P}2P$[a]	5′-T**P**T**P**T**U**^{P}T**U**^{P}TT**P**T	15 nM ± 2	3200 nM ± 500	n.d	-
$1^{Me}P$	5′-TCT**P**^{Me}TTTTTTCT	50 nM ± 8	n.d	-	-
1BAU	5′-TCTCTTT**B**TTCT	400 nM ± 200	n.d	-	-
$1^{Me}P1B$	5′-TCT**P**^{Me}TTT**B**TTCT	500 nM ± 300	n.d	-	-
2BAU	5′-TCTCT**B**T**B**TTCT	29 nM ±10	6900 nM ± 1400	n.d	-
$2^{Me}P2B$	5′-TCT**P**^{Me}T**B**T**B**TT**P**^{Me}T	39 nM ± 8	200 nM ± 100	600 nM ± 100	n.d
$3^{Me}P$	5′-T**P**^{Me}T**P**^{Me}TTTTTT**P**^{Me}T	200 nM ± 100	3200 nM ±1000	n.d	-
3BAU	5′-TCTCT**B**T**B**T**B**CT	8.3 nM ± 2	21 nM ± 2.0	n.d	-
$3^{Me}P3B$	5′-T**P**^{Me}T**P**^{Me}T**B**T**B**T**BP**^{Me}T	2.8 nM ± 1	7.6 nM ± 5.4	35 nM ± 4.0	0.2 μM ± 0.1
$3^{Me}P3B_{clu}$	5′-T**P**^{Me}**BP**^{Me}**BB**TTTT**P**^{Me}T	40 nM ± 7	400 nM ± 100	n.d	-
5BAU	5′-**B**C**B**C**B**T**B**TT**B**CT	< 1 nM	1.5 nM ± 0.9	5.5 nM ± 1.3	80 nM ± 11

[a] = 2.5 mM magnesium was employed as binding was not observed at [TFO] as high as 30 μM

n.d. = no footprint observed at [TFO] as high as 30 μM

Table 4.5 C_{50} values determined by DNase I footprinting for the interaction of several unmodified and modified TFOs containing different combinations of the nucleoside analogues P, P^{Me}, U^{P} and BAU (B) with different portions of 18 bp polypurine tract of the *tyr*T(43-58) DNA fragment.

4.4 Discussion

The data presented in this chapter clearly show that it is possible to achieve high affinity recognition of oligopurine tracts at physiological pH using triplex-forming oligonucleotides containing appropriately positioned nucleoside analogues. The affinity, specificity, and use of such analogues alone and in combination are discussed.

4.4.1 5-Propargylamino-dU and 2´-aminoethoxy,5-propargylamino-U

5-propargylamino-dU (U^P) and 2´-aminoethoxy,5-propargylamino-U (BAU) have previously been shown to form more stable triplets with AT base pairs than T (Bijapur *et al*, 1999; Sollogoub *et al*, 2002). The selectivity and affinity of these analogues was further examined by fluorescence melting and/or DNase I footprinting.

The results obtained from fluorescence melting showed that the replacement of a single T.AT triplet with U^P.AT or BAU.AT within an *inter*molecular 18mer triplex increased the T_m of the complex by 4 and 8 °C at pH 6.0 respectively. In this sequence context, both triplets were more stable than C^+.GC at all pHs, in contrast to T.AT, which produces less stable complexes than C^+.GC. These results confirm those previously obtained from the thermal melting studies undertaken on *intra*molecular triplexes containing each of these analogues (Bijapur *et al.*, 1999; Sollogoub *et al.*, 2002).

DNase I footprinting was used to examine DNA triplex formation at a 12 base pair oligopurine.oligopyrimidine sequence, using oligonucleotides that contain several substitutions of BAU for T. The results demonstrated a clear relationship between the number of substitutions and triplex stability. At pH 5.0, the unmodified TFO 5´-TCTCTTTTTTCT failed to produce a footprint in the absence of magnesium. A TFO where two of the third strand Ts were replaced with U^P also failed to generate a complex. In contrast, replacement of a single T with BAU generated a footprint with a C_{50} value of 400 nM. The addition of further BAU residues into the TFO caused a substantial increase in affinity. TFOs containing 3 and 5 substitutions generated footprints that gave C_{50} values in the low nM range (< 10 nM). The TFO containing 5 BAU residues exhibited a C_{50} value at least 30, 000 times higher than the unmodified oligonucleotide.

Increasing the pH to 6.0 showed again that the unmodified TFO did not generate a footprint, this time even in the presence of magnesium. This is as expected due to the presence of three Cs within the third strand that required low pH conditions for protonation. In contrast, the TFOs containing 2 and 3 BAU residues extended triplex formation to pH 6.0, whilst the TFO containing 5 residues generated a footprint with a C_{50} value of 80 nM at a pH as high as 7.5. These results demonstrate that BAU.AT triplets can sufficiently enhance triplex stability and compensate for the loss of binding energy at un-protonated C.GC triplets. However, it is also possible that Cs within a BAU-containing TFOs exhibit higher pK values, thereby facilitating triplex formation at higher pH.

An oligonucleotide contiguous BAU residues, 5´-BBBBBBCBT, was also prepared and examined by DNase I footprinting. This oligonucleotide formed a stable complex with its 9 base pair target site even at pH 7.5 and the absence of magnesium, yielding a C_{50} value of 400 nM. As well as producing a footprint at its intended target site, the TFO also produced several other secondary footprints at higher oligonucleotide concentrations. These were most notable within the oligopurine tract and at the sequence 5´-GTAA, suggesting interactions with purine bases. The binding of a TFO to secondary target sites has previously been observed (Fox *et al.*, 2000). These TFOs were shown to be able to form single and double base bulges. It is likely that this TFO is also binding in a similar manner.

A recent study on the oligonucleotide 5´-BTBTBTCBT which contains separated BAU substitutions produced a single footprint at the same target site, yielding a C_{50} value of 0.5 μM (Sollogoub *et al.*, 2002). Unlike this study, magnesium was also employed in the footprinting assay to stabilise triplex formation. Both C_{50} values obtained for the fully and partially substituted TFOs were very similar. As a further increase in stability would be observed for the fully modified TFO with the inclusion of magnesium, these results suggest that positioning BAU at adjacent positions within a TFO is not destabilising. This is in contrast to adjacent cytosine residues. This agrees with the results observed with oligonucleotides composed of contiguous U^P residues (Bijapur *et al.*, 1999) and 2´-aminoethoxy residues (Cuenod *et al.*, 1998; Buchini & Leumann, 2004). In contrast to C, it is likely that contiguous BAU residues are stabilised by hydrophobic and/or base stacking interactions between adjacent propargyl side chains. Also, BAU should be less affected by protonation competition, as the pK_a values for the

amino functions are much higher than that of C and they are screened by interactions with the phosphates.

These results suggest that even though TFOs containing multiple adjacent BAU substitutions produce complexes of high affinity, they will have to be designed carefully so as to minimize their interactions with non-target sites.

The above studies have highlighted that incorporation of a single BAU residue within a TFO effectively removes the magnesium dependence normally associated with the formation of parallel triplexes (Moser & Dervan, 1987; Völker *et al.*, 1994). This is not surprising for an analogue that stabilises predominantly by electrostatic interactions (Cuenod *et al.*, 1998; Bijapur *et al.*, 1999; Sollogoub *et al.*, 2002). It can be seen that the oligonucleotide 5′-TCTCTU^{P}TU^{P}TTCT did not form a stable complex in the absence of magnesium, whereas 5′-TCTCTTTBTTCT generated a footprint with a C_{50} value of 0.4 μM. Interestingly, both oligonucleotides contain the same number of positive charges and therefore might have been expected to exhibit a similar cation requirement. It might be argued that distributing the charge within an oligonucleotide (as in the U^{P}-containing oligonucleotide) could be advantageous but the opposite is observed. This lower cation requirement might be attributed to the ability of BAU to neutralize negative charges within the third stand and the duplex, unlike U^{P} which only interacts within the third strand. This decreased cation dependence would be useful for any biological applications of TFOs, where the physiological concentrations of these ions is much lower than those usually employed experimentally.

Footprinting studies were undertaken to examine whether BAU could stabilise triplexes that were formed in the GT-motif, since these structures are known to be less stable than parallel (CT-containing) triplexes. The oligonucleotides 5′-TGBGTBTBTBGT and 5′-TGBTBTBTGBGT were designed to bind in either a parallel or antiparallel orientation to their target sequence respectively. At pH 5.0 neither oligonucleotide produced a footprint at a concentration as high as 30 μM, a similar result was observed for the unmodified control oligonucleotides. The failure to form a stable complex is probably attributed to the structural distortion imposed at the GpBAU and BAUpG junctions, due to the lack of isomorphism between the BAU.AT and G.GC triplets. Although this result was disappointing, it demonstrates that the stabilisation of parallel triplexes by

BAU results from specific interactions with the amino substituents, and not from non-specific charge interactions.

4.4.1.2 Effect on triplex specificity

The affinity of U^P and BAU for each base pair relative to T has not previously been investigated. The results obtained from fluorescence melting demonstrated that both the U^P and BAU nucleosides are highly selective for AT relative to all other Watson–Crick DNA base pairs. This was observed as difference in melting temperatures between the most stable (X.AT) and second most stable (X.GC) triplets formed by these bases of at least 11 °C, this is the same as that exhibited by T. Footprinting experiments at physiological pH also corroborated these findings with BAU exhibiting a 20-fold difference between triplexes containing the most stable and second most stable triplets formed by this base. Furthermore, both analogues exhibited enhanced discrimination against pyrimidine-purine base pairs (X.TA and X.CG), as the triplets formed by them were similar or less stable than those formed by unmodified T. The reason for this enhanced discrimination is unclear and is especially noteworthy since T.CG is the most stable natural triplet at CG inversions.

NMR and molecular modelling studies have suggested that the amino functions of both the aminoethoxy and propargylamino side chains are suitably positioned to interact with nearby phosphates (Blommers *et al.,* 1999; Sollogoub *et al.*, 2002) and both are required for maximum stabilisation. It is therefore likely that one or both of these contacts do not occur in BAU.YR and U^P.YR triplets.

4.4.1.3 Effect on hysteresis

Using a fast rate of temperature change when melting and annealing triplexes generates hysteresis between melting profiles. This is greatest for complexes that exhibit slow dissociation and/or association steps in their formation. In this study, both nucleosides exhibit much greater hysteresis than T at a rate of 6 °C min^{-1}. This hysteresis was still present at a rate of 0.2 °C min^{-1} for BAU but had completely disappeared for U^P and T. Furthermore BAU still exhibited hysteresis at a temperature gradient of 0.067 °C min^{-1}. This suggests that there are very slow steps in the dissociation/and or association of this triplet. Hysteresis was greatest with BAU positioned against AT and much less opposite

another base pair. As mismatched triplets do not affect k_{on} but effect k_{off} in a manner that is dependent on the nature of the mismatch (Rougée *et al.*, 1992) the data suggest that the hysteresis for this triplet arises from slow dissociation and not slow association rates.

4.4.2 Deoxyuridine derivatives

4.4.2.1 5-Propargylguanidino-dU and 2´-guanidinoethoxy,5-propargylguanidino-U

The replacement of the amine functions of U^P and BAU with guanidine functions, generates 5-propargylguanido-dU (U^{PG}) and 2´-guanidinoethoxy ,5-propargylguanido-U (BGU). These analogues were investigated alongside BAU and U^P by fluorescence melting. The results demonstrated that, whilst both modifications were stabilising relative to T, neither produced triplets that were more stable than BAU and U^P. Previously reported studies on U^{PG} have demonstrated similar results (Roig & Asseline, 2003). In contrast, a recent study has suggested that the 2´-guanidinoethoxy modification is more stabilising than the 2´-aminoethoxy modification (Prakash *et al.*, 2004). A greater stabilisation by BGU might therefore have been expected. The study by Prakash *et* al. was undertaken at a higher pH than in this study. Under these conditions the guanidine functions are more likely to be protonated than the amine functions due to their higher pK_a, this therefore may account for the greater stabilisation observed.

The selectivity of both bases was also similar to U^P and BAU, though in some cases each was slightly more destabilising against mismatch base pairs. An effect likely to stem from steric factors due to the presence of the bulkier guanidine moieties.

4.4.2.2 5-Dimethylaminopropargyl-dU

It is possible than the amino functions of U^P and BAU contribute to stability by additional H-bonding within the major groove. The novel analogue 5-dimethylaminopropargyl U (U^{DMP}) is protonated like U^P but is incapable of forming hydrogen bonds within the major groove. Fluorescence melting of triplexes containing U^{DMP} exhibited lower melting temperatures than those containing U^P. This suggests that hydrogen bonding may be a stabilising factor, though the lower stability could be

attributed to the altered basicity of the analogue or unfavourable steric effects due to the presence of the methyl groups. Interestingly, it has been observed that the similar monomethylaminoethoxy sugar modification is as stabilising as the aminoethoxy modification (Blommers *et al.*, 1998). The selectivity of this analogue was unchanged relative to U^P.

4.4.2.2 5-Amino-dU

The base analogue 5-amino-dU (U^A) was studied because it positions a hydrophilic amino group at an identical position to the hydrophobic 5-methyl group of T. Unlike the previous analogues the pK_a of the base is 4.2 and is therefore unlikely to protonated at physiological pH. DNase I footprinting was used to examine triplex formation at a 10 base pair oligopurine.oligopyrimidine sequence, using oligonucleotides substituted with U^A. The results demonstrated that the U^A.AT triplet is about three times less stable than a T.AT triplet. As both the NH_2 and CH_3 groups have similar sizes and differ only in their polarity, it is likely that the lower stability stems from a loss in hydrophobic stacking interactions within the major groove. This is in agreement with reports that suggest the addition of a methyl group to the 5-position of a pyrimidine base is stabilising (Lee *et al.*, 1994; Povsic & Dervan, 1989; Xodo *et al.*, 1991).

4.4.3 Cytosine analogues

4.4.3.1 2-Aminopyridine and 3-methyl,2-aminopyridine

Both 2-aminopyridine (P) and 3-methyl,2-aminopyridine (^{Me}P) exhibit higher pK_a values than C and previous reports indicate that these bases allow triplex formation at a more physiological pH (Bates *et al.*, 1996; Hildbrand *et al*, 1996; Cassidy *et al.*, 1997). The results obtained from fluorescence melting showed that the substitution of a single P^{Me}.GC triplet for a C^+.GC triplet within an *inter*molecular 18mer triplex did increase the T_m of the complex and this was greater at higher pH. A difference in T_m of 3.5 °C was observed at pH 6.0.

Further studies on the specificity of ^{Me}P for each base pair revealed that this base compares favourably to C. A difference of at least 16 °C was observed between triplexes containing the most stable and the second most stable triplet formed by this

analogue at pH 6.0. This compares to C with a difference of 11 °C. ^{Me}P also forms less stable triplets with CG and AT base pairs but more stable triplets with TA relative to C. These results corroborate the previous footprinting selectivity studies obtained by Hildbrand *et al.* (Hildbrand *et al.*, 1997). It is likely that the loss of the 2-carbonyl group is the reason for this altered selectivity relative to C.

DNase I footprinting was used to examine DNA triplex formation at the same 12 base pair oligopurine.oligopyrimidine sequence as used in the BAU studies, using oligonucleotides that contain several substitutions of P or ^{Me}P for C. Replacement of a single C residue for P^{Me} resulted in a triplex that was as stable as the unmodified triplex at pH 5.0, though both triplexes did not generate footprints at pH 6.0. Replacement of all three Cs with P or P^{Me} caused a slight reduction in triplex stability at pH 5.0 but extended triplex formation to pH 6.0. This decreased pH dependency can be attributed to the higher pK_a values exhibited by both bases.

These results also confirm that adding a methyl group at the 3-position of P does not increase its affinity for GC base pairs (Hildbrand *et al*, 1997). This also agrees with similar results observed for 6-oxo dC and its methyl derivative (Berressedm *et al.*, 1995). This is in contrast to reports that show T.AT is more stable than U.AT and C^{Me}.GC is more stable than C.GC (Xodo *et al.*, 1991; Povsic & Dervan, 1989). The reason for this difference is unclear.

4.4.3.2 2´-Aminoethoxy,N7G

The addition of deoxyribose to the N7 position of guanine orients it such that the groups involved in hydrogen bond formation mimic those seen in the C^+.GC triplet (Hunziker *et* al., 1995; Koshlap *et al.*, 1997). In this study the 2´-aminoethoxy derivative of this analogue was examined. The results obtained from fluorescence melting showed that the substitution of a single ^{AE}N7G.GC triplet for a C^+.GC triplet led to a decrease in the stability of the triplex at pH 5.0, but produced a complex of a similar stability at pH 6.0. The selectivity of this base is similar to C with a 10 °C difference in the most stable and second most stable triplet formed by this base at pH 5.0. G normally recognises TA better than GC but it is clear that the altered positioning of this base results in a loss of TA recognition. A direct comparison with the deoxyribo derivative was not possible but these results suggest no dramatic increase in stability by addition of the 2´-aminoethoxy

group. As this base is not isostructural with other parallel triplets (Koshlap *et al.*, 1997), it is likely that the positioning of the 2´-aminoethoxy group is not ideal.

4.4.3.3 2´-aminoethoxy,6-oxo-C

Both 6-oxo-C and its methyl derivative have been shown to exhibit pH independent recognition of GC (Xiang *et al.,* 1994; Berressem *et al.*, 1995). In this study the 2´-aminoethoxy derivative of this base was investigated. Fluorescence melting of triplexes composed of several substitutions with this base revealed that in all cases these were less stable than their unmodified counterparts. However, the extent of this destabilisation was dependent on the pH. It was seen that the triplex composed of three ^{AE}6-oxo-C.GC triplets was only 1 °C less stable than the unmodified triplex. This modification therefore compares favourable to a study that showed a single substitution of 6-oxo-C led to a decrease in T_m of 14 °C (Xiang *et al.*, 1994). At lower pH the reason for the lower stability has been attributed to unfavorable stacking interactions and/or steric hindrance due to the 6-carbonyl group. These results suggest that the addition of a 2´-aminoethoxy group partly alleviates this lower stability.

Recent studies have suggested a further increase in stability for 2´-aminoethoxy modified nucleosides when incorporated into a fully-aminoethoxy modified TFO (Puri *et al.*, 2004; Buchini & Leumann, 2004), this may also be the case for ^{AE}6-oxo-C and ^{AE}N7G.

4.4.4 Combining favourable nucleoside analogues

The above studies have highlighted that when used alone BAU and ^{Me}P can be used to enhance triplex affinity and to extend the useful pH range for triplex formation respectively. DNase I footprinting was used to examine how these nucleoside analogues can be used in combination to achieve high affinity recognition of a 12 base oligopurine.oligopyrimidine sequence at physiological pH. It was shown that the addition of a single BAU and ^{Me}P residue into the third strand (^{Me}PBAU) had little affect on the affinity and pH dependency as compared to the TFO containing a single BAU residue (1BAU). However, addition of two of each of these residues to the TFO (2^{Me}P2BAU) enhanced triplex affinity at pH 6.0, and generated a footprint at pH 7.0. This TFO was more stable than TFOs containing either two substitutions of BAU or

^{Me}P. The addition of three substitutions of each residue to the TFO generated a triplex with enhanced affinity at pH 5.0, which was also stable at pH 7.0 and generated a footprint at pH 7.5 that exhibited a C_{50} value of 200 nM at pH 7.5. This oligonucleotide produced the strongest complex which extends to a higher pH than all the others. An equivalent TFO was examined with the same base composition as this TFO, with three ^{Me}P and three BAU residues, but in this instance the modifications are placed close together towards the 5´-end of the oligonucleotide, rather than being distributed throughout the third strand. This complex is stable at pH 5.0 in the absence of magnesium, and so clearly binds better than the unmodified oligonucleotide. It also produces a stable complex at pH 6.0. However, this oligonucleotide failed to produce a footprint at pH 7.0 and above, suggesting that the arrangement of modified residues is important and that distribution, rather than clustering, of positively charged residues produces the most stable complexes. A similar effect has previously been observed for U^P; a U^P residue positioned adjacent to a protonated C produces a triplex of lower stability compared to when U^P is separated by one uncharged nucleotide (Gowers *et al.*, 1999).

These results demonstrate that the cooperative enhancement in triplex stability obtained with these two analogues depends on the sequence arrangement of the third strand. Their effect is much greater when they are evenly distributed throughout the oligonucleotide instead of being clustered at one end. This contrasts with studies using 2´-aminoethoxy modified oligonucleotides, which suggested a greater effect when the modifications were clustered together (Puri *et al.*, 2004), though these experiments were performed with psoralen-linked oligonucleotides. However, the greater affinity obtained when there is an alternation of positive and neutral nucleosides is similar to that seen with third strand using T and C for which the most stable triplexes are obtained with alternating C^+.GC and T.AT triplets (Roberts *et al.*, 1996; James *et al.*, 2003).

Table 4.5 summarises the C_{50} values determined for the interaction of the modified and unmodified TFOs investigated in this chapter. Interestingly, this table highlights that the TFO containing 5 substitutions of BAU (5BAU) produces a complex of greater stability than any other TFO at all pHs. At pH 7.5 this TFO produces a complex that is about twice as stable as the complex formed by 3^{Me}P3BAU. This is surprising because this TFO contains adjacent cytosine and BAU residues. This highlights that one possible

means of overcoming the requirement to separate charged residues is to incorporate additional BAU residues into the TFO to further increase stability.

5 RECOGNISING PYRIMIDINE BASES USING OLIGONUCLEOTIDES CONTAINING NUCLEOSIDE ANALOGUES

5.1 Introduction

Triplex formation is usually restricted to oligopurine.oligopyrimidine target sites since only the purine strand of the duplex is recognised. The recognition of pyrimidine residues is much harder to achieve as C and T present a single hydrogen bond donor or acceptor site for binding within the major groove. The bulky 5-methyl group of T imposes an additional steric barrier to third strand binding. This chapter investigates the triplex-forming properties of several novel nucleoside analogues designed to recognise CG or TA base pairs, within the parallel motif.

5.1.1 Recognition of CG base pairs

Both C and T can bind to a CG base pair with moderate affinity (Mergny *et al.* 1991; Yoon *et al.*, 1992). This interaction involves the formation of a single hydrogen bond between the 2-carbonyl of the third strand base and the free C4-amino proton on the duplex cytosine (Radhakrishnan & Patel, 1994). The use of these bases for the recognition of CG is limited as both bases prefer to generate C^+.GC or T.AT triplets. One potential solution to this selectivity problem is to synthesise analogues that possess an altered array of hydrogen bonding contacts. To this end, the base analogue 5-propargylamino-dC (C^P; Figure 5.1A) was examined. It was reasoned that the introduction of an electron-withdrawing propargylamino group to the 5-position of C would lower its pK_a. As protonation of C is required for the recognition of GC, this base should offer a lower affinity for this base pair. Furthermore, the propargylamino group may impart other stabilising interactions as previously seen for the thymine analogue U^P (Bijapur *et al.*, 1999). A similar strategy has previously been applied in the preparation of the analogue 1-isoquinolone (Hari *et al.*, 2003). In this instance, the introduction of an aromatic ring across the 3 and 4 positions of C results in a loss of the hydrogen bond contacts required to recognise GC (or AT). This base was synthesised as its LNA sugar derivative to further increase triplex stability. In this study its 2´-aminoethoxy sugar derivative (^{ae}Q; Figure 5.1B) is examined. This modification locks the sugar pucker to a favourable N-type conformation and suitably positions a positive charge so as to interact with a negatively charged phosphate residue within the duplex (Cuenod *et al.*,

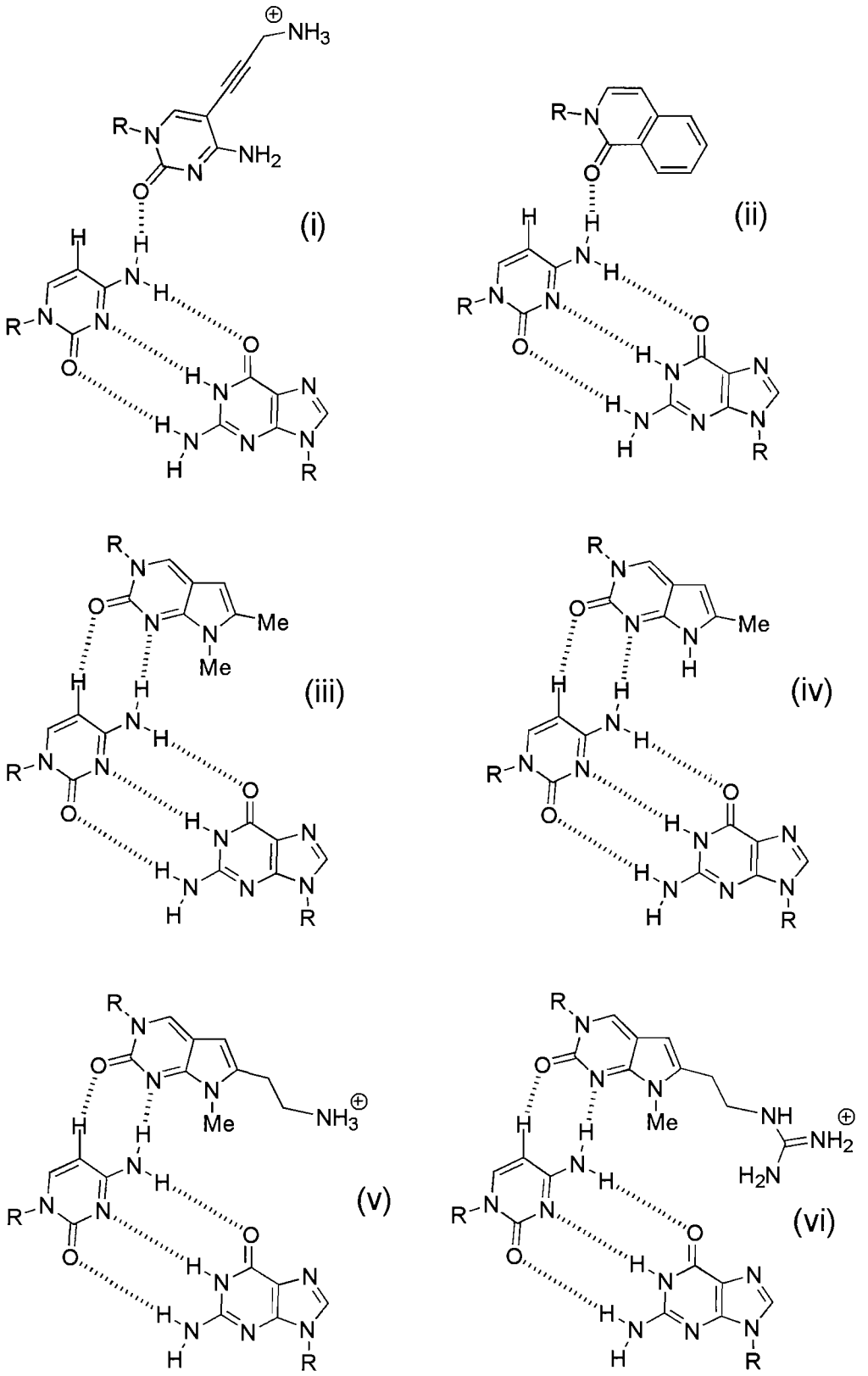

Figure 5.1 Chemical structures and proposed hydrogen bonding patterns of the nucleotide analogues designed to recognise CG interruptions; (i) C^{P}.CG (ii) ^{AE}Q.CG (iii) ^{7H}MP.CG (iv) MP.CG (v) ^{AE}P.CG and (vi) ^{G}EP.CG.

1998; Sollogoub *et al.*, 2002; Buchini & Leumann, 2004).

Several analogues based on the pyrrolopyrimidin-2-one ring system were also investigated. These nucleobases are similar in structure to T but lack the 4-carbonyl and 3-NH groups, both of which are required for the recognition of AT. In this configuration, these bases are capable of forming a hydrogen bond involving N3 and the free C4-amino proton of the duplex C. The 2-carbonyl group is also free to form an unconventional C-H...O bond at the 5-position of C (Prevot-Halter & Leumann, 1999; Marfut & Leumann, 1998). The analogue ^{7H}MP (Figure 5.1D) was initially examined to assess the suitability of the pyrrolopyrimidone-2-one core for CG recognition. As this base presents a hydrogen bond donor at position 7 it may recognise GC as well as CG. The analogue MP (Figure 5.1C) was therefore studied, as it is incapable of hydrogen bonding at this position, due to the presence of a methyl group. Further derivatives containing substituents at the 6-position were also examined. These offer the potential to form additional hydrogen bonds with N7 or O6 of G or to participate in electrostatic interactions with the anionic phosphate residues. ^{A}EP and ^{A}PP (Figure 5.1E and 5.2A) contain protonated amine functions, while ^{G}EP and ^{G}PP (Figure 5.1F and 5.2B) contain protonated guanidine functions. Two derivatives containing less flexible side chains were also characterised. ^{MA}BP and ^{PA}BP (Figure 5.1D and E) contain benzylamine side groups and position amine functions within the major groove. As the benzene ring may also participate in stacking interactions within the major groove and as an additional control, the analogue BP (Figure 5.1C) was examined. Lastly, the 2´-aminoethoxy derivative of ^{A}PP (^{AE}PP; Figure 5.2F) was investigated for its triplex-forming properties.

5.1.2 Recognition of TA base pairs

G has been previously been identified to bind a TA base pair with moderate affinity (Griffin & Dervan, 1989; Mergny *et al.* 1991). This interaction involves the formation of a single hydrogen bond between the C2 amino proton of the third strand base and the 4-carbonyl group on the duplex thymine (Radhakrishnan & Patel, 1991). The use of this base for the recognition of a TA base pair is limited to certain sequence contexts, as it forms more stable triplets when flanked by T.AT than C^{+}.GC (Kiessling *et al.*, 1992). In this study 7- and 2´-substituted derivatives of deoxyguanosine were assessed for their ability to target TA interruptions. These are protonated under physiological conditions

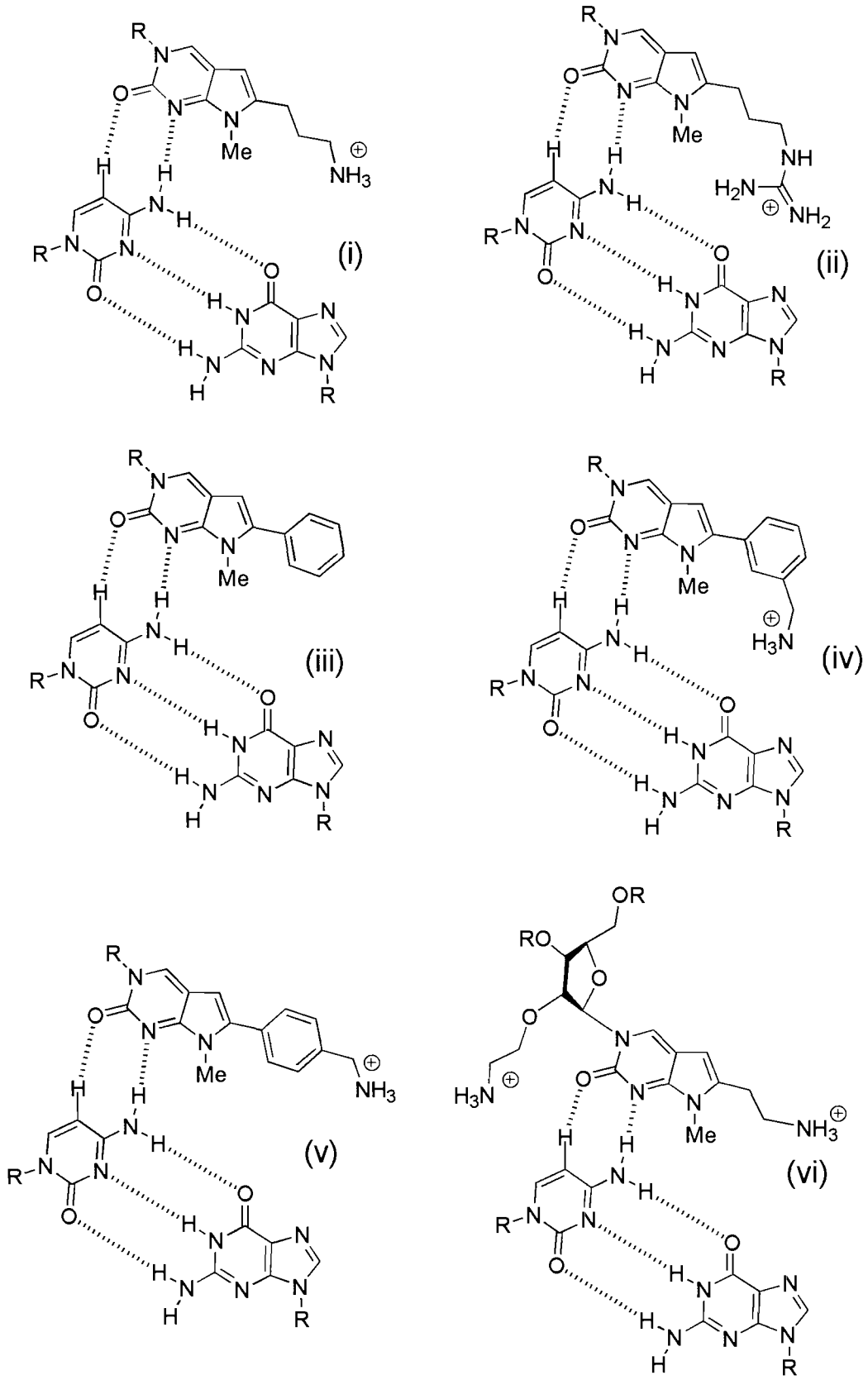

Figure 5.2 Chemical structures and proposed hydrogen bonding patterns of the nucleotide analogues designed to recognise CG interruptions; (i) ^{A}PP.CG (ii) ^{G}PP.CG (iii) BP.CG (iv) ^{MA}BP.CG (v) ^{PA}BP.CG and (vi) ^{AE}PP.CG.

and might position the positive charge so as to interact with the negative phosphodiester residues within the triplex backbone. The analogues 7-deaza-7-propargylamino-dG (G^P; Figure 5.3A) and 7-deaza-7-propargylguanido-dG (G^{PG}; Figure 5.3A) contain acyclic amine and guanidine functions at the 7-position of the base respectively. The analogue 2´-aminoethoxy-G (^{AE}G; Figure 5.3C) contains an acyclic amine attached to the 2´-position of the sugar.

An alternative strategy to increase triplex stability at pyrimidine inversions is to design analogues that can form hydrogen bonds with both partners of the target base pair. Recently, Guinvarc'h *et al.* reported on the triplex-forming properties of the unnatural *C*-nucleoside *N*-(4-(3-acetamidophenyl)thiazol-2-yl-acetamide (Guinvarc'h *et al., 2001;* S; Figure 5.3D). In their study this analogue was shown by UV melting to bind to a TA base pair with an affinity comparable to that of the T.AT triplet. It was proposed that the interaction of this base involved the formation of three hydrogen bonds to the N7 atom and the 6-amino group of A, and to the 4-carbonyl group of T. In this study the 2´-aminoethoxy derivative of this base (^{AE}S; Figure 5.3D) is examined and compared to S.

5.2 Experimental design

The triplex-forming properties of TFOs containing these novel nucleosides were evaluated using DNase I footprinting and thermal melting experiments. These were compared to TFOs containing natural bases. Each nucleoside (X) was positioned within a TFO so as to form a central X.ZY triplet upon triplex formation, where ZY is each bp in turn (AT, TA, GC or CG).

5.2.1 Thermal denaturation experiments

The sequences of the oligonucleotides used in the thermal melting experiments are illustrated in Figure 5.4A. For the fluorescence experiments the purine strand of the duplex (boxed) was labelled at the 5´-end with a fluorophore (F; fluorescein), while the third strand was labelled at the 5´-end with a quencher (Q; pyrene or methyl red). For the UV experiments the duplex and TFO were unlabelled. Melting temperatures (T_m) for these intermolecular triplexes were determined as described in Chapter 3 using a rate of temperature change of either 0.2 °C min^{-1} (fluorescence experiments) or 0.1 °C min^{-1} (UV experiments). Recordings were taken during both the heating and cooling steps and

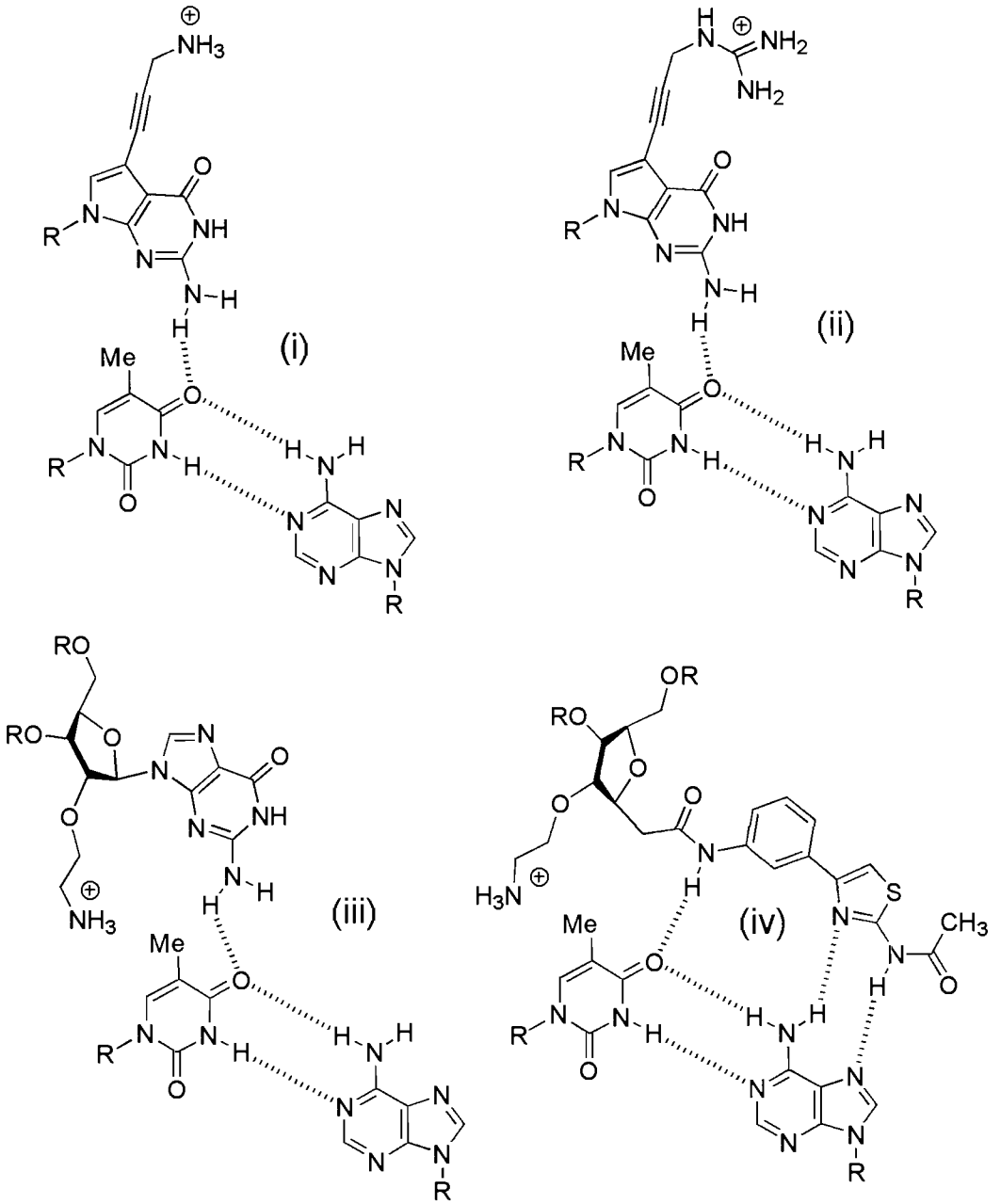

Figure 5.3 Chemical structures and proposed hydrogen bonding patterns of the nucleotide analogues designed to recognise TA interruptions; (i) G^{P}.TA (ii) G^{PG}.TA (iii) ^{AE}G.TA and (iv) ^{AE}S.TA.

A

(i)

5′-Q-TCTCTCTT**X**TCCTCCTCC

5′-F-AGAGAGAA**Z**AGGAGGAGG

3′-TCTCTCTT**Y**TCCTCCTCC

(ii)

5′-Q-TCTCTCT**X**TCT**X**TCCTCC

5′-F-AGAGAGA**T**AGA**T**AGGAGG

3′-TCTCTCT**A**TCT**A**TCCTCC

B

5′-TCTCTT**X**TTTCT

5′-TCBCTB**X**BTBCT

5′..AGAGAA**Z**AAAGA..

3′..TCTCTT**Y**TTTCT..

Figure 5.4 Sequence of oligonucleotides used in Chapter 5; A) Oligonucleotides used in the fluorescence and UV melting experiments. For fluorescence melting, the duplexes were labelled with fluorescein (F) at the 5′-end of the purine strand, whereas the TFOs are labelled with either methyl red serinol, methyl red threoninol or pyrene (Q) at the 5′-end. For UV melting, the duplex and TFO strands were unlabelled. (i) Sequences used for the single substitution studies, ZY is each base pair in turn (AT, TA, GC, CG), whereas X is each base or analogue in turn. (ii) Sequences used for the double substitution studies, X is either G, S or ^{2AE}S and is positioned opposite a TA base pair. B) Sequences of the *tyr*T (43-59) fragments and third strand oligonucleotides used in the footprinting experiments. The 12 base pair triplex target site is shown and ZY corresponds to each base pair in turn. The DNA was labelled at the 3′-end of the *Eco*RI site (upper strand). In the single substitution experiments X in the TFO corresponds to each base or analogue in turn and B is the nucleoside analogue BAU.

no significant hysteresis was observed. As the 18mer third strands contained several cytosine residues triplex formation using these oligonucleotides was pH dependent and was restricted to low pH conditions (pH < 6.0). All melting experiments were undertaken in 50 mM sodium acetate buffer containing 200 mM sodium chloride at a pH between 5.0 and 6.0. No additional stabilising factors were employed in the assay, so as to maximize the intrinsic affinity of each analogue. The concentration of duplex in the fluorescence assay was 0.25 μM and the concentration of third strand was 3 μM. The concentration of the duplex in the UV assay was 1 μM and the concentration of third strand was 5 μM. The excess of third strand in each assay was used to facilitate triplex formation. T_m values were calculated from the first derivatives of the melting and annealing profiles. Each value was recorded in triplicate and usually differed by less than 0.5 °C.

The sequences shown in Figure 5.4A(i) were used for single substitution selectivity studies, where X was each base or analogue and ZY is AT, TA, GC and CG. Fluorescence melting experiments were also performed on triplexes containing two seperated TA interruptions. The sequences used are shown in Figure 5.4A(ii). These positions were targeted using third-strand oligonucleotides containing S, ^{AE}S, and G.

5.2.1 DNase I footprinting studies

The relative affinities of 12mer oligonucleotides of sequence 5′-TCTCTTXTTTCT (where X is each base or analogue) with duplex targets containing the oligopurine. oligopyrimidine tract 5′-AGAGAAZAAAGA/3′-TCTCTTYTTTCT were examined by quantitative DNase I footprinting. The sequences of the third strand oligonucleotides and their duplex targets are shown in Figure 5.4B. The fragments containing these target sites were generated by site-directed mutagenesis of the 105 bp *tyr*T(43-59) fragment and were radiolabelled at the 3′-end of the *Eco*RI site using reverse transcriptase and [α-^{32}P]dATP. The 12-bp target site within the polypurine tract contains three GC base pairs and triplex formation was strongly pH dependent. Experiments were therefore undertaken at pH 5.0 in 50 mM sodium acetate containing 10 mM magnesium chloride and the complexes were left to equilibrate overnight at 20 °C. Quantitative analysis of the bands within each footprint allowed calculation of C_{50} values, indicating the TFO concentration that reduced the band intensity by 50%. Table

5.7 summarises the C_{50} values obtained for the interaction of all the oligonucleotides examined in this chapter.

5.3 Results

5.3.1 Triplex formation with unmodified oligonucleotides

The interaction of the oligonucleotides 5′-TCTCTTXTTTCT (where X is A, G, C or T) with each of the four *tyr*T(43-59) fragments was measured by DNase I footprinting. Representative cleavage patterns for the interactions of these oligonucleotides are shown in Figure 5.5 and 5.6. In the appropriate combinations (considered below) the oligonucleotides produced a footprint at the intended target site, at the 3′-end of the 17 bp oligopurine tract, without altering the cleavage patterns for the remainder of the 105 bp fragment. The concentration dependence of the footprint (but not its location) varied according to the nature of X.ZY.

The left hand panel of Figure 5.5 shows the DNase I digestion pattern of the four duplex fragments in the presence of the oligonucleotide 5′-TCTCTTATTTCT. A clear footprint is evident for the interaction of this oligonucleotide with the target containing a central GC bp, which persists into the low μM range. Quantitative analysis of the bands within this footprint yielded a C_{50} value of 0.3 ± 0.1 μM. No footprints are apparent for the three remaining fragments, however, it can be seen that the bands at the 3′-end of the polypurine tract are enhanced for the AT and TA-containing targets at oligonucleotide concentrations of 3 μM and above. This is indicative of a weaker interaction of the oligonucleotide and the DNA duplex, though in this instance this could not be accurately measured. These results demonstrate that adenine can generate a stable triplet with a GC bp and to a certain extent can interact weakly with AT and TA bps.

The right hand panel of Figure 5.5 shows the DNase I digestion pattern of the four duplex fragments in the presence of the oligonucleotide 5′-TCTCTTGTTTCT. In this instance a clear footprint is evident for the interaction of the oligonucleotide and the fragments containing a GC and TA bp. The C_{50} values determined for these interactions were 0.2 ± 0.1 μM and 2.5 ± 0.5 μM respectively. No interactions were evident with the AT and CG-containing fragments. These results indicate that guanine can form a stable

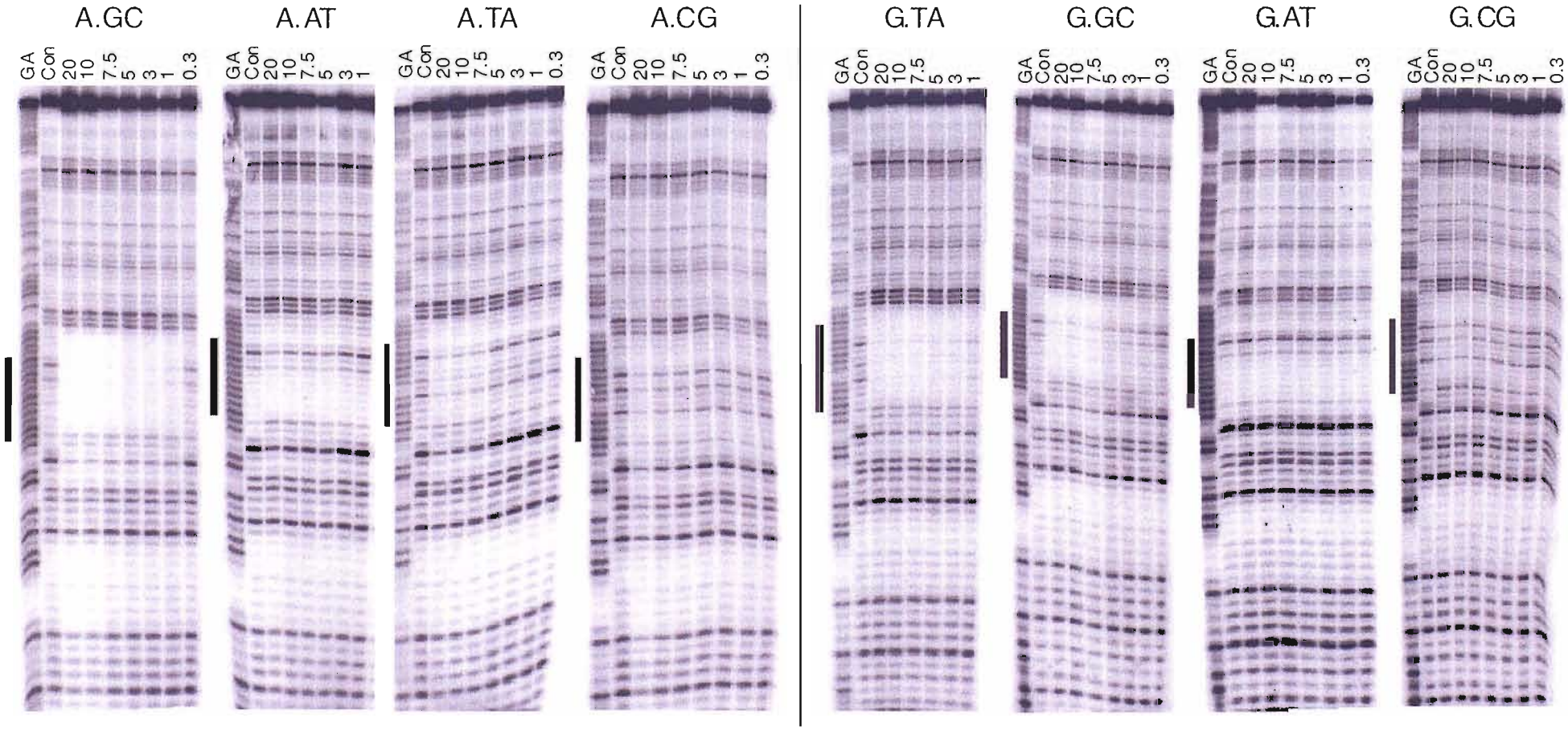

Figure 5.5 DNase I cleavage patterns of different *tyr*T(43-59) fragments in the presence of oligonucleotides 5´-TCTCTTATTTCT (left panel) and 5´ TCTCTTGTTTCT (right panel) at pH 5.0. Each triplex differed by a single central triplet X.AT, X.TA, X.GC and X.CG. The experiments were performed in 50 mM sodium acetate containing 10 mM magnesium chloride, and the complexes were left overnight at 20 °C to equilibrate. The oligonucleotide concentration (μM) is shown at the top of each gel lane. Tracks labelled 'GA' are Maxam-Gilbert markers specific for purines, while 'con' indicates DNase I cleavage in the absence of added oligonucleotide. The filled boxes show the position of the triplex target sites.

triplet with a TA base pair, producing a C_{50} value 10-fold higher than its interaction with a GC base pair.

The left hand panel of Figure 5.6 illustrates the DNase I digestion pattern of the four duplex fragments in the presence of the oligonucleotide 5′-TCTCTTCTTTCT. As expected a clear footprint is evident against the GC and CG duplex targets whilst no interaction with the AT or TA targets is observed at concentrations as high as 20 μM. It was not possible to calculate a C_{50} value for the footprint produced by the oligonucleotide with the GC-target as the footprint persisted to oligonucleotide concentrations lower than that employed. It can therefore be estimated that the C_{50} would be lower than the lowest TFO concentration (< 0.1 μM). The interaction of the oligonucleotide with the CG target could be quantified and yielded a C_{50} value of 0.8 ± 0.3 μM. These data suggest that, as expected, C generates the most stable triplet with GC but can also generate triplets with CG, albeit with a lower affinity.

The right hand panel of Figure 5.6 shows the DNase I digestion pattern of the four duplex fragments in the presence of the oligonucleotide 5′-TCTCTTTTTTCT. This oligonucleotide produced footprints with every duplex target except for the one containing a central TA bp. The C_{50} values calculated for the interactions of this oligonucleotide with the AT, CG and GC targets were 0.2 ± 0.1 μM, 0.7 ± 0.4 μM and 2.1 ± 0.3 μM, respectively. These results highlight that thymine generates the most stable triplet with an AT bp but can also form relatively stable triplets with CG and GC bps. Under these conditions the second most stable triplet, T.CG, produced a C_{50} value at least 7-fold lower than the most stable triplet, T.AT.

These results are summarised in Table 5.7, from which it can be seen that the stability (C_{50}) of the complexes formed by the interaction of these unmodified oligonucleotides varied according to the identity of the central triplet in the order T.AT = C^+.GC > A.GC > G.TA > T.CG = C.CG. As expected G.TA, C.CG and T.CG are the most stable triplets formed at pyrimidine interruptions, albeit with a lower affinity and selectivity than the standard T.AT and C^+.GC triplets. These results are consistent with the results obtained from fluorescence melting experiments presented in Chapter 3.

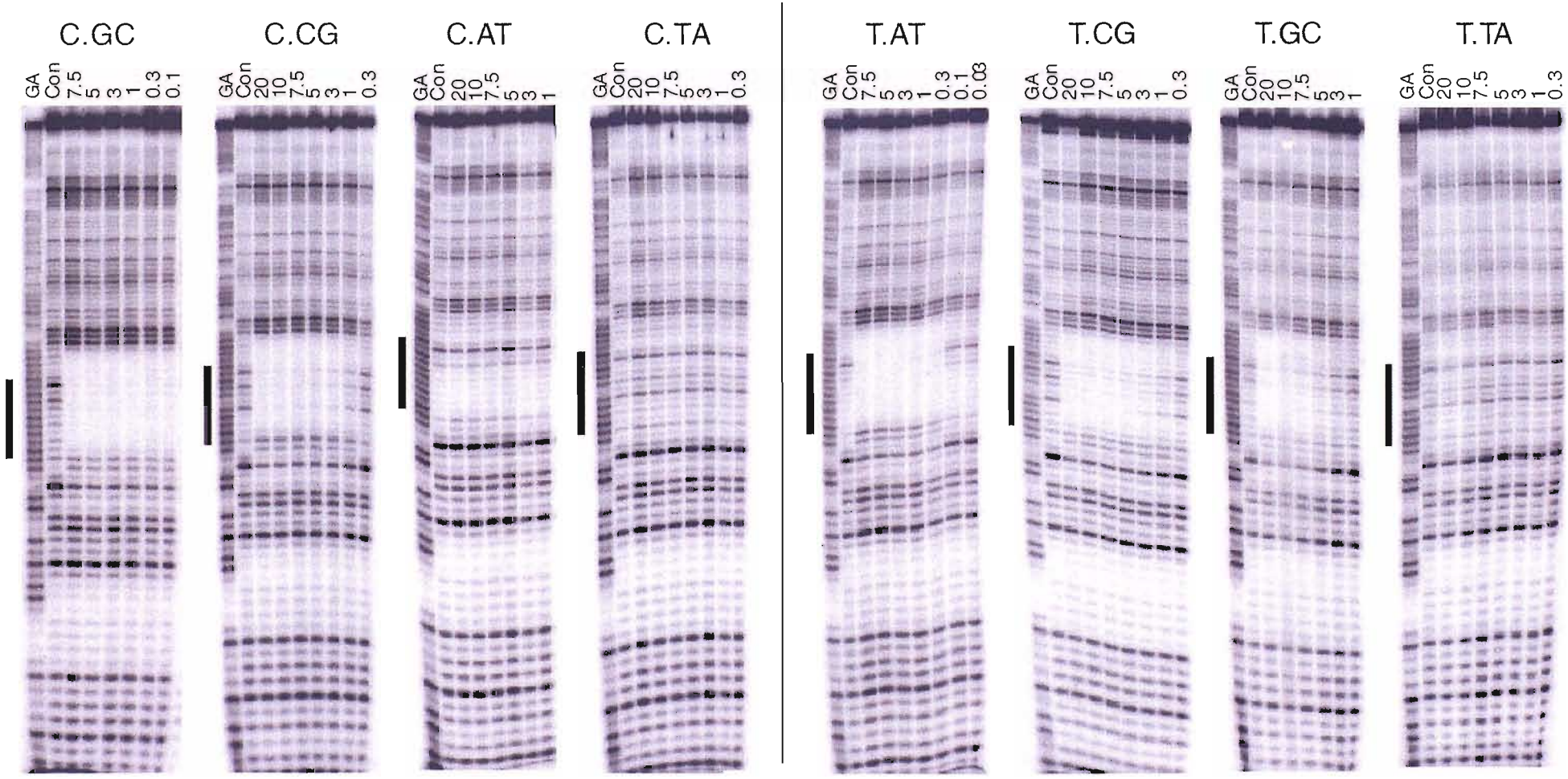

Figure 5.6 DNase I cleavage patterns of different *tyr*T(43-59) fragments in the presence of oligonucleotides 5´-TCTCTTCTTTCT (left panel) and 5´ TCTCTTTTTTCT (right panel) at pH 5.0. Each triplex differed by a single central triplet X.AT, X.TA, X.GC and X.CG. The experiments were performed in 50 mM sodium acetate containing 10 mM magnesium chloride, and the complexes were left overnight at 20 °C to equilibrate. The oligonucleotide concentration (μM) is shown at the top of each gel lane. Tracks labelled 'GA' are Maxam-Gilbert markers specific for purines, while 'con' indicates DNase I cleavage in the absence of added oligonucleotide. The filled boxes show the position of the triplex target sites.

5.3.2 Triplex formation with 5-propargylamino-dC

The specificity of C^P in triplex formation was examined by determining the melting temperatures of the fluorescently-labelled triplexes shown in Figure 5.4, where X is C^P and ZY is each bp in turn. Since protonation of the ring nitrogen is pH-dependent, the melting experiments were carried out at different pH values. The melting profiles obtained for the four triplexes at pH 6.0 are presented in Figure 5.7 (top panel). The T_m values determined for these profiles and those obtained at lower pH values are shown in Table 5.1. This table includes T_m values for the corresponding C-containing triplexes for reference (taken from the data in Chapter 3).

It can be clearly seen that with C^P in the third strand the most stable triplex was generated with the duplex containing a central GC bp (green line). The T_m value for this complex was 41.1 °C and is 4 °C lower than the T_m obtained with the C-containing third strand. However, the difference in T_ms produced by these two triplets was dependent on the pH of the solution. As the pH decreased, so did the difference in affinity between the two triplets and at pH 5.0 both exhibited similar T_ms. This observation is consistent with the expectation that C^P, with a lower pK_a than C, will be less protonated the higher the pH. The unprotonated form will be unable to form two hydrogen bonds to GC and will exhibit a lower affinity for this base pair.

		ZY			
X	pH	AT	TA	GC	CG
C	5.0	56.0 (56.3)	54.9 (55.0)	67.2 (66.8)	59.3 (59.2)
	5.5	42.7 (42.7)	41.4 (42.8)	59.0 (59.1)	46.7 (46.9)
	6.0	< 28.0	< 28.0	45.1 (45.2)	31.9 (31.9)
C^P	5.0	58.3 (58.8)	55.7 (56.0)	66.8 (66.6)	62.0 (62.2)
	5.5	45.0 (45.5)	42.0 (41.3)	57.1 (57.4)	49.8 (50.2)
	6.0	28.8 (28.9)	< 28.0	41.1 (41.0)	33.7 (33.9)

Table 5.1 T_m values determined by fluorescence melting for triplexes composed of triplets containing C^P using a temperature gradient of 0.2 °C min^{-1} and the quencher pyrene. T_m values in parenthesis were calculated from the annealing phase.

The second most stable triplex generated with C^P in the third strand was with the duplex containing the central CG bp (black line) and was 7 °C lower than that obtained with GC. This triplet exhibited T_m values that were 2-3 °C higher than those exhibited by the corresponding triplet generated by C. As the extent of this increase was not dependent

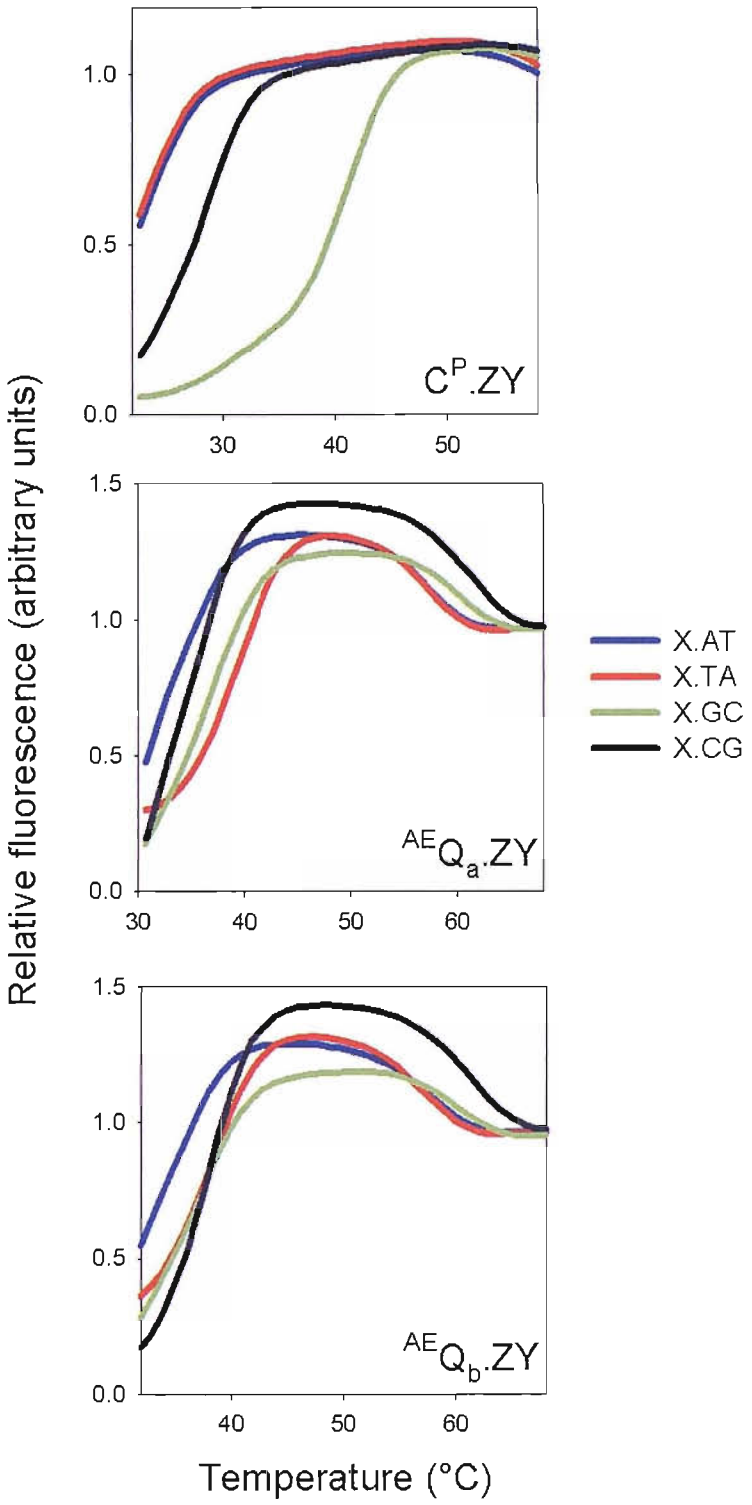

Figure 5.7 Fluorescence melting curves showing the interaction of TFOs containing 5-propargylamino-dC or 2′-aminoethoxy,1-isoquinolone with duplex targets containing a variable central base pair. Each TFO contains either C^P, $^{AE}Q_\alpha$ or $^{AE}Q_\beta$ at an identical position, generating X.ZY triplets, where ZY is AT, TA, GC or CG. The experiments were performed in 50 mM sodium acetate containing 200 mM NaCl at either pH 6.0 (C^P) or pH 5.5 ($^{AE}Q_\alpha$ or $^{AE}Q_\beta$). The y-axes show the normalised fluorescence (arbitrary units), while the x-axes shows the temperature (°C). The samples were heated at a rate of 0.2 °C min^{-1}.

on pH it suggests that the interaction of C^P with CG predominantly involves the 2-carbonyl group and not the ring nitrogen of the base. The next most stable triplet was generated opposite AT and a similar increase in affinity was also observed relative to C. Again this was not dependent on pH and suggests that the 2-carbonyl group participates in the recognition of A. Interestingly, no stabilisation was observed for a TA base pair, suggesting that the propagylamino chain is not suitably positioned to enhance the stability of this triplet.

To confirm these results, the formation of triplexes containing C^P were examined by DNase I footprinting. The DNase I digestion patterns of the four duplex fragments in the presence of the oligonucleotide 5´-TCTCTT$\underline{C^P}$TTTCT are shown in Figure 5.8. As expected a clear footprint is evident with the target containing a central GC bp (left hand panel) that persists to the low μM range. It was not possible to quantify the bands within this footprint but visual estimation yields a C_{50} value of between 1 and 0.3 μM. This is at least 3-fold lower than the C_{50} estimated for the equivalent C-containing TFO. A weaker footprint is also evident for both fragments containing a central CG and AT bp. Quantitative analysis of the bands within these footprints yields C_{50} values of 1.2 ± 0.2 μM and 1.1 ± 0.1 μM respectively. Therefore, the C_{50} value for C^P.AT is 30-fold greater than that obtained for C.AT, whilst the C_{50} value for C^P.CG is only 1.5-fold greater than C.CG. This is in contrast to the results obtained from fluorescence melting that suggests both triplets are equally stabilised by the introduction of the propargylamino group. The reason for this difference is unclear. No interaction of the oligonucleotide was observed with the target containing a central TA base pair.

Taken together it appears that the addition of the propargylamino group to C decreases its affinity for GC, presumably due to a lowering of the pK_a of the heterocycle while it increases the affinity for AT and CG. Unfortunately, under the low pH conditions employed in this study it was not possible to determine whether C^P retains its recognition of GC at pH 7.0.

5.3.3 Triplex formation with 2´-aminoethoxy-1-isoquinolone

The sequence specificities of both the α and β anomers of ^{AE}Q in triplex formation were assessed by determining the melting temperature of the fluorescently-labelled triplexes shown in Figure 5.4, where X is ^{AE}Q and ZY is each bp in turn. Representative

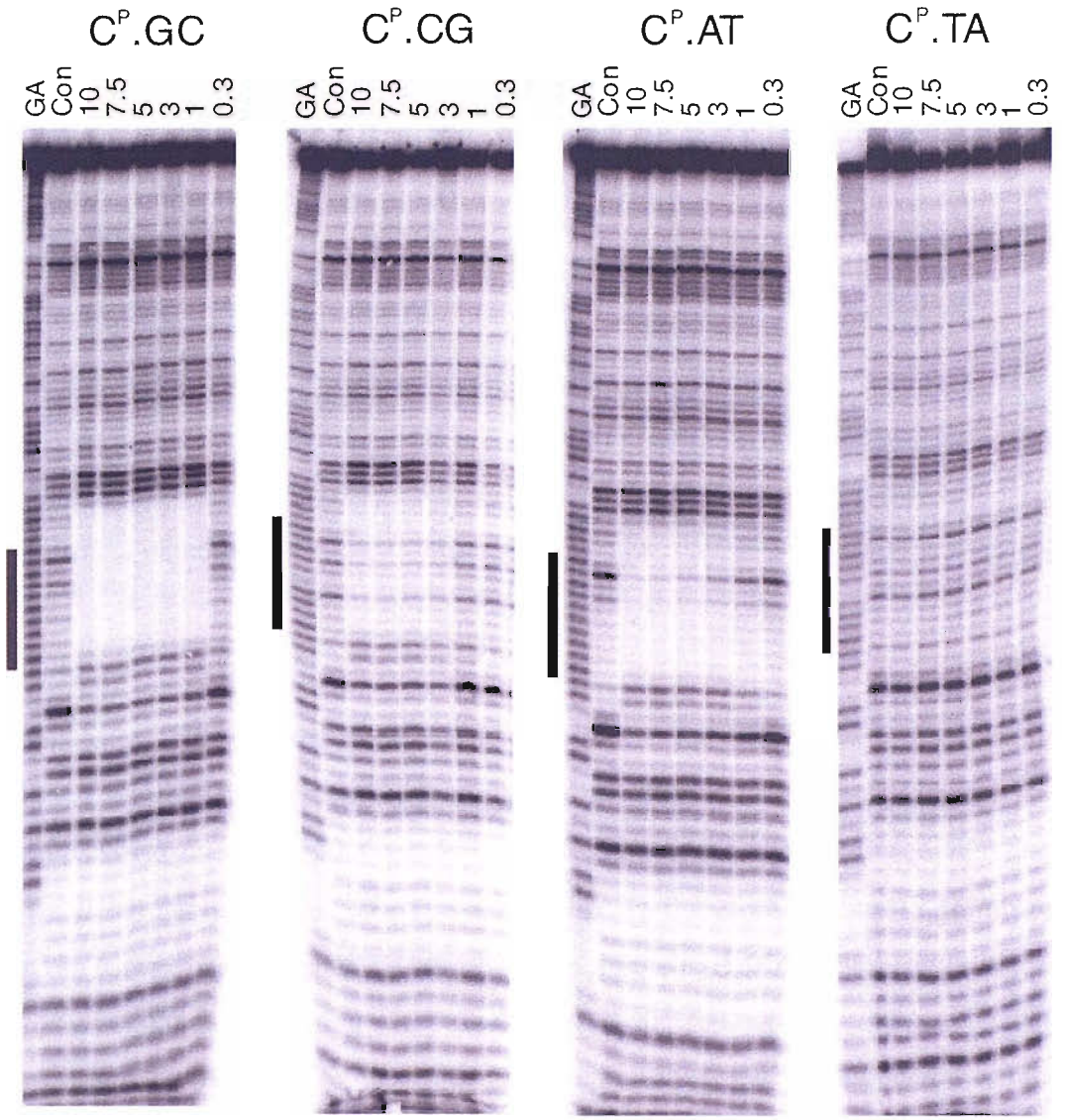

Figure 5.8 DNase I cleavage patterns of different *tyr*T(43-59) fragments in the presence of oligonucleotide 5´-TCTCTTC^{P}TTTCT at pH 5.0. Each triplex differed by a single central triplet X.AT, X.TA, X.GC and X.CG. The experiments were performed in 50 mM sodium acetate containing 5 mM magnesium chloride, and the complexes were left overnight at 20 °C to equilibrate. The oligonucleotide concentration (μM) is shown at the top of each gel lane. Tracks labelled 'GA' are Maxam-Gilbert markers specific for purines, while 'con' indicates DNase I cleavage in the absence of added oligonucleotide. The filled boxes show the position of the triplex target sites.

fluorescence melting profiles for the complexes containing the α (middle panel) and β (bottom panel) anomers of ^{AE}Q at pH 5.5 are illustrated in Figure 5.8. The T_ms determined from these profiles and those obtained at other pH values (pH 6.0 and 5.0) are shown in Table 5.2.

		ZY			
X	pH	AT	TA	GC	CG
C	5.0	55.3 (55.2)	53.4 (53.7)	67.4 (65.9)	57.6 (57.7)
	5.5	39.8 (39.4)	38.7 (38.6)	56.6 (56.7)	43.7 (43.4)
	6.0	< 28.0	< 28.0	41.1 (41.2)	28.9 (28.7)
$^{AE}Q_\alpha$	5.0	50.3 (50.0)	54.2 (54.2)	52.6 (52.6)	51.6 (51.4)
	5.5	< 35.0	38.7 (<35)	37.3 (<35)	39.2 (<35)
	6.0	< 28.0	< 28.0	< 28.0	< 28.0
$^{AE}Q_\beta$	5.0	52.3 (52.1)	54.8 (55.0)	54.3 (54.1)	54.5 (54.6)
	5.5	37.2 (<35)	40.2 (<35)	39.2 (<35)	39.2 (<35)
	6.0	< 28.0	< 28.0	< 28.0	< 28.0

Table 5.2 T_m values determined by fluorescence melting for triplexes composed of triplets containing $^{AE}Q_\alpha$ and $^{AE}Q_\beta$ using a temperature gradient of 0.2 °C min^{-1} and the quencher methyl red. T_m values in parenthesis were calculated from the annealing phase.

Examination of the melting profiles and T_ms reveals that both anomers form complexes of lower stability and selectivity than those formed by natural bases. The T_ms of these complexes vary between 50.3 and 54.2 °C for the α anomer and between 52.3 and 54.2 °C for β the anomer at pH 5.0. The complexes are therefore at least 13 °C less stable than the triplex containing C$^+$.GC. It was not possible to detect triplex formation for any of the complexes containing these analogues at pH 6.0, as the complexes melted at temperatures lower than 28 °C. Under these conditions both analogues are effectively acting as 'null bases' in which they make little or no contribution to the affinity or specificity of the TFO.

The sequence selectivity and affinity of ^{AE}Q in triple helix formation was investigated further by DNase I footprinting. The interactions of the 12mer oligonucleotides 5´-TCTCTT^{AE}Q$_\alpha$TTTCT and 5´-TCTCTT^{AE}Q$_\beta$TTTCT with the four *tyr*T(43-59) DNA fragments were examined. The left hand panel of Figure 5.9 shows the DNase I digestion pattern of the four duplex fragments in the presence of the $^{AE}Q_\alpha$ -containing oligonucleotide. The cleavage pattern for each fragment remains unaltered in the presence of the oligonucleotide indicating no interaction at oligonucleotide concentrations as high as 20 μM

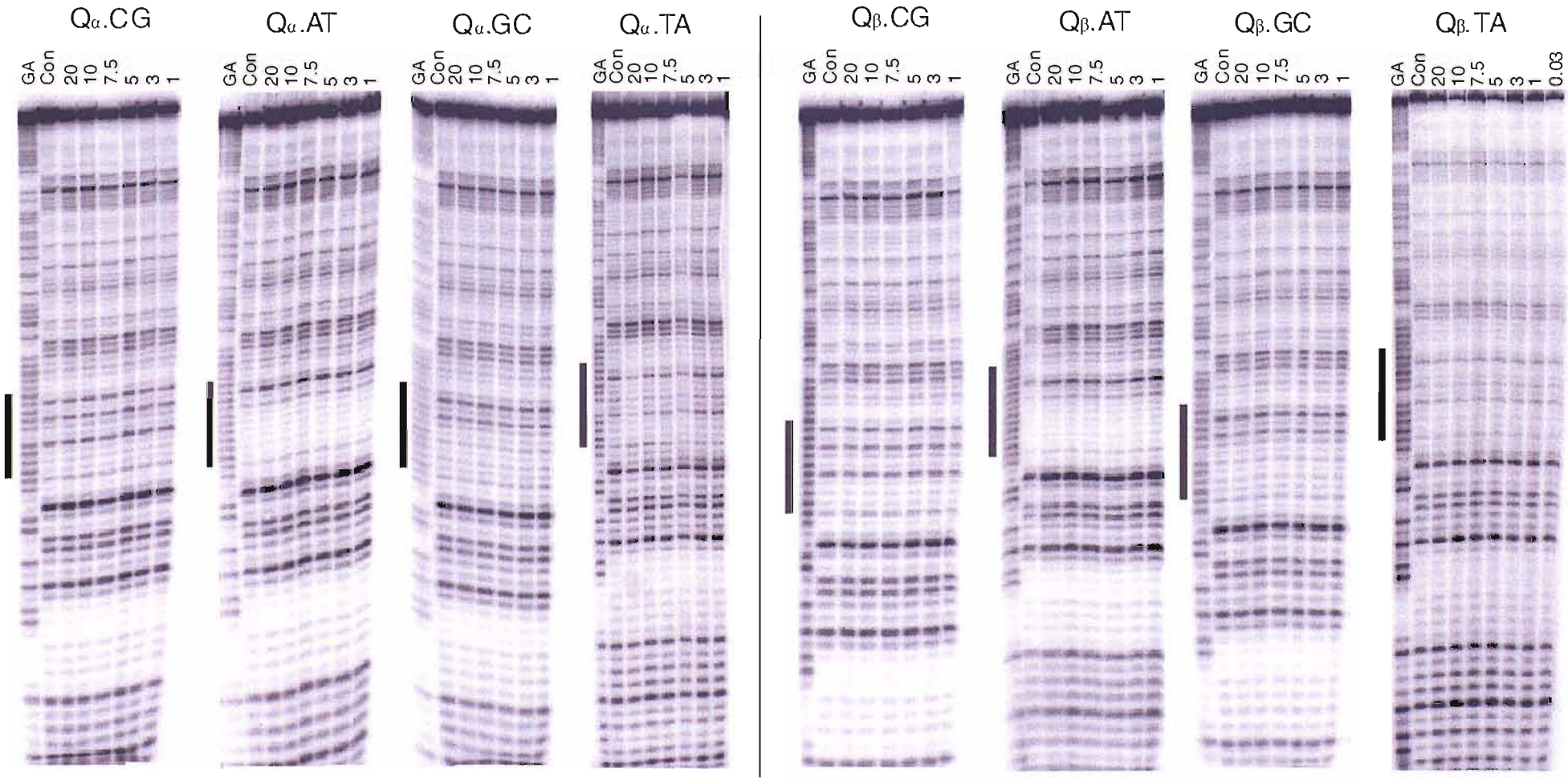

Figure 5.9 DNase I cleavage patterns of different *tyr*T(43-59) fragments in the presence of oligonucleotides 5'-TCTCTTQ$_{\alpha}$TTTCT (left panel) and 5'-TCTCTTQ$_{\beta}$TTTCT (right panel) at pH 5.0. Each triplex differed by a single central triplet X.AT, X.TA, X.GC and X.CG. The experiments were performed in 50 mM sodium acetate containing 10 mM magnesium chloride, and the complexes were left overnight at 20 °C to equilibrate. The oligonucleotide concentration (μM) is shown at the top of each gel lane. Tracks labelled 'GA' are Maxam-Gilbert markers specific for purines, while 'con' indicates DNase I cleavage in the absence of added oligonucleotide. The filled boxes show the position of the triplex target sites.

A similar result can be seen for the interaction of the $^{AE}Q_{\beta}$ -containing oligonucleotide, which is illustrated on the right hand panel of Figure 5.9. These results confirm those obtained from fluorescence melting, suggesting that in this context the 2´-aminoethoxy derivative of Q is not effective for the recognition of CG.

5.3.4 Triplex formation with substituted pyrrolopyrimidin-2-ones

The nucleobases ^{7H}MP and MP were initially examined to assess the suitability of the pyrrolopyrimidin-2-one core for the recognition of a CG inversion. These bases differ in the presence of a methyl group at position 7. The sequence specificity and pH dependence of MP and ^{7H}MP in triplex formation was assessed by determining the melting temperature of the fluorescently-labelled triplexes shown in Figure 5.4, where X is either MP or ^{7H}MP and ZY is each bp in turn. The top panel of Figure 5.10 illustrates the melting profiles obtained for the triplexes containing these bases at pH 5.5. The T_ms for these profiles and those obtained at other pH values (pH 5.0 and 6.0) are shown in Table 5.3. The top left hand graph clearly shows that ^{7H}MP recognises a GC bp (green line), whilst MP recognises CG bp (black line), with the highest affinity. The presence of the N-methyl group of MP is therefore essential to prevent the nucleobase from acting as a cytosine analogue. The difference in T_m of ^{7H}MP.GC and MP.CG (~ 8 °C) suggests that ^{7H}MP is forming two conventional hydrogen bonds to GC compared to just one between MP and CG. The ^{7H}MP.GC triplet also exhibits similar T_m values as the T.AT triplet whereas the MP.CG triplet exhibits a T_m value at least 4 °C lower. Both analogues exhibit increased affinity for CG relative to T, with an increase in T_m of between 2-3 °C. Interestingly, the selectivity of each nucleobase for the remaining base pairs was dependent on the pH. At pH 5.5 and 6.0 both bases generated triplets with AT and MP generated a triplet with GC that produced complexes at least 4 °C less stable than when positioned opposite GC. However, at pH 5.0 a difference of about 2 °C is observed. This suggests that a protonation event could be occurring on the ring nitrogen, which may allow the recognition of GC and AT by the formation of a hydrogen bond with the purines at N7.

The sequence selectivity and affinity of ^{7H}MP and MP was further corroborated by DNase I footprinting. The interactions of 5´-TCTCTT^{7H}MPTTTCT and 5´-TCTCTTMPTTTCT with the four DNA fragments were examined. The right hand

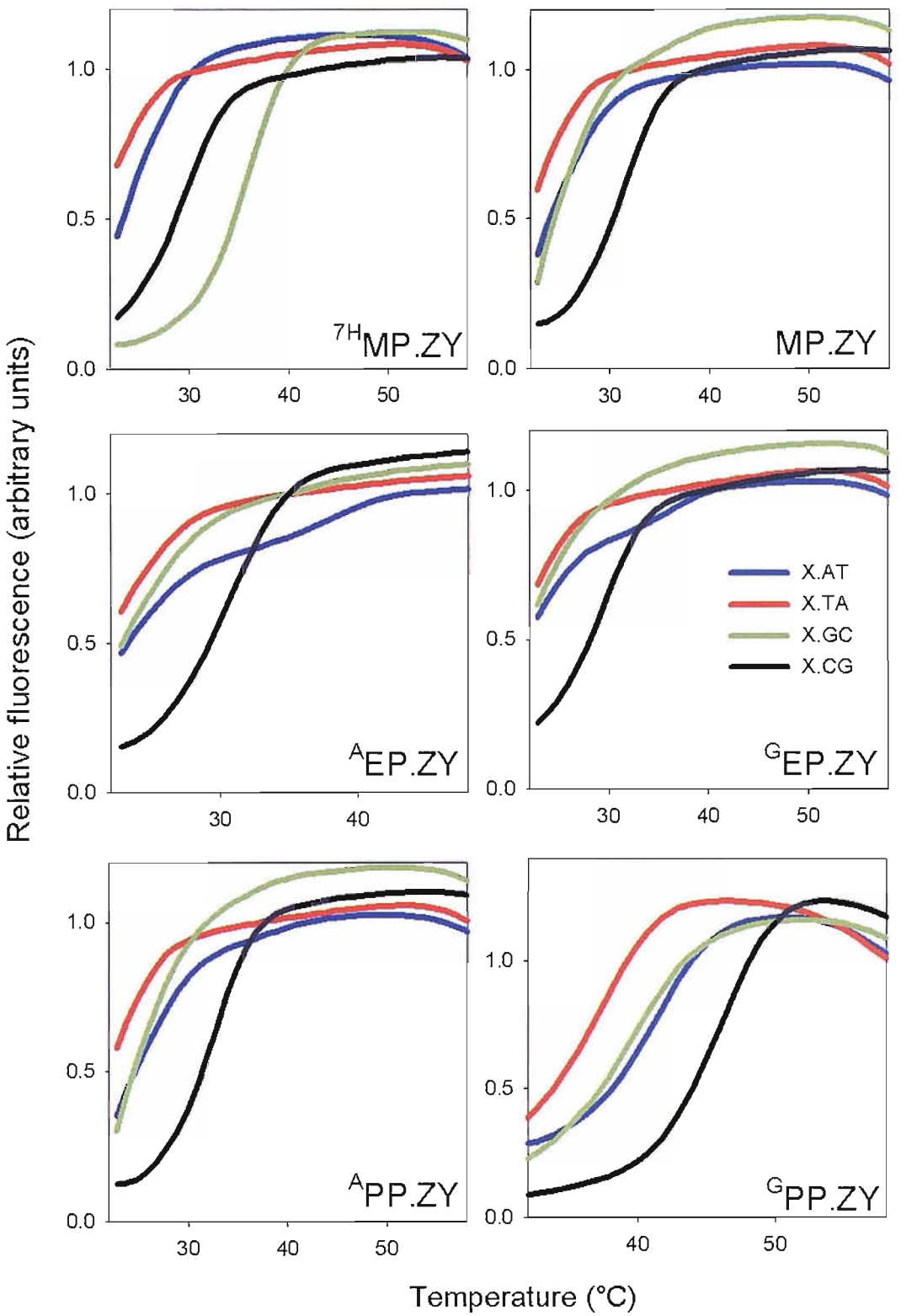

Figure 5.10 Fluorescence melting curves showing the interaction of TFOs containing pyrrolopyrimidin-2-ones with duplex targets containing a variable central base pair. Each TFO contains either ^{7H}MP, MP, ^{A}EP, ^{G}EP, ^{A}PP or ^{G}PP at an identical position, generating X.ZY triplets. The experiments were performed in 50 mM sodium acetate containing 200 mM NaCl at either pH 6.0 (^{7H}MP, MP, ^{A}EP, ^{G}EP, ^{A}PP) or pH 5.5 (^{G}PP). The y-axes show the normalised fluorescence (arbitrary units), while the x-axes shows the temperature (°C). The samples were heated at a rate of 0.2 °C min^{-1}.

X	pH	ZY			
		AT	TA	GC	CG
T	5.0	63.8 (62.5)	52.7 (53.1)	56.8 (57.3)	57.4 (57.5)
	5.5	54.0 (54.0)	38.1 (38.3)	42.9 (43.0)	43.3 (43.4)
	6.0	39.4 (39.4)	< 28.0	27.7 (27.7)	28.3 (28.3)
^{7H}MP	5.0	57.4 (57.8)	53.3 (53.5)	65.4 (64.3)	59.8 (59.3)
	5.5	42.8 (42.8)	39.0 (38.8)	54.1 (54.2)	46.2 (46.1)
	6.0	< 28.0	< 28.0	36.2 (36.6)	29.9 (30.1)
MP	5.0	57.8 (58.0)	53.1 (53.3)	58.8 (59.2)	60.3 (60.2)
	5.5	42.7 (42.5)	38.7 (38.2)	41.4 (42.0)	46.4 (46.5)
	6.0	< 28.0	< 28.0	< 28.0	31.5 (31.7)
^{A}EP	5.0	55.7 (56.6)	52.2 (52.2)	56.7 (56.4)	59.0 (59.1)
	5.5	40.4 (40.5)	37.8 (37.7)	40.2 (39.7)	45.6 (45.6)
	6.0	< 28.0	< 28.0	< 28.0	30.5 (30.6)
^{G}EP	5.0	56.3 (57.0)	52.9 (53.0)	57.4 (57.1)	59.6 (59.7)
	5.5	40.3 (40.6)	38.1 (37.9)	39.4 (39.5)	45.9 (45.8)
	6.0	< 28.0	< 28.0	< 28.0	29.6 (29.9)
^{A}PP	5.0	57.3 (58.0)	52.4 (53.0)	60.3 (58.8)	60.3 (60.8)
	5.5	42.1 (42.3)	37.6 (37.4)	41.4 (41.5)	47.1 (47.0)
	6.0	< 28.0	< 28.0	< 28.0	32.1 (32.4)
^{G}PP	5.0	56.9 (57.0)	52.5 (52.5)	56.7 (56.4)	59.7 (59.9)
	5.5	41.1 (41.1)	37.5 (37.1)	39.4 (39.4)	46.0 (45.6)
BP	5.0	58.4 (59.0)	53.2 (53.5)	58.2 (58.2)	60.4 (60.7)
	5.5	43.2 (43.6)	37.5 (37.6)	40.6 (41.1)	46.8 (47.1)
	6.0	28.1 (28.4)	< 28.0	< 28.0	32.9 (33.1)
^{PA}BP	5.0	57.2 (58.0)	52.8 (53.1)	58.1 (57.6)	60.4 (60.6)
	5.5	41.3 (41.6)	37.3 (37.2)	38.6 (39.1)	46.1 (46.4)
	6.0	< 28.0	< 28.0	< 28.0	31.0 (31.3)
^{MA}BP	5.0	64.6 (59.4)	53.2 (59.4)	57.2 (57.7)	60.4 (60.7)
	5.5	51.6 (46.5)	37.7 (37.6)	40.0 (40.2)	46.1 (46.0)
	6.0	37.9 (35.7)	< 28.0	< 28.0	31.3 (31.5)
^{AE}PP	5.0	70.3 (62.0)	52.3 (52.6)	60.5 (58.9)	60.3 (60.5)
	5.5	52.5 (51.1)	37.7 (37.7)	43.5 (42.9)	47.1 (47.5)
	6.0	39.9 (37.6)	< 28.0	31.1 (31.1)	32.4 (32.2)

Table 5.3 T_m values determined by fluorescence melting for triplexes composed of triplets containing pyrrolopyrimidones using a temperature gradient of 0.2 °C min^{-1} and the quencher methyl red. T_m values in parenthesis were calculated from the annealing phase.

panel of Figure 5.11 shows the DNase I digestion pattern of the four duplex fragments in the presence of the oligonucleotide 5′-TCTCTT^{7H}MPTTTCT. Footprints are evident for the targets containing a GC, CG and AT bp whilst no interaction is observed with target containing a TA bp. It was not possible to calculate a C_{50} value for the footprint produced by this oligonucleotide with the GC-target as the footprint persisted to oligonucleotide concentrations lower than that employed. It can therefore be estimated that the C_{50} would be lower than the lowest TFO concentration (< 0.3 μM). C_{50} values determined for the remaining footprints were 0.8 ± 0.2 μM and 1.7 ± 0.2 μM for the targets containing a CG or AT bp respectively.

The left hand panel of Figure 5.11 shows the DNase I digestion pattern of the four duplex fragments in the presence of the oligonucleotide 5′-TCTCTTMPTTTCT. Again, footprints are evident for the targets containing a GC, CG and AT bp whilst no interaction is observed with target containing a TA bp, although the order of affinity was different in this case. C_{50} values calculated from these footprints were 0.5 ± 0.1 μM, 1.6 ± 0.2 μM, and 6.0 ± 1.7 μM for the CG-, AT- and GC-containing targets respectively. The ^{7H}MP.GC triplet produced a C_{50} value at least 20-fold greater than that produced by MP.GC, again highlighting the requirement for the methyl group at position 7 to stop the recognition of GC. A 2.5 fold difference in C_{50} between T.AT and MP.CG again suggests this triplet is less stable.

Taken together, the results from fluorescence melting and DNase I footprinting suggest that the pyrrolopyrimidin-2-one core provides an effective means for selectively recognising CG base pairs, producing triplets that are more stable than the T.CG triplet. A methyl group is required at the 7-position to stop recognition of GC. There is scope for improvement as the MP.CG triplet is still less stable than T.AT or C^+.GC.

5.3.4.1 Positively charged derivatives

The nucleobases ^{A}EP, ^{G}EP, ^{A}PP and ^{G}PP were examined to assess whether the addition of substituents at the 6-position of pyrrolopyrimidin-2-one core could further stabilise the MP.CG triplet. The melting temperature of the fluorescently-labelled triplexes shown in Figure 5.4 were determined, where X is ^{A}EP, ^{G}EP, ^{A}PP and ^{G}PP and ZY is each bp in turn. Representative fluorescence melting profiles for the complexes containing these bases are illustrated in Figure 5.10 and the T_ms calculated for these

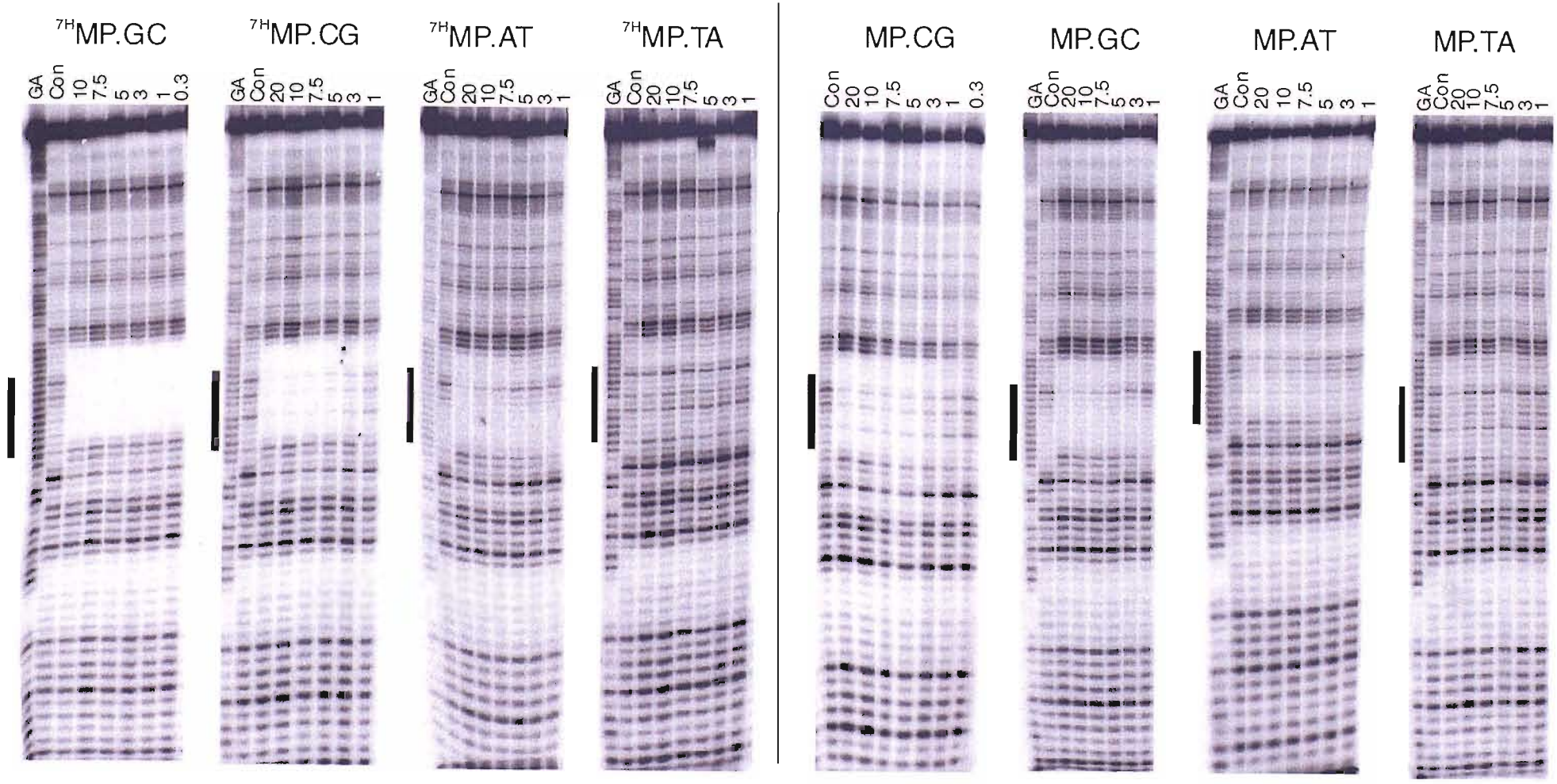

Figure 5.11 DNase I cleavage patterns of different *tyr*T(43-59) fragments in the presence of oligonucleotides 5'-TCTCTTMPTTTCT (left panel) and 5'-TCTCTT^{7H}MPTTTCT (right panel) at pH 5.0. Each triplex differed by a single central triplet X.AT, X.TA, X.GC and X.CG. The experiments were performed in 50 mM sodium acetate containing 10 mM magnesium chloride, and the complexes were left overnight at 20 °C to equilibrate. The oligonucleotide concentration (μM) is shown at the top of each gel lane. Tracks labelled 'GA' are Maxam-Gilbert markers specific for purines, while 'con' indicates DNase I cleavage in the absence of added oligonucleotide. The filled boxes show the position of the triplex target sites.

complexes and those at lower pH values (pH 5.0 and 5.5) are shown in Table 5.3. It is clear that all the substituted pyrrolopyrimidin-2-one bases showed enhanced selectivity and affinity for a CG bp as compared to T at pH 5.5 and 6.0, and in a similar manner to MP, their selectivity is reduced at pH 5.0. The T_ms for the complexes formed by positioning ^{A}EP, ^{G}EP, ^{A}PP and ^{G}PP against CG at pH 5.5 were 45.6 °C, 45.9 °C, 47.1 °C and 46.0 °C. It is therefore clear that, although there is not a great difference between these bases, the order of affinity for CG of these nucleosides is therefore ^{A}PP = MP > ^{G}PP > ^{A}EP = ^{G}EP. For each nucleobase the order of stability of triplets is X.CG > X.AT > X.GC > X.TA.

Interestingly, in some instances the melting profiles obtained for these nucleobase when positioned against AT showed a secondary transition at high temperatures (see figure 5.10, middle graphs, blue line). These transitions were not evident for T, ^{7H}MP or MP. The presence of these transitions will be discussed later in the chapter.

The interactions of the oligonucleotides 5′-TCTCTTXTTTCT (where X is ^{A}EP, ^{G}EP, ^{A}PP and ^{G}PP) with the four *tyr*T(43-59) fragments were determined as before. Representative cleavage patterns for the interaction of each of the oligonucleotides with the four DNA fragments are shown in Figure 5.12 and 5.13. The left hand panel of Figure 5.12 shows the DNase I digestion pattern of the four duplex fragments in the presence of the oligonucleotide 5′-TCTCTT^{A}EPTTTCT. Footprints were generated by this oligonucleotide with the CG, AT and GC-containing targets, yielding estimated C_{50} values of 0.8 ± 0.4 μM, 2 ± 1 μM and 12 ± 5.1 μM respectively. This order of affinity is similar to that observed in fluorescence melting experiments and is the same as the analogue MP. It is therefore evident that in this instance the introduction of the protonated amine does not increase the affinity of this analogue. The right hand panel of Figure 5.12 shows the DNase I digestion pattern of the four duplex fragments in the presence of the oligonucleotide 5′-TCTCTT^{G}EPTTTCT. Footprints were generated by this oligonucleotide with the CG, AT and GC targets, yielding C_{50} values of 0.7 ± 0.1 μM, 1.5 ± 0.6 μM and 8.7 ± 3.3 μM respectively. Again this analogue shows no altered affinity as compared to MP.

The left hand panel of Figure 5.13 shows the DNase I digestion pattern of the four duplex fragments in the presence of the oligonucleotide 5′-TCTCTT^{A}PPTTTCT. Footprints were generated by this oligonucleotide with the CG, AT and GC targets,

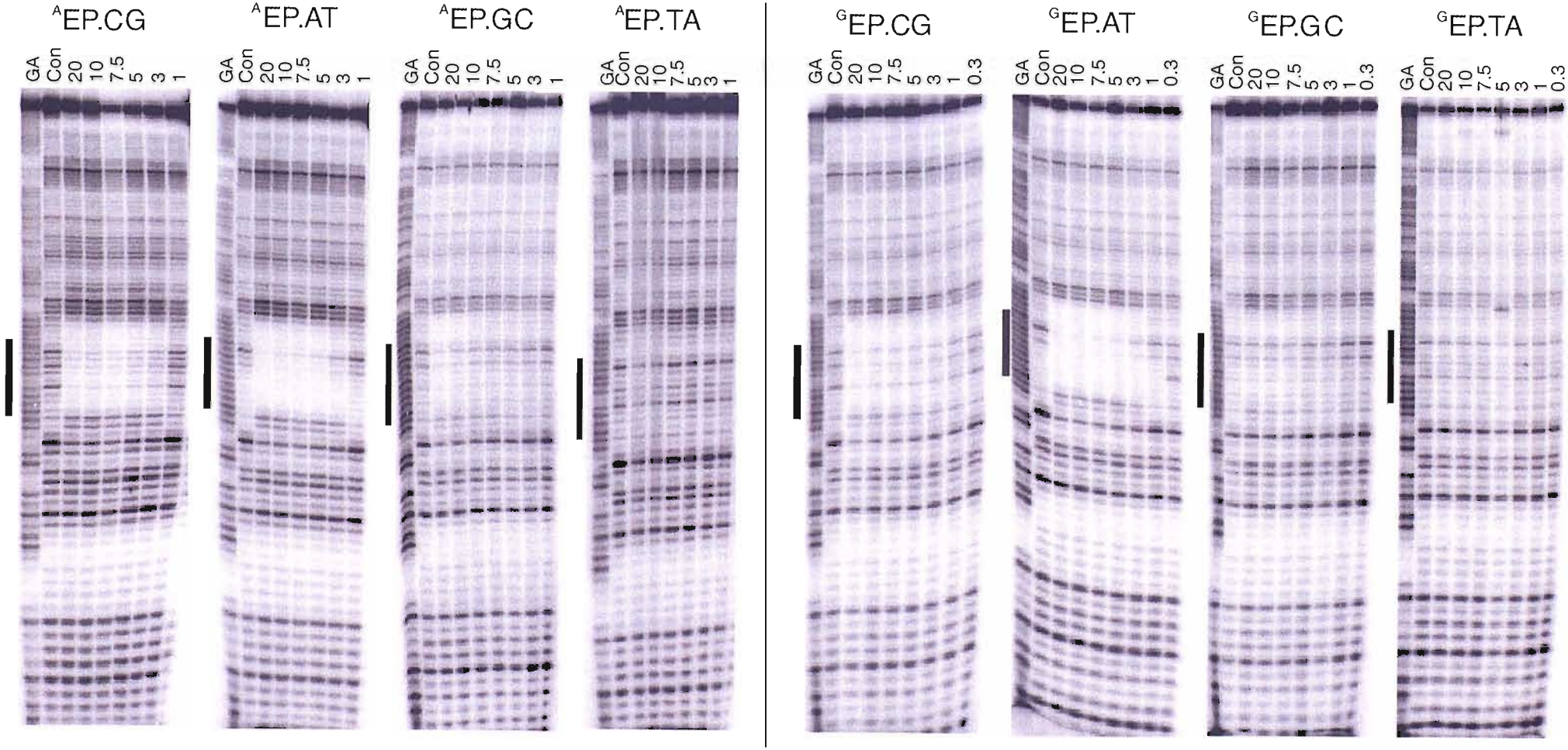

Figure 5.12. DNase I cleavage patterns of different *tyr*T(43-59) fragments in the presence of oligonucleotides 5'-TCTCTT^{A}EPTTTCT (left panel) and 5'-TCTCTT^{G}EPTTTCT (right panel) at pH 5.0. Each triplex differed by a single central triplet X.AT, X.TA, X.GC and X.CG. The experiments were performed in 50 mM sodium acetate containing 10 mM magnesium chloride, and the complexes were left overnight at 20 °C to equilibrate. The oligonucleotide concentration (μM) is shown at the top of each gel lane. Tracks labelled 'GA' are Maxam-Gilbert markers specific for purines, while 'con' indicates DNase I cleavage in the absence of added oligonucleotide. The filled boxes show the position of the triplex target sites.

yielding C_{50} values of 0.3 ± 0.1 μM, 1.2 ± 0.5 μM and 4.8 ± 1.5 μM respectively. The right hand panel of Figure 5.12 shows the DNase I digestion pattern of the four duplex fragments in the presence of the oligonucleotide 5′-TCTCTT^{G}PPTTTCT. Footprints were only generated by this oligonucleotide with the CG, AT and GC targets, yielding C_{50} values of 0.8 ± 0.2 μM, 1.4 ± 0.2 μM and 9.7 ± 2.5 μM respectively. Both nucleobases therefore exhibit a similar affinity and selectivity as MP.

The data from these two techniques suggest no dramatic increase in stability by the addition of a protonated side chain to the pyrrolopyrimidin-2-one core, although ^{A}PP did produce a complex that was slightly more stable than MP at each pH value. The flexibility and rotational freedom of these protonated side chains might account for their lack of stabilisation.

5.3.4.2 Benzylamine derivatives

To assess whether the introduction of more rigid side chain may impart a better stabilising effect, the bases ^{MA}BP and ^{PA}BP, containing benzylamine groups, were investigated. These were compared to the base BP that lacks any amino functions. Again, the melting temperatures for the triplexes shown in Figure 5.4 were determined, where X is BP, ^{MA}BP and ^{PA}BP and ZY is each bp in turn. Representative fluorescence melting profiles for the complexes containing these bases are illustrated in Figure 5.14 and the T_ms calculated for these complexes and those at lower pH values are shown in Table 5.3.

The top left hand panel shows the interaction of the BP-containing TFO. The melting profiles obtained for this analogue suggest no altered selectivity as compared to MP. All T_m values for each BP.ZY triplet differed by less than 1 °C as compared to MP.ZY, however, a slight increase in T_m of 1.4 °C is observed against CG at pH 6.0. It seems that the ability of the benzene ring to stack favourably with neighbouring bases is only slightly better than that of the methyl group at the same position. As expected the addition of this group does not alter triplex specificity.

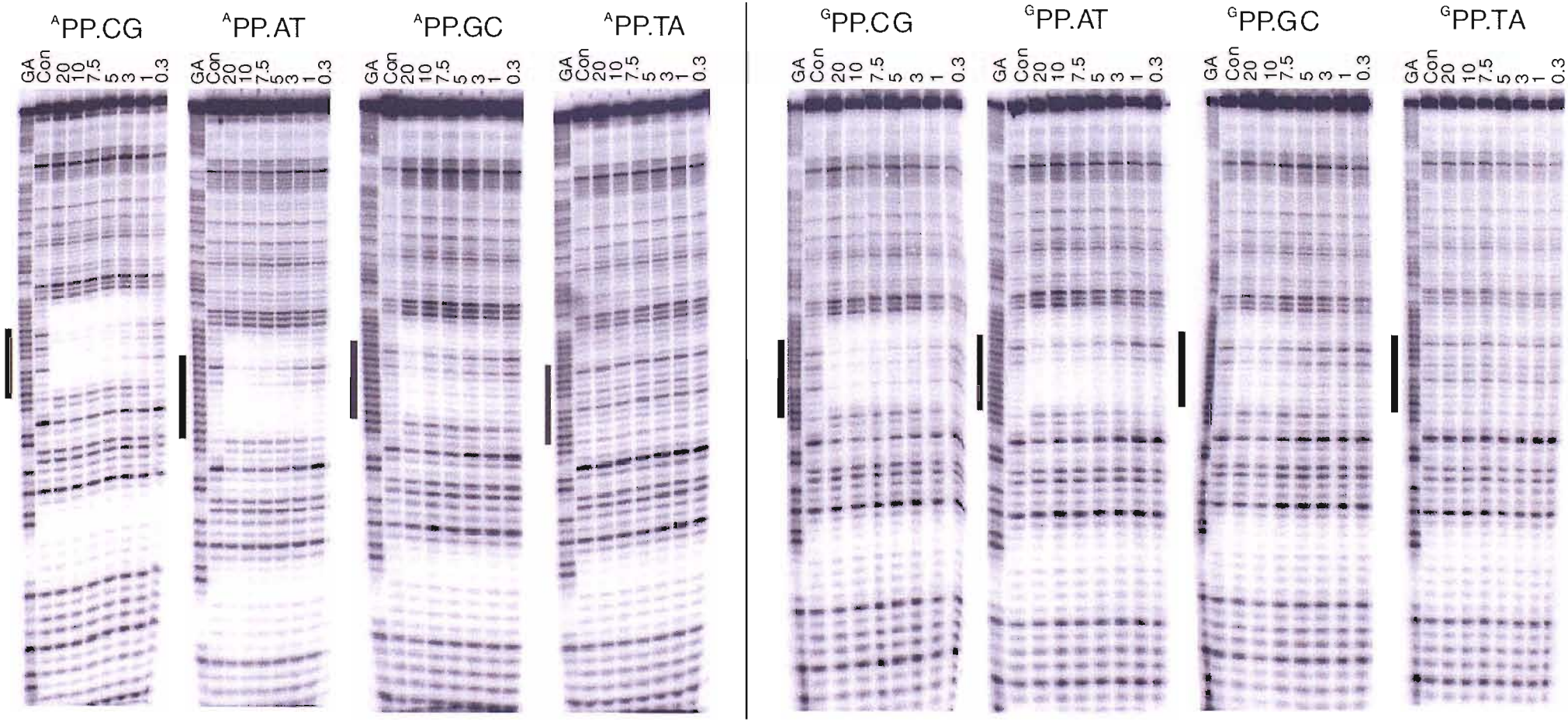

Figure 5.13 DNase I cleavage patterns of different *tyr*T(43-59) fragments in the presence of oligonucleotides 5'-TCTCTT^{A}PPTTTCT (left panel) and 5'-TCTCTT^{G}PPTTTCT (right panel) at pH 5.0. Each triplex differed by a single central triplet X.AT, X.TA, X.GC and X.CG. The experiments were performed in 50 mM sodium acetate containing 10 mM magnesium chloride, and the complexes were left overnight at 20 °C to equilibrate. The oligonucleotide concentration (μM) is shown at the top of each gel lane. Tracks labelled 'GA' are Maxam-Gilbert markers specific for purines, while 'con' indicates DNase I cleavage in the absence of added oligonucleotide. The filled boxes show the position of the triplex target sites.

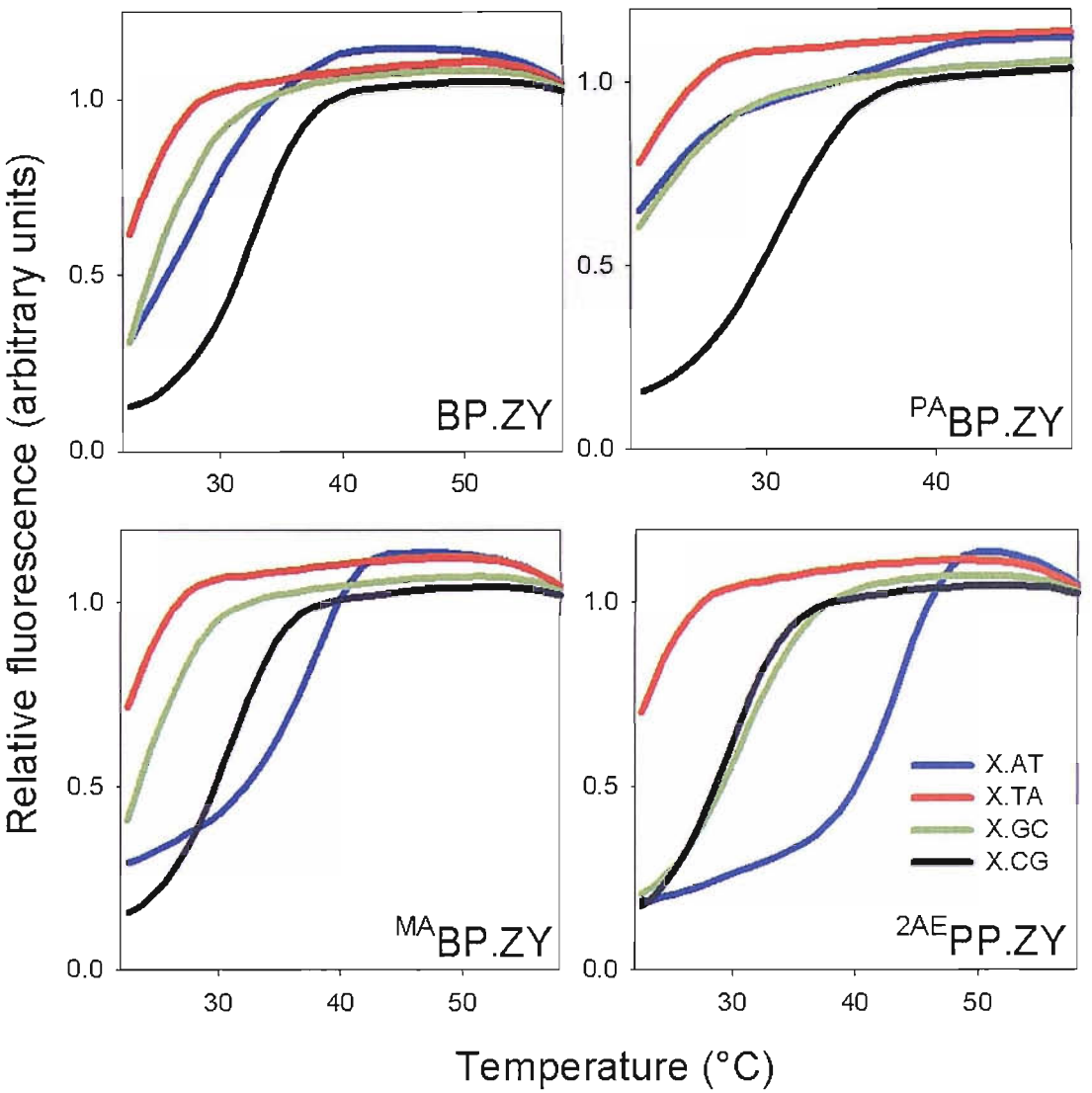

Figure 5.14 Fluorescence melting curves showing the interaction of TFOs containing pyrrolopyrimidin-2-one benzylamine derivatives with duplex targets containing a variable central base pair. Each TFO contains either BP, ^{MA}BP, ^{PA}BP or ^{AE}PP at an identical position, generating X.ZY triplets.The experiments were performed in 50 mM sodium acetate containing 200 mM NaCl at pH 6.0. The y-axes show the normalised fluorescence (arbitrary units), while the x-axes shows the temperature (°C). The samples were heated at a rate of 0.2 °C min^{-1}.

The top right hand graph shows the interaction of the ^{PA}BP-containing third strand. In this instance an amino group is introduced at the *para* position of the ring. This positions it away from the Hoogsteen face of guanine. Again the T_m data suggest no increase in affinity for CG relative to MP and this triplet is actually destabilising relative to BP.CG. The selectivity of this base remains essentially the same, with only minor differences at all pHs. The bottom left hand graph shows the interaction of the ^{MA}BP-containing third strand. In this instance an amino group is introduced at the *meta* position of the ring, positioning it towards the Hoogsteen face of guanine. This analogue closely resembles ^{G}PP, in terms of the positioning of the hydrogen bonding residues. Examination of the T_m data reveals that this analogue offers the greatest affinity for an AT base pair, whilst its selectivity for the remaining base pairs remains unchanged. Furthermore, the melting and annealing profiles of the ^{MP}BP.AT- containing triplex exhibited hysteresis. The T_m for ^{MP}BP.AT triplet is estimated to be 36.5 °C and is therefore 3 °C less stable than T.AT but 5 °C more stable than MP.CG. This increase in stability suggests the formation of two hydrogen bonds, and that the H-bonding contacts on the base and the amine are ideally positioned to recognise AT over CG. This base is therefore not useful for selectively recognising CG.

5.3.4.3 2´-Aminoethoxy derivatives

Lastly, the 2´-aminethoxy derivative of ^{A}PP was examined to assess whether the addition of an amino group to the 2´-position of the sugar may increase the affinity of this analogue for CG, without compromising its selectivity. The T_ms of the triplexes shown in Figure 5.4 were determined by fluorescence melting as before. The bottom right hand graph of Figure 5.14 shows the melting profiles obtained for this analogue positioned against each base pair in turn. It can be seen that with ^{AE}PP in the third strand the most stable triplex was generated with the duplex containing a central AT bp (blue line). The annealing and melting profiles for this complex exhibited hysteresis, an effect previously observed for BAU, another 2´-aminoethoxy modified nucleoside, at this rate of temperature change. This suggests slow kinetics for the formation of this triplet. At pH 6.0, the T_m value for the ^{AE}PP.AT complex was 39.9 °C which is 12 °C higher than the T_m obtained with the ^{A}PP.AT at the same pH. The selectivity of this nucleoside is also slightly different than previously observed for the pyrrolopyrimidones (see Section 5.3.4.1). It can be seen that the affinity for GC increases whilst the affinity for CG and TA remains the same. The T_m of the ^{AE}PP.GC triplet is 3 °C greater than that obtained

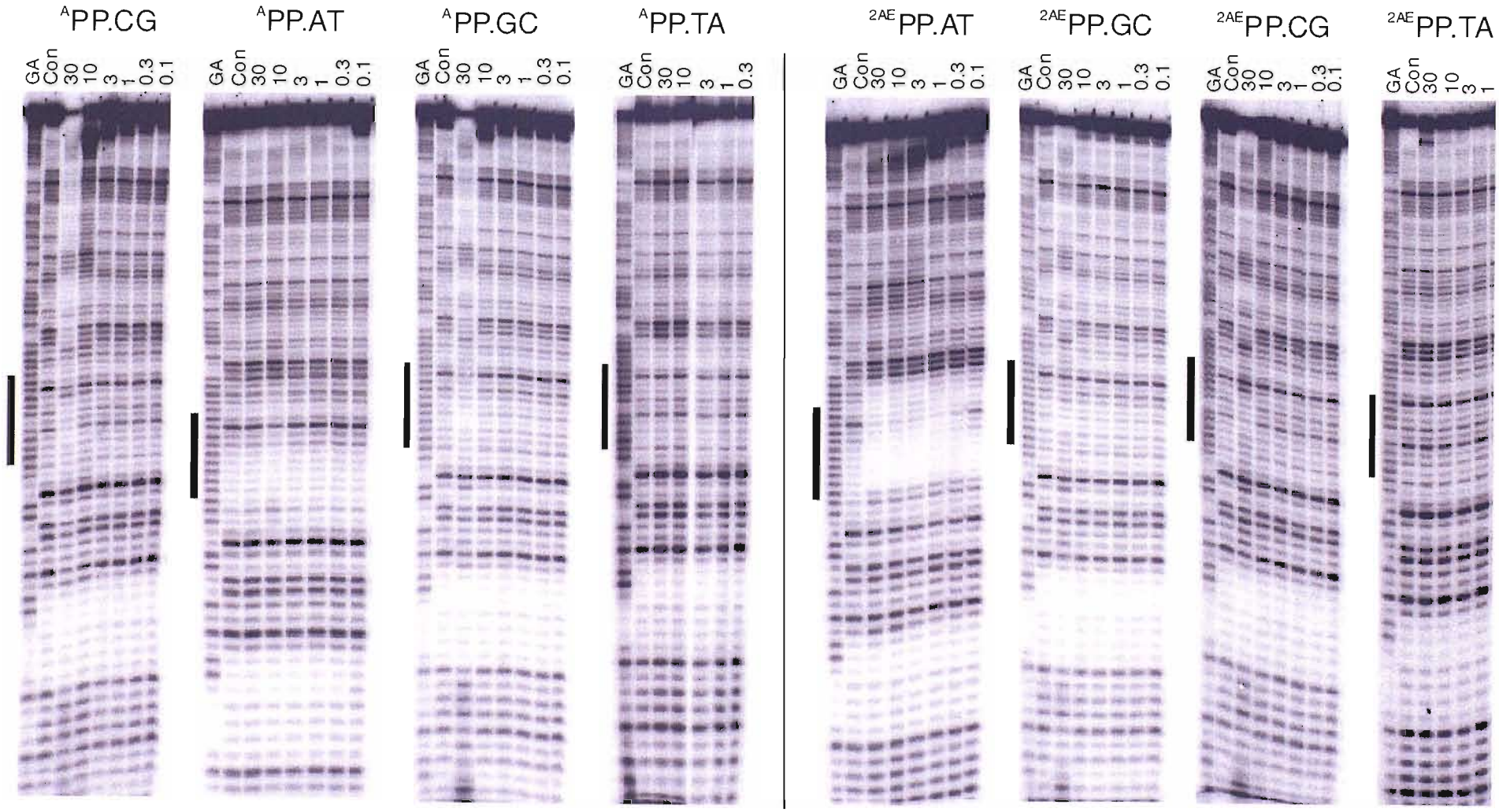

Figure 5.15 DNase I cleavage patterns of different *tyr*T(43-59) fragments in the presence of oligonucleotides 5'-TCBCTB^{A}PPBTBCT (left panel) and 5'-TCBCTB^{AE}PPBTBCT (right panel) at pH 5.0. Each triplex differed by a single central triplet X.AT, X.TA, X.GC and X.CG. The experiments were performed in 50 mM sodium acetate containing 10 mM magnesium chloride, and the complexes were left overnight at 20 °C to equilibrate. The oligonucleotide concentration (μM) is shown at the top of each gel lane. Tracks labelled 'GA' are Maxam-Gilbert markers specific for purines, while 'con' indicates DNase I cleavage in the absence of added oligonucleotide.

for ^{A}PP.GC. These results are consistent with the results obtained for BAU (Chapter 3) that suggest that the 2-aminoethoxy modification increases stability at purine.pyimidine base pairs and not at pyrimidine.purine base pairs.

To further examine this interaction at physiological pH the oligonucleotides 5´-TCBCTBXBTBCT (where X is ^{A}PP or ^{AE}PP and B is BAU) were studied with the four *tyr*T(43-59) fragments at pH 7.0. These TFOs contained four additional BAU substitutions to stabilise triplex formation at this pH. Representative cleavage patterns for the interaction of each of the oligonucleotides with the four DNA fragments are shown in Figure 5.15. The left hand panel shows the cleavage pattern of the four fragments in the presence of the oligonucleotide containing ^{A}PP. It is evident that at this pH the affinity of this TFO is too low to observe as the cleavage patterns for the gels remain unaltered in the presence of this oligonucleotide. The right hand panel shows the cleavage pattern of the four fragments in the presence of the oligonucleotide containing ^{AE}PP. In contrast to ^{A}PP, a clear footprint is evident for this oligonucleotide and the AT-containing fragment while no interaction for the remaining three fragments is observed. It was not possible to calculate a C_{50} value for the footprint produced by the oligonucleotide with the AT-target but is estimated visually at about 0.1 μM. This clearly confirms the results obtained from fluorescence melting and suggests this nucleoside prefers to generate triplets with AT and not CG base pairs.

5.3.5 Triplex formation with analogues of dG

Several analogues of deoxyguanosine were examined for their ability to recognise a TA interruption within an oligopurine tract. Representative melting profiles for the triplexes containing G^{P}, G^{PG} or ^{AE}G positioned against each bp in turn are illustrated in Figure 5.16. The T_ms calculated from these profiles and from those obtained at lower pH values are shown in Table 5.4. The T_ms for the corresponding G-containing triplexes are also included in this table.

It can clearly be seen that with G^{P} in the third strand the most stable triplexes were generated with the duplexes containing either a central TA bp (red line) or central GC bp (green line). The T_m values of these complexes were 31.0 and 30.2 °C respectively. Examination of Table 5.4 reveals that both G^{P} and G exhibit similar T_ms when positioned opposite a TA bp at all the pH values tested. It therefore appears that

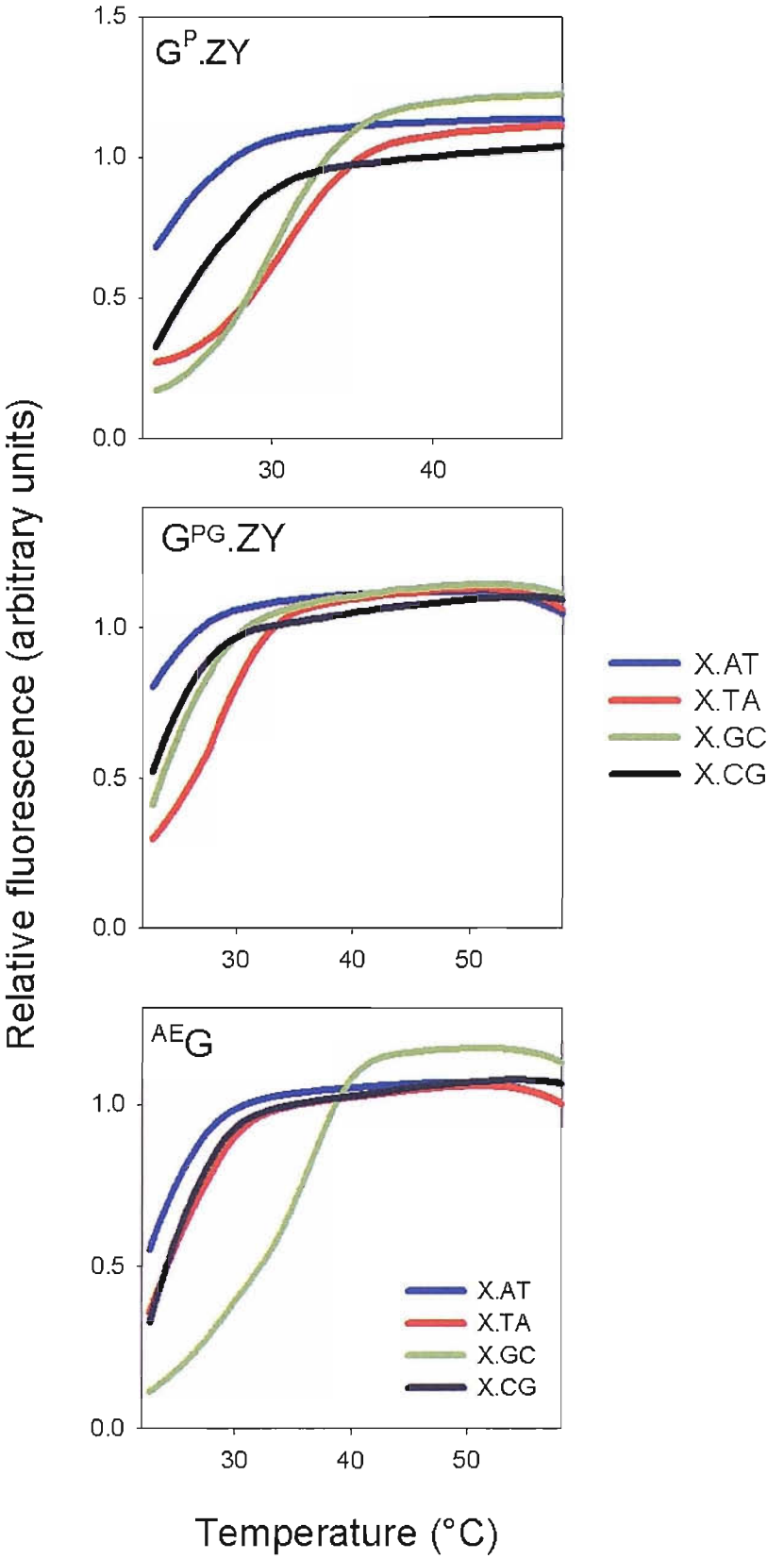

Figure 5. 16 Fluorescence melting curves showing the interaction of TFOs containing deoxyguanosine derivatives with different duplex targets containing a variable central base pair.Each TFO contains either G^{P}, G^{PG} or ^{AE}G at an identical position, generating X.ZY triplets.The experiments were performed in 50 mM sodium acetate containing 200 mM NaCl at pH 6.0.The y-axes show the normalised fluorescence (arbitrary units), while the x-axes shows the temperature (°C). The samples were heated at a rate of 0.2 °C min^{-1}.

introducing a propargylamino group to the 7-position of dG does not increase the stability of the G.TA triplet. In contrast, the stability of the G^P.GC triplet is greater than the G.GC triplet, with a typical increase in T_m of about 2 °C at the pH values tested. The same is seen for the interaction of G^P with AT, though the increase in T_m was lower, with a typical increase in T_m of about 1 °C. No increase in affinity was observed for the interaction with a CG bp. It therefore appears that only the affinity for purine.pyrimidine base pairs is increased by the introduction of the propargylamino group to the 7-position of G.

		ZY			
X	pH	AT	TA	GC	CG
G	5.0	54.2 (54.5)	58.7 (46.7)	57.3 (57.3)	56.3 (56.4)
	5.5	38.2 (38.4)	46.7 (46.8)	43.1 (43.4)	41.2 (41.5)
	6.0	< 28.0	30.6 (30.7)	28.0 (27.9)	< 28.0
G^P	5.0	54.9 (55.0)	58.5 (58.7)	59.0 (59.2)	56.4 (56.5)
	5.5	39.5 (39.0)	46.2 (46.1)	45.3 (45.4)	40.9 (40.9)
	6.0	< 28.0	31.0 (31.4)	30.2 (30.3)	< 28.0
G^{PG}	5.0	54.9 (55.3)	57.8 (58.0)	58.6 (58.5)	55.9 (55.9)
	5.5	39.4 (38.7)	45.2 (44.7)	43.8 (43.6)	40.0 (39.7)
	6.0	< 28.0	29.2 (29.1)	< 28.0	< 28.0
^{AE}G	5.0	53.8 (54.1)	55.4 (55.5)	63.8 (60.3)	55.1 (55.3)
	5.5	39.1 (39.1)	41.5 (41.4)	50.8 (47.9)	40.0 (40.1)
	6.0	< 28.0	< 28.0	36.5 (32.2)	< 28.0

Table 5.4 T_m values determined by fluorescence melting for triplexes composed of triplets containing deoxyguanosine derivatives using a temperature gradient of 0.2 °C min^{-1} and the quencher methyl red. T_m values in parenthesis were calculated from the annealing phase.

The middle panel of Figure 5.16 shows the melting profiles obtained for the propargylguanidino derivative of G (G^{PG}). At pH 6.0, all the triplexes generated by this base were of lower thermal stability than those generated by G. However, at pH 5.0 only the triplexes generated with G^{PG} opposite CG and TA were less stable and those generated with AT and GC were between 0.7-1.3 °C more stable than those generated by G. The reason for this difference is not known but it is clear that the triplex-forming properties of this analogue are inferior to unmodified G.

The bottom panel of Figure 5.16 shows the melting profiles for the complexes containing the 2´-aminoethoxy derivative of G (^{AE}G). Examination of these profiles reveals that the most stable triplet generated by this base was against GC (green line), with a T_m of 34 °C. Again, at the rate of heating and cooling, hysteresis was evident for

this complex at low pH. The selectivity of this base for the remaining base pairs is altered as compared to G. When positioned in the third strand, this base produced complexes of lower stability when positioned opposite TA and CG base pairs. This was greatest against TA and these complexes were at least 3 °C less stable than those formed by G depending on the pH.

DNase I footprinting experiments were used to confirm the results obtained from fluorescence melting on the analogues G^P and G^{PG}. Figure 5.17 presents the cleavage patterns for the interaction of the oligonucleotides 5′-TCTCTT$\underline{G}^P$TTTCT and 5′-TCTCTT$\underline{G}^{PG}$TTTCT with the four fragments derived from *tyr*T(43-59). It is clear that both oligonucleotides produce footprints with the fragments containing central TA and GC bps, while the cleavage patterns for the TA and CG fragments remains unaltered in the presence of these oligonucleotides. The C_{50} values calculated for the interactions of the G^P and G^{PG}-containing oligonucleotides with the fragment containing TA were 1.0 ± 0.1 μM and 2.5 ± 1.2 μM respectively. The same experiment conducted with the unmodified oligonucleotide yielded a C_{50} of 0.2 ± 0.1, therefore the order of stability of these triplets is G.TA > G^P.TA > G^{PG}.TA. Under these conditions these analogues produce C_{50} values that are at least 5-fold lower than G. The C_{50} values for the interaction of these oligonucleotides with the GC duplex targets were 2.5 ± 0.6 μM and 2.5 ± 0.5 μM, respectively. A comparison with the data obtained for the oligonucleotide containing G shows that these triplets are less stable.

5.3.6 Triplex formation with S and 2′-aminoethoxy-S

Guinvarc'h *et al.* recently reported on the synthesis and recognition properties of the nucleoside S in triplex formation (Guinvarc'h *et al.*, 2001). We desired to further characterise this analogue and to study the binding properties of its novel 2′-aminoethoxy derivative (^{AE}S). The stabilities of triplexes that contain a single S or ^{AE}S residue in the centre of the third-strand oligonucleotide were examined by fluorescence melting. Representative melting profiles for these complexes at pH 6.0 are presented in Figure 5.18. The T_m data obtained for these and those obtained at lower pH values are shown in Table 5.5. Examination of this table reveals that S exhibited a greater affinity than G for a TA base pair, with an increase in T_m of 2 °C at pH 5.0 and 4 °C at pH 6.0. However, in this sequence context the S.TA triplet is still less stable than the T.AT triplet, exhibiting a T_m value at least 5 °C lower. S also produced stable complexes with the three remaining base pairs, although the relative stability of these triplets was

dependent on the pH of the solution. At pH 5.0, the melting temperatures of the S.TA and S.CG containing triplexes are essentially the same (61.0 °C and 61.1 °C) and are only marginally higher than S.GC and S.AT (60.1 °C and 59.2 °C). A difference of just 2 °C is observed between the most stable triplet and the least stable triplet at this pH. However at pH 6.0 the discrimination of this base is slightly improved. A difference in T_m of 1.5 °C between S.TA and S.CG and a difference in T_m of 4.2 °C between the most stable and least stable triplet is observed. This still compares unfavourably to T, which exhibits a difference of 11 °C between the most stable and the second most stable triplet produced by this base. This pH dependence suggests the involvement of protonated species. S exhibits a very poor selectivity with an order of affinity of TA < CG < GC = AT.

		ZY			
X	pH	AT	TA	GC	CG
S	5.0	59.2 (59.3)	61.0 (60.7)	60.1 (59.9)	61.1 (61.3)
	5.5	47.2 (47.0)	50.5 (50.4)	46.8 (46.5)	49.1 (49.0)
	6.0	30.6 (30.9)	34.6 (34.6)	30.4 (30.7)	33.0 (33.2)
^{AE}S	5.0	59.5 (59.9)	62.3 (61.0)	60.3 (60.5)	61.7 (61.6)
	5.5	47.5 (47.5)	51.7 (51.6)	47.5 (47.4)	49.3 (49.3)
	6.0	31.3 (31.3)	36.5 (36.4)	31.2 (31.2)	33.6 (63.6)

Table 5.5 T_m values determined by fluorescence melting for triplexes composed of triplets containing S and ^{AE}S using a temperature gradient of 0.2 °C min^{-1} and the quencher methyl red. T_m values in parenthesis were calculated from the annealing phase. The third strands were labelled with methyl red.

Examination of the T_m data for ^{AE}S reveals that the addition of the 2´-aminoethoxy group to S leads to an increase in triplex stability at TA by a further 2 °C at pH 6.0. Therefore of the nucleosides examined in this study, ^{AE}S produced the most stable triplets with TA base pairs. At the higher pH values, the ^{AE}S.TA triplet is only 3 °C less stable than T.AT, compared with G.TA, which is less stable than T.AT by 9 °C. The discrimination of this base also appears to be superior to S. The difference in T_m in the recognition of TA and CG is now 2.9 °C at pH 6.0, about double the difference in T_m observed between S.TA and S.CG (1.6 °C). This also compares favourably to G, where the difference in T_m between the most stable and second most stable triplet formed by this base was 2.6 °C. The order of affinity of this ^{AE}S for each base pair remains the same, though it again seems that the 2´-aminoethoxy modification stabilises triplex formation to a different extent depending on the base pair to be targeted. The lowest stabilisation was observed against CG.

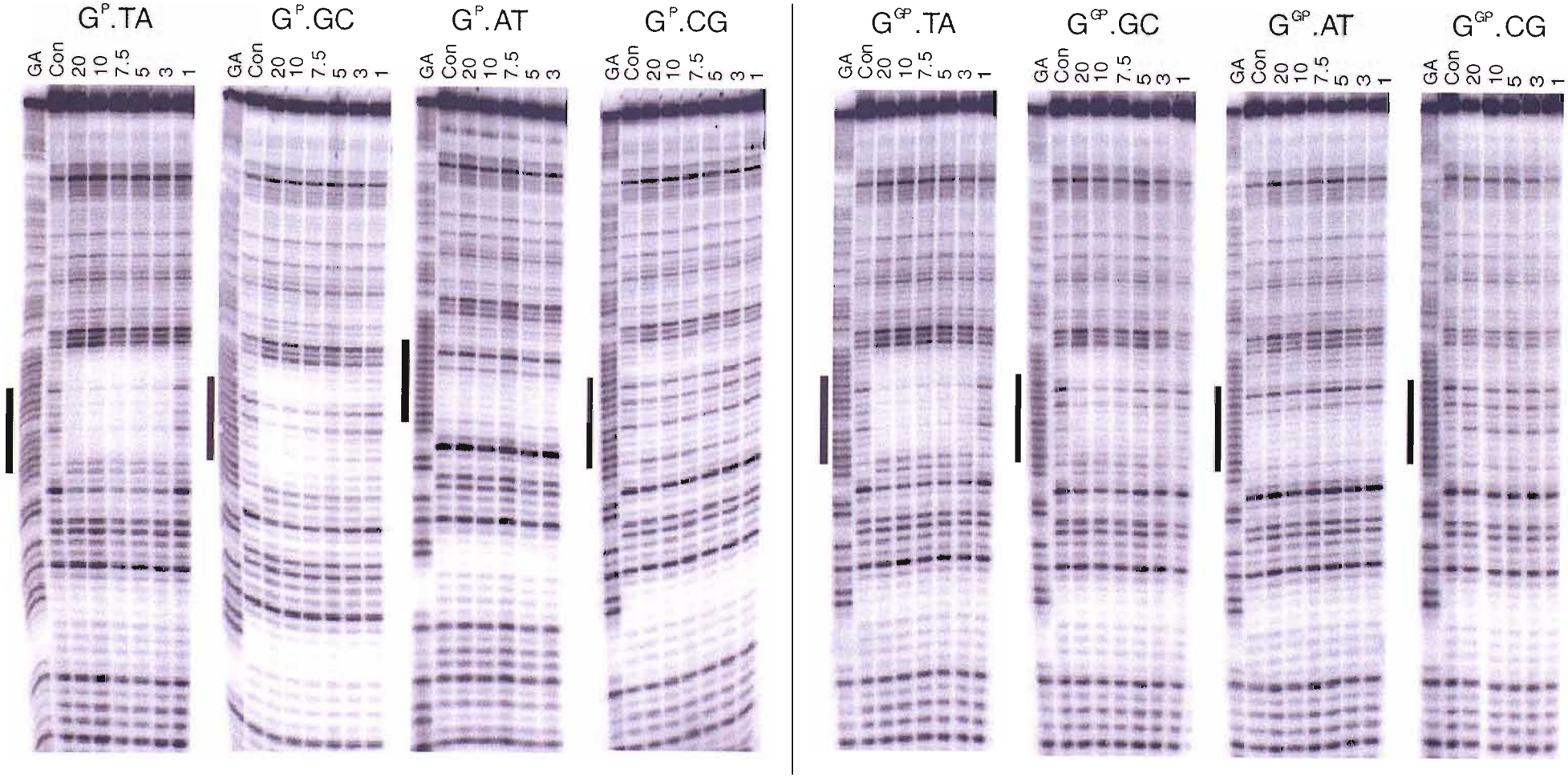

Figure 5.17 DNase I cleavage patterns of different *tyr*T(43-59) fragments in the presence of oligonucleotides 5'-TCBCTBG^{PG}BTBCT (left panel) and 5'-TCBCTBG^{PG}BTBCT (right panel) at pH 5.0. Each triplex differed by a single central triplet X.AT, X.TA, X.GC and X.CG. The experiments were performed in 50 mM sodium acetate containing 10 mM magnesium chloride, and the complexes were left overnight at 20 °C to equilibrate. The oligonucleotide concentration (μM) is shown at the top of each gel lane. Tracks labelled 'GA' are Maxam-Gilbert markers specific for purines, while 'con' indicates DNase I cleavage in the absence of added oligonucleotide. The filled boxes show the position of the triplex target sites.

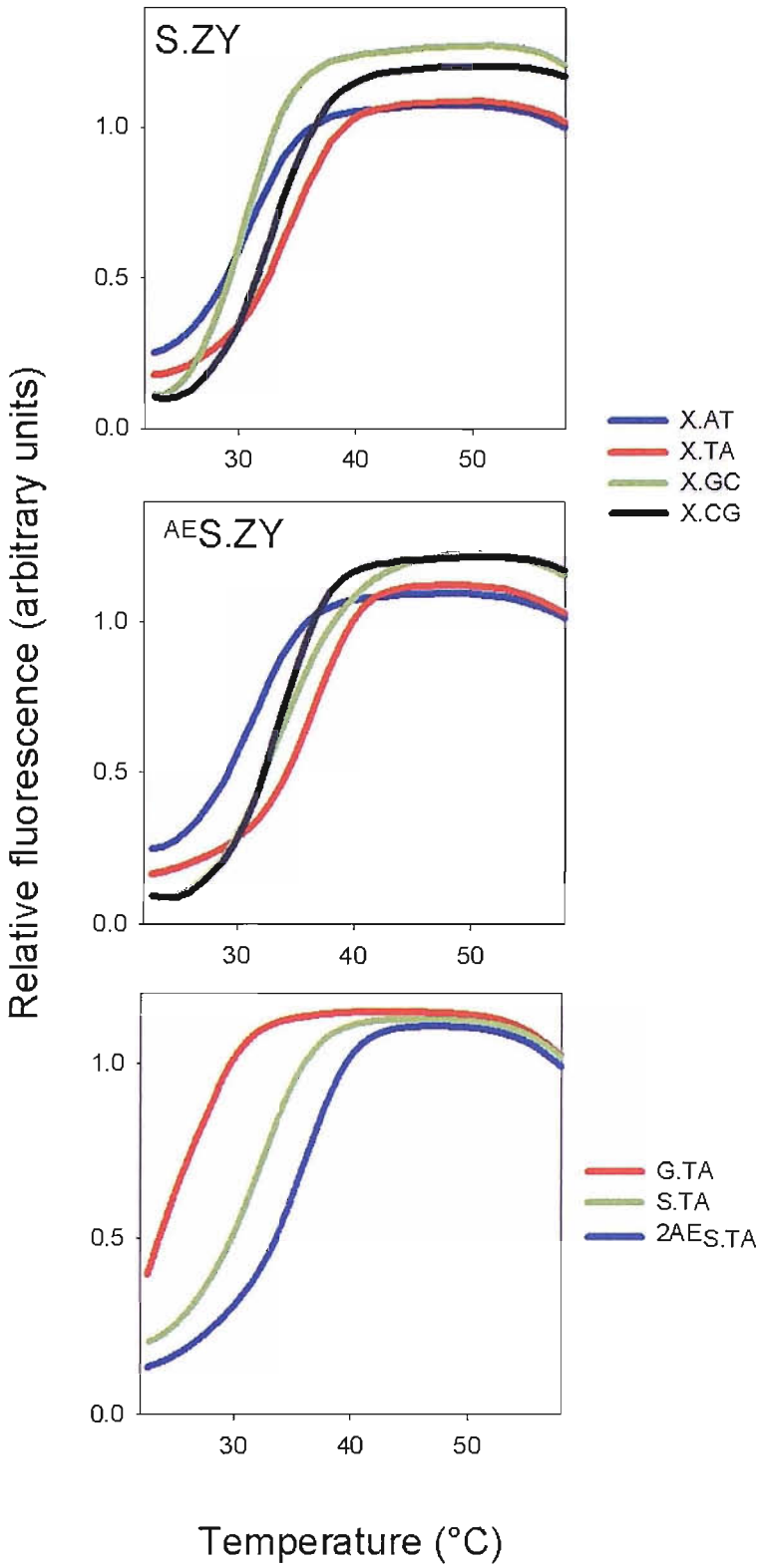

Figure 5.18 Representative fluorescence melting curves showing the interaction of TFOs with target sites containing TA interruptions; A) Melting curves showing the interaction of TFOs containing either S, or ^{AE}S, generating the triplets X.AT, X.TA, X.GC and X.CG; B) Melting curves showing the interaction of TFOs containing two S, ^{AE}S, or G substitutions with a duplex containing two TA interruptions.

In order to obtain a greater insight into the binding properties of S and ^{AE}S, fluorescence melting experiments were performed on triplexes containing two separated TA interruptions. These positions were targeted using third-strand oligonucleotides containing S, ^{AE}S, and G, the sequence of which can be seen in Figure 5.4B. Representative fluorescence melting curves for the complexes at pH 6.0 are shown in Figure 5.18 (bottom panel), and the T_m values are summarised in Table 5.6. At pH 6.0, the presence of two G.TA triplets is sufficiently destabilising to prevent triplex formation above 28 °C (note that a single G.TA triplet gave a T_m of only 30.6 °C). In contrast, the complex with two S.TA triplets displayed a T_m of 32.1 °C, and the stability was further enhanced by incorporation of two ^{AE}S residues with a T_m of 36.3 °C. In this general sequence context, there is little difference in stability between the complexes with one and two ^{AE}S.TA triplets whereas G is strongly destabilising. Again, the relative stability of the three complexes were greater at pH 6.0, showing an increase in T_m of about 2 °C for the addition of each ^{AE}S monomer relative to S.

X	pH	T_m
G	5.0	52.3 (52.4)
	5.5	40.3 (40.3)
	6.0	< 28.0
S	5.0	56.7 (56.8)
	5.5	46.3 (46.4)
	6.0	32.1 (32.1)
^{AE}S	5.0	58.9 (58.4)
	5.5	49.2 (49.2)
	6.0	36.3 (36.3)

Table 5.6 T_m values determined by fluorescence melting for triplexes containing two TA interruptions, targeting these positions with third strands containing G, S and ^{AE}S triplets. T_m values in parenthesis were calculated from the annealing phase.

UV melting experiments were undertaken to support the results obtained from fluorescence melting for ^{AE}S. Representative absorbance vs temperature plots for the triplexes shown in Figure 5.4 (where X is ^{AE}S) are presented in Figure 5.19. For each profile two clear transitions are present; one at low temperatures that corresponds to the melting of the triplex and one at high temperatures that corresponds to the melting of the underlying duplex. The T_m of the triplex was dependent upon the nature of the triplex formed and the pH of the solution. These experiments were carried out at pH 5.8 under the same buffer conditions as above, this pH was employed so as to separate the

melting transitions as much as possible. The rate of temperature change employed was 0.1 °C min^{-1} and hysteresis was not evident between melting and annealing profiles.

It is clear from examining the data that the third-strand oligonucleotide with a central ^{AE}S residue exhibited the same relative selectivity as seen in the earlier fluorescence melting experiments (TA > CG > AT > GC) giving T_m values of 44, 41, 39 and 38 °C, respectively. As expected these values are intermediate between those observed at pH 5.5 and 6.0 using fluorescence melting. Repeating the experiment with the equivalent G-containing third strand produced a complex when positioned opposite TA with a T_m of only 36 °C. Under these conditions, a difference of 8 °C is observed between the ^{AE}S.TA and G.TA triplets and emphasizes the stabilising effect of this base on triplex formation. This study also emphasizes that the reporter groups used in fluorescence melting does not lead to any significant change in triplex stability or specificity.

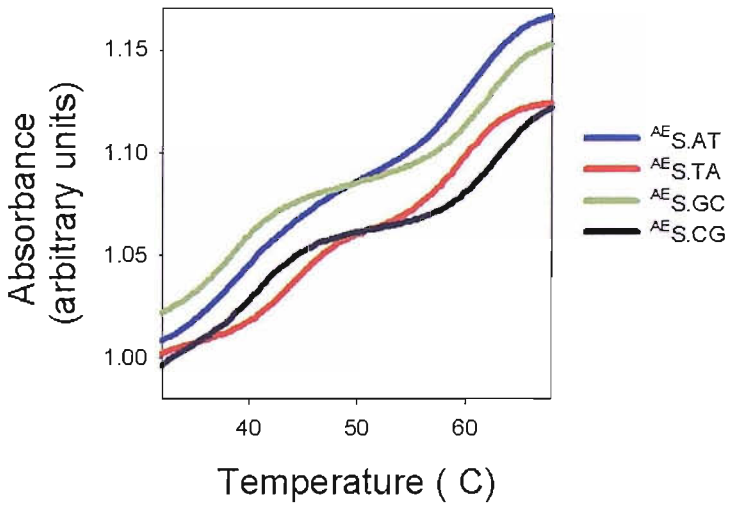

Figure 5.20 UV melting curves showing the interaction of TFOs containing 2′-aminoethoxy-S with different duplex targets containing a variable central base pair. The experiments were performed in 50 mM sodium acetate containing 200 mM NaCl at pH 5.8. The samples were heated at a rate of 0.1 °C min^{-1}.

Lastly, DNase I footprinting experiments were undertaken on triplexes containing the S and ^{AE}S nucleosides. Figure 5.20 shows the cleavage patterns of the four fragments derived from *tyr*T(43-59) in the presence of the oligonucleotides 5′-TCTCTTSTTTCT and 5′-TCTCTT^{AE}STTTCT. It can be seen that in contrast to any other natural base or analogue, these TFOs produced footprints at all four target sites, although the footprints

persisted to different oligonucleotide concentrations. The concentration of the S-containing oligonucleotide required to decrease the band intensity within the footprint by 50 % was 0.11 ± 0.05, 0.6 ± 0.2, 2.1 ± 0.3 and 2.1 ± 0.7 μM for the TA, CG, AT and GC duplex targets respectively. This again confirms the order of affinity of this base for the four duplex targets. In this instance S exhibited about a 5-fold selectivity for a TA bp over a CG bp. The C_{50} value for the S.TA triplet was also about twice that produced by G.TA (0.3 ± 0.1 μM).

The concentration of the ^{AE}S-containing oligonucleotide required to decrease the band intensity within the footprint by 50 % was 0.5 ± 0.1, 0.8 ± 0.1 and 1.2 ± 0.2 μM for the CG, AT and GC duplex targets respectively. However, it was not possible to calculate a C_{50} value for the interaction of ^{AE}S with TA and is estimated as being < 0.1 μM. It can therefore appears that as expected the addition of the 2′-aminoethoxy group further increased the affinity of S for all the targets, although the increase in affinity was greatest for targets with a central TA and AT. Again ^{AE}S.TA is more stable than G.TA. ^{AE}S also appears to be able to discriminate between TA and CG with at least a 4-fold difference in C_{50} values.

	ZY			
X	AT	TA	GC	CG
A	n.d	n.d	0.3 ± 0.1	n.d
G	n.d	0.2 ± 0.1	2.5 ± 0.5	n.d
C	n.d	n.d	< 0.1	0.8 ± 0.3
T	< 0.1	n.d	2.1 ± 0.3	0.7 ± 0.4
C^P	1.1 ± 0.1	n.d	< 0.3	1.2 ± 0.2
$^{AE}Q_\alpha$	n.d	n.d	n.d	n.d
$^{AE}Q_\beta$	n.d	n.d	n.d	n.d
^{7H}MP	1.7 ± 0.2	n.d	< 0.3	0.8 ± 0.2
MP	1.6 ± 0.2	n.d	6.0 ± 1.7	0.5 ± 0.1
^{A}EP	2 ± 0.1	n.d	12 ± 5.1	0.8 ± 0.4
^{G}EP	1.5 ± 0.6	n.d	8.7 ± 3.3	0.7 ± 0.1
^{A}PP	1.2 ± 0.5	n.d	4.8 ± 1.5	0.3 ± 0.1
^{G}PP	1.4 ± 0.2	n.d	9.7 ± 2.5	0.8 ± 0.2
G^P	n.d	1.0 ± 0.1	2.5 ± 0.6	n.d
G^{GP}	n.d	2.5 ± 1.2	2.5 ± 0.5	n.d
S	2.1 ± 0.3	0.11 ± 0.1	2.1 ± 0.7	0.6 ± 0.2
^{AE}S	0.8 ± 0.1	< 0.1	1.2 ± 0.2	0.5 ± 0.1

Table 5.7 C_{50} values determined by DNase I footprinting for the interaction of TFOs 5′-TCTCTTXTTTCT, where X is either a natural base or analogue, with target duplexes containing the sequence 5′-AGAGAAZAAAGA/ 3′-TCTCTTYTTTCT, where YZ is AT, TA, GC or CG. The experiments were performed in 50 mM sodium acetate at pH 5.0.0 containing 10 mM magnesium chloride.

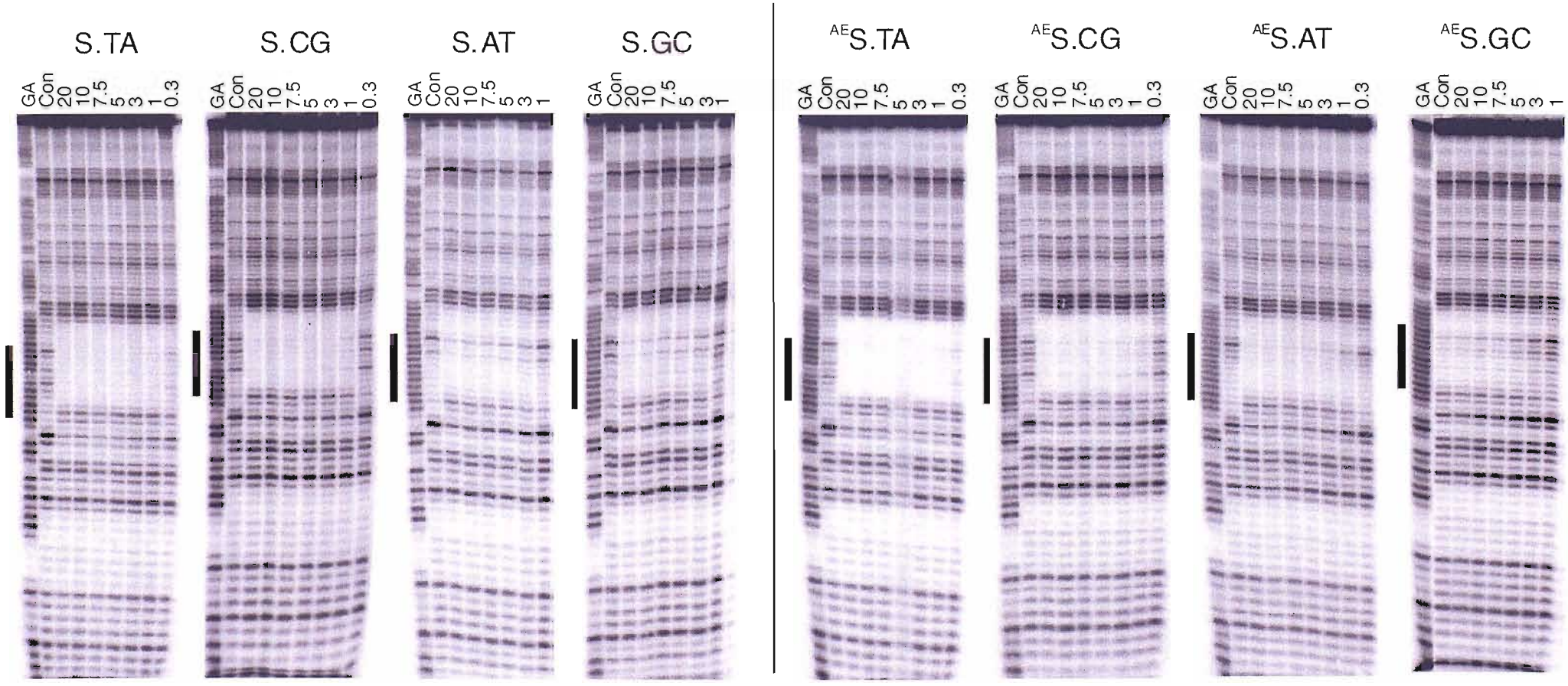

Figure 5.19 DNase I cleavage patterns of different *tyr*T(43-59) fragments in the presence of oligonucleotides 5'-TCTCTTSTTTCT (left panel) and 5'-TCTCTT^{AE}STTTCT (right panel) at pH 5.0. Each triplex differed by a single central triplet X.AT, X.TA, X.GC and X.CG. The experiments were performed in 50 mM sodium acetate containing 10 mM magnesium chloride, and the complexes were left overnight at 20 °C to equilibrate. The oligonucleotide concentration (μM) is shown at the top of each gel lane. Tracks labelled 'GA' are Maxam-Gilbert markers specific for purines, while 'con' indicates DNase I cleavage in the absence of added oligonucleotide. The filled boxes show the position of the triplex target sites.

5.4 Discussion

The experiments in this chapter examined the triplex-binding properties of several nucleoside analogues designed to recognise pyrimidine bases within a target oligopurine tract. The affinity and specificity of these nucleosides is discussed.

5.4.1 5-Propargylamino-dC

The introduction of a propargylamino group at the 5-position of C should lower the pK_a of its ring nitrogen. It should therefore be less protonated at high pH, disabling its ability to form two hydrogen bonds to a GC base pair. This has previously been demonstrated using the C5 propyne analogue of dC (Froehler *et al.*, 1992), although in this instance the decrease in pK_a should be greater due to the introduction of an electron withdrawing amino group. The results from fluorescence melting experiments indicated that, as expected at higher pHs, the affinity of C^P for GC was lower than that of C, confirming a requirement for protonation. However, the extent of this destabilisation was not as dramatic as initially anticipated; at pH 5.0 both C^P and C formed triplets that exhibited similar melting temperatures. In contrast, footprinting studies at pH 5.0 indicated that the C^P.GC was less stable than C^+.GC. This minor difference maybe attributed to the presence of magnesium in the buffer, which may affect the pK_a of the base. There are several potential reasons why the affinity of this base is only slightly lower than C at the pH values tested: (i) the propargylamino group may stabilise the C^P.GC triplet, as previously shown for the formation of the U^P.GC triplet (ii) the electron withdrawing property of the amino group is partially lowered due to electrostatic interactions with a positively charged phosphate residue (iii) the pK_a of C^P is higher upon triplex formation as previously shown for C (Rajopal & Feignon, 1989; Asensio *et al.*,1999).

From these results it also appears that the introduction of a propargylamino group at the 5-position of C alters its specificity in triplex formation. This is not surprising, as similar results were seen for the thymine analogue 5-propargylamino-dU in Chapter 4. The triplets formed by C^P with CG and AT were at least 2 °C more stable than those formed by C, whilst the affinity for TA was not affected. However, the magnitude of this stabilisation was not as great as seen with U^P. In the absence of ring protonation C^P should present two hydrogen bond acceptors, both of which are capable of forming a

single hydrogen bond with AT or CG. As selectivity was not dependent on pH, it suggests that the carbonyl, not the ring nitrogen, plays the predominant role as the acceptor used for recognition of these base pairs. In this configuration, additional stabilisation is likely to stem from increased stacking or electrostatic interactions of the propargylamino group within the major groove.

The results obtained from footprinting studies with this analogue were slightly different; most notably the stabilisation afforded by C^P was greater for AT than for CG; the C_{50} value for C^P.AT is 30-fold greater than that obtained for C.AT, whilst the C_{50} value for C^P.CG is only 1.5-fold greater than C.CG. The reason for this difference is unclear but it is most likely to stem from the different sequences used or different buffer conditions.

It remains to be seen whether C^P would offer a greater affinity for CG than GC at physiological pH as in this experimental system triplex formation was restricted to low pH. The increased pK_a within a triplex might disfavour the usefulness of this base for targeting CG inversions. Further experiments with TFOs composed solely of T would remove this pH restriction and would allow this to be determined.

5.4.2 2′-Aminoethoxy-1-isoquinolone

CG recognition has previously been reported using LNA bearing a 1-isoquinolone base (Hari *et al.*, 2003). In the present study the binding properties of the 2′-aminoethoxy derivative of this nucleoside were examined. Both α and β anomers were studied, as α-anomers have been reported to bind favourable within triplex DNA (Thuong *et al.*,1987; Bates *et al.*, 1996; Marfut *et al.*, 1997). Disappointingly the results obtained indicated that at all pH values the selectivity and affinity of both anomers was poor. Of all the analogues studied, these bases were the most destabilising positioned against any base pair. These results therefore indicate that the stabilisation previously afforded by this base must have stemmed predominantly from the LNA modification. The reason for this is not obvious as both modifications lock the sugar in an N-type conformation. However, it is possible that this base prefers to generate a *syn* conformation when the aminoethoxy modification is introduced into the sugar.

5.4.3 Substituted pyrrolopyrimidin-2-one nucleosides

Several nucleosides based on the 3*H*-pyrrolo[2,3-*d*]pyrimidin-2(7*H*)-one ring system were examined for their ability to recognise CG base pairs. These nucleosides present double acceptor sites, either of which could participate in forming a hydrogen bond with the free C4-amino proton of the duplex C. Initially the nucleobases MP and ^{7H}MP were studied to assess the suitability of the pyrrolopyrimidin-2-one core for CG recognition. In both cases T_m measurements indicated that triplexes containing a MP.CG or ^{7H}MP.CG triplet were on average 3 °C more stable than those containing T.CG or C.CG. Furthermore, the C_{50} values determined by footprinting experiments indicated that these nucleosides produced triplets with CG that are at least as stable as those produced by C or T. This increase in affinity for CG relative to T could stem from two major factors: (i) In a structural model for CG recognition that involves N3, the carbonyl group may form an additional dipolar interaction with H-C(5) of cytosine (Marfut & Leumann, 1998; Buchini & Leumann, 1999); (ii) the extended aromatic surface of this base may provide additional stacking interactions within the major groove. These results also confirmed that a methyl group is required at position 7 (as in MP) to disable the recognition of a GC base pair. ^{7H}MP produced a very stable triplet with GC that was about 8 °C more stable than ^{7H}MP.CG. The difference in stability between these two triplets suggests that this base is forming two hydrogen bonds to GC and suggests that it may also be protonated at N3 (Figure 5.21A).

The selectivity of both MP and ^{7H}MP was also dependent on pH and at low pH the specificity of these analogues was decreased. At pH 5.0, the difference in melting temperatures between the most stable (MP.CG) and second most stable triplets (MP.GC and MP.AT) was only 1.5 °C. At pH 6.0, this difference was increased to a more favourable 5 °C. One simple explanation for this is the recognition of the bases at low pH may be the result of protonation event at N3. In this configuration a hydrogen bond could form with the N7 atoms of AT and GC and would account for the higher affinity for these base pairs. Despite this altered selectivity it is clear that at pH values above 5.5 this base is specific for CG.

The stabilising effect of introducing amino or guanidino groups at the 6-position of the pyrrolopyrimidin-2-one ring was then examined. These replace the methyl group present at the 6-position of MP. The amino and guanidinoethyl-modified nucleobases

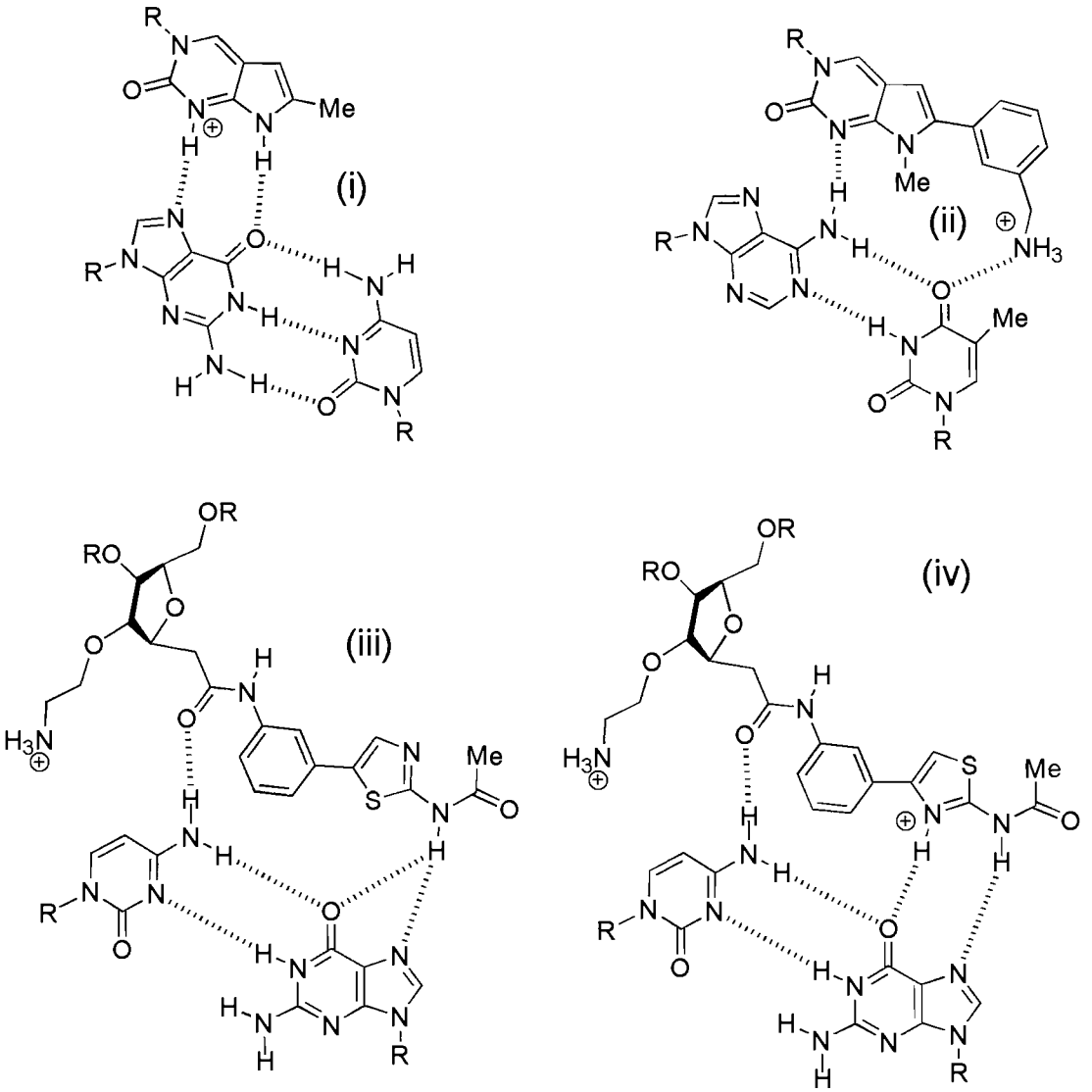

Figure 5.21 Chemical structures and proposed hydrogen bonding patterns of triplets containing novel nucleoside analogues; (i) ^{7H}MP.GC (ii) ^{MA}BP.AT (iii) S.CG and (iv) ^{AE}S.CG.

^{A}EP and ^{G}EP and the amino and guanidinopropyl-modified nucleobases ^{A}PP and ^{G}PP were investigated. Surprisingly, no dramatic increase in affinity or altered specificity was observed for any of these nucleobases relative to MP. The order of affinity for CG of these nucleosides is ^{A}PP = ^{M}PP > ^{G}PP > ^{A}EP = ^{G}EP and their selectivity at high pH remained X.CG < X.GC < X.GC < X.TA. From these data it appears that the protonated groups were not suitably positioned to participate with H-bonding within the major groove or in electrostatic interactions with the phosphodiester backbone. A study on the affinities of aminopropyl and propargylamino-modified T recently suggested that the lack of rigidity of the propyl chain resulted in destabilisation of the triple helix (Brazier *et al.*, 2005). A similar situation is therefore likely in this instance.

As noted in Section 5.3.3.1 a small secondary transition was observed at high temperatures for the melting profiles obtained for certain pyrrolopyrimidin-2-ones with the target containing an AT base pair. One suggestion for the occurrence of this transition could be that an additional species was present in the sample. A recent study on the stability of the structurally similar furanopyrimidin-2-one nucleosides suggested that under certain conditions, such as UV melting, these nucleosides may undergo facile hydrolytic ring opening in aqueous solution (Jiao & Burgess, 2004). Furthermore, this paper suggested that the substituent at the 7-position has a relatively strong influence on the ease at which ring opening occurs and may explain why this transition was only observed for certain substituted pyrrolopyrimidin-2-ones. Opening of the ring is likely to generate uracil derivatives and might explain why the transition was only observed with the target containing an AT base pair. Interestingly, this transition was less prominent when heating the samples at a faster rate of heating.

As the initial attempt to enhance the thermodynamic stability by the incorporation of pendant protonated groups was unsuccessful, a further set of derivatives were evaluated. It was rationalised that a more rigid platform for the amine may reduce the rotational freedom and the flexibility of the side chain and could be used as a better scaffold to position amine functions to interact with G of the CG base pair. The planar aromatic ring could also participate in stabilising interactions with the neighbouring bases. Initially the analogue BP was examined and contained a benzene ring at the 7-position. From T_m measurements it appears that this nucleobase offered only a slight increase in affinity (ΔT_m ~1 °C) for CG relative to MP, and again exhibited the same selectivity as the previous nucleobases. ^{PA}BP and ^{MA}BP were then studied and contain amino groups

at the *para* and *meta* positions of the benzene ring respectively. Again the stability of these nucleobases was not improved for the recognition of CG. However, ^{MA}BP unexpectedly formed a more stable triplet with AT. The T_m value for this interaction was similar to that obtained for the standard T.AT triplet and therefore suggests the formation of two hydrogen bonds. The amino group is therefore likely to be in a suitable position to interact with the 4-carbonyl of T (Figure 5.21(ii)). This corroborates the viability of this approach and suggests that further altering the position of the amino group may be useful for increasing the stability at CG. Despite the limited success of these modifications, it should be noted that as protonated amino groups have been reported to enhance binding kinetics of TFOs (Puri *et al.*, 2004), these analogues maybe more useful in this respect.

The last substituted pyrollopyrimidin-2-one to be investigated was the 2′-aminoethoxy derivative of ^{A}PP. The T_m values determined for triplexes containing this nucleoside indicated that it recognised AT with a higher affinity than CG. An increase in T_m was also observed against GC. As this interaction might stem from a protonation event at N3, further footprinting experiments were undertaken at pH 7.0. Again AT recognition was confirmed. This result is surprising but is similar to the results observed for BAU in Chapter 4, where addition of the 2′-aminoethoxy group to T stabilised its interaction with purine.pyrimdine and not pyrimidine.purine base pairs. The reason for this is unclear.

5.4.4 Deoxyguanosine derivatives

7- and 2′-substituted derivatives of dG were assessed for their novel triplex-forming properties. T_m values determined for the analogues containing a 7-propargylamino or 7-propargylguanidino group on the base, or a 2′-aminoethoxy group on the sugar, indicated no increase in affinity for a TA base pair relative to G. In fact both G^{PG} and ^{AE}G actually destabilised the triplex by 1 °C and 3 °C respectively. In contrast, all modifications enhanced the affinity of G for a GC base pair. At pH 6.0, the ^{AE}G.TA triplet was 6 °C more stable than G.GC, whilst the G^{P}.GC and G^{PG}.GC triplets were between 2-3 °C more stable. The strength of binding of ^{AE}G for GC is almost comparable to that of T for AT, suggesting that this analogue is forming two hydrogen bonds. Footprinting experiments were also carried out on G^{PG} and G^{P} and confirmed that these bases were destabilising opposite TA. However, the standard deviations for

the values obtained for triplexes containing these bases opposite GC base pair were too large to allow unambiguous interpretation. It is therefore clear that these modifications do not result in useful bases for the selective recognition of TA base pairs.

Both the G.TA and G.GC triplets can be accomodated within parallel triplexes and the relative stability of each triplets is dependent on the local sequence context (Griffin & Dervan, 1989; Sun *et al.*, 1991). G.TA is more stable when flanked by T.AT than C^+.GC triplets, due to the formation of an additional hydrogen bond between the unused amino proton of G and the duplex T of a 3´-adjacent T.AT triplet (Radhakrishnan & Patel, 1991/1994). As a result G produces more stable triplets with TA than GC only when flanked with T.AT. However in this instance, the dG derivatives favoured GC recognition, despite flanking T.AT triplets. The reason for this might be that (i) the addition of these modification disrupts the favourable neighbouring interactions (ii) the positioning of the propargyl or aminoethoxy side chains are only suitable for interacting with phosphates when situated opposite GC.

These analogues might find a better use within the antiparallel triplex motif, not just because this modification is stabilising but also because they may reduce the propensity of G-rich oligonucleotides to form secondary structures; the formation of a G-quadruplex utilizes both the Watson-Crick and Hoogsteen faces of G and therefore the introduction of the relatively large propargyl chain at the seven position is likely to disrupt the formation of such structures.

5.4.4 S and 2-aminoethoxy-S

The unnatural thiazolylaniline deoxyribonucleoside (S) has been reported to recognise a TA base pair with a comparable affinity to that of T for an AT base pair (Guinvarc'h *et al.*, 2001). This chapter presents fluorescence melting data obtained with this analogue and showed that it increased triplex stability at a TA base pair by 2-4 °C relative to G, producing a triplet that was 3-5 °C less stable than T.AT. These T_m measurements are similar to those obtained by Guinvarc'h *et al.* measured by UV absorbance. To confirm these results, footprinting experiments were undertaken on shorter TFOs. It was observed that the interaction of a TFO containing a single substitution of S with a duplex target containing a TA base pair in an identical position yielded a C_{50} value that was 3-fold greater than the equivalent G-containing TFO. Again this triplex was less

stable than the triplex containing T.AT. In the hydrogen bonding scheme proposed by Guinvarc'h *et al.*, S recognises a TA base pair by forming three hydrogen bonds (Figure 5.3(iv)); one to O4 of thymine and two to adenine (N7 and N6). The relatively high T_m and C_{50} values for the triplexes containing a single S.TA triplet support this suggestion though the lower stability compared to T.AT, where only 2 hydrogen bonds are formed, may seem surprising. This suggests that the arrangement of hydrogen-bonding groups in S or its stacking within the third strand is not optimal.

Although these results demonstrate that S is effective in stabilising TA interruptions, this nucleoside offers a limited selectivity. At pH 5.0, the melting studies showed a difference of just 2 °C between most stable (S.TA) and least stable (S.AT) triplets generated by this base. This compares with a 14 °C difference between the two most stable triplet combinations formed by C. Furthermore, at pH 5.0 the complexes containing S.AT and S.CG exhibited identical T_ms, although at pH 6.0 selectivity was increased and a difference in T_m of 1.6 °C was observed between the two triplets. This low selectivity was also confirmed by footprinting studies and S was the only base to enable stable triplex formation when positioned opposite each of the base pairs. A 5-fold selectivity for TA over CG was evident, which compares to greater than an 8-fold difference in selectivity for the recognition of GC and CG by C.

It should be noted that S is structurally related to the nucleoside analogue D_3 (Figure 1.15(i); Griffin *et al.*, 1992), which was designed for specific recognition of CG base pairs but was subsequently found to intercalate at YpR steps instead of binding within the major groove (Kiessling *et al.*, 1992; Koshlap *et al.*, 1993). Although S could potentially bind in the same manner, a study on nearest neighbour effects suggested this is not the case (Guinvarc'h *et al.*, 2003). However, the conformational flexibility of S may permit hydrogen-bond formation with other base pairs in addition to TA, and schemes for putative S.CG triplets are shown in Figure 5.21. In one of these (Figure 5.21(iii)), S forms a hydrogen bond to N4 of cytosine and a bifurcated hydrogen bond to O6 and N7 of guanine, although there are no hydrogen bonds to the thiazole ring. An alternative structure for the recognition of CG, which involves protonation of the thiazole nitrogen and consequent hydrogen bonding to O6 of guanine, is shown in the Figure 5.21(iv). The latter triplet, which could exist at low pH, is likely to be the more stable, explaining why S shows greater selectivity for TA at elevated pH values.

However, detailed structural studies will be necessary to properly elucidate the binding modes of S.

2′-aminoethoxy-S was studied alongside S to investigate whether this derivative could enhance triplex affinity further. This nucleoside analogue increased triplex stability at a TA by a further 2 °C relative to S, producing a triplet that was only 3 °C less stable than T.AT. UV melting was undertaken and this base was shown to generate a triplex with a T_m 8 °C higher than the triplex containing G.TA triplet. Both fluorescence and UV melting indicated a difference in T_m of 3 °C between the thermal stability of the triplexes containing ^{AE}S.TA and ^{AE}S.CG triplets, this difference is similar to that afforded by G for TA and GC. Again ^{AE}S was shown to increase triplex stability when positioned against each base pair and this was greatest against TA and the least against CG, hence the slightly better discrimination observed. The lower stabilisation afforded for CG is similar to the results obtained with the previous 2′-aminoethoxy modified bases (BAU, ^{AE}G). This suggest that modifications that leave the Hoogsteen face of a base unaltered may still be useful for altering the triplex specificity of the base.

Finally, experiments were performed with duplex targets containing two separated TA interruptions, targeting these positions with third strands containing G, S and ^{AE}S. These experiments were undertaken to gain a further insight into the binding properties of these nucleosides. At pH 6.0, the presence of two G.TA triplets was sufficiently destabilising to prevent triplex formation above 28 °C. In contrast, the complex with two S.TA triplets displayed a T_m at least 4 °C higher and the complex with two ^{AE}S.TA triplets displayed a T_m at least 8 °C higher. This indicates that the increase in binding affinity of these substitutions is additive.

6 TOWARDS FOUR BASE RECOGNITION IN PARALLEL TRIPLEX FORMATION AT PHYSIOLOGICAL PH

6.1 Introduction

Triplex formation using oligonucleotides composed only of natural bases suffers from several intrinsic limitations; (i) the binding of the third strand may not be strong, due to electrostatic repulsion between the three polyanionic DNA strands; (ii) formation of the C^+.GC triplet requires conditions of low pH (< 6.0), necessary for protonation of third strand cytosines; (iii) there are no stable means for recognising TA or CG base pairs using natural DNA bases. The preceding chapters identified several nucleoside analogues that when substituted into TFOs could be used to overcome one or more of these restrictions. 2´-aminoethoxy-5-propargylamino-U (BAU; Figure 6.1(i)) forms more stable triplets with AT than T and does not require divalent metal ions for binding. The specificity of this analogue is greater than T, offering enhanced discrimination against pyrimidine-purine base pairs. 3-methyl-2-aminopyridine (^{Me}P; Figure 6.1(ii)) binds to GC base pairs at higher pHs than C and when used in combination with BAU extends high affinity triplex formation to physiological pH. 6-(3-aminopropyl)-7-methyl-*3H*-pyrrolopyrimidin-2-one (^{A}PP; Figure 6.1(iii)) forms stable and selective triplets with CG. While, *N*-(4-(3-acetamidophenyl)thiazol-2-yl-acetamide (S; Figure 6.1(iv)) forms more stable triplets with TA than G, albeit with a lower selectivity.

There have been many studies investigating the effects of single nucleotides on triplex stability, each addressing one or other aspects of the problem (pH dependency, affinity and recognition of pyrimidine inversions). However, there are very few examples where they have been combined to achieve high binding affinity to mixed sequence duplex DNA targets at physiological pH. This chapter examines the ability of a TFO containing multiple substitutions of BAU, ^{Me}P, S and ^{A}PP to selectively target a mixed sequence duplex target at physiological pHs.

6.2 Experimental design

The triplex-forming properties of the oligonucleotides shown in Figure 6.2 were examined by fluorescence melting and DNase I footprinting.

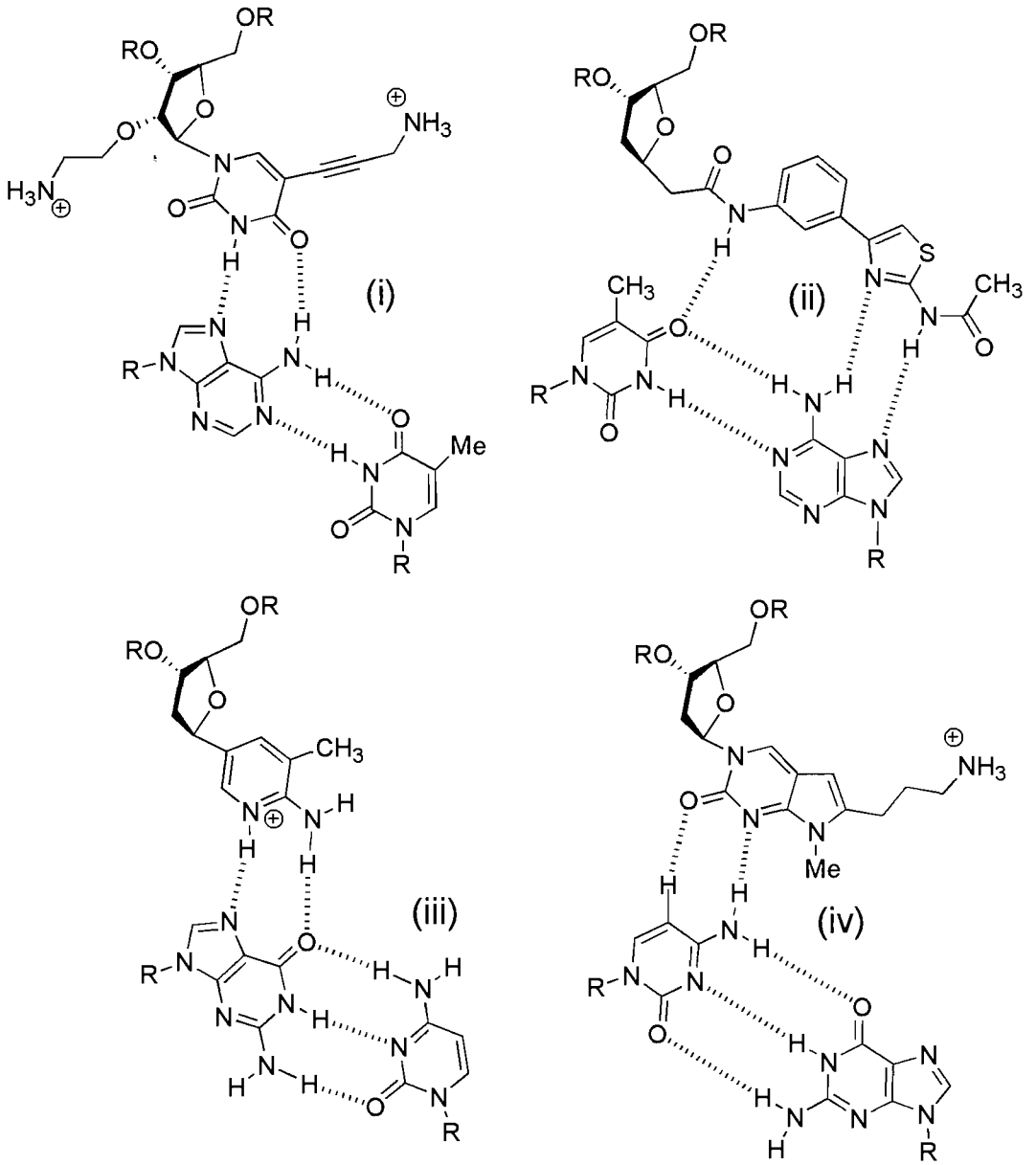

Figure 6.1 Chemical structures and proposed hydrogen bonding patterns of the nucleotide analogues designed to recognise each of the four base pairs.; (i) BAU.AT; (ii) ^{Me}P.GC; (iii) ^{A}PP.GC; (iii) S.TA.

A

TFO-2	5′-Q-TCTTTGTTCTCTTGCTCTT
TFO-1	5′-Q-BMBPBSBTMTMPTSMTMBT
Duplex 1	5′-F-AGACATAAGAGCATGAGAA 3′-TCTGTATTCTCGTACTCTT
Oligo-1	3′-Q-TCTGTATTCTCGTACTCTT
Oligo-2	3′-F-AGACATAAGAGCATGAGAA
Oligo-3	3′-F-AAGAGTACGAGAATACAGA
Duplex 2	5′-F-AGACA**1**AAGAGCATGAGAA 3′-TCTGT**2**TTCTCGTACTCTT
Duplex 3	5′-F-AGACAT**3**AGAGCATGAGAA 3′-TCTGTA**4**TCTCGTACTCTT
Duplex 4	5′-F-AGACATAA**5**AGCATGAGAA 3′-TCTGTATT**6**TCGTACTCTT
Duplex 5	5′-F-AGACATAAGAG**7**ATGAGAA 3′-TCTGTATTCTC**8**TACTCTT
Duplex 6	5′-F-AGACATAAGAG**C**ATGAGAA 3′-TCTGTATTCTC**G**TACTCTT

B

Fragment 1	5′..AGACATAAGAGCATGAGAA.. 3′..TCTGTATTCTCGTACTCTT..
Fragment 2	5′..AGACA**A**AAGAGCATGAGAA.. 3′..TCTGT**T**TTCTCGTACTCTT..
Fragment 3	5′..AGACAT**T**AGAGCATGAGAA.. 3′..TCTGTA**A**TCTCGTACTCTT..
Fragment 4	5′..AGACATAA**T**AGCATGAGAA.. 3′..TCTGTATT**A**TCGTACTCTT..
Fragment 5	5′..AGACATAAAAG**T**ATGAGAA.. 3′..TCTGTATTTTC**A**TACTCTT..

Figure 6.2 Sequence of the oligonucleotides and DNA fragments used in Chapter 6; A) Oligonucleotides used in the fluorescence melting melting experiments, where B is BAU, M is ^{Me}P, P is ^{A}PP and S is S.The duplexes are boxed and labelled with fluorescein (F) at the 5'-end of the purine strand, whereas the TFOs are labelled with methyl red serinol (Q) at the 5'-end. Oligo 1-3 contained appropriately positioned fluorophores and quenchers. Duplexes 2-5 are identical to duplex 1, except that single base pair changes are introduced at different positions, opposite one of the third strand bases; positions 1.2, 3.4, 5.6 and 7.8 correspond to each base pair (A.T, T.A, G.C and C.G) in turn. Duplex 6 positions a single substitution of S opposite a CG base pair. B) The duplex target sequences used in DNase I footprinting experiments. Only the 19 bp target sites are shown. Fragment 1 is identical to Duplex 1, while Fragments 2-5 contain single base pair changes at different positions, opposite one of the third strand bases. Each fragment was labelled at the 3'-end of the *Eco*R1 site (on the purine strand).

6.2.1 Fluorescence melting experiments

The sequences of the oligonucleotides used in the fluorescence melting experiments are illustrated in Figure 6.2A. The purine-containing strand of the duplex (boxed) was labelled at the 5´-end with fluorescein, and the third strand was labelled at the 5´-end with methyl red. Duplex 1 contains a 19 bp oligopurine.oligopyrimidine tract that is interrupted by two CG and two TA base pairs. The oligonucleotide TFO-1 was designed to form a specific triplex with this targets generating BAU.AT, ^{Me}P.GC, S.TA and ^{A}PP.CG triplets as well as conventional T.AT triplets. The oligonucleotide TFO-2 was designed to recognise the same target generating the best triplets using only natural DNA bases (T.AT, C.GC. G.TA and T.CG). Experiments were undertaken in either 50 mM sodium acetate (pH 5.0, 5.5 and 6.0) or 50 mM sodium phosphate (6.5, 7.0 or 7.5) containing 200 mM NaCl. The concentration of duplex and TFO in each experiment was 0.25 μM and 3 μM, respectively. There was no hysteresis between the heating and melting curves at a heating and cooling rate of 0.2°C/min, though significant hysteresis was observed at faster rates of temperature change (0.1°C/sec). This is consistent with the known slow rates of triplex formation. Several other oligonucleotides were also prepared, with appropriately positioned fluorophores and quenchers. Oligo-1 was combined with the labelled strand of duplex 1, to estimate the melting temperature of the duplex. Whereas oligo-2 and 3 were combined with TFO-1, to ensure parallel triplex formation was being observed.

The sequence specificity of triplex formation was assessed by determining the melting profiles of TFO-1 with a further 12 duplexes. Duplexes 2-5 are identical to duplex 1 except that single base pair changes are introduced at different positions, opposite one of the modified third strand bases; positions 1.2, 3.4, 5.6 and 7.8 correspond to each base pair (AT, TA, GC and C.G) in turn.

6.2.2 DNase I footprinting experiments

The affinity and selectivity of the modified oligonucleotides was further assessed by DNase I footprinting experiments, using DNA fragments that contain similar target sites (Figure 6.2B). The TFOs are the same as those employed in fluorescence melting studies. The fragments were prepared by cloning synthetic oligonucleotides into the *Bam*HI site of pUC19. These contained the same target sites as used for the

fluorescence melting studies. Radiolabelled fragments were produced by digesting each plasmid with *Eco*RI and *Hind*III and labelling at the 3´-end of the *Eco*RI site on purine-containing strand using reverse transcriptase and [α-^{32}P]dATP. Footprinting experiments at pH 5.0 were performed in 50 mM sodium acetate, at pH 6.0 in 10 mM PIPES containing 50 mM NaCl and at pH 7.0 in 10 mM Tris-HCl containing 50 mM NaCl. Fragment 1 contains the same perfect match target site as duplex 1, while fragments 2-5 contain single base pair substitutions opposite each of the modified nucleotides in turn.

6.3 Results

6.3.1 Fluorescence melting experiments

Representative melting profiles showing the interaction of TFO-1 with duplex 1 at different pH values are shown in Figure 6.3. These melting profiles clearly demonstrate successful triplex formation at all pH values tested. As expected, the T_m is still pH dependent due to the presence of the ^{Me}P.GC triplet; between pH 5.0 and 6.0 the T_m values obtained are greater than 60 °C, while increasing the pH to 6.5, 7.0 and 7.5 gave T_m values of 58.2, 48.8 and 37.4 °C respectively. The T_m decrease at higher pH is presumably because the pK_a of ^{Me}P is between 6.5 and 7.5 in this system. The apparent relative fluorescence for the triplex is higher at pH 7.0 and 7.5 as the affinity of the third strand is weaker and there is a significant amount of unbound fluorescent duplex in the equilibrium. In contrast TFO-2, which only contains natural nucleotides, failed to generate a stable triplex, even at pH 5.0. This indicates that as expected, the four pyrimidine interruptions in the target site are highly destabilising.

6.3.1.1 Comparing with duplex stability

Examination of the melting profiles reveals a second transition at high temperatures, a decrease in fluorescence, and is presumably due to the melting of the underlying duplex (see Section 3.4.2). This transition is only observed for the triplexes formed at pH 7.0 and 7.5, suggesting that the triplexes formed at lower pH are more stable than the underlying duplex. To examine this further, the stability of the duplex was estimated by similar melting experiments, replacing the unlabelled pyrimidine-rich strand of duplex 1 with oligo 1 (bearing a 3´-methyl red). Representative melting profiles showing this

interaction at three pH values are shown in the left hand panel of Figure 6.4. The T_m values for these profiles varied between 58.5 and 62.5 °C depending on the pH; at a lower pH the thermal stability of the duplex was lower. It is therefore evident that between pH 5.0 and 6.0 the triplexes formed with TFO-1 are more stable than that of the duplex alone.

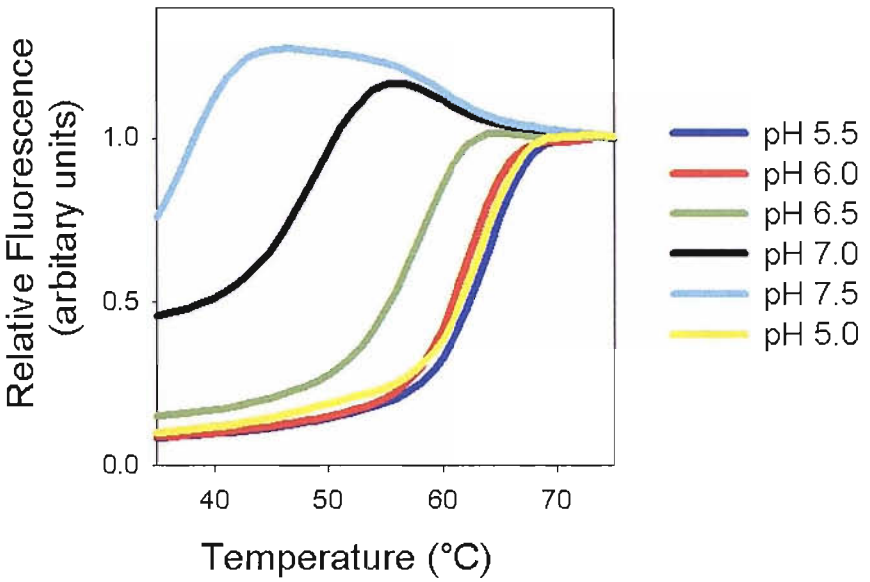

Figure 6.3 Fluorescence melting curves showing the interaction of TFO-1 with its intended duplex target. The experiments were performed at varying pHs in an appropriate buffer. The *y*-axis shows the normalised fluorescence (arbitrary units), whereas the *x*-axis shows the temperature (°C).

6.3.1.2 Orientation of third strand binding

Several other oligonucleotides were also prepared, with appropriately positioned fluorophores and quenchers, to ensure that parallel triplex formation was being observed. The melting of these oligonucleotides can be seen in Figure 6.4. Addition of TFO-2 to the purine strand of the duplex, which could theoretically generate a parallel Hoogsteen duplex, failed to show the formation of a complex at any pHs. Addition of TFO-2 to oligo-2, which could form an antiparallel Watson-Crick duplex by generating BAU.A ^{Me}P.G ^{A}PP.C and S.T base pairs, also failed to show the formation of a complex at all pHs. Finally, oligo-3 corresponding to the opposite orientation of the purine strand of the duplex, also showed no interaction with TFO-2. This would have required reverse Hoogsteen interactions to form a duplex with the third strand.

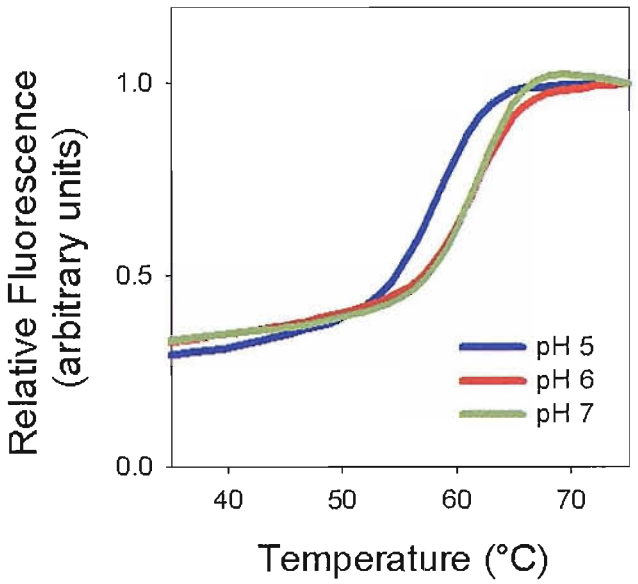

Figure 6.4 Fluorescence melting curves showing the interaction of Oligo 1 with the purine-containing strand of the duplex, forming a Watson-Crick duplex at different pH values. The *y*-axes shows the normalised fluorescence (arbitrary units), whereas the *x*-axes shows the temperature (°C).

6.3.1.3 Effect of magnesium concentration

Stable triplex formation normally requires the addition of divalent metal ions to screen the charge interaction between the three polyanionic backbones. This was not required for the formation of these triplexes, presumably due to the presence of multiple positive charges within the TFO on the BAU residues. Representative melting profiles showing the interaction of TFO-1 with duplex 1 at pH 7.0 in the presence of varying concentrations of magnesium are shown in the right hand panel of Figure 6.5. The T_m values calculated from the first derivatives of these profiles were 48.8, 49.2, 50.9, 51.8, 53.4 and 55.2 °C in the presence of 5, 10, 20, 30, 40 and 50 mM magnesium chloride. This increase in T_m can be attributed to the increase in ionic strength, and is much less than typically seen with TFOs containing natural bases. As the concentration of magnesium increases it can be seen that the overall level of fluorescence decreases; a decreased of about 60 % is observed in the presence of 50 mM magnesium chloride. This effect is most likely attributed to quenching effects of these divalent ions on fluorescein.

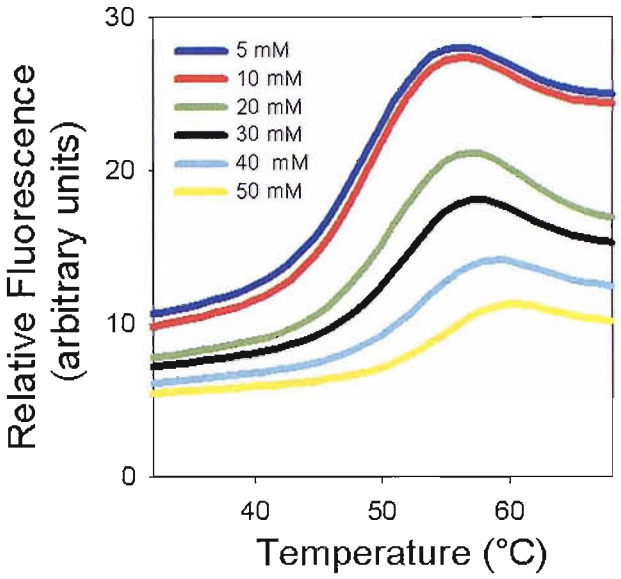

Figure 6.5 Fluorescence melting curves showing the interaction of TFO-1 with duplex 1 at pH 7.0 in the presence of various concentrations of magnesium. The *y*-axes shows the normalised fluorescence (arbitrary units), whereas the *x*-axes shows the temperature (°C).

6.3.1.4 Triplex specificity

The sequence specificity of triplex formation was examined by determining the melting profiles of TFO-2 with a further 12 duplexes, each of which differed from duplex 1 by a single base pair opposite one of the modified nucleotides. Duplexes 2, 3, 4 and 5 shown in Figure 6.2 were used to assess the selectivity of S, BAU, ^{Me}P and ^{A}PP respectively, in the context of this sequence. Each duplex, therefore, generated a single triplet X.YZ, where X is BAU, ^{Me}P, S or ^{A}PP, and YZ is each base pair in turn. The fluorescent melting profiles of these complexes at pH 5.0 are shown in Figure 6.6, and at pH 7.0 in Figure 6.7. T_m values, together with those determined at other pHs, are shown in Table 6.1.

It can be seen that the sequence specificity of BAU is maintained over the entire pH range; BAU always produced the most stable triplex when positioned opposite an AT base pair (blue line) and each single base pair mismatch decreased the T_m by at least 10 °C, an effect that was greater at higher pHs. A similar effect is seen with ^{Me}P which always generated the most stable triplex when positioned opposite a GC base pair (green line), and exhibited at least a 15°C decrease in T_m for each of the triplet mismatches. However, ^{A}PP always formed the most stable triplexes with CG (black

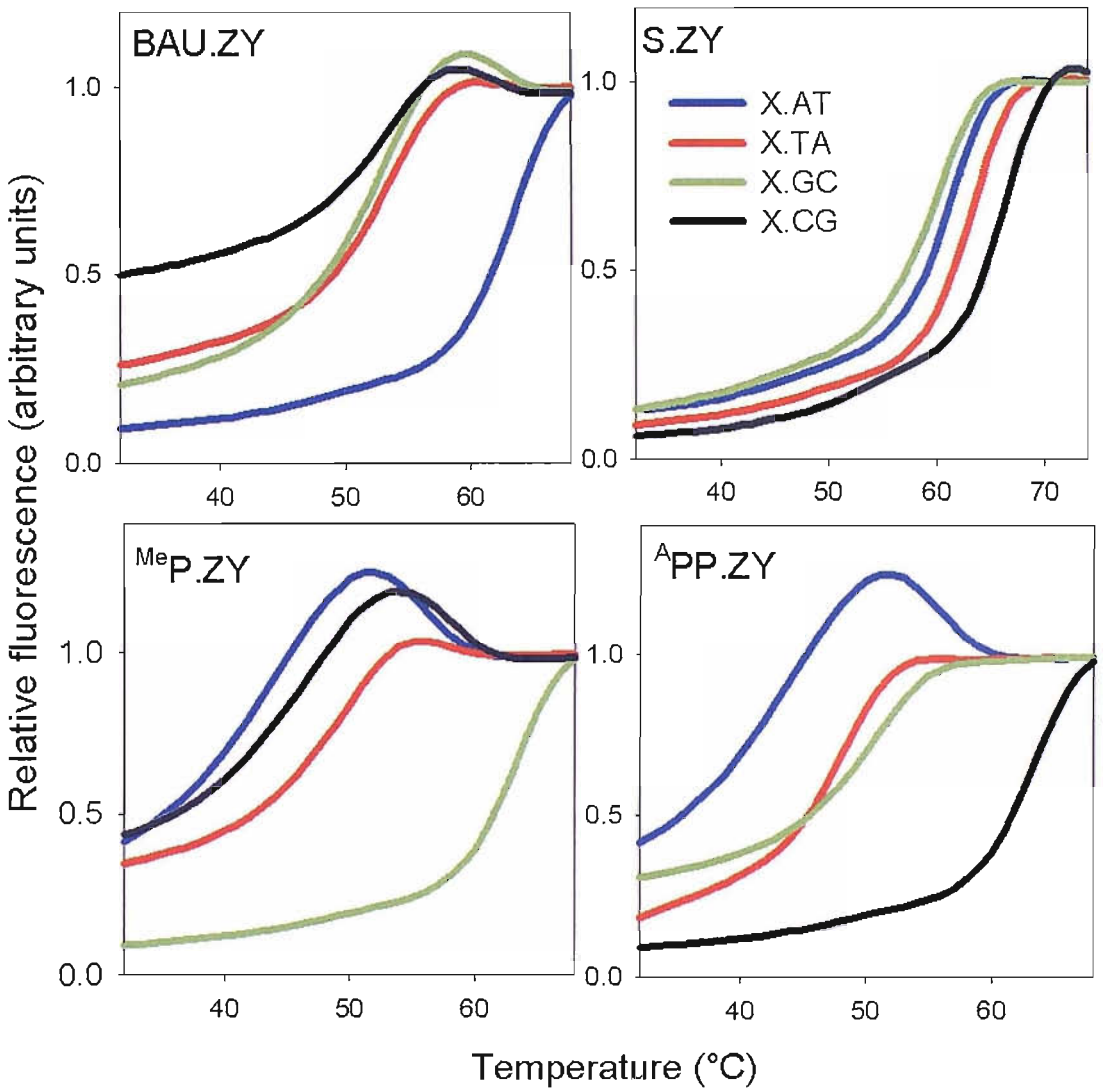

Figure 6.6 Fluorescence melting curves showing the interaction of TFO-1 with duplexes that differ by a single base pair opposite each synthetic third strand nucleotide at pH 5.0. Duplex 3 was used for BAU, duplex 2 for S, duplex 4 for ^{Me}P and duplex 5 for ^{A}PP. The *y*-axes shows the normalized fluorescence (arbitrary units), whereas the *x*-axes shows the temperature (°C).

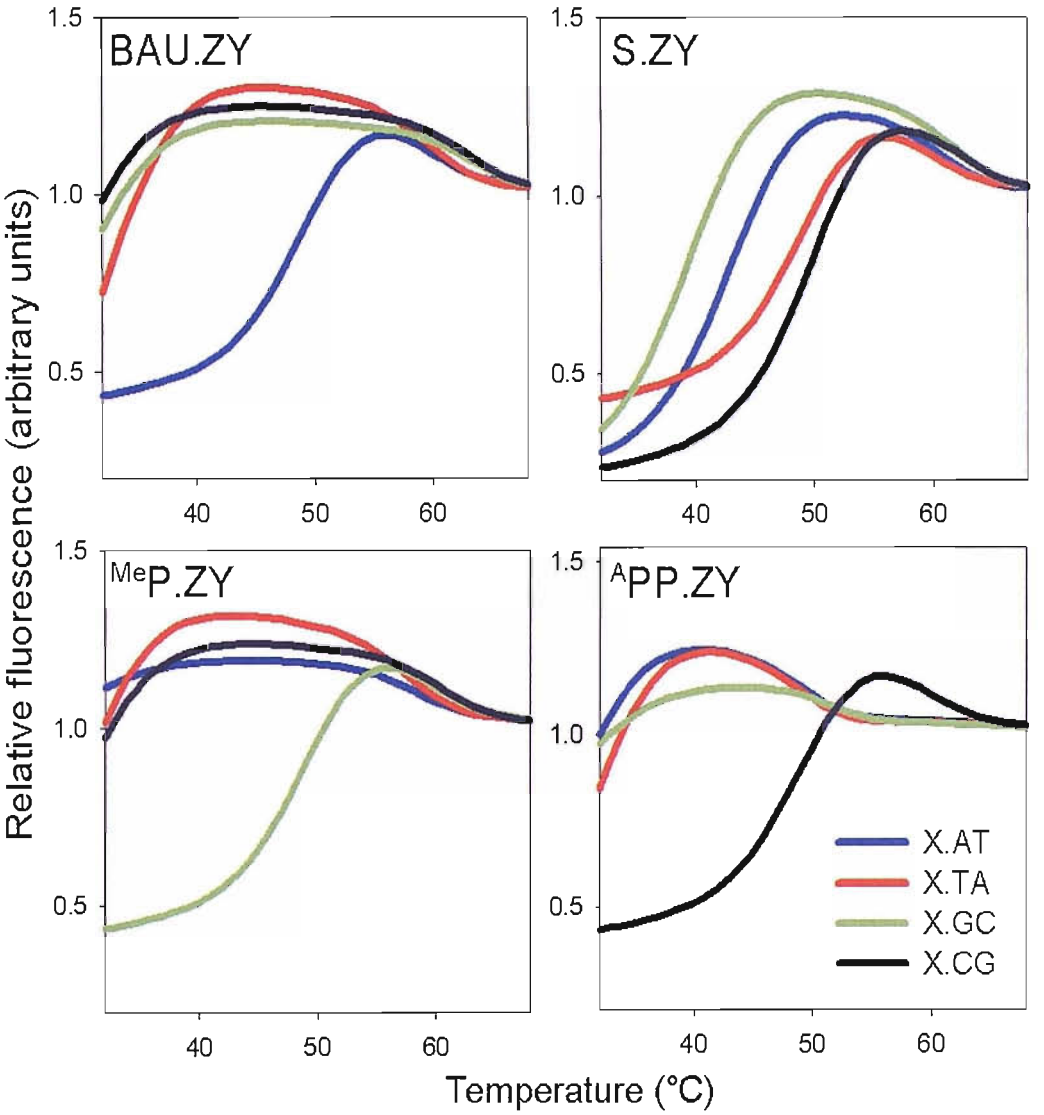

Figure 6.7 Fluorescence melting curves showing the interaction of TFO-1 with duplexes that differ by a single base pair opposite each synthetic third strand nucleotide at pH 7.0. Duplex 3 was used for BAU, duplex 2 for S, duplex 4 for ^{Me}P and duplex 5 for ^{A}PP. The *y*-axes shows the normalized fluorescence (arbitrary units), whereas the *x*-axes shows the temperature

Line) but its selectivity for the other 3 base pair was dependent on the pH. Examination of the bottom left hand graph of Figure 6.6 (pH 5.0) reveals that the next most stable triplex was generated with ^{A}PP positioned opposite a GC base pair (green line), the T_m for this complex was 13°C lower showing a high level of discrimination. In contrast, examination of the bottom left hand graph of Figure 6.7 (pH 7.0) reveals that the next most stable triplex was generated with a TA base pair (red line). This pH dependent selectivity indicates protonation plays a role in the recognition of GC at lower pH. This effect was previously observed in the context of an unmodified sequence (see Section 5.4.3). The monomers BAU, ^{Me}P and ^{A}PP therefore retain exquisite sequence selectivity and the stability of these 19mer triplexes decreases by ~15°C for single mismatches at pH 7.0.

Conversely, the nucleotide S exhibited a much lower level of selectivity; at low pH there was just a ~ 6 °C difference between the best and the worst complexes formed by this base. Also at low pH S recognises a CG base pair (black line) with a greater affinity than a TA base pair (green line), exhibiting a difference of ~ 3 °C in T_ms. This result was unexpected. At higher pHs the discrimination of this base increases and at pH 7.0 produced higher T_ms with TA and CG than with GC and AT, although the S.CG triplet was still as stable as the S.TA . To gain a greater insight into whether the triplets flanking S affect its affinity for CG, the interaction of TFO-2 with a further duplex was examined. Duplex 6, which is shown in Figure 6.2A, differs to duplex 1, the intended target, by a CG base pair at the 3´-end of the sequence. Upon triplex formation this positions the second S substitution opposite this base pair. At both positions S is flanked by different base triplets; at the 5´-end these are BAU.AT triplets whereas at the 3´-end these are T.AT and ^{Me}P.GC triplets. The T_ms calculated for the new triplex were 66.5, 66.8, 65.2, 60.8 and 51.2 °C at pH 5.0, 5.5, 6.0, 6.5 and 7.0 respectively. A comparison with the T_ms obtained for the triplex containing the S.CG at the 3´-end (Table 6.1) shows the new triplex is of identical thermal stability. It is therefore evident that the the stability of the S.CG triplet is not dependent on the flanking base triplets.

Overall, these data clearly show that TFO-1 forms a stable triplex at pH 7.0 with its intended mixed sequence duplex target containing four pyrimidine inversions and four GC base pairs. This compares with the unmodified TFO-2, where triplex formation was not observed even at pH 5.0.

pH	ZY	X			
		BAU	^{Me}P	^{A}PP	S
5.0	AT	63.5 (63.5)	43.9 (43.5)	48.3 (48.3)	61.5 (61.9)
	TA	53.6 (53.2)	49.8 (49.0)	48.4 (48.3)	63.5 (63.5)
	GC	53.3 (52.6)	63.5 (63.5)	50.8 (49.0)	60.4 (60.4)
	CG	53.6 (53.0)	47.2 (45.8)	63.5 (63.5)	66.5 (66.6)
5.5	AT	63.9 (63.8)	43.7 (42.6)	48.1 (48.2)	62.0 (62.8)
	TA	52.8 (52.2)	49.5 (49.0)	48.3 (48.2)	63.9 (63.8)
	GC	53.0 (52.5)	63.9 (63.8)	48.1 (48.0)	60.6 (60.4)
	CG	51.5 (50.5)	46.3 (46.2)	63.9 (63.8)	66.4 (66.7)
6.0	AT	62.4 (62.4)	40.4 (40.1)	45.7 (45.3)	60.5 (60.6)
	TA	50.7 (49.6)	47.0 (46.2)	46.4 (46.0)	62.4 (62.4)
	GC	49.0 (48.9)	62.4 (62.4)	45.3 (44.7)	57.7 (57.0)
	CG	48.0 (47.0)	44.5 (43.3)	62.4 (62.4)	64.5 (64.3)
6.5	AT	58.2 (57.6)	n.d	38.8 (37.5)	54.1 (53.1)
	TA	42.9 (41.8)	39.1 (38.0)	40.4 (39.5)	58.2 (57.6)
	GC	42.6 (41.6)	58.2 (57.6)	37.3 (36.5)	50.3 (49.6)
	CG	40.2 (39.2)	37.7 (36.6)	58.2 (57.6)	59.6 (59.0)
7.0	AT	48.8 (47.4)	n.d	n.d	43.2 (41.5)
	TA	n.d	n.d	n.d	48.8 (47.4)
	GC	n.d	48.8	n.d	39.7 (37.9)
	CG	n.d	n.d	48.8	49.8 (48.3)
7.5	AT	37.4 (36.0)	n.d	n.d	n.d
	TA	n.d	n.d	n.d	37.4 (36.0)
	GC	n.d	37.4 (36.0)	n.d	n.d
	CG	n.d	n.d	37.4 (36.0)	37.8 (37.4)

Table 6.1 T_m values determined by fluorescence melting for triplexes formed by the fully modified oligonucleotide TFO-1 at different pHs using a temperature gradient of 0.2 °C min^{-1}. The values in bold correspond to those for TFO-1 at its intended target site (employing BAU.AT, S.TA ^{Me}P.GC and ^{A}PP triplets). For all the other cases, 1 bp in the target was changed opposite one of the modified bases, as shown in Figure 6.1 using duplexes 2-5 (1.2 opposite S, duplex 2; 3.4 opposite BAU, duplex 3; 5.6 opposite ^{Me}P, duplex 4; 7.8 opposite ^{A}PP, duplex 5). T_m values in parenthesis were calculated from the annealing phase. Each T_m value was repeated in triplicate and usually differed by less than 0.5 °C.

6.3.2 DNase I footprinting experiments

The affinity and selectivity of these modified oligonucleotides was further assessed by DNase I footprinting, using DNA fragments that contained similar targets sites. For these experiments the same third strand oligonucleotides were used as in fluorescence melting studies. The interactions of TFO-1 and TFO-2 with the perfect match target site at different pHs are shown in Figure 6.8 and the C_{50} values calculated from these are summarised in Table 6.2. It can be seen that TFO-2, which contains only natural nucleotides, does not affect the cleavage pattern, even at the highest oligonucleotide concentration (30 μM). In contrast, clear footprints are evident with TFO-1 at the intended target site, with the remainder of the cleavage pattern remaining unaltered. At pH 5.0, the footprint persists to concentrations < 10 nM and although higher oligonucleotide concentrations are required at elevated pH values, a footprint is still evident at micromolar concentrations even at pH 7.0. It was not possible to obtain an accurate C_{50} value for the interaction of TFO-1 at pH 5.0, but it can be estimated as being < 0.01 μM. Quantitative analysis of the bands within the remaining footprints yielded C_{50} values of 0.011 ± 0.002 μM and 1.1 ± 0.1 μM for the interaction of this TFO at pH 6.0 and 7.0. It is therefore evident that increasing the pH from 5.0 to 7.0 led to a 100-fold decrease in the C_{50} for the interaction of this oligonucleotide. As with fluorescence melting studies, divalent metal ions were not required for binding, though these are present for a short while during the DNase I digestion.

The next step was to study selectivity of these modified TFOs. Four further footprinting substrates were prepared, which contained single base pair substitutions opposite one of the novel nucleotides, generating S.AT, BAU.TA, ^{Me}P.TA and ^{A}PP.TA triplets in turn. The results of these experiments at pH 5.0, 6.0 and 7.0 are shown in Figure 6.9 and 6.10. The C_{50} values, at all pH values, are summarised in Table 6.2. The left hand panel of Figure 6.9 shows the cleavage patterns for the four mismatch targets in the presence of the unmodified TFO-2 at pH 5.0. In each instance it is clearly seen that the oligonucleotide does not bind at TFO concentrations as high as 30 μM. This is as expected as no interaction was seen with the intended target site. The right hand panel of Figure 6.9 shows the cleavage pattern of the four fragments in the presence of TFO-1 at pH 5.0. In each case, a clear footprint is evident at the target site. It was not possible to quantify the bands in the footprint generated by the triplex containing an S.AT mismatch. It is therefore estimated that the C_{50} for this interaction was < 0.01 μM.

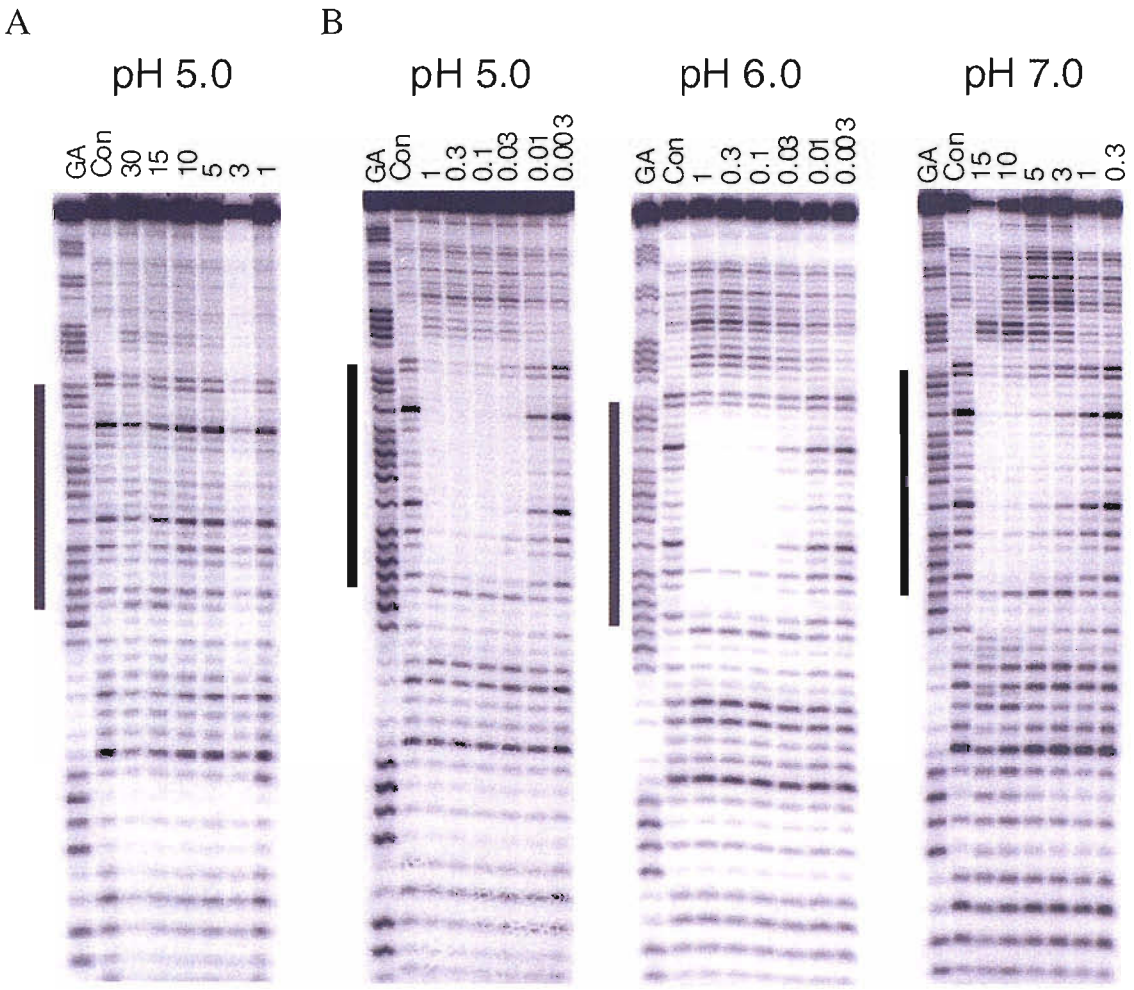

Figure 6.8 DNase 1 footprinting experiments showing the interaction of the oligonucleotides TFO-1 (B) and TFO-2 (A) with their intended duplex target sites. The experiments were performed at pH 5.0, 6.0 and 7.0 in appropriate buffers. The oligonucleotide concentrations (μM) are shown at the top of each gel lane. Tracks labelled 'GA' are Maxam-Gilbert markers specific for purines, while 'con' indicates DNase I cleavage in the absence of added oligonucleotide. The filled boxes show the position of the triplex target site.

Quantitative analysis of the bands within the footprint for the triplexes containing BAU.TA and ^{Me}P.TA mismatches yielded C_{50} values of 0.013 ± 0.002 μM and 0.0019 ± 0.005 μM. An unusual effect is seen with the combination generating an ^{A}PP.TA triplet at low pH, for which a partial footprint is evident, covering only the upper part of the target. This suggests partial binding of the TFO

	C_{50} (μM)		
	pH 5.0	pH 6.0	pH 7.0
Perfect match	<0.01	0.011 ± 0.002	1.1 ± 0.1
S.AT	<0.01	0.020 ± 0.005	4.5 ± 0.7
BAU.TA	0.013 ± 0.002	0.04 ± 0.02	n.d
^{Me}P.TA	0.019 ± 0.005	n.d	n.d
^{A}PP.TA	[a]	[a]	n.d

[a] For this target, TFO-1 only produced a partial footprint that did not cover the entire site.
n.d. indicates that no footprint was detected.

Table 6.2 C_{50} values determined by DNase I footprinting for the interaction of the modified oligonucleotide TFO-1 with target sites that differed by a single base pair, generating a triplex mismatch opposite one of the novel nucleotides. The identity of the mismatch (S.AT, BAU.TA, ^{Me}P.TA or ^{A}PP.TA) is indicated. The experiments were performed at pH 5.0, 6.0 and 7.0 in an appropriate buffer containing 50 mM NaCl.

The cleavage pattern of the four fragments in the presence of the modified oligonucleotide at pH 6.0 is shown in the left hand panel of Figure 6.10. A clear footprint is evident for the interaction of the TFO generating a S.AT mismatch. While a footprint that persists to a lower TFO concentration is also evident for the combination producing a BAU.TA mismatch. No interaction is observed for the ^{Me}P.TA mismatch and a similar partial footprint is observed for the ^{A}PP.TA combination as seen at pH 5.0. The C_{50} values for the S.AT and BAU.TA triplexes were 0.020 ± 0.005 μM and 0.04 ± 0.02 μM. Again it can be seen that the mismatch reduces the binding affinity of the TFO, requiring higher oligonucleotide concentrations to generate a footprint. The triplex containing the BAU.TA triplet generates a C_{50} value 4-fold lower than that with the perfect match, whilst, the triplex with the S.AT triplet generates a C_{50} 2-fold lower.

The cleavage pattern of the four fragments in the presence of the modified oligonucleotide at pH 7.0 is shown in the right hand panel of Figure 6.10. It can be seen that at this pH single base pair changes opposite BAU, ^{Me}P and ^{A}PP abolished the footprint, however a footprint is still present for S. The C_{50} for this footprint is 4.5 ± 0.7 μM and is therefore 3-fold lower than that obtained for the interaction of this TFO with its intended target. This highlights that the selectivity of TFO-1 is less pronounced at

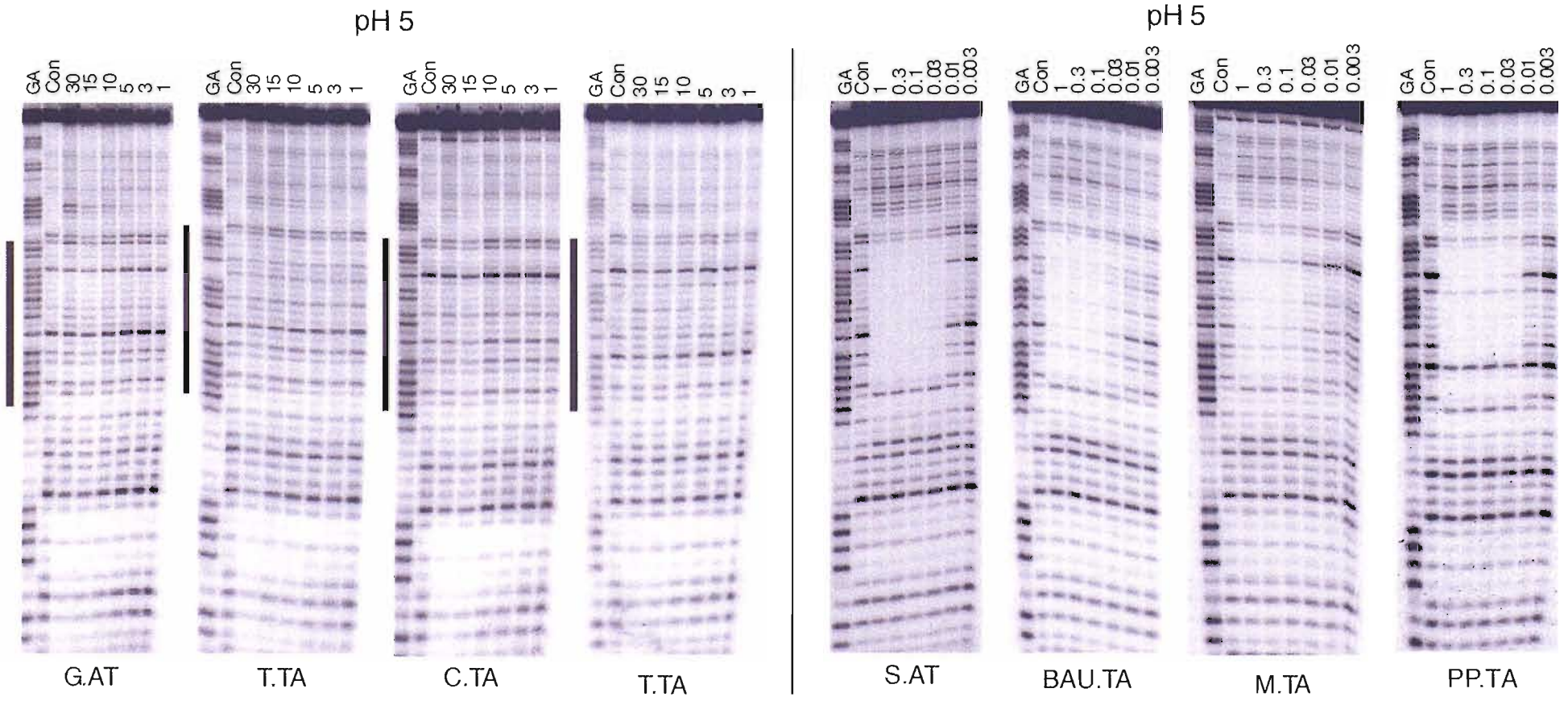

Figure 6.9 DNase I footprinting experiments showing the interaction of TFO-2 (left panel) and TFO-1 (right panel) with four different target sites that contain 1 bp change relative to the intended target site, generating the mismatches (shown beneath the gel in bold). The experiments were performed at pH 5.0. The oligonucleotide concentration (μM) is shown at the top of each gel lane. Tracks labelled 'GA' are Maxam-Gilbert markers specific for purines, while 'con' indicates DNase I cleavage in the absence of added oligonucleotide. The filled boxes show the position of the triplex target sites.

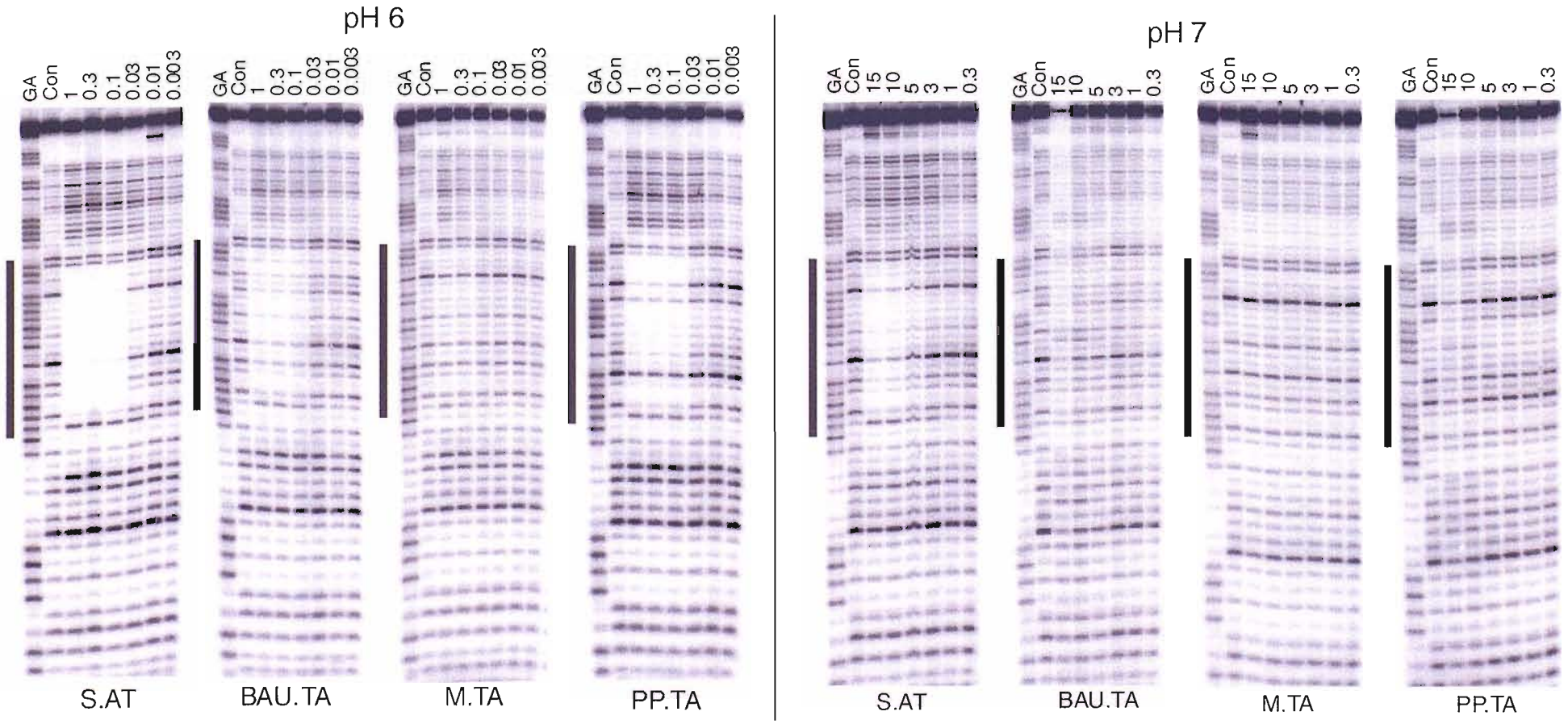

Figure 6.9 DNase I footprinting experiments showing the interaction of TFO-1 with four different target sites that contain 1 bp change relative to the intended target site, generating S.AT, BAU.TA, ^{Me}P.TA and ^{A}PP.TA triplet (shown beneath each gel in bold). The experiments were performed at pH 6.0 (left panel) and 7.0 (right panel). The oligonucleotide concentration (μM) is shown at the top of each gel lane. Tracks labelled 'GA' are Maxam-Gilbert markers specific for purines, while 'con' indicates DNase I cleavage in the absence of added oligonucleotide. The filled boxes show the position of the triplex target sites.

lower pH values although at pH 7.0 triplex specificity is high for all of the monomers apart from S.

These results, together with fluorescence melting studies, demonstrate that triplex formation can be achieved at this mixed sequence target site at pH 7.0, and that BAU, ^{Me}P and ^{A}PP are highly selective. S permits stable triplex formation at TA inversions but shows much less discrimination between the 4 base pairs.

6.4 Discussion

The formation of stable triple helices at mixed sequence target sites, at physiological pH is a major challenge for the general use of the antigene triplex strategy. The results presented in this chapter unambiguously show that, by incorporating several different synthetic nucleotides in a single a TFO, it is possible to form stable triplexes at a mixed sequence duplex targets that contain four pyrimidine inversions at physiological pH.

6.4.1 Triplex stability

The triplexes formed at this target site have similar T_m and C_{50} values to those generated at similar length uninterrupted oligopurine sites using third strands containing only C and T, for which T_m values between 63 and 67°C are observed at pH 5.0 (see Section 3.3.5). However, since the results presented in Chapter 4 show that the inclusion of a single BAU residue increases the T_m by ~5 °C, it might be expected that the stability of the triplexes formed with this multiply modified oligonucleotide would be greater than that observed. This emphasizes that the ^{A}PP.CG and S.TA triplets have a lower stability than C^+.GC and T.AT. This is to be expected, because these triplets are not isomorphous with each other or with the BAU.AT and ^{Me}P.GC triplets. The stability of the modified triplex was clearly still dependent on the pH; T_m and C_{50} values determined for the triplex at pH 5.0 and 6.0 were similar, whilst those determined at pH 7.0 were much lower as evidenced by a 15 °C drop in T_m or a 100-fold decrease in the C_{50} value. This is presumably because the pK_a of ^{Me}P is between 6.5 and 7.5 in this system and is consistent with the reported pK_a of 6.86 for the similar 2-aminopyridine (Albert *et al.*, 1948). Although the affinity of the ^{Me}P.GC triplet is enhanced by the presence of the very strong BAU.AT triplet at pH 7.0, there is clearly still need for further cytosine derivatives.

The formation of this triplex was not dependent on any other stabilising factors, such as high concentrations of divalent metal ions or the addition triplex binding ligands. A similar observation was noted for the formation of triplexes containing one or more BAU substitutions (see Section 4.4.1.1) and is attributed to the presence of the positive charges on this nucleoside. In this instance it is also likely that ^{Me}P and ^{A}PP will contribute, as these nucleosides also contain positive charges. Interestingly, the addition of relatively high concentrations of magnesium resulted in an increase in triplex stability; a T_m increase of 6 °C was observed for the addition of 50 mM magnesium chloride. This is to be expected due to the increase in ionic strength. Even with 18 positive charges within the TFO, when ^{Me}P is protonated, there will still be an overall negative charge.

Several groups have recently suggested that the 2´-aminoethoxy modification, which is present in BAU, can stabilise a range of triplets, and it has been suggested that contiguous 2´-aminoethoxy modifications further increase triplex stability (Cuenod *et al.*, 1998; Buchini & Leumann, 2004; Puri *et al.*, 2004). This has been attributed to its effect on oligonucleotide conformation (DNA versus RNA), as well as the presence of the positive charge. The oligonucleotides used in the present study did not contain any contiguous BAU residues, and these were all separated by at least one other base. It is, therefore, possible that further improvements in triplex affinity might be achieved by either increasing the number of BAU modifications or by changing their distribution within the oligonucleotide. Further improvement might also be possible by using the 2´-aminoethoxy derivative of S in place of S.

6.4.2 Triplex specificity

Several control experiments were performed to ensure parallel triplex formation was being observed in the fluorescence melting experiments. These indicated that the TFO was not forming Watson-Crick, Hoogsteen or reverse Hoogsteen duplexes with the purine-containing strand. This was to be expected for the W-C duplex for several reasons; (i) protonation of ^{Me}P would disable recognition of G (Hildbrand *et al.*, 1997); (ii) ^{A}PP would require protonation to recognise cytosine; (iii) S is incompatible for the recognition of T. The lack of formation of a Hoogsteen duplex was surprising, especially at low pH, since these had been observed previously (see Section 3.4.2) and suggests highly specific interactions between third strand and TFO.

Interestingly, the selectivity of BAU, ^{Me}P and ^{A}PP within the context of the multiply modified TFO was enhanced. At pH 5.0, a difference of 10, 14, 13 °C drop in T_m was observed when positioning each base opposite a mismatch. This compares to 8, 11, 1 °C in the context of the previously studied CT-containing TFOs. A similar effect was previously reported for a nucleoside within the context of 2´-aminoethoxy-TFOs (Buchini & Leuman, 2004). Although a mismatch in any sequence context is likely to disrupt the cooperative interaction between neighbouring triplets, this may be greater for 2´-aminoethoxy-modified nuclesides since any alteration in the position of the third strand is likely to disrupt the positioning of the charge, resulting in a loss of favourable charge-charge interactions. As expected increasing the pH of the solution also enhanced the selectivity of the nucleosides of BAU, ^{Me}P and ^{A}PP displayed a decrease in T_m of ~15 °C for triplexes containing the most stable and second most stable triplet formed by each base.

At all pHs the S monomer, which is designed to recognise TA inversions, also recognised CG base pairs with a similar affinity and at pH 5.0 the S.CG triplet was actually more stable than S.TA. These results are similar to those obtained previously, however, in that instance S.CG was only ever as stable as S.TA. It was suggested that CG recognition involves protonation of the thiazole nitrogen and consequent hydrogen bonding to O6 of guanine (Figure 5.21). An increase in the pK_a of this nucleoside within the context of this TFO might therefore be the reason for the increased affinity for CG. It is obvious that there is the need for further development of monomers designed to recognise TA base pairs. It would be interesting to see what improvement might be obtained by using 2'-aminoethoxy S as this base was shown to offer enhanced selectivity against CG base pairs.

In a similar manner the selectivity of ^{A}PP was also dependent on the pH. At pH 5.0, the second most stable triplet generated by this base was opposite a GC base pair, whereas at pH 7.0, this was with a TA base pair. This effect is most likely to be attributed to a protonation event at N3 of the base, which can participate in the formation of a second hydrogen bond with N7 of guanine. In each case these triplets were much less stable than the triplets generated at CG. Another unusual effect was observed in footprinting the triplex containing the mismatched ^{A}PP.TA triplet. A partial footprint was evident, covering only the upper part of the target. This is most likely an effect of the position of the mismatch and not the specificity of the base. This mismatch is 8 triplets from the

triplex termini, and would still allow the formation of a relatively weak triplex composed of 11 triplets. This suggests that increasing the length of the modified TFO may also decrease its selectivity, more work should be undertaken to delineate this effect.

7 TRIPLEX FORMATION AT TARGET SITES CONTAINING DUPLEX MISMATCHES OR 5-AMINOURACIL

7.1 Introduction

The binding of a triplex-forming oligonucleotide within the DNA major groove is highly asymmetric; the bases of a TFO usually only make contacts with the bases on the purine strand of the duplex and not its partner on the opposing pyrimidine strand. Recognition of the duplex purine strand may therefore be insensitive to the identity of the base to which it is paired, i.e. whether it is paired with its Watson-Crick partner or forms a mismatch base pair. Previous studies suggested that triplets formed at duplex mismatches can have increased stability and T.AC and C.GA triplets were shown to be more stable than the standard T.AT and C^+.GC triplets (Sun *et al.*, 1991). (The notation N.XZ refers to a triplet, in which the third strand base N interacts with the duplex XZ base pair, forming hydrogen bonds to base Z). This increase in stability was attributed to the greater structural flexibility of the mismatched base pair, allowing for more favourable interactions with the third strand. In this chapter we have examined the stability of all 64 possible triplet combinations (N.XZ, where Y and Z are each base in turn), using fluorescence melting experiments. These studies were extended to examine the interaction of the nucleoside analogues S (for recognition of TA interrptions) and BAU (for recognition of AT base pairs) with duplex mismatches.

Several base analogues have been examined for their effect on triplex stability when positioned in the purine-containing strand of a duplex (Robles *et al.*, 2003). Generally, these bases retain the Watson-Crick face of a standard base but incorporate additional hydrogen bonding sites available for binding in the major groove. The 8-amino derivatives of A and G were shown to enhance triplex stability when substituted for A and G within the T.AT and C^+.GC triplets, respectively (Güimil-Garcia *et al.*, 1999; Soliva *et al.*, 2000; Cubero *et al.*, 2001). The pyrimidine analogue pseudouridine (Ψ) was also shown to form a stable triplets when positioned in the central strand of a triplex (Trapane *et al.*, 1994). More recently, the T analogue 5-amino-dU (U^A; Figure 7.1A), which is derived from a simple replacement of the hydrophobic 5-methyl group of T by the hydrophilic 5-amino group, was shown to bind to TFOs containing C, T and A (Rana & Ganesh, 2000). This result is interesting because unlike T a third strand G is not recognised by U^A. The second part of this chapter further examines the binding

properties of this analogue under different sequence contexts using fluorescence melting and circular dichroism.

7.2 Experimental design

The sequences of the oligonucleotides used in the fluorescence melting experiments are illustrated in Figure 7.1. The purine strand of the duplex (boxed) was labelled at the 5′-end with a fluorophore (F; fluorescein), while the third strand was labelled at the 5′-end with a quencher (Q; methyl red). Melting temperatures (T_m) for these intermolecular triplexes were determined as described in Chapter 3 using a rate of temperature change of 0.2 °C min^{-1}. Recordings were taken during both the heating and cooling steps and no significant hysteresis was observed. As the 18mer third strands contained several cytosine residues triplex formation using these oligonucleotides was pH dependent and was restricted to low pH conditions (pH < 6.0). All melting experiments were undertaken in 50 mM sodium acetate buffer containing 200 mM sodium chloride at a pH 5.5. The concentration of duplex was 0.25 μM and the concentration of third strand was 3 μM. T_m values were calculated from the first derivatives of the melting and annealing profiles. Each value was recorded in triplicate and usually differed by less than 0.5 °C.

The sequences of the oligonucleotides used in circular dichroism (CD) experiments are shown in Figure 7.1B(ii). The purine strand of the duplex (boxed) was labelled at the 5′-end with a fluorophore (F; fluorescein), while the third strand was unlabelled. The CD spectra for each triplex were determined as described in Chapter 2. The triplexes were first heated to 95 °C then allowed to cool slowly to room temperature, to ensure correct annealing of the complex. All experiments were undertaken in 50 mM sodium acetate buffer containing 200 mM sodium chloride at pH 6.0. The concentration of duplex was 1 μM and the concentration of third strand was 5 μM. Each spectrum was accumulated 16 times, smoothed and the buffer spectrum subtracted.

7.3 Results

The oligonucleotides illustrated in Figure 7.1 were used to generate 64 different triplex combinations, each varying by a single triplet N.XZ, where N, X and Z are each base in turn. 16 of these combinations contain standard Watson-Crick (WC) base pairs in the

A

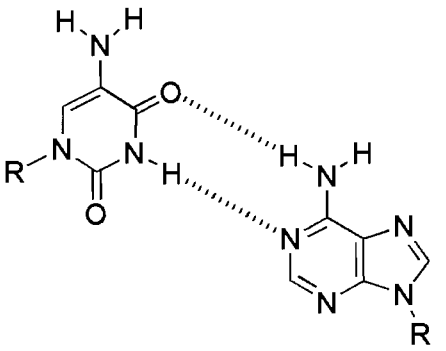

B

(i)

5′-Q-TCTCTCTTNTCCTCCTCC
5′-F-AGAGAGAAXAGGAGGAGG
3′-TCTCTCTTZTCCTCCTCC

(ii)

5′-Q-TCTCTCTTNTCCTCCTCC
5′-F-AGAGAGAAXAGGAGGAGG
3′-TCTCTCTTATCCTCCTCC

(iii)

5′-Q-TCTCTCTCNCCCTCCTCC
5′-F-AGAGAGAGXGGGAGGAGG
3′-TCTCTCTCACCCTCCTCC

Figure 7.1 Chemical structure of the 5-amino-dU.adenine base pair and sequence of oligonucleotides used in Chapter 7; A) The analogue 5-aminouracil (U^A) generating a base pair with adenine; B) Sequence of the oligonucleotides used in fluorescence melting experiments: the duplexes are boxed and were labelled with fluorescein (F) at the 5′-end of the purine strand, whilst the third strands were labelled with methyl red or pyrene (Q) at an identical position; (i) oligonucleotides used for Watson-Crick mismatch studies, where N, X and Z are each base in turn, generating 64 triplet combinations; (ii) oligonucleotides used to examine the specificity of 5-amino-dU in triplex formation when flanked with T.AT triplets, where N is A, G, C or T and X is T or U^A; (iii) oligonucleotides used to examine the specificity of 5-amino-dU in triplex formation when flanked with C^+.GC triplets, where N is A, G, C or T and X is T or U^A.

duplex and the data for these were presented in Section 4.6.3.1, while the remaining 48 combinations contain mismatched base pairs in the duplex.

7.3.1 Triplexes containing C.XZ triplets

Representative melting profiles for triplexes containing cytosine in the third strand are shown in Figure 7.2. For each panel, the N.X bases of the N.XZ triplet are constant, whilst the base Z is substituted with each base in turn. The T_m values determined for these profiles, which were performed at pH 5.5, are shown in Table 7.1. The values in parentheses show the differences in T_m between the triplet formed at a Watson-Crick base pair (e.g. C.AT) and the triplet containing a duplex mismatch (e.g C.AG). The profiles obtained for the triplexes containing C.AZ triplets are shown on the top left hand panel. It can be seen that more stable triplexes were generated with cytosine was positioned opposite a mismatch AZ base pair than opposite a standard AT bp (black line). This was most notable for the triplex containing a C.AA triplet (blue line) for which the T_m is 4.4 °C higher than for C.AT.

	N			
XZ	A	G	C	T
AA	43.5 (-0.9)	44.3 (+5.3)	44.2 (+4.4)	50.4 (-4.1)
AG	46.6 (+2.2)	41.3 (+2.3)	39.2 (-0.8)	51.6 (-2.9)
AC	47.0 (+2.6)	40.7 (+1.7)	41.4 (+1.6)	52.1 (-2.4)
AT	44.4	39.0	39.8	**54.5**
GA	44.1 (-3.9)	43.6 (-0.4)	53.4 (-3.2)	43.2 (-0.5)
GG	43.7 (-4.7)	45.2 (+1.1)	51.1 (-5.5)	43.6 (-0.1)
GC	48.4	**44.1**	**56.6**	43.7
GT	45.7 (-2.7)	43.8 (-0.4)	51.9 (-4.7)	44.4 (+0.8)
CA	43.9 (+2.2)	44.8 (+2.9)	47.0 (+3.3)	44.8 (+0.3)
CG	40.7	41.9	**43.7**	**44.5**
CC	43.1 (+2.4)	44.3 (2.4)	45.5 (+1.8)	42.3 (-2.2)
CT	41.3 (+0.6)	41.9 (0.0)	44.2 (+0.5)	40.5 (-4.0)
TA	40.7	**47.3**	38.7	37.8
TG	41.5 (+0.8)	41.3 (-6.0)	40.3 (+1.6)	40.3 (+2.5)
TC	42.3 (+1.6)	42.1 (-5.2)	39.4 (+0.7)	40.2 (+2.4)
TT	41.3 (+0.6)	41.3 (-6.0)	39.0 (+0.3)	39.8 (+2.0)

Table 7.1 T_m values for different triplet combinations determined by fluorescence melting. Experiments were performed in 50 mM sodium acetate pH 5.5 containing 200 mM NaCl. Each T_m value was repeated in triplicate and differed by less than 0.5°C. The purine strand of the duplex was labelled with fluorescein while the third strands were labelled with methyl red. The values in parentheses show the differences in T_m between the triplet formed at a Watson-Crick base pair and the triplet containing a duplex mismatch. The values in bold correspond to the well known C^+.GC, T.AT, G.TA, G.GC, T.CG and C.CG triplets.

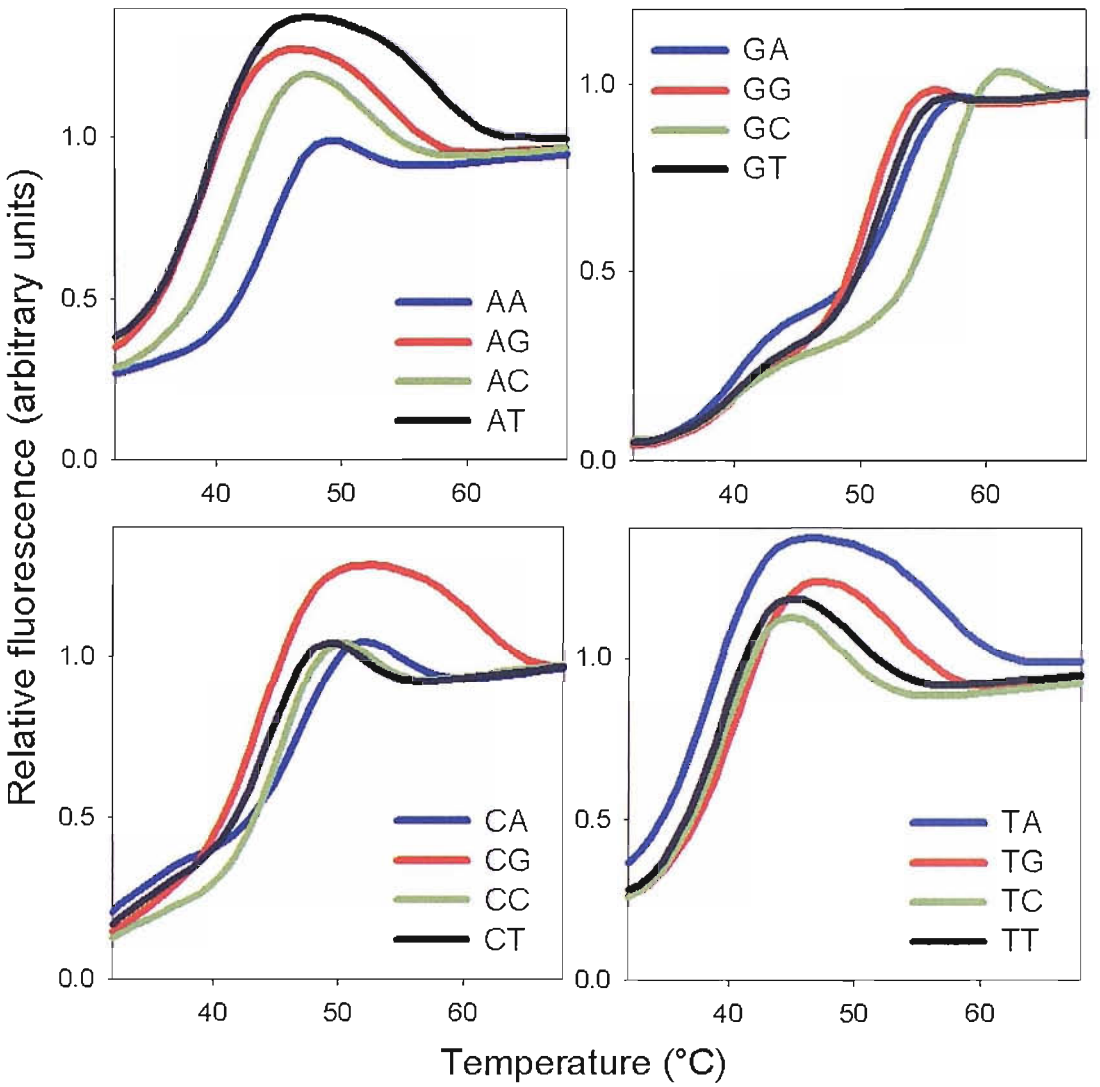

Figure 7.3 Fluorescence melting curves for different triplexes containing the base cytosine opposite each possible standard or mismatched base pair (C.ZY). The experiments were performed in 50 mM sodium acetate, pH 5.5 containing 200 mM NaCl. The y-axis show the normalised fluorescence (arbitrary units), while the x-axis shows the temperature (°C). The samples were heated at a rate of 0.2 °C/min.

The top right hand panel shows the profiles for the triplexes containing C.GZ triplets. In this instance the triplex containing the C^+.GC triplet (green line) was more stable than any of the triplexes containing C.GZ mismatches, with a T_m 3.2 °C higher than the next most stable. As expected, these C.GZ triplets were more stable than all the other C.XZ triplets. Further examination of the melting profiles reveals a secondary transition at lower temperatures. This is most likely to be attributed to the formation of a Hoogsteen duplex between the third strand and the purine-containing strand of the duplex (see Section 3.4.2). It is also noteworthy that the T_ms determined for these transitions (~ 40 °C) are the same irrespective of the duplex pyrimidine strand, which again suggests this interaction occurs between the third strand and purine-containing strand of the duplex.

The bottom panels show the profiles for the triplexes containing C.CZ or C.TZ triplets. In all cases the triplexes generated with C against a mismatched base pair were more stable than with a standard base pair (CG or TA). It is interesting to note the increased affinity of C for CA relative to CG, as C has been proposed for recognition of CG base pairs.

7.3.2 Triplexes containing T.XZ triplets

Representative melting profiles for the triplexes containing thymine in the third strand are shown in Figure 7.3. The top left panel shows the profiles for the triplexes containing T.AZ triplets. The most stable triplex was generated with T opposite an AT base pair, forming the usual T.AT triplet (black line) rather than with an AZ mismatch. The T.AA triplet (blue line) was the least stable, with a T_m 4.1 °C lower than T.AT (black line). The melting curves obtained for the triplexes containing T.GZ triplets are shown in the top right hand panel. All these triplexes exhibited similar T_m values (~ 44 °C), irrespective of the base that is paired with G.

The bottom right panel shows the profiles for triplexes containing T.CZ triplets. In this instance the triplexes containing T.CT and T.CC triplets are between 2 and 4 °C less stable than T.CG and T.CA. The most stable triplets produced similar T_m values to the T.GZ triplets. The melting profiles for the triplexes containing T.TY triplets are shown in the bottom right panel. The triplets containing mismatched base pairs are more stable than the T.TA triplet displaying T_m values between 2 and 5 °C higher, though these triplets are less stable than T.AT.

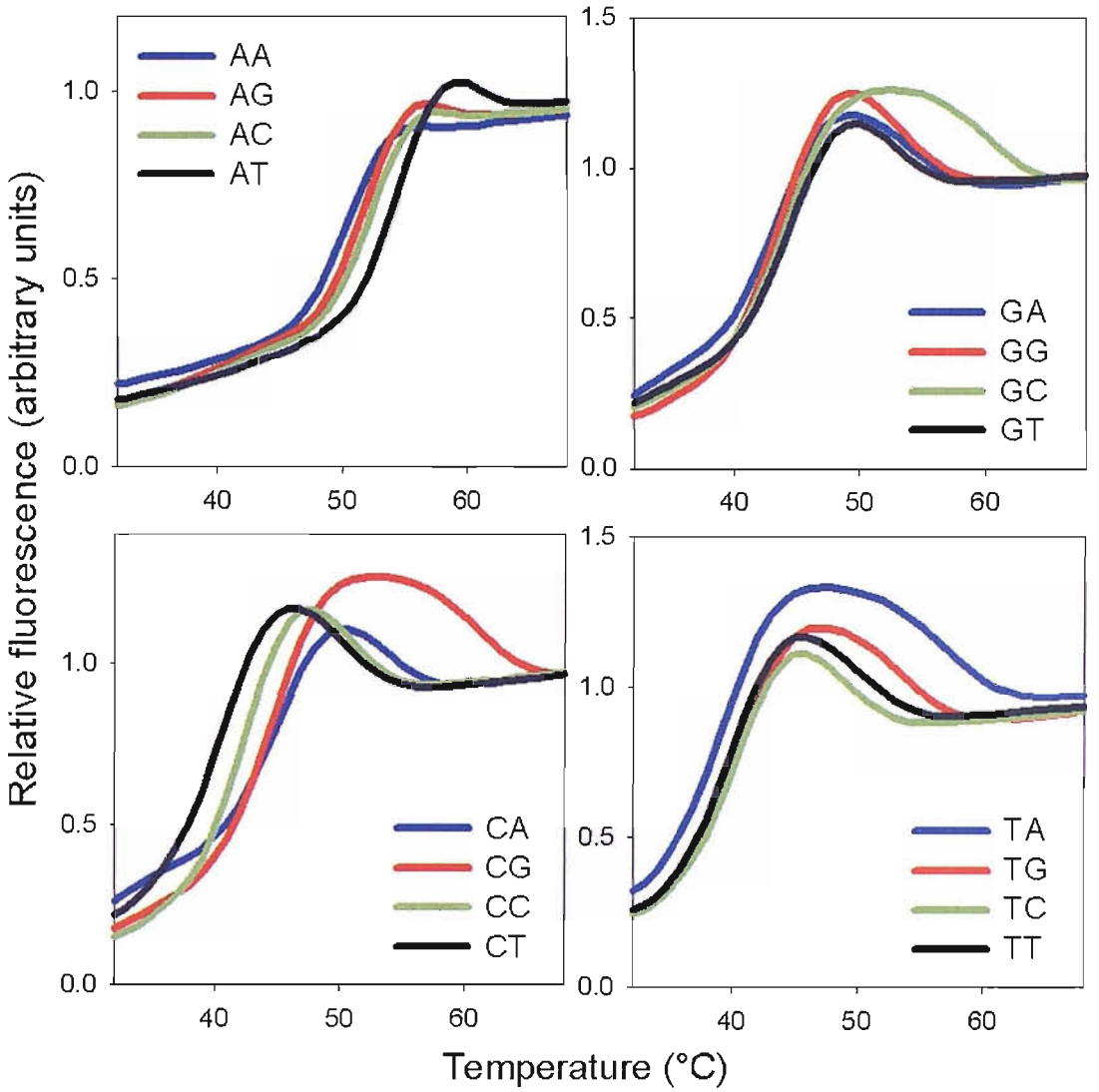

Figure 7.4 Fluorescence melting curves for different triplexes containing the base thymine opposite each possible standard or mismatched base pair (T.ZY). The experiments were performed in 50 mM sodium acetate, pH 5.5 containing 200 mM NaCl. The y-axis show the normalised fluorescence (arbitrary units), while the x-axis shows the temperature (°C). The samples were heated at a rate of 0.2 °C/min.

7.3.3 Triplexes containing G.XZ triplets

Representative melting profiles for the triplexes containing guanine in the third strand are shown in Figure 7.4. The top left hand panel shows the profiles for the triplexes containing G.AZ triplets. It is evident that the triplexes generated opposite a mismatched base pair are more stable than against AT. The G.AA triplet (blue line) was the most stable, exhibiting a T_m that is 5.3 °C higher than that observed with G.AT (black line). The top right hand panel shows the profiles obtained for the triplexes containing G.GZ triplets. These all have similar stabilities, exhibiting T_ms of about 44 °C.

The bottom left panel illustrates the profiles for the triplexes containing G.CZ triplets. The triplex containing a G.CG (red line) triplet exhibited a T_m of 41.9 °C, while the triplexes with duplex mismatches were more stable; G.CA (blue line) and G.CC (green line) triplets exhibited T_m values of about 44.5 °C. The bottom left hand panel shows the profiles for the triplexes containing G.TZ triplets. In this instance the most stable triplex was generated with G opposite a TA base pair (generating the well-known G.TA triplet) with a T_m of 47.3 °C. This triplet was at least 6 °C more stable than with any TZ mismatch.

7.3.4 Triplexes containing A.XZ triplets

Representative melting profiles for the triplexes containing adenine in the third strand are shown in Figure 7.5. The top left hand panel shows the profiles obtained for triplexes containing A.AZ triplets. It can be seen that the most stable triplexes were generated with adenine positioned opposite an AC (green line) and AG (red line) duplex mismatch; these complexes exhibited T_ms of about 47 °C. This compares to a T_m of about 44 °C for the A.AT triplet (black line). In contrast, the triplex containing the A.AA (blue line) triplet was no more stable than A.AT.

The top right hand graph shows the profiles obtained for the triplexes containing A.GZ triplets. The most stable triplex was generated with adenine opposite a standard GC base pair, exhibiting a T_m of about 48 °C. Substituting the three remaining bases at position Z produced triplexes that were at least 2 °C less stable. The bottom panels show the profiles obtained for the triplexes containing either A.CZ or A.TZ triplets. In

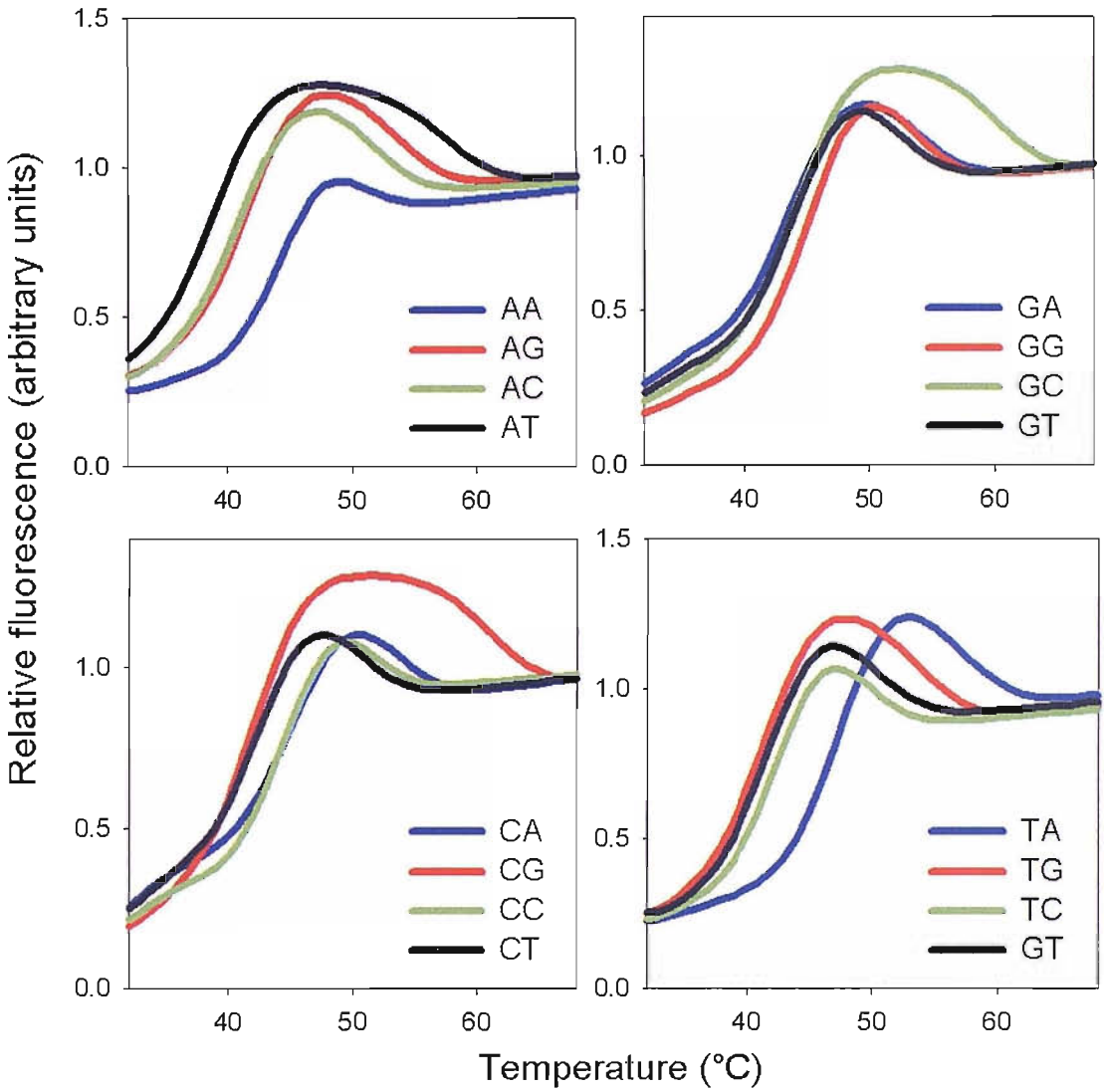

Figure 7.3 Fluorescence melting curves for different triplexes containing the base guanine opposite each possible standard or mismatched base pair (G.ZY). The experiments were performed in 50 mM sodium acetate, pH 5.5 containing 200 mM NaCl. The y-axis show the normalised fluorescence (arbitrary units), while the x-axis shows the temperature (°C). The samples were heated at a rate of 0.2 °C/min.

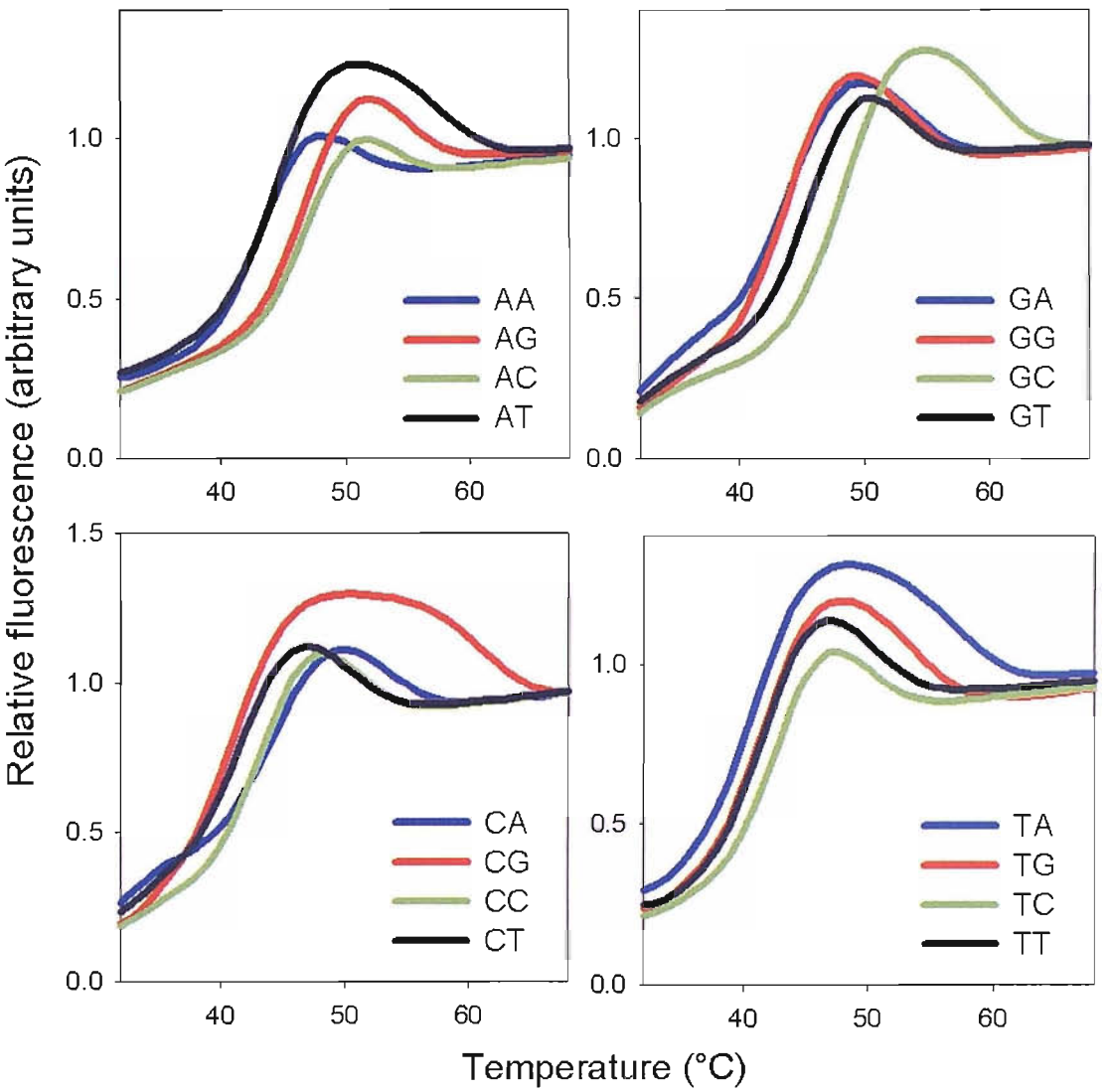

Figure 7.6 Fluorescence melting curves for different triplexes containing the base adenine opposite each possible standard or mismatched base pair (A.ZY). The experiments were performed in 50 mM sodium acetate, pH 5.5 containing 200 mM NaCl. The y-axis show the normalised fluorescence (arbitrary units), while the x-axis shows the temperature (°C). The samples were heated at a rate of 0.2 °C/min.

both cases positioning A opposite a duplex mismatch generated a complex of greater stability than opposite a standard base pair; this was most evident for the triplexes containing A.CA and A.CC triplets (green and red lines). The triplexes formed with these base pairs were less stable than those generated with the above AZ and GZ base pairs.

7.3.5 Triplex containing BAU.XZ triplets

We examined the stability of triplexes containing the modified nucleoside BAU opposite each possible mismatched base pair. Representative melting profiles for the triplexes containing this analogue are shown in Figure 7.6. The T_m values determined from these profiles, which were performed at pH 5.5 are shown in Table 7.2. The top left hand panel shows the profiles obtained for triplexes containing BAU.AZ triplets. It can be seen that the most stable triplex is formed with BAU opposite the W-C AT base pair (black line) with a T_m of 59.5 °C. Substituting T of the BAU.AT triplet with A, G and C resulted in complexes with T_m values that are all about 4 °C lower. The top right hand panel shows the melting curves obtained for the triplexes containing BAU.GY triplets. It can be seen that BAU displayed a lower affinity for a GZ mismatch than a GC base pair (green line), generating triplexes with T_m values 1.6-5 °C lower. This destabilisation was greatest for triplex containing the BAU.GA triplet. The melting profiles obtained for the triplexes that contained BAU.CZ and BAU.TZ triplets are illustrated in the bottom graphs. The T_m data reveal that all CZ mismatches generated triplexes with T_m values that are 1.4-3.2 °C higher than CG, the degree of stabilisation was greatest for CA, with a T_m of 45.2 °C. All TY mismatches were also stabilising relative to TA, but to a lesser extent than CY, with an increase in T_m of between 1-2 °C.

7.3.6 Triplex containing S.XZ triplets

Representative melting profiles for the triplexes containing the nucleoside analogue S in the third strand are shown in Figure 7.7 and the T_m values determined from these are shown in Table 7.2. The top left hand panel shows the profiles obtained for triplexes containing S.AZ triplets. It can be seen that with S in the third strand the most stable triplexes are formed opposite the three mismatches with T_m values between 2.4 and 3.4 °C higher than the triplex containing an AT base pair. The top right hand panel shows the profiles obtained for triplexes containing S.GZ triplets. Again, triplexes generated

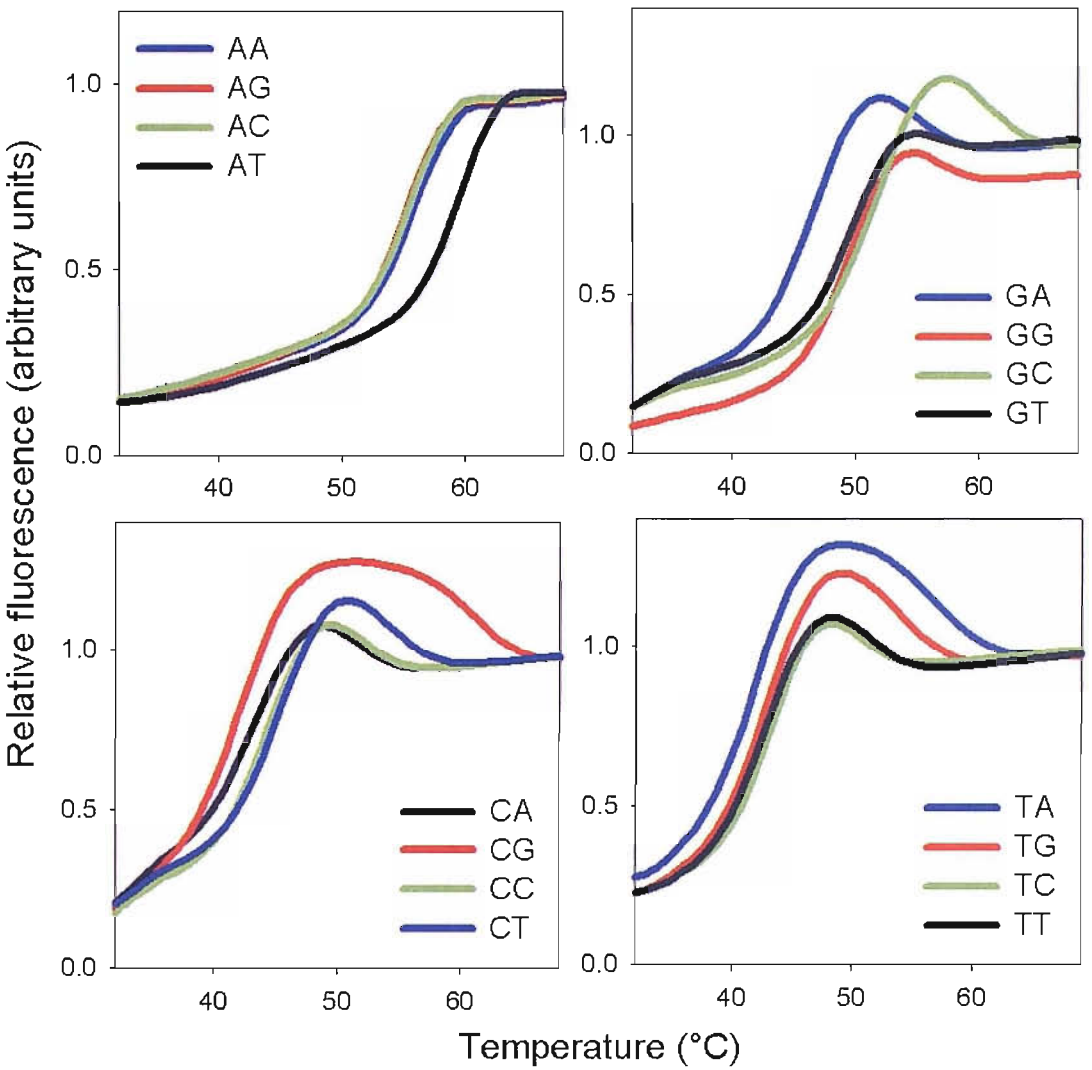

Figure 7.6 Representative fluorescence melting curves for different triplexes containing BAU positioned opposite each possible standard or mismatched base pair (BAU.ZY). The experiments were performed in 50 mM sodium acetate, pH 5.5 containing 200 mM NaCl. The y-axis show the normalised fluorescence (arbitrary units), while the x-axis shows the temperature (°C). The samples were heated at a rate of 0.2 °C/min.

with duplex mismatches were more stable than with a GC base pair, with a difference of between 3.2-4.0 °C, which was greatest for the S.GC triplet. The melting temperatures determined for these triplexes are similar to those obtained for S.AZ triplexes.

The bottom left hand panel shows the profiles obtained for triplexes containing S.CZ triplets. The triplexes generated with triplexes are between 1.6-3.6 °C more stable than those generated with S.CG. This was most notable for the S.CA and S.CC triplet which exhibited T_ms of about 53°C. The bottom right hand panel shows the melting curves obtained for triplexes containing S.TZ triplets. Again, the triplex generated with the mismatch base pairs are more stable than with the standard TA base pair, though the difference was less pronounced. The greatest increase was for the S.TT triplet which exhibited a T_m of 52.5 °C compared to 51.2 °C for S.TA. Overall, it can be seen that the triplexes formed by S differed in T_m values between 46.8 and 53.1 °C. The most stable triplexes were generated with S.CA, S.CC and S.TT triplexe

.

	N	
XZ	BAU	S
AA	55.7 (-3.8)	50.9 (+3.4)
AG	55.2 (-4.3)	49.9 (+2.4)
AC	55.4 (-4.1)	50.2 (+2.7)
AT	59.5	47.5
GA	46.8 (-5.0)	50.0 (+3.2)
GG	49.8 (-1.9)	50.1 (+3.3)
GC	51.8	46.8
GT	49.9 (-1.6)	50.7 (+4.0)
CA	45.2 (+3.2)	53. 1 (+3.6)
CG	42.0	49.5
CC	44.3 (+2.4)	53.0 (+3.5)
CT	43.4 (+1.4)	51.1 (+1.6)
TA	41.8	51.0
TG	42.9 (+1.1)	51.9 (+0.9)
TC	43.3 (+1.5)	51.2 (+0.2)
TT	42.8 (+1.0)	52.5 (+1.5)

Table 7.2 T_m values determined by fluorescence melting for triplexes composed of different triplet combinations containing the analogues BAU and S opposite duplex mismatches using a temperature gradient of 0.2 °C min^{-1} and the quencher methyl red at pH 5.5. Each T_m value was repeated in triplicate and usually differed by less than 0.5 °C.

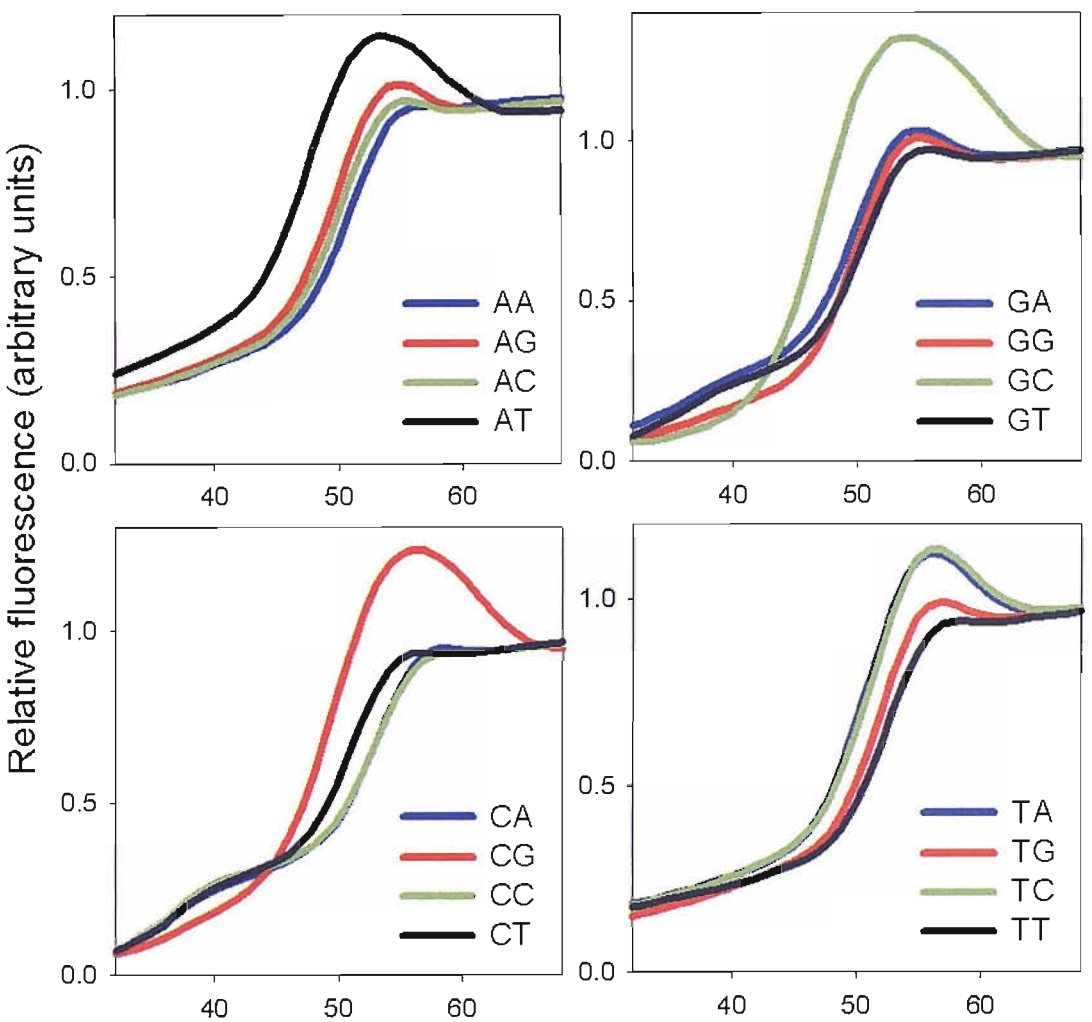

Figure 7.7 Fluorescence melting curves for different triplexes containing the nucleoside S opposite each possible standard or mismatched base pair (S.ZY). The experiments were performed in 50 mM sodium acetate, pH 5.5 containing 200 mM NaCl. The y-axis show the normalised fluorescence (arbitrary units), while the x-axis shows the temperature (°C). The samples were heated at a rate of 0.2 °C/min.

7.3.7 Triplex formation with 5-amino-dU in the purine strand

5-aminouracil (U^A) is a pyrimidine analogue of T in which the 5-methyl group is replaced by a 5-amino group. This analogue retains the required contacts to form a base pair with adenine but positions two additional hydrogen bonding sites within the major groove. The stability of triplexes in which this base (and T) were positioned in the purine-containing strand of a duplex were examined by determining the melting temperatures of the fluorescently-labelled triplexes shown in Figure 7.1B(ii), where N is A, G, C or T and X is U^A or T. Representative melting temperatures for these triplexes at pH 5.5 are illustrated in Figure 7.8. The T_m values determined from these and other experiments performed at pH 5.5 are shown in Table 7.3.

		N			
ZY	pH	A	G	C	T
TA	5.5	44.4 (44.4)	50.5 (50.4)	41.4 (42.8)	42.6 (42.7)
	6.0	30.1 (30.3)	37.1 (37.1)	28.4 (46.8)	29.6 (30.2)
U^AA	5.5	46.6 (46.8)	47.7 (47.9)	44.0 (44.1)	44.6 (44.9)
	6.0	33.6 (33.8)	34.4 (34.5)	30.5 (30.7)	30.0 (30.3)

Table 7.3 T_m values determined by fluorescence melting for triplexes containing 5-amino-dU in the purine strand of the duplex, flanked by T.AT. Values were obtained using a temperature gradient of 0.2 °C min^{-1} and the quencher methyl red. Values in parenthesis were calculated from the annealing phase.

The left hand panel of Figure 7.8 shows the interaction of TFOs containing each of the four natural bases with the TA-containing duplex target. Examination of these curves reveals that, as expected, the least destabilising base positioned opposite a TA base pair was guanine (red line). At pH 6.0, the triplex containing this triplet is about 7 °C more stable than the second most stable complex generated with TA. The order of selectivity of this base pair was G > A > T = C and was not affected by the pH.

The melting profiles obtained for the interaction of TFOs containing each of the four natural bases with the U^AA-containing duplex target are shown in the right hand panel of Figure 7.8. It can be seen that the most stable triplexes were generated with G and A positioned opposite the U^AA base pair (red and blue lines). The triplexes generated by these combinations were of similar stability but were 3 °C less stable than the triplex containing G.TA. This suggests that guanine has lower affinity, while adenine has a greater affinity for a U^AA base pair relative to TA. The low T_ms obtained for these

triplexes relative to triplexes containing T.AT or C^+.GC triplets (see Section 3.3.6.1) suggests that the only a single hydrogen bond is forming between U^A and the third strand base. Examination of the T_ms obtained for the triplexes positioning C and T opposite U^A reveals that both were more stable than when positioned opposite T, by 2-3 °C. The overall affinity of U^A was therefore G = A < C = T in this sequence context. The selectivities determined in this study are different to those obtained previously by Rana & Ganesh (2000) and will be discussed later.

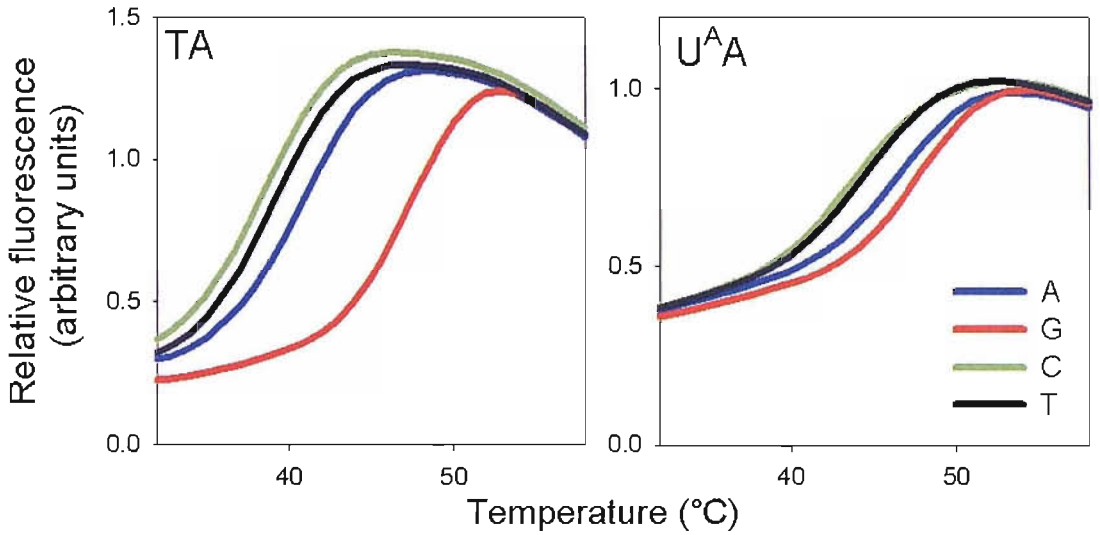

Figure 7.8_ Representative fluorescence melting curves for triplexes containing X.TA (left) or X.U^AA (right) triplets, where X is A, G, C or T. Each triplet was flanked by T.AT triplets. The experiments were performed in 50 mM sodium acetate, pH 5.5 containing 200 mM NaCl. The y-axis show the normalised fluorescence (arbitrary units), while the x-axis shows the temperature (°C). The samples were heated at a rate of 0.2 °C/min.

We also determined whether the selectivity of this base was affected by the nature of the flanking bases. This was investigated by determining the melting temperatures of the fluorescently-labelled triplexes shown in Figure 7.1B(iii). These sequences contained C^+.GC triplets flanking the X.TA or X.U^AA triplets. Representative melting profiles for these triplexes are illustrated in Figure 7.9. These experiments were determined at pH 5.5 and pH 6.0. The T_m values determined for these complexes are shown in Table 7.4. The left hand panel of Figure 7.8 shows the interaction of TFOs containing each of the four natural bases with the duplex target containing a TA base pair. It can be seen that the difference in T_m between each of the triplexes is much lower than observed previously (when this triplet is flanked by T.AT triplets). At pH 5.5, the triplexes

containing A.TA, C.TA and T.TA triplets were more stable than previously and the magnitude of this increase was greatest for C (ΔT_m ~7 °C). In contrast the triplex containing the G.TA triplex was less stable than before, with a T_m decrease of 2 °C. At pH 6.0, a similar selectivity is observed.

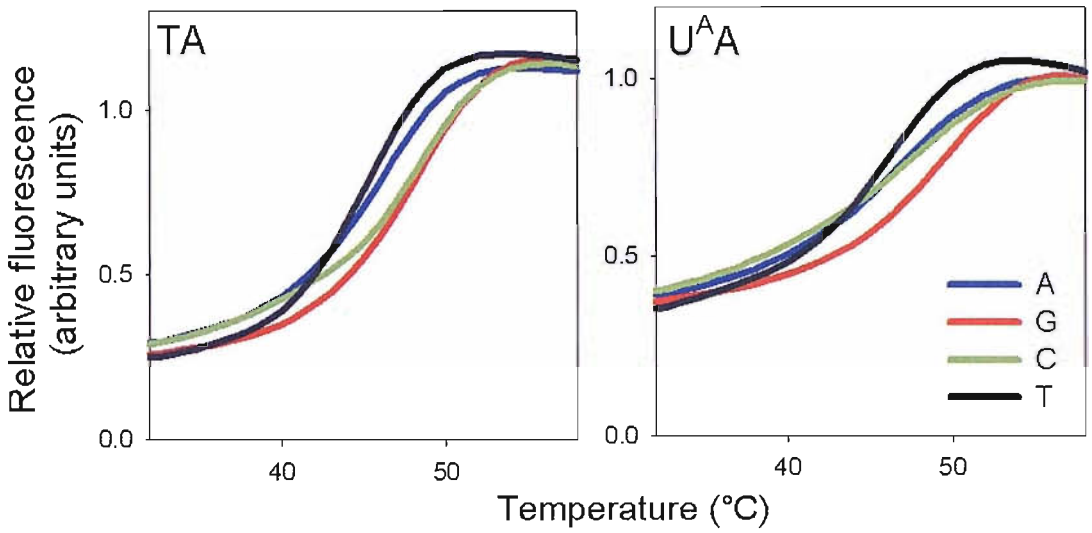

Figure 7.9 Representative fluorescence melting curves for triplexes containing X.TA (left) or X.U^{A}A (right) triplets, where X is A, G, C or T. Each triplet was flanked by C$^+$.GC triplets. The experiments were performed in 50 mM sodium acetate, pH 5.5 containing 200 mM NaCl. The y-axis show the normalised fluorescence (arbitrary units), while the x-axis shows the temperature (°C). The samples were heated at a rate of 0.2 °C/min.

		N			
ZY	pH	A	G	C	T
TA	5.5	46.3 (46.6)	48.4 (48.6)	48.3 (48.5)	45.0 (45.1)
	6.0	29.9 (30.1)	32.3 (32.3)	32.2 (32.2)	29.1 (29.4)
U^{A}A	5.5	47.0 (46.8)	50.1 (50.2)	47.4 (48.2)	46.3 (46.7)
	6.0	31.4 (31.7)	34.4 (34.5)	31.0 (31.3)	31.3 (31.3)

Table 7.4 T_m values determined by fluorescence melting for triplexes containing 5-amino-dU in the purine strand of the duplex, flanked by C$^+$.GC. Values were obtained using a temperature gradient of 0.2 °C min^{-1} and the quencher methyl red. Values in parenthesis were calculated from the annealing phase.

The right hand panel of Figure 7.9 shows the interaction of TFOs containing each of the four bases with the duplex target containing a U^{A}A base pair flanked by GC base pairs. An increase in triplex stability is also observed and is most notable for the triplexes containing G.U^{A}A, C.U^{A}A and T.U^{A}A triplets, with little difference in the stability of the triplex containing A.U^{A}A. In this sequence context, the G.U^{A}A triplet is more stable

than the G.TA triplet, exhibiting a difference in T_m of 2 °C; however, it is still 3 °C less stable than G.TA when flanked with T.AT. At pH 6.0 the triplexes were of similar stability to the previous triplexes with one exception, the triplex containing A.U^{A}A was 3 °C less stable than in the previous sequence context.

Taken together these data indicate sequence dependent differences in the selectivity of the base pairs TA and U^{A}A for each of the natural bases when positioned in a TFO. When flanked by T.AT both triplets generate the most stable triplets with G, though U^{A}A also shows a similar affinity for A. The G.TA triplet is more stable than G.U^{A}A. In contrast, when flanked by C$^+$.GC triplets U^{A}A produces more stable triplets with G than TA, an effect that is greater at higher pH. Interestingly, increasing the pH also decreases the stability of the A.U^{A}A triplet.

To further investigate these findings circular dichroism was performed on the triplexes containing X.U^{A}A triplets. These experiments were performed at pH 6.0 in the same buffer as used in fluorescence melting. The CD spectra were first determined for the duplex and single strands separately and these are shown in Figure 7.10A. It can be seen that the U^{A}A-containing duplex (dashed line) exhibits a negative band at 245 nm and positive band at 280 nm, suggesting no perturbation from the standard B-type duplex (Gray *et al.*, 1978, Gray *et al.*, 1992). The coloured lines represent the spectra obtained with the single strand labelled oligonucleotides and as expected, the spectra are different to those obtained for the duplex. An intense positive band is observed at 290 nm and a negative band is observed at 260 nM. Interestingly, the intensity of the band at 290 nm is different for the four oligonucleotides. It is greatest for the C-containing TFO, followed by T, and then the purine-containing TFOs. The CD spectra of cytosine-rich oligonucleotides are known to show evidence of helicity at low pH.

We next determined the CD spectra of the triplexes generated by addition of each of the third strands to the U^A-containing duplex, and these spectra are shown in Figure 7.10B. The spectra obtained are, as expected, different to those observed for the individual components of each triplex. Most notably, an increased negative band is observed below 220 nm. This is a characteristic that has been associated with A-like DNA conformations and the formation of triplex structures (Gray *et al.*, 1978; Rana *et al.*, 2000; Bernal-Mendéz & Leumann, 2002). Interestingly, the intensity of this negative peak is greatest for the A- and G-containing TFOs, which may suggest a greater

A

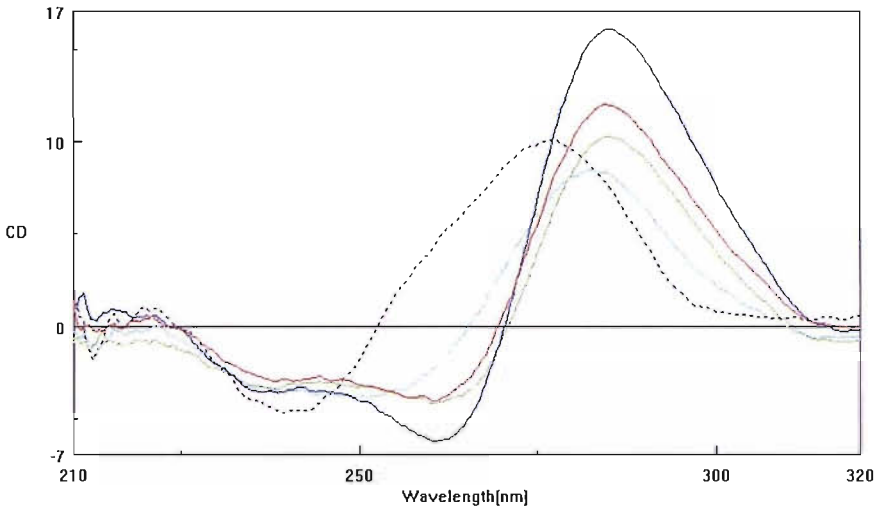

B

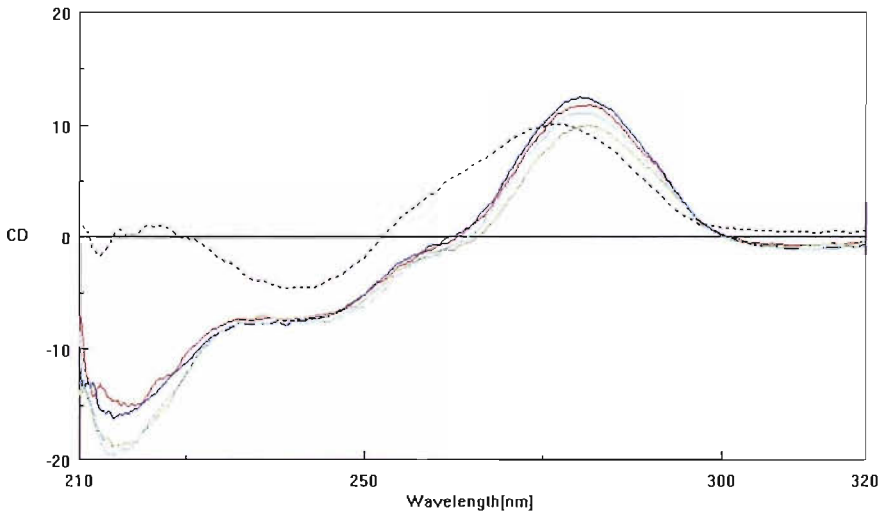

Figure 7.10 CD spectra of duplexes and triplexes formed by 5-amino-dU. A) CD spectra of target U^A-duplex (dashed line) and third strands containing A (light blue), G (green), C (blue), and T (red) at a central position; B) CD spectra of target U^A-duplex and triplex strutures containing a single A.U^AA (light blue), G.U^AA (green), C.U^AA (blue), and T.U^AA (red) triplets. The experiments were performed in 50 mM sodium acetate, pH 6.0 containing 200 mM NaCl.

proportion of triplexes formed with these oligonucleotides. The positive maxima observed with the duplex alone is also shifted to a higher wavelength upon triplex formation.

7.4 Discussion

The results presented in this paper demonstrate that triplex stability is affected by the identity of the base that is paired with the recognised duplex base; in some instances a duplex mismatch increase triplex affinity, while others show a decrease in stability. The affinity and specificity of each natural base and the analogues BAU and S for each of the duplex mismatches is discussed.

7.4.1 Natural bases

With cytosine in the third strand the most stable triplet was generated opposite a GC base pair, generating the familiar C^+.GC triplet. Substituting the duplex with A, G or T destabilised the triplet by at least 4 °C and this effect was greatest against GG. This contrasts the findings of Sun *et al.* (1991) which suggested that C.GA is more stable than C.GC. This difference is presumably due to the different sequence contexts in which these triplets have been assessed. In the present study the N.XZ triplets are flanked by T.AT triplets, whereas the previous study had a C^+.GC triplet on the 3´-side of the triplet. The C.AZ, C.CZ and C.TZ triplexes were all more stable when Z was a mismatch instead of a W-C base pair. In particular C.CA and C.AA triplets displayed T_ms which are 3.3 and 5 °C higher than C.CG and C.AT respectively.

With thymine in the third strand the most stable triplex was generated with the AT-containing target, generating the T.AT triplet. Substituting the duplex T led to a decrease in T_m of between 3-4 °C. Again this contrasts with the results previously obtained by Sun *et al.* (1991) which suggested that the T.AC triplet is more stable than T.AT. T also recognised GC and CG base pairs with moderate affinity. Replacing the G of T.CG decreased the stability of this triplet, whilst replacing the C of T.GC had little effect. This suggests that the interaction of T with GC is flexible and can tolerate some structural flexibility. The weaker binding of T to CA than to CG contrasts with C, for

which C.CA is more stable than C.CG. This difference is surprising since both T and C are thought to interact with CG, via the 2-carbonyl groups.

With G in the third strand it was seen that the most stable triplexes were generated with the target containing a TA base pair. Positioning this base opposite a TZ mismatch decreased the T_m of this triplet by about 6 °C. The stability of the G.TA triplet is known to be dependent on the formation of an additional hydrogen bond to the T of an adjacent T.AT triplet (Radhadkrishnan & Patel, 1991), and it is possible that this contact is not made when G is positioned opposite a mismatched T. G is also known to form a parallel triplet with GC base pairs, though this isolated triplet is less stable than G.TA. Substituting the C of the G.GC triplet for the three other bases leads a decrease in triplex stability, though the destabilisation is less than that with G.TZ mismatches. This suggests that the affinity of G for GC is less dependent on the position of G. The triplexes generated with G opposite AZ and CZ triplexes were more stable when Z was a mismatch and was greatest for the G.AA, G,CA and G.CC triplets.

With adenine in the third strand the most stable triplexes were generated with a standard GC base pair. Replacing the C of the A.GC base pair with A, G and T decreased the stability and this was greatest for the purines, presumably due to their larger size, distorting the triplex structure. The triplexes generated with A opposite the remaining AZ, CZ and TZ base pairs were more stable when Z was a mismatch than the correct base and was greatest for the A.AC and A.AG triplets.

Overall, it can be seen that the most stable triplexes were generated when T was positioned opposite TA and C opposite a GC base pair. The next most stable triplexes generated contained the triplets G.TA, C.CA, C.CC, A.GC, A.AG and A.AC which were all of similar stability; C.CA and C.CC were more stable than C.CG, whilst, A.AG and A.AC were of a similar stability to A.GC. It is clear that, within this sequence context, there were no triplet combinations that produced triplexes of greater stability than those containing standard C^+.GC and T.AT triplets.

7.4.2 Modified nucleosides

This study was then extended to assess the effect of duplex mismatches on the stability of triplexes containing modified bases in the third strand. The analogue BAU was

previously shown to form more stable and selective triplets with AT than T, whilst S recognises TA base pairs with a higher affinity than G.

Replacing the T of the BAU.AT triplet with A, G and C led to a decrease in triplex stability in a similar manner to that observed with T.AT. A T_m decrease of 4 °C was evident in each case, which is slightly more than that observed with T.AZ, for which there was a T_m decrease of 2-4 °C. Replacing C of the BAU.GC triplet was also destabilising, with a T_m decrease of 2-5 °C, whereas the stability of T.GC was unaltered by replacement of C. In contrast, positioning BAU opposite a CZ or TZ mismatch led to an increase in triplex stability relative to CG and TA. This was greatest with the CZ mismatches and was most notable for the BAU.CA triplet, with a T_m increase of 3 °C. Again this is different to the results with the T.CZ triplets, where the mismatches were destabilising. Previous results have demonstrated that BAU binds to AT and GC base pairs with a higher affinity than T. This was attributed to the suitable positioning of the 5-propargylamino and 2′-aminoethoxy groups so as to interact with the negative phosphate residues at these base pairs. The greater destabilisation exhibited by BAU against AY and GY mismatches is likely to be a consequence of altering the positioning of these groups, disrupting the favourable charge-charge interactions. Previous results also demonstrated that BAU exhibited an enhanced discrimination against CG base pairs, in this instance it is likely that the propargylamino and aminoethoxy groups are not ideally positioned. The increase in affinity of BAU for a CY mismatch, compared to T which is destabilising at a CY mismatch, is likely to be the results of more suitable positioning of these moieties due to the increased structural flexibility of the duplex at a mismatch.

Positioning S opposite any duplex mismatch increased triplex stability, in contrast to any other base studied. This was most evident for S.CA and S.CC triplets were 4 °C more stable than S.CG. The S.GZ and S.AZ triplex mismatches were the next most stabilising, increasing stability by 2-3 °C, depending on the mismatch. The least stabilising mismatches were formed at S.TZ, where a difference in T_m of only 1 °C was observed relative to interaction with the W-C base pairs. Overall, it can be seen that the triplexes formed by S differed in T_m values between 46.8 and 53.1 °C. The low selectivity of this base was previously noted in Chapter 5 and 6 and was attributed to possible protonation effects, the conformational flexibility of this analogue, an

intercalative mode of binding or the presence of hydrogen bond contacts that span the entire major groove.

7.4.3 The analogue 5-aminouracil in the central strand of a triplex

The thymine analogue 5-amino-dU (U^A) contains a 5-amino group in place of the 5-methyl group of T. When substituted for T in a TA base pair this analogue presents an additional two hydrogen bond donor sites in the major groove. The triplex-forming properties of this base were examined by fluorescence melting and compared to T in the same position. When flanked by T.AT on both sides the most stable triplets generated by this base were with A and G, exhibiting T_ms of 34 °C at pH 5.5. Whilst, as expected, the G.TA triplet was the most stable triplet generated by T, with a T_m of ~ 37 °C. These results differ from those obtained by Rana and Ganesh (2000) who showed that A offered the highest affinity for U^AA. In the binding scheme proposed by the authors, the 4-carbonyl and 5-amino group of U^A form hydrogen bonds to the N1 atom and 6-amino group of A (Figure 7.11A). As the A.U^AA triplet was less stable than T.AT, displaying a T_m 5 °C lower, it is unlikely that two hydrogen bonds are forming between the third strand and duplex. It is more likely that a single hydrogen bond forms between the N1 atom of A and the exocyclic 5-amino group of U^A (Figure 7.11B). This also gives a better backbone geometry than in the previously scheme. The decreased stability of the G.U^AA triplet relative to the G.TA triplet suggests that G is no longer suitably positioned to form an additional H-bond with the adjacent T.AT triplet, as mentioned above. However, it is still likely that G recognises U^A in a similar manner to T (Figure 7.11C).

In contrast, the selectivity of both U^A and T was altered when these bases were flanked by C^+.GC triplets on both sides. U^A generated less stable triplets with A (ΔT_m 3 °C) whilst its affinity for G was unchanged. Conversely, T generated less stable triplets with G (ΔT_m 5 °C) when flanked by C^+.GC triplets and confirms previously reported results (Kiessling *et al.*, 1993). This suggests that in a similar manner to G and its interaction with TA, the stability of the A.U^AA triplet is dependent on interactions other than just hydrogen bonding. The remaining triplets formed by these bases were more stable at low pH, presumably due to the increased stability of C^+.GC relative to T.AT. Under these conditions, G.U^AA was more stable than G.TA, however, the difference was not

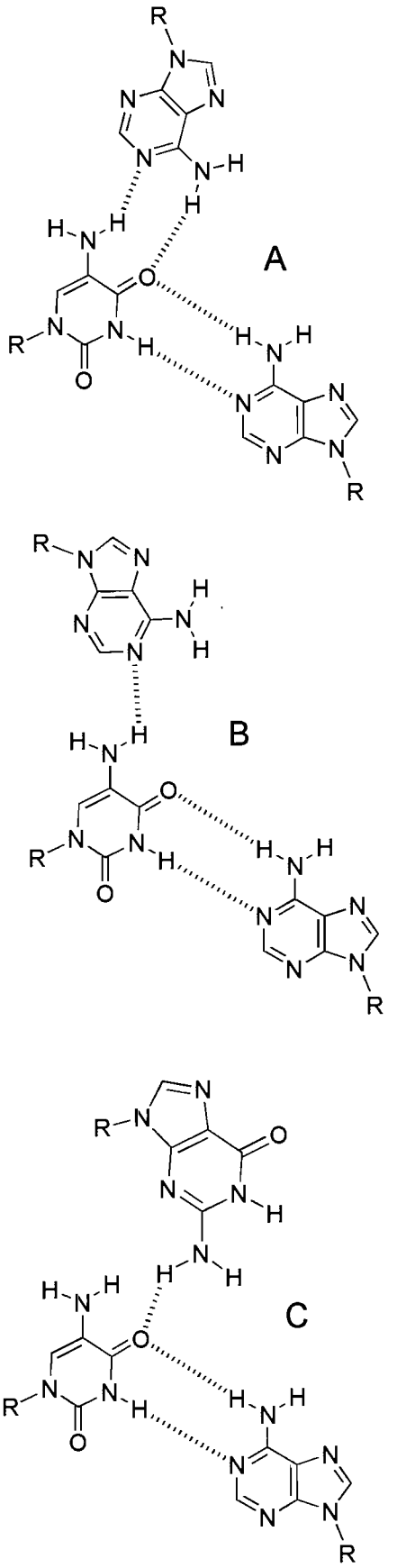

Figure 7.11 Chemical structure and proposed hydrogen bonding patterns for the triplets generated with the base analogue 5-aminouracil; A) A.U^{A}T B) A.U^{A}T and C) G.U^{A}T.

substantial. These results indicate that 5-aminouracil does not possess useful recognition properties.

8 GENERAL CONCLUSIONS

In recent years triplex-forming oligonucleotides (TFOs) have received extensive research interest for their application in such diverse areas as gene-based therapeutics, functional genomics and molecular biology (Rice *et al.,* 2001; Seidman & Glazer, 2003; Potaman, 2003). The most encouraging advances have shown that TFOs can be used to elicit site-specific mutagenesis and to inhibit tumour growth in mice (Vasquez *et al.*, 2000; Re *et al.*, 2004). Despite this, triplex formation is hampered by several restrictions; (i) there are no stable means for recognising TA or CG base pairs (pyrimidine interruptions) using natural DNA bases; (ii) formation of the C^+.GC triplet requires conditions of low pH (< 6.0), necessary for protonation of the third strand cytosine; (iii) the binding of the third strand may not be strong, due to electrostatic repulsion between the three polyanionic DNA strands. The work described in this thesis examined the triplex-forming properties of several novel nucleoside analogues that might be used to overcome each of these restrictions. From this study we propose the first generation of modified nucleotides for forming stable triple helices at mixed sequences at physiological pHs.

8.1 Techniques

DNase I footprinting and thermal melting (fluorescence and UV) experiments were used to determine the specificity and affinity of the modified TFOs examined in this thesis. At the start of this work the fluorescence melting technique had not been applied to the study of *inter*molecular triplex formation. Before applying this technique to the study of modified triplexes its validity was assessed and the results of which were presented in Chapter 3. In these experiments oligonucleotides were suitably labelled with a fluorophore and quencher so as to produce intermolecular triplexes with a low fluorescence upon formation. Heating these complexes led to an increase in fluorescence signal which translated to a melting profile for each complex. It was initially anticipated that the slow nature of triplex formation would limit the ability to determine accurate T_ms under equilibrium conditions. It was found that by adjusting several experimental parameters (i.e. pH, ionic conditions) the complexes associated and dissociated at a suitable rate. The LightCycler could also be programmed to heat and cool in a slow enough fashion so that triplex formation was completely reversible.

To further validate this method the stability of all possible combinations of natural bases opposite each base pair was investigated and showed good agreement with previously reported data (Griffin & Dervan, 1989; Yoon *et al.*, 1991; Mergny *et al.*, 1991). There was also a good correlation between footprinting and fluorescence melting experiments despite several experimental differences (constant vs variable temperature, differences in buffer conditions, sequence length effects). The results obtained by UV melting on unlabelled TFOs were the same as those obtained using fluorescence melting on labelled TFOs. This highlights that the reporter groups did not significantly affect triplex specificity.

8.2 Nucleoside analogues for stabilising DNA triplexes

Several studies have suggested that at low pH the C^+.GC triplet is more stable than T.AT due to the presence of the positive charge (Roberts & Crothers, 1996; Keppler *et al.*, 1997; James *et al.*, 2003). With this in mind the thymine analogue 5-propargylamino-dU was synthesised (Bijapur *et al.*, 1999) and later its 2′-aminoethoxy derivative (Sollogoub *et al.*, 2002). Both analogues contain positively charged amino functions suitably positioned to interact with the negative phosphodiester residues within the duplex purine-strand and/or the TFO. The results presented in Chapter 4 further investigated these analogues alongside several of their derivatives. Fluorescence melting showed that modifications at the 5-position of dU increased triplex stability in the order propargylamino = propargylguanidino > dimethylpropargylamino. At pH 6.0 an increase in T_m of 2, 4 and 4 °C per modification was observed for the dimethylamine, guanidine and amine derivatives respectively. As each modification contains a positive charge in a similar position it is likely that the lower stabilisation afforded by the dimethylamine is a result of a loss of hydrogen bonding contacts within the major groove. Conversely, the methyl groups may result in a steric clash with the triplex backbone. The results obtained with the 2′-aminoethoxy,5-propargylamino (BAU) and 2′-guanidinoethoxy,5-propargylguanidino analogues also suggest that replacement of each amine with a guanidine does not alter triplex stability. In both instances an increase in T_m of 8 °C was observed. As a guanidine is protonated over a greater range than the amine this modification is likely to offer greater stabilisation at higher pH values.

It was also observed that all of the nucleosides were highly selective for AT relative to

all other Watson–Crick DNA base pairs. Furthermore, each analogue exhibited enhanced discrimination against pyrimidine-purine base pairs (X.TA and X.CG), as the triplets formed by them were similar or less stable than those formed by unmodified T. The reason for this enhanced discrimination is unclear and is especially noteworthy since T.CG is the most stable natural triplet at CG inversions. Footprinting studies were also undertaken to examine whether BAU could stabilise triplexes that were formed in the GT-motif, since these structures are known to be less stable than parallel (CT-containing) triplexes. Triplex formation was not detected in either binding orientation. This confirms that stabilisation of parallel triplexes by this analogue results from specific interactions with the amino substituents, and not from non-specific charge interactions.

8.2 Nucleoside analogues for decreasing the pH dependence of DNA triplexes

The requirement for low pH in the parallel binding motif, necessary for protonation of third strand cytosines, has led to the synthesis of a variety of cytosine mimics. Two bases that have been designed for the pH independent recognition of GC are N7-dG (Hunziker *et al.*, 1995) and 6-oxo-dC (Xiang *et al.*, 1994). Both bases were shown to offer a lower affinity than C for GC under low pH conditions, presumably due to the lack of a positive charge. The 2′-aminoethoxy derivative of each base was examined in Chapter 4 by fluorescence melting. Again, it was seen that both derivatives produced less stable complexes with GC than C at pH 5.0 but were of a similar stability at pH 6.0. These results are similar to those obtained with the deoxyribose variants (Hunziker *et al.*, 1995; Xiang *et al.*, 1994). The lack of stabilisation is likely to stem from structural effects; ^{AE}N7G is not isostructural within the surrounding parallel triplets, whilst 6-oxo-C may suffer from unfavourable stacking interactions and/or steric hindrance due to the 6-carbonyl group. In both cases the altered N-type conformation of the sugar may further contribute to these sequence effects.

The analogue 2-aminopyridine and its 3-methyl derivative (^{Me}P) were investigated. The addition of the 3-methyl group did not affect the affinity of this base, consistent with the findings of a previous report (Hildbrand *et al.*, 1997). It was seen that triplexes containing ^{Me}P were more stable than C at pH 6.0 with a ΔT_m increase of 3.5 °C per modification but did not form at pH 7.0. A better approach was achieved by combining ^{Me}P with BAU within the same TFO. A complex containing three substitutions of each

analogue exhibited nanomolar binding affinity at pH 7.5. However, the affinity depended on the number of substitutions and their arrangement; oligonucleotides in which these analogues were evenly distributed throughout the third strand bound much better than those in which they are clustered. There are several potential reasons for this; (i) repulsion may occur between adjacent charges; (ii) pseudonucleosides such as ^{Me}P are expected to adopt an S-type sugar pucker in contrast to C which adopts a more favourable N-type conformation upon triplex formation (Plavec *et al.*, 1994; Imanishi *et al.*, 2002); (iii) base stacking interactions between the 3-methyl group of ^{Me}P and the 5-propargylamino group of an adjacent BAU may alter the positioning of the amine unfavourably. The last point could be assessed by replacing 3-methyl,2-aminopyridine with 2-aminopyridine within the TFO.

8.4 Nucleoside analogues for recognising pyrimidine interruptions

The use of C and T to recognise a CG base pair is limited as both bases also generate C^+.GC or T.AT triplets which have a higher stability. 5-propargylamino-dC was investigated in Chapter 5 because the addition of the propargylamino group should lower the pK_a of the ring nitrogen, thereby decreasing its recognition of GC. However, the extent of this destabilisation was not as dramatic as initially anticipated; at pH 6.0 a T_m decrease of 4 °C was observed against a GC base pair. There are several potential reasons for this; (i) the propargylamino group may stabilise the C^P.GC triplet, as previously shown for the formation of the U^P.GC triplet (ii) the electron withdrawing property of the amino group is partially lowered due to electrostatic interactions with a positively charged phosphate residue (iii) the pK_a of C^P is higher upon triplex formation as previously shown for C (Rajopal & Feignon, 1989; Asensio *et al.*,1999). Interestingly, the addition of the propargylamino chain stabilised the interaction with CG by just 2 °C per modification. This is consistent with the above findings suggesting the 5-propargylamino modification is most suited for increasing stability at RY base pairs.

The base 1-isoquinolone was also investigated as its 2´-aminoethoxy ribose derivative. At all pH values this analogue effectively acted as a 'null base' in which it made little or no contribution to the affinity or specificity of the TFO. In previous studies this base had shown good CG recognition properties when incorporated into LNA, indicating that the stabilisation previously afforded by this base stemmed predominantly from the

sugar modification (Hari *et al.*, 2003). As both modifications lock in the same sugar pucker it is not clear why each exhibits different affinities. It is possible that this base prefers to generate a *syn* conformation when the aminoethoxy modification is introduced into the sugar.

The most successful analogues designed for the recognition of CG were based on the pyrrolopyrimidin-2-one ring system. These nucleobases are similar in structure to T but lack the 4-carbonyl and 3-NH groups, both of which are required in the recognition of AT. In this configuration, these bases are capable of forming a hydrogen bond involving N3 and the free C4-amino proton of the duplex C. The 2-carbonyl group is also free to form an unconventional C-H...O bond at the 5-position of C (Prevot-Halter & Leumann, 1999; Marfut & Leumann, 1998). Of the 10 derivatives studied, the analogue ^{A}PP was the most stabilising. However, there was very little difference in stability between each of the derivatives. At pH 6.0 the ^{A}PP.CG triplet was 3 °C more stable than T.CG. Again, the 2´-aminoethoxy derivative of ^{A}PP exhibited a greater affinity for AT than CG suggesting that this modification favours recognition of RY base pairs.

As the G.TA triplet is the most stable triplet generated at TA by any natural base, several deoxyguanosine derivatives were examined for their ability to recognise this base pair. The addition of a propargylamino chain to the 7 position of the base or an aminoethoxy group to the 2 position of the sugar did not increase affinity for TA, rather a slightly increased affinity for GC was observed (ΔT_m = 2-5 °C). This is consistent with each modification favouring a RY base pair.

Lastly, the analogues S and its 2´-aminoethoxy derivative were investigated. S has previously been shown to generate stable triplexes at TA base pairs (Guinvarc'h *et al.*, 2001). The presence of two G.TA triplets was sufficiently destabilising to prevent triplex formation above 28 °C at pH 6.0. In contrast, a complex containing two S.TA triplets displayed a T_m of 32.1 °C, and the stability was further enhanced by incorporation of two ^{AE}S residues (T_m = 36.3). This demonstrates a T_m of 2 °C for each addition of ^{AE}S relative to S. Furthermore, ^{AE}S was more selective than S, discriminating between TA and CG by 3 °C. It is likely that the low selectivity of these bases is attributed to protonation effects, the conformational flexibility of each analogue, and an intercalative mode of binding or the presence of hydrogen bond contacts that span the entire major groove.

8.5 Four base recognition by triplex-forming oligonucleotides

There have been many studies investigating the effects of single nucleotides on triplex stability, each addressing one or other aspects of the problem (pH dependency, affinity and recognition of pyrimidine inversions). Chapter 6 examined the ability of a TFO containing multiple substitutions of the previously studied BAU, ^{Me}P, S and ^{A}PP to selectively target a mixed sequence duplex target at physiological pHs. With this combination it was possible to generate a triplex footprint at a 19-mer target site that contains four pyrimidine interruptions. As expected the complex was sensitive to pH, since it contained several ^{Me}P.GC triplets, but it formed at low micromolar concentration at pH 7.0 and exhibited a T_m of 37 °C at pH 7.5. Footprinting and melting experiments demonstrated that this heavily modified oligonucleotide retains its sequence specificity and that changing one of the base pairs opposite any one of the modified nucleoside leads to a large decrease in affinity. The only exception is S which appears to form stable complexes opposite both TA and CG base pairs. These results show a good correlation with the results presented for each analogue in previous chapters.

8.5 Implications and future work

The results presented here on BAU, alongside those of Sollogoub *et al.* (2002), highlight that this nucleoside needs no further optimization. There are, however, several sequence composition effects that need to be assessed, such as the effect of clustering or separating substitutions. It has recently been shown that very stable triplexes are obtained if all the sugars in the TFO are 2´-aminoethoxy-substituted (Puri *et al.*, 2004) this may also be the case with this analogue.

Recent studies have suggested that the association rates of TFOs correlate better with their bioactivity than T_m values (Puri *et al.*, 2004). It has been postulated that fast association rates are required for TFOs to compete with DNA binding proteins (e.g. transcription factors) and will increase the probability of TFOs rebinding after elution by cellular mechanisms. Preliminary temperature jump experiments have been performed on BAU, the results of which suggest that the affinity of BAU is predominantly the result of a much slower dissociation rate. It would therefore be

interesting to determine the kinetic parameters associated with other modified analogues and to see how this affects triplex stability.

Although M has good recognition characteristics it does not bind tightly to GC at pHs above 6.0. A more useful base to use would be pseudoisocytosine, as this base offers pH independent recognition of GC. It is not possible to synthesise its 5-propargylamino derivative but the 2′-aminoethoxy variant ($^{AE}\Psi$; Figure 8.1) may prove useful for applications alongside BAU.

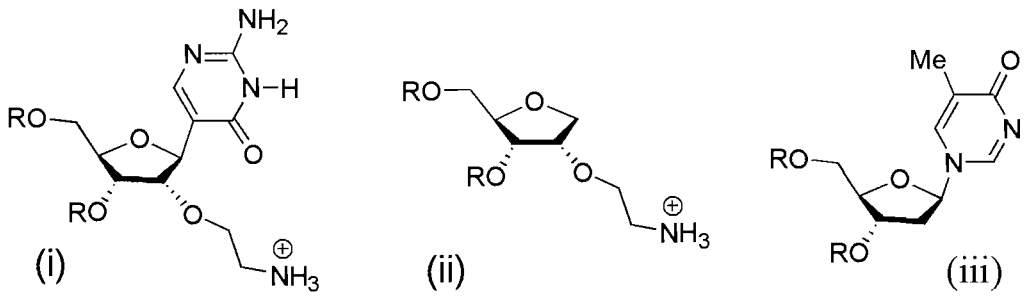

Figure 8.1 Potential nucleoside analogues for triplex formation; (i) 2′-aminoethoxy pseudoisocytosine; (ii) abasic 2′-aminoethoxy; (iii) ^{2H}T.

Although ^{AE}S provides the most stable means for recognising TA interruptions, the ^{AE}S.TA triplet is still less stable than T.AT or C^+.GC. There is still therefore a need for further nucleotides capable of recognising TA with high affinity and specificity.

The initial attempts to further enhance the affinity of the pyrrolopyrimidin-2-ones by the introduction of pendant protonated amino groups was not successful and requires further investigation. A significant problem with targeting pyrimidine inversions is the lack of isomorphism of the triplets generated with these base pairs. It may therefore be worthwhile studying a base that could generate a more isomorphous triplet. A potential base that could do this may be ^{2H}T (Figure 8.1(iii)). This base is capable of forming a hydrogen bond involving the 4-carbonyl and the free C4-amino proton of the duplex C. In this configuration the N3 atom is also free to form an unconventional C-H...N bond at the 5-position of C.

The results presented in this thesis suggest that the 2′-aminoethoxy modification favours stabilisation at purine.pyrimidine base pairs. It is therefore likely that this modification will have more success when introduced into nucleosides designed to

target AT or GC. Synthesis and evaluation of a 2′-aminoethoxy abasic monomer (Figure 8.1(ii)) may provide further insight into the binding properties of this particular modification.

APPENDIX

Representative footprinting plots generated by the oligonucleotide 5'-TCTCTTTXTTCT, where X is A, G, C or T with different fragments derived from *tyr*T(43-48).

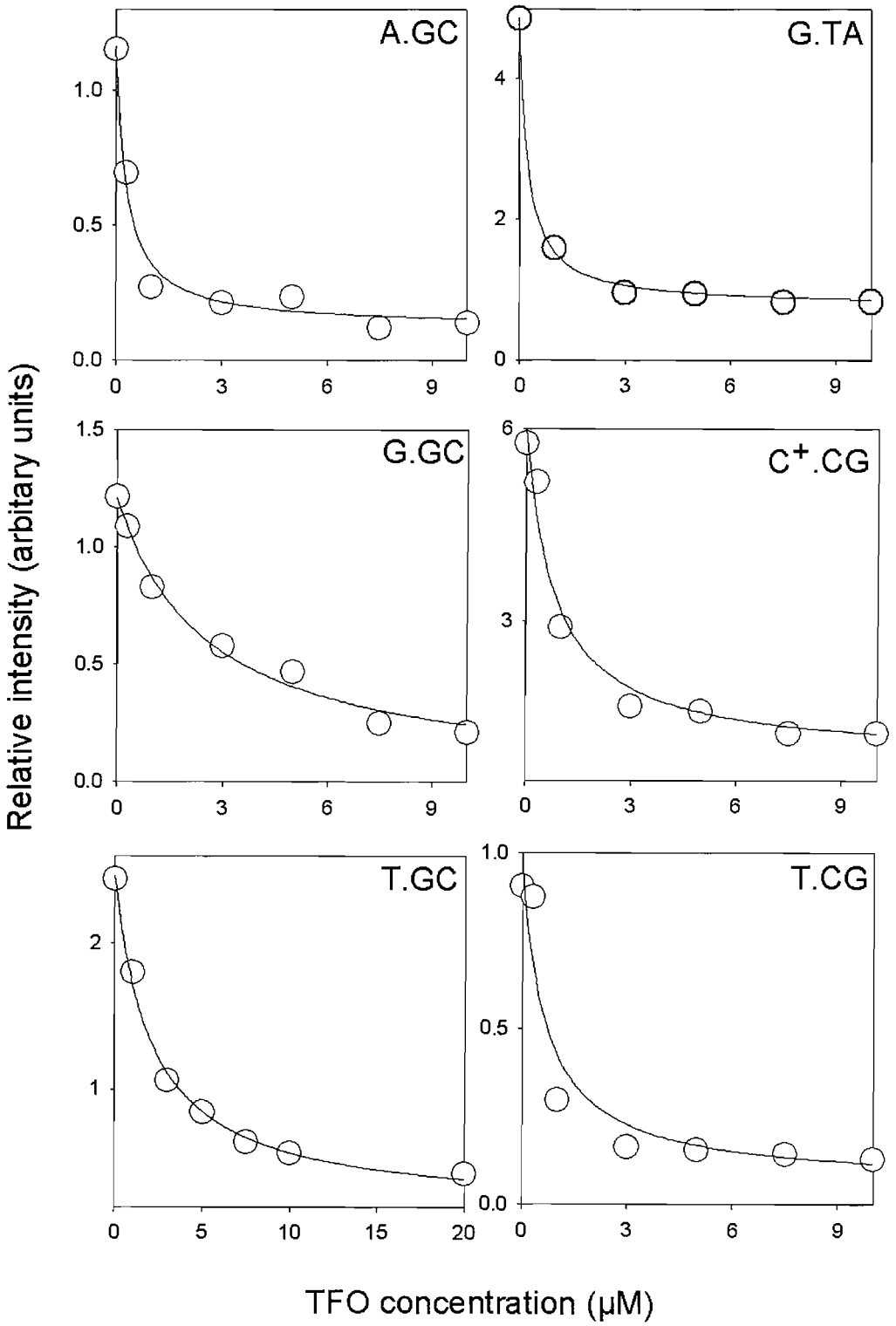

The chemical structures of the analogues prepared by the Brown group, Chemisty Dept, Southampton University and examined within this thesis;

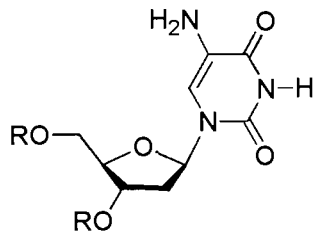

^{A}U

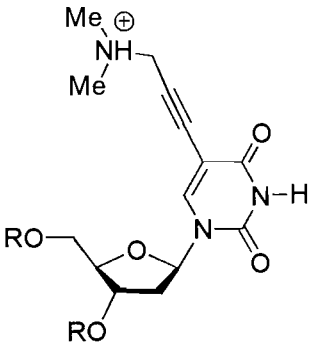

U^{DMAP}

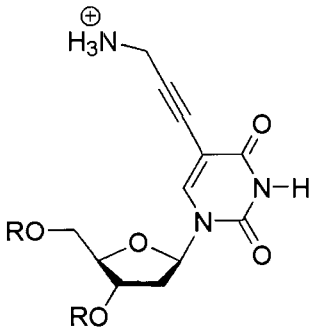

U^{P}

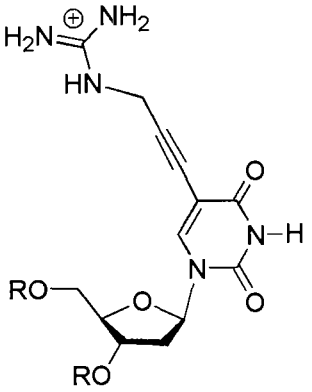

U^{PG}

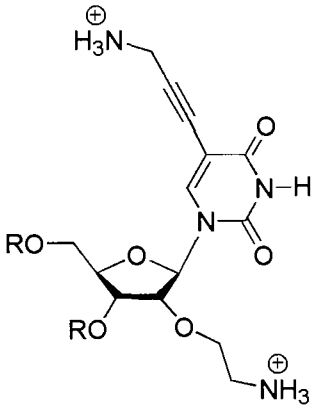

BAU

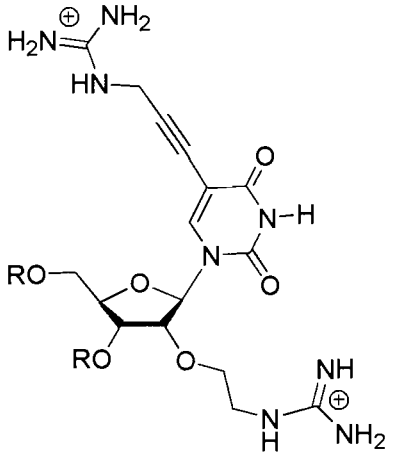

BGU

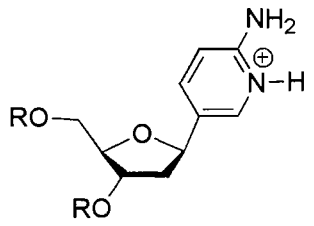

P

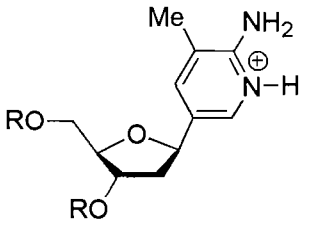

P^{Me}

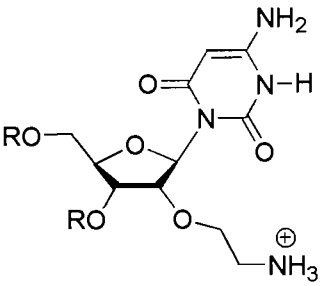

^{AE}6-oxo-C

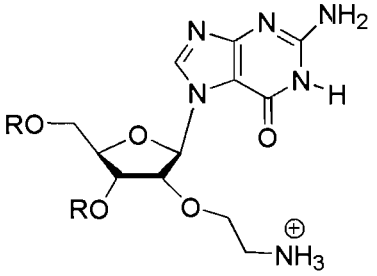

^{AE}N7G

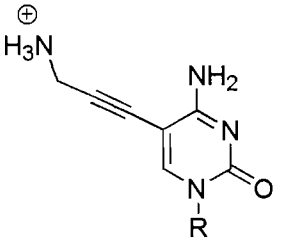

C^P

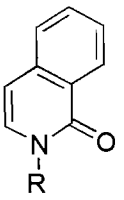

^{AE}Q

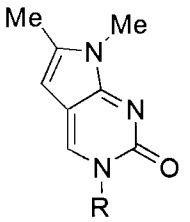

MP

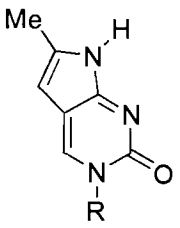

^{7H}MP

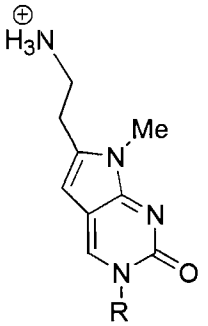

^{A}EP

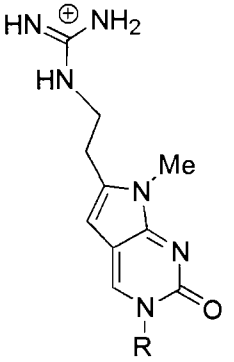

^{G}EP

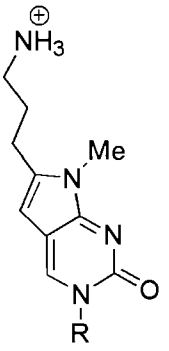

^{A}PP

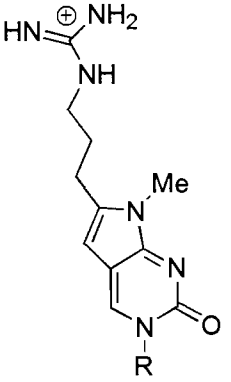

^{G}PP

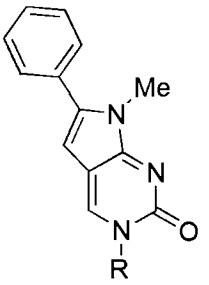

BP

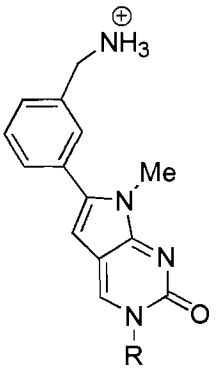

^{MA}BP

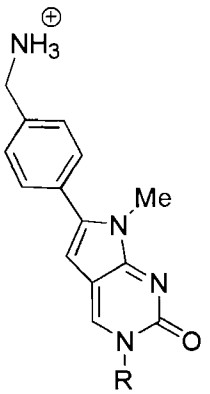

^{PA}BP

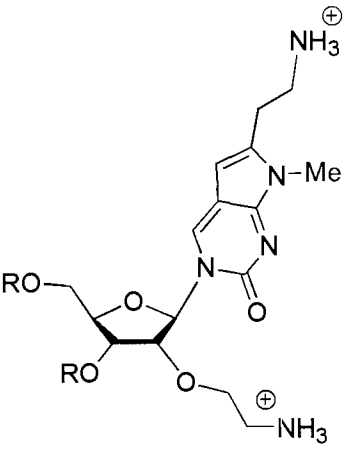

^{AE}PP

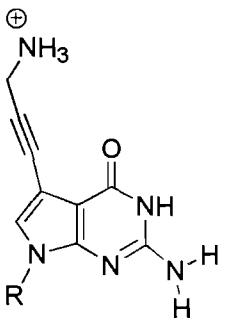

G^{P}

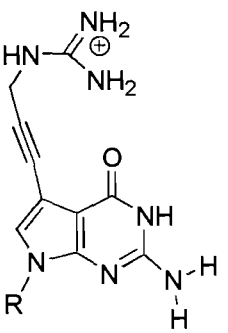

G^{PG}

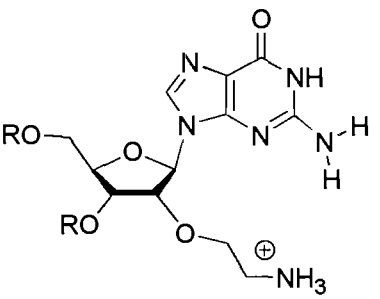

^{AE}G

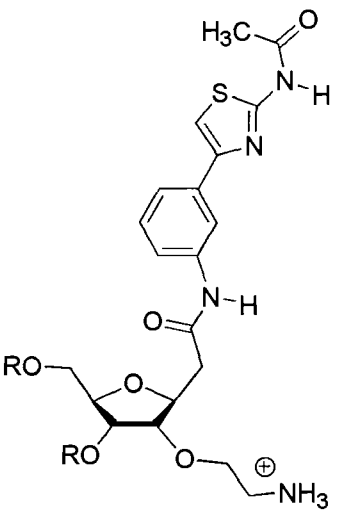

^{AE}S

REFERENCES

Alberti, P., Arimondo, P.B., Mergny, J-L., Garestier, T., Hélène, C., and Sun, J-S. (2002) A directional nucleation-zipping mechanism for triple helix formation. *Nucleic Acids Res.* 24, 5407-5415.

Amosova, O.A., and Fresco, J.R. (1999) A search for base analogs to enhance third-strand binding to 'inverted' target base pairs of triplexes in the pyrimidine/parallel motif. *Nucleic Acids Res.* 27, 4632-4635.

Anthony, T., and Subramaniam, V. (2001) Molecular beacons: nucleic acid hybridization and emerging applications. *J. Biomol. Struct. Dyn.* 19, 497-504.

Arnott, S., Hukins, D.W., Dover, S.D., Fuller, W., and Hodgson, A.R. (1973) Structures of synthetic polynucleotides in the A-RNA and A'-RNA conformations: x-ray diffraction analyses of the molecular conformations of polyadenylic acid-polyuridylic acid and polyinosinic acid-polycytidylic acid. *J. Mol. Biol.* 81, 107-172.

Arnott, T.S., Bond, P.J., Selsing, E., Smith, P.L.C. (1976) Models of triple-stranded polynucleotides with optimised stereochemistry. *Nucleic Acids Res.* 3, 2459-70.

Arya, D.P., Coffee, R.L.,Willis, B., and Abramovitch, A.I.J (2001) Aminoglycoside-nucleic acid interactions: remarkable stabilization of DNA and RNA triple helices by neomycin. *J. Am. Chem. Soc.* 123, 5385-5395.

Arya, D.P., Xue, L., and Tennant, P. (2003) Combining the best in triplex recognition: synthesis and nucleic acid binding of a BQQ-neomycin conjugate. *J. Am. Chem. Soc.* 125, 8070-8071.

Asensio, J.L., Brown, T., and Lane, A.N. (1998) Thermodynamic, kinetic, and conformational properties of a parallel intermolecular DNA triplex containing 5′ and 3′ junctions. *Biochemistry.* 37, 15188-15198.

Asensio, J.L, Lane, A.N., Dhesi, J., Bergqvist, and Brown, T. (1998) The contribution of cytosine protonation to the stability of parallel DNA triple helices. *J. Mol. Biol.* 275, 811-822.

Asensio, J.L., Brown, T., and Lane, A.N. (1999) Solution conformation of a parallel DNA triple helix with 5′ and 3′ triplex-duplex junctions. *Structure.* 7, 1-11.

Asseline, U., Hau, J.F., Czernecki, S., Le Diguarher, T., Perlat, M.C., Valery, J.M., and Thuong, N.T. (1991) Synthesis and physiochemical properties of oligonucleotides built with either alpha-L or beta-L nucleotide units and covalently linked to an acridine derivative. *Nucleic Acids Res.* 19, 4067-4074.

Atsumi, N., Ueno, Y., Kanazaki, M., Shuto, S., and Matsuda, A. (2002) Nucleosides and nucleotides. Part 214: Thermal stability of triplexes containing 4′ α-*C*-aminoalkyl-2′-deoxynucleosides. *Biorg. Med. Chem.* 10, 2933-2939.

Barawker, D.A., Rajeev, K.G., Kumar, V.A., and Ganesh, K.N. (1996) Triplex-formation at physiological pH: comparative studies on DNA triplexes containing 5-Me-dC tethered at N4 with spermine and tetraethyleneoxyamine. *Nucleic Acids Res.* 25, 4187-93.

Bartley, J.P., Brown, T., and Lane, A.N. (1997) Solution conformation of an intramolecular DNA triplex containing a nonnucleotide linker: comparison with the DNA duplex. *Biochemistry.* 36, 14502-14511.

Basye, J., Trent, J.O, Gao, D., and Ebbinghaus, S.W. (2001) Triplex formation by morpholino oligodeoxyribonucleotides in the HER-2/neu promoter requires the pyrimidine motif. *Nucleic Acids Res.* 29, 4873-4880.

Bates, P.J., Laughton, C.A., Jenkins, T.C., Capaldi, D.C., Roselt, P.D., Reese, C.B., and Neidle, S. (1996) Efficient triple helix formation by oligodeoxyribonucleotides

containing α- or β- 2-amino-5-(2-deoxy-D-ribofuranosyl) pyridine residues. *Nucleic Acids Res.* 24, 4176-4184.

Beal, P.A., and Dervan, P.B. (1991) Second structural motif for recognition of DNA by oligonucleotide-directed triple-helix formation. *Science.* 251, 1360-1363.

Behe, M.J. (1995) An overabundance of long oligopurine tracts occurs in the genome of simple and complex eukaryotes. *Nucleic Acids Res.* 23, 689-695.

Bernal-Méndez, E., and Leumann, C.J. (2002) Stability and kinetics of nucleic acid triplexes with chimaeric DNA/RNA third strands. *Biochemistry.* 41, 5312-5322.

Berressem, B., and Engels, J.W. (1995) 6-oxocytosine a novel protonated C base analogue for stable triple helix formation. *Nucleic Acid Res.* 23, 3465-3475.

Best, G.C., and Dervan, P.B. (1995) Energetics of formation of sixteen triple helical complexes which vary at a single position within a pyrimidine motif. *J.Am. Chem. Soc.* 117, 1187-1193.

Bidichandani, S.I., Ashizawa, T., and Patel, P.I. (1998) The GAA triplet repeat expansion in Friedreich's ataxia interferes with transcription and may be associated with an unusual DNA structure. *Am. J. Hum. Genet.* 62, 111-121.

Bijapur, J., Keppler, M.D., Bergqvist, S., Brown, T., and Fox, K.R. (1999) 5-(1-propargylamino)-2′-deoxyuridine (U^P): a novel thymidine analogue for generating DNA triplexes with increased stability. *Nucleic Acids Res.* 27, 1802-1809.

Brazier, J.A., Shibata, T., Townsley, J., Taylor, B.F., Frary, E., Williams, N.H., and Williams, D.M. (2005) Amino-functionalized DNA: the properties of C5-amino-alkyl substituted 2′-deoxyuridines and their application in DNA triplex formation. *Nucleic Acids Res.* 33, 1362-1371.

Broitman, S.L., Dwight, D.I., and Fresco, J.R. (1987) Formation of the triple-stranded polynucleotide helix, poly(A.A.U). *Proc. Natl. Acad. Sci. USA.* 84, 5120-5124.

Brown, P.M., Madden, C.A., and Fox, K.R. (1998) Triple-helix formation at different positions on nucleosomal DNA. *Biochemistry.* 37, 16139-16151.

Buchini, S., and Leumann, C.J. (2003) Recent improvements in antigene technology. *Curr. Opin. Chem. Biol.* 7, 717-726.

Buchini, S., and Leumann, C.J. (2003) Dual recognition of a C-G pyrimidine-purine inversion sites: synthesis and binding properties of triplex forming oligonucleotides containing 2′-aminoethoxy-5-methyl-1*H*-pyrimid-2-one ribonucleosides. *Tett. Letts.* 5065-5068.

Buchini, S., and Leumann, C.J. (2004) Stable and selective recogntion of three base pairs in the parallel triple-helical DNA binding motif. *Angew. Chem.* 116, 4015-4018.

Blaskó, A., Dempcy, O.D, Minyat, E.E., and Bruice, T.(1996) Association of short-strand DNA oligomers with guanidium-linked nucleosides. A kinetic and thermodynamic study. *J. Am. Chem. Soc.* 118, 7892-7899.

Blommers, M.J.J, Natt. F., Jahnke, W. and Cuenoud, B. (1998) Dual recognition of double-stranded DNA by 2′-aminoethoxy-modified oligonucleotides: the solution structure of an intramolecular triplex obtained by NMR spectroscopy. *Biochemistry.* 37, 17714-17725.

Cain, R.J., and Glick, G.D. (1998) Use of cross-links to study the conformationl dynamics of triplex DNA. *Biochemistry.* 37, 1456-64.

Capobianco, M.L., Champdore, M., Arcamone, F., Garbesi, A., Guinvarc'h, D., and Arimondo, P.B. (2005) Improved synthesis of daunomycin conjugates with triplex-forming oligonucleotides. The polypurine tract of HIV-1 as a target. *Biorg. Med. Chem.* 13, 3209-3218.

Cassidy, S.A., Slickers, P., Trent, J.O., Capaldi, D.C., Roselt, P.D., Reese, C.B., Neidle, S., and Fox, K.R. (1997) Recognition of GC base pairs by triplex forming

oligonucleotides containing nucleosides derived from 2-aminopyridine. *Nucleic Acids Res.* 25, 4891-4898.

Chaires, J.B., Ren, J., Henary, M., Zegrocka, O., Bishop, G.R., and Strekowski, L. (2003) Triplex selective 2-(2-Naphthyl)quinoline compounds: origins of affinity and new design principles. *J. Am. Chem. Soc.* 125, 7272-7283.

Chandler, S.P, and Fox, K.R. (1993) Triple helix formation at A_8XA_8•T_8YT_8. *FEBS Letts.* 332, 189-192.

Chandler, S.P., and Fox, K.R. (1996) Specificity of antiparallel DNA triple helix formation. *Biochemistry.* 35, 15038-15048.

Chaturvedi, S. Horn., T., and Letsinger, R.L. (1996) Stabilization of triple-stranded oligonucleotide complexes: use of probes containing alternating phosphodiester and stereo-uniform cationic phosphoramidate linkages. *Nucleic Acid Res.* 24, 2318-2323.

Chen, D.L., and McLaughlin, L.W. (2000) Use of PK_a to enhance the formation of base triplets involving C-G and G-C base pairs. *J. Org. Chem.* 65, 7469-7474.

Cheng, A.J., and Van Dyke, M.W. (1998) Oligodeoxyribonucleotide length and sequence effects on intramolecular and intermolecular G-quartet formation. *Antisense Nucleic Acid Drug Dev.* 8, 215-225.

Chin, T-M., Lin, S-B., Lee, S-Y., Chang, M-L., Cheng, A.Y-Y., Chang, F-C, Psaternack, L., Huang, D.H., and Kan, L-S. (2000) 'Paper-Clip' type triple helix formation by 5′-d-$(TC)_3Ta(CT)_3Cb(AG)_3$ (a and b = 0 -4) as a function of loop size with and without the pseudoisicytosine base in the hoogsteen strand. *Biochemistry*, 39, 12457-12464.

Chomilier, J., Sun, J-S., Collier, D.A., Montenay-Garestier, T., Hélène, Lavery, R. (1992) A computational and experimental study of the bending induced at a double-triple helix junction. *Biophys. Chem.* 45, 143-152.

Coman, D., and Russu, I.M. (2004) Site-resolved stabilization of a DNA triple helix by magnesium ions. *Nucleic Acids Res.* 32, 878-883.

Cooney, M., Czernuszewicz, G., Postel, E.H., Flint, S.J., and Hogan, M.E. (1988) Site-specific oligonucleotide binding repress transcription of the human *c-myc* gene in vitro. *Science.* 241, 456-459.

Craig, M.E., Crothers, D.M., and Doty, P. (1971) Relaxation kinetics of dimer formation by self complementary oligonucleotides. *J. Mol. Biol.* 62, 383-401.

Cubero, E., Guimil-Garcia, R., Luque, F.J., Eritja, R., and Orozco, M. (2001) The effect of amino groups on the stability of DNA duplexes and triplexes based on purines derived from inosine. *Nucleic Acids Res.* 29, 2522-34.

Cuenod, B., Casset, F., Hüsken, D., Natt, F., Wolf, R.M., Altmann, K-H., Martin, P., and Moser, H.E. (1998) Dual recognition of double-stranded DNA by 2′-aminoethoxy-modified oligonucleotides. *Angew. Chem. Int. Ed.* 37, 1288-1291.

Dabrowiak, J.C (1997) Quantitative DNA footprinting. *Methods in Molecular Biology,* Humana press.

Dagle, J.M., and Weeks, D.L. (1996) Positively charged oligonucleotides overcome potassium-mediated inhibition of triplex formation. *Nucleic Acids Res.* 24, 2143-2149.

Darby, R.A.J., Sollogoub, M., McKeen, C., Lynda, B., Risitano, A., Brown, N., Brown, T., Fox. K.R. (2002) High throughput measurement of duplex, triplex and quadruplex melting curves using molecular beacons and a lightcycler. *Nucleic acids res.* 9, e39.

Debart, F., Meyer, A., Vasseur, J-J., and Rayner, B. (1998) Anomeric inversion (from β to α) in methylphosphonates oligonucleosides enhances their affinity for DNA and RNA. *Nucleic Acids Res.* 26, 4551-4556.

Dey, I. and Rath, P. (2005) A novel rat genomic simple repeat DNA with RNA-homology shows triplex (H-DNA)-like structure and tissue specific RNA expression. *Biochem. Biophys. Res. Commun.* 327, 276-286.

Demidov, V.V., and Frank-Kamenetskii, M.D. (2004) Two sides of the coin: affinity and specificity of nucleic acid interactions. *Trends Biochem. Sci.* 29, 62-71.

Dempcy, R.O., Browne, K.A., and Bruice, T.C. (1995) Synthesis of the polycation thimidyl DNG, its fidelity in binding polyanionic DNA/RNA, and the stability and nature of hybrid complexes. *Proc. Natl. Acad. Sci. U S A.* 92, 6097-6101.

Durland, R.H., Kessler, D.J., Gunnel, S., Duvic, M., Pettitt, B.M., and Hogan, M.E. (1991) Binding of triple helix forming oligonucleotides to sites in gene promoters. *Biochemistry.* 30, 9246-9255.

Durland, R.H., Rao, T.S., Revenkar, G.R., Tinsley, J.H., Myrick, M.A., Seth, D.M., Rayford, J., Singh, P., and Jayaraman, K. (1994) Binding of T and T analogs to CG base pairs in antiparallel triplexes. *Nucleic Acids Res.* 22, 3233-3240.

Egholm, M., Christensen, L., Dueholm, K.L., Buchardt, O., Coull, J., and Nielsen, P.E. (1995) Efficient pH-independent sequence-specific DNA binding by pseudoisocytosine-containing bis-PNA. *Nucleic Acids Res.* 23, 217-222.

Eldrup, A.B., Dahl, O. and Nielsen, P.E. (1997) A novel peptide nucleic acid monomer for recognition of thymine in triple-helix structures. *J. Am. Chem. Soc.* 119, 11116-11117.

Escudé, C., Sun, J-S., Rougée, M., Garestier, T., and Hélène, C. (1992) Stable triple helices are formed upon binding of RNA oligonucleotides and their 2′-*O*-methyl derivatives to double helical DNA. *Acad Sci. III.* 315, 521-525.

Escudé, C. Nguyen, C.H., Kukreti, S., Janin, Y., Sun, J-S., Bisagni, E., Garestier, T., and Hélène, C. (1998) Rational design of a triple helix-specific intercalating ligand. *Proc. Natl. Acad. Sci.* 95, 3591-3596.

Escudé, C., Garestier, T., and Sun, J-S. (2001) Drug interactions with triple-helical nucleic acids. *Methods Enzym.* 340, 340-357.

Felsenfeld, G., Davies, D.R., and Rich, A. (1957) Formation of a three-stranded polynucleotide molecule. *J. Am. Chem. Soc.* 79, 2023-2024.

Fox, K.R. (2000) Targeting DNA with triplexes. *Curr. Med. Chem.* 7, 17-37.

Fox, K.R., Flashman, E., and Gowers, D.M. (2000) Secondary sites for triplex-forming oligonucleotides containing bulges, loops, and mismatches in the third strand. *Biochemistry.* 39, 6714-6725.

François, J-C., Saison-Behmoaras, T., and Hélène., C. (1988) Sequence-specific recognition of the major groove of DNA by oligonucleotides via triple helix formation. Footprinting studies. *Nucleic Acids Res.* 16, 11431-11440.

Frank-Kamenetskii, M.D. (1987) DNA H form requires a homopyrimidine-homopyrimidine mirror repeat. *Nature.* 330, 495-497.

Froehler, B.C., Wadwani, S., Terhost, T.J., and Gerrard, S.R. (1992) Oligonucleotides containing C-5 propyne analogs of 2′-deoxyuridine. *Tett. Lett.* 37, 5307-5310.

Galas, D.J., Schmitz, A. (1978) DNase footprinting: a simple method for the detection of protein-DNA binding specificity. *Nucleic Acids Res.* 5, 157-170

Giovannangeli, C., Rougée, M., Garestier, T., Thuong, N.T., and Hélène, C. (1992) Triple-helix formation by oligonucleotides containing the three bases thymine, cytosine, and guanine. *Proc. Natl. Acad. Sci.* 89, 8631-8635.

Godde, F., Toulme, J-J., and Moreau, S. (1998) Benzoquinazoline derivatives as substitutes for thymine in nucleic acid complexes. Use of fluorescence emission of benzo[g]quinazoline-2,4-(1*H*,3*H*)-dione in probing duplex and triplex formation. *Biochemistry.* 37, 13765-13775.

Goni, J.R., de la Cruz, X., and Orozco, M. (2004) Triplex-forming oligonucleotide target sequences in the human genome. *Nucleic Acids Res.* 126, 354-360.

Goobes, R., and Minsky, A. (2001) Thermodynamic aspects of triplex DNA formation in crowded environments. *J. Am. Chem. Soc.* 123, 12692-12693.

Gowers, D.M., and Fox, K.R (1997) DNA triple helix formation at oligopurine sites containing multiple contiguous pyrimidines. *Nucleic Acids Res.* 25, 3787-3794.

Gowers, D.M, Bijapur, J., Brown, T., and Fox, K.R. (1999) DNA triple helix formation at target sites containing several pyrimidine interruptions: stabilization by protonated cytosine or 5-(1-propargylamino) dU. *Biochemistry.* 38, 13747-13758.

Gray, D.M., Morgan, A.R., and Ratliff, R.L. (1978) A comparison of the circular dichroism spectra of synthetic DNA sequences of the homopurine. homopyrimidine and mixed purine–pyrimidine types. *Nucleic Acids Res.* 5, 3679–3695.

Gray, D.M., Hung, S.H., and Johnson, K.H. (1995) Absorption and circular dichroism spectroscopy of nucleic acid duplexes and triplexes. *Meth. Enzymol.* 246, 19–34.

Griffin. L.C., and Dervan, P.B (1989) Recognition of thymine adenine base pairs in the parallel triple helix motif. *Science*, 245, 967-971.

Griffin, L.C., Kiessling, L.L., Beal, P.A., Gillespie, P., and Dervan, P.B. (1992) Recognition of all four base pairs of double-helical DNA by triple-helix formation: design of nonnatural deoxyribonucleosides for pyrimidine-purine base pair binding. *J. Am. Chem. Soc.* 114, 7976-7982.

Gryaznov, S.M., Lloyd, D.H., Chen, J.K., Schultz, R.G., DeDionisio, L.A., Ratmeyer, L., and Wilson,W.D. (1995) Oligonucleotide N3'->P5' phosphoramidates. *Proc. Natl Acad. Sci. USA.* 92, 5798–5802.

Guimil-Garcia, R., Bachi, A., Eritja, R., Luque, F.J., and Orozco, M. (1998) Triple helix stabilization propeties of oligonucleotides containing 8-amino-2-deoxyguanosine. *Bioorg. Med. Chem. Lett.* 8, 3011-3016.

Guinvarc'h, D., Fourrey, J-L., Maurisse, R., Sun, J-S and Benhida, R. (2001) Incorporation of a novel nucleobase allows stable oligonucleotide-directed triple helix formation at the target sequence containing a purine.pyrimidine interruption. *Chem. Commun.* 1814-1815.

Guinvac'h, D., Fourrey, J-L., Maurisse, R., Sun, J-S., and Benhida, R. (2002) Synthesis, incorporation into triplex-forming oligonucleotides, and binding properties of a novel 2´-deoxy-*C*-nucleoside featuring a 6-(thiazolyl-5)benzimidazole nucleobase. *Org. Letts.* 14, 4209-4212.

Guinvarc'h, D., Fourrey, J-L., Maurisse, R., Sun, J-S, and Benhida, R. (2003) Design of artificial nucleobases for the recognition of the AT inversion by triple-helix forming oligonucleotides: A structure-stability relationship study and neighbour bases effect. *Bioorg. Med. Chem.* 2751-2759.

Han, H., and Dervan, P.B. (1994) Different conformational families of pyrimidine.purine.pyrimidine triple helices depending on backbone composition. *Nucleic Acids Res.* 22, 9831-9844.

Hari, Y., Obika, S., Sekiguchi, M., and Imanishi, T. (2003) Selective recognition of CG interruption by 2´,4´-BNA having 1-isoquinolone as a nucleobase in a pyrimidine motif triplex. *Tetrahedron.* 59, 5123-5128.

Hari, Y., Obika, S., Inohara, H., Ikejiri, Une, D., and Imanishi, T. (2005) Synthesis and triplex-forming ability of 2´,4´-BNAs bearing imidazoles as a nucleobase. *Chem. Pharm. Bull.* 53, 843-846.

Hélène, C., and Toulme, J.J. (1990) Specific regulation of gene expression by antisense, sense and antigene nucleic acids. *Biochim. Biophys. Acta.* 1049, 99-125.

Hildbrand, S., and Leumann, C.J. (1996) Enhancing DNA triple helix stability at neutral pH by the use of oligonucleotides containing a more basic deoxycytidine analog. *Angew. Chem. Int. Ed.* 35, 1968-1970.

Hilbrand, S., Blaser, A., Parel, S.P., and Leumann, C.J. (1997) 5-substituted 2-aminopyridine *C*-nucleosides as protonated cytidine equivalents: increasing efficiency and selectivity in triple helix formation. *J. Am. Chem. Soc.* 119, 5499-5511.

Hogan, M.E., Roberson, M.W., and Austin, R.H. (1989) DNA flexibility variation may dominate DNase I cleavage. *Proc. Natl. Acad. Sci. USA.* 86, 9273-9277.

Horn, V., Lacroix, L., Gautier, T., Takasugi, M., Mergny, J-L., and Lacoste, J. (1994) Triple helix formation with *Drosophila* satellite repeats. Unexpected stabilization by copper ions. *Biochemistry.* 43, 11196-11205.

Horne, D.A., and Dervan, P.B. (1991) Effects of an abasic site on triple helix formation characterized by affinity cleaving. *Nucleic Acids Res.* 19, 4963-4965.

Howard, F.B., Frazier, J., Lipsett, M.N. and Mills, T. (1964) Infrared demonstration of two- and three-strand helix formation between poly C and guanosine mononucleotides and oligonucleotides. *Biochem. Biophys. Res. Comm.* 17, 93-102.

Htun, H., and Dahlberg, J.E (1988) Single strands, triple strands, and kinks in H-DNA. *Science.* 241, 1791-1796.

Huang, C-Y., Cushman, C.D., and Miller, P.S. (1993) Triplex formation by an oligonucleotide containing N^4-(3-acetamidepropyl)cytosine. *J. Org. Chem.* 58, 5048-5049.

Huang, C-Y., and Miller, P.S. (1993) Triplex formation by an oligodeoxyribonucleotide containing N^4-(6-aminopyridinyl)cytosine. *J. Am. Chem. Soc.* 115, 10456-10457.

Huang, C-Y., Guixia, B., and Miller, P.S. (1996) Triplex formation by oligonucleotides containing novel deoxycytidine derivatives. *Nucleic Acids Res.* 24, 2606-2613.

Hunziker, J., Prietley, S.E., Brunar, H., and Dervan, P.B. (1995) Design of an N7-glycosylated purine nucleoside for recognition of GC base pairs by triple helix formation. *J. Am. Chem. Soc.* 117, 2661-2662.

Imanishi, T., and Obika, S. (2002) BNAs: novel nucleic acid analogs with a bridged sugar moiety. *Chem. Commun.* 21, 1653-1659.

James, P.L., Brown, T., and Fox, K.R. (2003) Thermodynamic and kinetic stability of intermolecular triple helices containing different proportions of C^+.GC and T.AT triplets. *Nucleic Acids Res.* 31, 5598-5606.

Jetter, M.C, and Hobbs, F.W. (1993) 7,8-dihydro-8-oxoadenine as a replacement for cytosine in the third strand of triple helices. Triplex formation without hypochromicity. *Biochemistry*, 32, 3249-3254.

Jiao, G-S, and Burgess, K. (2004) On the stability of furanopyrimidin-2-one bases in oligonucleotides. *Chem. Comm.* 1304-1305.

Kalish, J.M., Seidman, M.M., Weeks, D.L., and Glazer, P.M. (2005) Triplex-induced recombination and repair in the pyrimidine motif. *Nucleic Acids Res.* 33, 3492-3502.

Keppler, M.D., and Fox, K.R. (1997) Relative stability of triplexes containing different numbers of T.AT and C^+.GC triplets. *Nucleic Acids Res.* 25, 4644-4649.

Keppler, M.D, Zegrocka, O., Strekowski, L., and Fox, K.R. (1999a) DNA triple helix stabilisation by a napthylquinone dimmer. *FEBS Letts.* 447, 223-226.

Keppler, M.D., Read, M.A., Perry, P.J., Trent, J.O., Jenkins, T.C., Reszka, A.P., Neidle, S., and Fox, K.R. (1999b) Stabilization of DNA triple helices by a series of mono- and disubstituted amidoanthraquinones. *Eur. J. Biochem.* 263, 817-825.

Keppler, M.D., James, P.L., Neidle, S., Brown, T., and Fox, K.R. (2003) DNA sequnce specificity of triplex-binding ligands. *Eur. J. Biochem.* 270, 4982-92.

Kibler-Herzog, L., Kell, B., Zon, G., Shinozuka, K., Mizan, S., and Wilson, W.D. (1990) Sequence dependent effects of methylphosphonate deoyribonucleotide double and triple helical complexes. *Nucleic Acids Res.* 18, 3545-3555.

Kiessling, L.L., Griffin, L.C., and Dervan, P.B. (1992) Flanking sequence effects within the pyrimidine triple helix motif characterized by affinity cleaving. *Biochemistry.* 31, 2829-2834.

Kohwi, Y and Kohwi-Shigematsu, T. (1988) Magnesium ion-dependent triple-helix structure formed by homopurine-homopyrimidinr sequences in supercoiled plasmid DNA. *Proc. Natl. Acad. Sci. USA.* 85, 3781-3785.

Koh, J.S., and Dervan, P.B. (1992) Design of a nonnatural deoxyribonucleoside for recognition of GC base pairs by oligonucleotide-directed triple helix formation. *J. Am. Chem. Soc.* 114, 1470-1478.

Koshlap, K.M., Gillespie, P., Dervan, P.B., and Feigon, J. (1993) Nonatural deoxyribonucleoside D_3 incorporated in an intramolecular DNA triplex binds sequence-specifically by intercalation. *J. Am. Chem. Soc.* 115, 7908-7909.

Koizumi, M., Morita, K., Daigo, M., Tsutsumi, S., Abe, K., Obika, S. and Imanishi, T. (2003) Triplex formation with 2′-*O*,4′-*C*-ethylene-bridged nucleic acids (ENA) having C3′-*endo* conformation at physiological pH. *Nucleic Acids Res.* 31, 3267-3273.

Koshlap, K.M., Schultz, P., Brunar, H., Dervan, P.B., and Feignon, J. (1997) Solution structure of an intramolecular DNA triplex containing an N7-glycosylated guanine which mimicks a protonated cytosine. *Biochemistry.* 36, 2659-2668.

Krawczyk, S.H., Milligan, J.F., Wadwani, S., Moulds, C., Froehler, B.C., and Matteucci (1992) Oligonucleotide-mediated triple helix formation using N3-protonated deoxycytidine analog exhibiting pH-independent binding within the physiological range. *Proc. Natl. Acad. Sci. USA.* 89, 3761-3764.

Krosigk, U.V., and Benner, S.A. (1995) pH-independent triple helix formation by an oligonucleotide containing a pyrazine-donor-accepor base. *J. Am. Chem. Soc.* 117, 5361-5362.

Kukreti, S., Sun, J-S., Garestier, T., and Hélène, C. (1997) Extension of the range of DNA sequences available for triple helix formation: stabilization of mismatched triplexes by acridine containing oligonucleotides. *Nucleic Acids Res.* 25, 4264-4270.

Lacroix, L., Lacoste, J., Reddoch, J.F., Mergny, J-L, Levy, D.D., Seidmann, M.M., Matteucci, M.D., and Glazer, P.M. (1999) Triplex formation by oligonucleotides containing 5-(1-propynl)2′-deoxyuridine: decreased magnesium dependence and improved intracellular gene targeting. *Biochemistry.* 38, 1893-1901.

Lacroix, L., Arimondo, P.B., Takasugi, M., Hélène, C., Mergny, J-L. (2000) Pyrimidine morpholino oligonucleotides form a stable triple helix in the absence of magnesium ions. *Biochem. Biopys. Res. Comm.* 270, 363-369.

Latimer, L.J.P., Hampel, K., and Lee, J.S. (1989) Synthetic repeating sequence DNAs containing phosphothiorates: nuclease sensitivity and triplex formation. *Nucleic Acids Res.* 17, 1549-1561.

Lawley, P.D., and Brookes, P. (1963) Further studies on the alkylation of nucleic acids and their constituent nucleotides. *Biochem. J.* 89, 127-138.

Lecubin, F., Devys, M., Fourrey, J-L, Sun, J-S, and Benhida, R. (2003) Synthesis and triplex binding properties of oligonucleotides containing a novel nucleobase. *Nucleosides, Nucleotides & Nucleic acids.* 22, 1281-1284.

Lee, J.S., Johnson, D.A., and Morgan, A.R. (1979) Complexes formed by $(pyrimidine)_n.(purine)_n$ DNAs on lowering the pH are three-stranded. *Nucleic Acids Res.* 6, 3073-3090.

Lee, J.S., Woodsworth, M.L., Latimer, L.J.P. and Morgan, R. (1984) Poly(purine). poly(pyrimidine) synthetic DNAs containing 5-methylcytosine form stable triplexes at neutral pH. *Nucleic Acids Res.* 12, 6603-6614.

Le Doan, T., Perrouault, L., Praseuth, D., Habhoub, N., Decout, J-L., Thuong, N.T., Lhomme., J., and Hélène, C. (1987) Sequence-specific recognition, photocrosslinking and cleavage of the DNA double helix by an oligo-[α]-thymidylate covalently linked to an azidoproflavine derivative. *Nucleic. Acids. Res.* 19, 7749-7760.

Lehmann, T.E., Greenberg, W.A., Liberles, D.A., Wada, C.K., and Dervan, P.B. (1997) Triple-helix formation by pyrimidine oligonucleotides containing nucleosides with extended aromatic nucleobases: intercalation from the major groove as a method for recognising C.G and T.A base pairs. *Helv. Chimie. Acta.* 80, 2002-2022.

Leitner, D., Schröder, W., and Weisz, K. (2000) Influence of sequence-dependant cytosine protonation and methylation on DNA triplex stability. *Biochemistry.* 39, 5886-5892.

Li, J.S., Fan, Y-H., Marky, L.A., and Gold, B. (2003) Design of triple helix forming C-glycoside molecules. *J. Am. Chem. Soc.* 125, 2084-2093.

Li, J.S., Shikiya, R., Marky, L.A. and Gold, B. (2004) Triple helix forming TRIPside molecules that target mixed purine/pyrimidine DNA sequences. *Biochemistry* 43, 1440-1448.

Loakes, D. (2001) The applications of universal DNA base analogues. *Nucleic Acids Res.* 29, 2437-2447.

Lyamichev, V.I., Mirkin, S.M., and Frank-Kamenetskii, M.D. (1985) A pH-dependant structural transition in the homopurine-homopyrimidine tract in superhelical DNA. *J. Mol. Biol. Struct. Dyn.* 3, 327-338.

Marck, C. and Thiele, D. (1978) Poly(dG).poly(dC) at neutral and alkaline pH: the formation of triple stranded poly(dG).poly(dG).poly(dC). *Nucleic Acids. Res.* 5, 1017-1028.

Macaya, R., Wang, E., Schultz, P., Sklenar, V., and Feignon, J. (1992) Proton nuclear magnetic resonance assignments and structural characterization of an intramolecular DNA triplex. *J. Mol. Biol.* 225, 755-73.

Malkov, V.A., Voloshin, O.N., Soyfer, V.N., and Frank-Kamenetskii, M.D. (1993) Cation and sequence effects on stability of intermolecular pyrimidine-purine-purine triplex. *Nucleic Acids Res.* 21, 585-591.

Manor, H., Rao, B.S., and Martin, R.G. (1988) Abundance and degree of dispersion of genomic d(GA)n.d(TC)n sequences. *J. Mol. Evol.* 27, 96-101.

Marfut, J., Hunziker, J., and Leumann, C.J. (2006) Recognition of a GC base pair by α-N7-deoxyinosine within the pyrimidine-purine-pyrimidine DNA triple helical motif. *Biorg. Med. Chem.*. 24, 3021-3024.

Marfut, J., Parel, S.P., and Leumann, C.J. (1997) Strong, specific, monodentate G-C base pair recogntion by N7-inosine derivatives in the pyrimidine.purine-pyrimidine triple-helical binding motif. *Nucleic Acids. Res.* 25, 1875-1882.

Marfut, J. and Leuman, C.J. (1998) Evidence for C-H...O hydrogen bond assisted recognition of a pyrimidine base in the parallel DNA triple-helical motif. *Angew. Chem. Int .Ed.* 37, 175-178.

Mayer, A., and Leumann, C.J. (2003) A short, efficient synthesis of 2′-deoxypseudoisocytosine based on heck chemistry. *Nucleosides, Nucleotides & Nucleic acids.* 22, 1919-1925.

Mayer, A., Häberli, A., and Leumann, C.J. (2005) Synthesis and triplex forming properties of pyrrolidino pseudoisocytosine containing oligodeoxynucleotides. *Org. Biomol. Chem.* 3, 1653-1658.

Mergny, J.L., Sun, J.S., Rougée, M., Montenay-Garester, T., Barcelo, F., Chomilier, J., and Hélène., C. (1991) Sequence specificity in triple-helix formation: experimental and theoretical studies of the effect of mismatches on triplex stability. *Biochemistry.* 30, 9791-9798.

Mergny, J.L., Duval-Valentin, G., Nguyen, C.H., Perroualt, L., Faucon, B., Rougée, M., Montenay-Garestier, T., Bisagni, E., and Hélène, C. (1992) Triple helix-specific ligands. *Science*. 256, 1681.

Mertz, E., Mattei, S., and Zimmerman, S.C. (2004) Synthesis and duplex DNA recognition studies of oligonucleotides containing a ureido isoindolin-1-one homo-N-nucleoside. A comparison of host-guest DNA recognition studies. *Bioorg. Med. Chem.* 12, 1517-1526.

Michel, J., Toulmé, J-J., Vercauteren, J., and Moreau, S. (1996) Quinazoline-2,4(1*H*,3*H*)-dione as a substitute for thymine in triple helix forming oligonucleotides: a reassessment. *Nucleic Acids Res.* 24, 1127-1135.

Michel, T., Debart, F., Vasseur, J-J., Geinguenaud, F., and Taillandier, E. (2003) FTIR and UV spectroscopy studies of triplex formation between alpha-oligonucleotides with non-ionic phosphoramidate linkages and DNA targets. *J. Biomol. Struct. Dyn.* 21, 435-445.

Michel, T., Debart., F., Heitz, F., and Vasseur, J-J. (2005) Highly stable DNA triplexes formed with cationic phosphoramidate pyrimidine α-oligonucleotides. *Chembiochem.* 6, 1254-1262.

Miller, P.S., Dreon, N., Pulford, S.M., and McParland, K.B. (1980) Oligothymidylate analogues having stereoregular, alternating methyl phosphonate/phosphodiester backbones. *J. Biol. Chem.* 255, 9659-9665.

Miller, P.S., Bhan, P., Cushman, C.D. and Trapane, T.L. (1992) Recognition of guanine-cytosine base pair by 8-oxoadenine. *Biochemistry,* 31, 6788-6793.

Mohan, V., Cheng, Y.K., Marlow, G.E., and Pettitt, B.M. (1993) Molecular recognition of Watson-Crick base pair reversals in triple-helix formation: use of nonatural oligonucleotide bases. *Biopolymers.* 33, 1317-1325.

Mokhir, A.A., Connors, W.H., and Richert, C. (2001) Synthesis and monitored selection of nucleotide surrogates for binding T.A base pairs in homopurine-homopyrimidine DNA triple helices. *Nucleic Acids Res.* 29, 3674-3684.

Morgan, A.R. and Wells, R.D. (1964) Specificity of the three-stranded complex formation between double-stranded DNA and single-stranded RNA containing repeating nucleotide sequences. *J. Mol. Biol.* 37, 63-80.

Moser, H.E., and Dervan, P.B. (1987) Sequence specific cleavage of double-helical DNA by triple helix formation. *Science*. 238, 645-238.

Nara, H., Ono, A., Matsuda, A. (1995) DNA duplex and triplex formation and resistance to nucleolytic degredation of oligodeoxynucleotides containing syn-norspermidine at the 5-position of 2´-deoxyuridine. *Bioconjug. Chem.* 6, 54-61.

Nielsen, P.E., Egholm, M., Berg, R.H., Buchardt, O. (1991) Sequence selective recognition of DNA by strand displacement with a thymine-substituted polyamide. *Science.* 254, 1497-1500.

Nielsen, P.E., Egholm, M., and Buchardt, O. (1994) Evidence for $(PNA)_2$/DNA triplex structure upon binding of PNA to dsDNA by strand displacement. *J. Mol. Recognit.* 7, 165-170.

Nielsen, P.E. (2001) Targeting double stranded DNA with peptide nucleic acid. *Curr. Med. Chem.* 8, 545-550.

Noonberg, S.B., François, J-C., Garestier, T., Hélèene, C. (1995) Effect of competing self-structure on triplex-formation with purine-rich oligodeoxynucleotides containing GA repeats. *Nucleic Acids Res.* 23, 1956-1963.

Obika, S., Hari, Y., Sekiguchi, M., and Imanishi, T. (2001) A 2',4'-bridged nucleic acid containing 2-pyridone as a nucleobase: efficient recognition of a C.G interruption by triplex formation with a pyrimidine motif. *Angew. Chem. Int. Ed. Engl.* 40, 2079–2081.

Obika, S., Onoda, M., Morita, K., Andoh, J., Koizumi, M., and Imanishi, T. (2003) 3'-amino-2',4'-BNA: novel bridged nucleic acids having an N3'->P5' phosphoramidite linkage. *Chem. Commun.*

Olsen, A.G., Dahl, O., and Nielsen, P.E. (2003) A novel PNA-monomer for recognition of thymine in triple-helix structures. *Nucleosides, Nucleotides and Nucleic Acids.* 22, 1331-1333.

Ono, A., Ts'o, P.O.P., and Kan, L. (1991) Triplex formation of oligonucleotides containing 2'-*O*-methylpseudocytosine in substitution for 2'-deoxycytidine. *J. Am. Chem. Soc.* 113, 4032-4033.

Ono, A., Ts'o, P.O.P. and Kan, L. (1992) Triplex formation of an oligonucleotide containing 2'-O-methylpseudoisocytosine with a DNA duplex at neutral pH. *J. Org. Chem.* 57, 3225-3230.

Osbourne, S., Powers, V.E.C., Rusling, D.A., Lack, O., Fox, K.R., and Brown, T. (2004) Selectivity and affinity of triplex-forming oligonucleotides containing 2´-aminoethoxy-5-(3-aminoprop-1-ynyl)uridine for recognising AT base pairs in duplex DNA. *Nucleic. Acids. Res.* 32, 4439-4447.

Ouali, M., Gousset, H., Geinguenaud, F., Liquier, J., Gabarro, A., Le Bret, M., and Taillandier, E. (1997) Hydration of the $dT_n.dA_nXdT_n$ parallel triple helix: a Fourier transform infrared and gravimetric study correlated with moleuclar dynamics simulations. *Nucleic Acids Res.* 25, 4816-4824.

Park, M., and Bruice, T.C. (2005) Binding studies of cationic uridyl ribonucleic guanidine (RNG) to DNA. *Biorg. Med. Chem. Lett.* 15, 3247-3251.

Parsch, U., Engels, J.W. (2000) pH-independent triple helix formation with 6-oxocytidine as cytidine analogue. *Chem. Eur. J.* 6, 2409-2424.

Perroualt, L., Asseline, U., Rivalle, C., Thung, N.T., Bisagni, E., Giovannangeli, C., Le Doan, T., and Helene, C. (1990) Sequence-specific photo-induced endonucleases based on triplex-forming oligonucleotides. *Nature.* 22, 358-360.

Phipps, A.K., Tarköy, M., Schult, P., and Feignon, J. (1998) Solution structure onf an intramolecular DNA triplex containing 5-(1-propynl)-2'-deoxyuridine residues in the third strand. *Biochemistry.* 37, 5820-5830.

Pilch, D.S., Levenson, C. and Shafer, R.H. (1990) Structural analysis of the $(dA)_{10}.2(dT)_{10}$ triple helix. *Proc. Natl. Acad. Sci. USA* 87, 1942-1946.

Plavec, J., Thibaudeau, C., and Chattopadhyaya, J. (1994) How does the 2´-hydroxy group drive the pseudorotational equilibrium in nucleoside and nucleotide by the tuning of the 3´-gauche effect. *J. Am Chem. Soc.* 116, 6558-6560.

Plum, G.E., Pilch, D.S., Singleton, S.F., Breslauer, K.J. (1995) Nucleic acid hybridization : triplex stability and energetics. *Annu. Rev. Biophys. Biomol. Struct.* 24, 319-50.

Porschke, D., and Eigen, M. (1971) Co-operative non-enzymic base recognition. 3. kinetics of the helix-coil transition of the oligoribouridylic-oligoriboadenylic acid system and of oligoriboadenylic acid alone at acidic pH. *J. Mol. Biol.* 62, 361-381.

Potaman, V.N., (2003) Applications of triple-stranded nucleic acid structures to DNA purification, detection and analysis. *Expert. Rev. Mol. Diagn.* 3, 481-495.

Povsic, T.J., and Dervan, P.B. (1989) Triple helix formation by oligonucleotides on DNA extended to the physiological pH range. *J. Am. Chem. Soc.* 111, 3059-3061.

Prakash, T.P., Puschl, A., Lesnik, E., Mohan, V., Tereshko, V., Egli, M., and Manoharan, M. (2004) 2'-*O*-[2-(guanidinium)ethyl]-modified oligonucleotides: stabilising effect on duplex and triplex structures. *Org. Lett.* 6, 1971-1974.

Prévot-Halter, I., and Leumann C.J. (1999) Selective recognition of a C-G base pair in the parallel DNA triple-helical binding motif. *Biorg. Med. Chem. Lett.* 9, 2657-2660.

Prévot, I, and Leumann, C.J. (2002) Evaluation of novel third strand bases for the recognition of a C.G base pair in parallel DNA triple-helical binding motif. *Helv. Chim. Acta.* 85, 502-514.

Puri, N., Majumdar, A., Cuenod, B., Natt, F., Martin, P., Boyd, B., Miller, P.S., and Seidman, M.M. (2002) Minimum number of 2'-*O*-(2-aminoethyl) residues required for gene knockout activity by triple helix forming oligonucleotides. *Biochemistry.* 41, 7716-7724

Puri, N., Majumdar, A., Cuenod, B., Millar, P.S. and Seidman., M.M. (2004) Importance of clustered 2'-O-(2-aminoethyl) residues for the gene targeting activity of triple helix-forming oligonucleotides. *Biochemsitry.* 43, 1343-1351.

Radhadkrishnan, I., Gao, Xiaolian, O., de los Santos, C., Live, D., and Patel, D.J. (1991) NMR structural studies of intramolecular $(Y+)_n \bullet (R+)_n(Y-)_n$ DNA triplexes in solution: imino and amino proton and nitrogen markers of G.TA base triple formation. *Biochemistry.* 30, 9022-9030.

Radhadkrishnan, I., Patel, D.J. (1994) DNA triplexes: Solution structures, hydration sites, energetics, interactions and function. *Biochemistry.* 33, 11405-11416.

Raghavan, S.C., Chastain, P., Lee, J.S., Hegde, B.G., Houston, S., Langen, R., Hsieh, C-L., Haworth, I.S., and Lieber, M.R. (2005) Evidence for a triplex DNA conformation at the Bcl-2 major breakpoint region of the t(14;18) translocation. *J. Biol. Chem.* 280, 22749-22760.

Rajopal, P., and Feigon, J. (1989) Triple-strand formation in the homopurine: homopyrimidine DNA oligonucleotides $d(G\text{-}A)_4$ and $(T\text{-}C)_4$. *Nature.* 339, 637-640.

Ranasinghe, R.T., Rusling, D.A., Powers, V.E.C., Fox, K.R., and Brown, T. (2005) Recognition of CG inversions in DNA triple helices by methylated 3*H*-pyrollo[2,3-*d*]pyrimidin-2(7*H*)-one nucleoside analogues. *Chem. Comm.* 2555-25557

Rao, B.S. (1996) Regulation of DNA replication by homopurine.homopyrimidine sequences. *Mol. Cell. Biochem.* 156, 163-168.

Re, R.N., Cook, J.L., and Giardina, J.F. (2004) The inhibition of tumour growth by triplex-forming oligonucleotides. *Cancer Letts.* 209, 51-53.

Rehfuss, R, Goodisman, J., and Dabrowiak, J.C. (1990) Quantitative footprinting analysis. Binding to a single site. *Biochemistry.* 29, 777-781.

Renneberg, D., and Leumann, C.J. (2004) Exploring Hoogsteen and reversed-Hoogsteen duplex and triplex formation with tricyclo-DNA purine sequences. *Chembiochem.* 5, 1114-1118.

Rhee, S., Han, Z-J., Liu, K., Miles, T., and Davies, D.R. (1999) Structure of a triple helical DNA with a triplex-duplex junction. *Biochemistry.* 38, 16810-16815.

Roberts, R.W., and Crothers, D.M. (1991) Specificity and stringency in DNA triplex formation. *Proc. Natl. Acad. Sci. USA.* 88, 9397-9401.

Roberts, R.W., and Crothers, D.M. (1992) Stability and properties of double and triple helices: dramatic effect of DNA or RNA backbone composition. *Science,* 258, 1463-1468.

Roberts, R.W., and Crothers, D.M. (1996) Prediction of the stability of DNA triplexes. *Proc. Natl. Acad. Sci. USA.* 93, 4320-4325.

Robles, J., Maseda, M., Beltran, M., Concernau, M., Pedroso, E., and Grandas, A. (1997) Synthesis and enzymatic stability of phosphodiester-linked peptide-oligonucleotide hybrids. *Bioconjug. Chem.* 8, 785-8.

Robles, J., Grandas, A., Pedroso, E., Luque, F.J., Eritja, R., and Orozco, M. (2002) Nucleic acid triple helices: stability effects of nucleobase modifications. *Curr. Org. Chem.* 6, 133-1368.

Rougée, M., Faucon, B., Mergny, J.L., Barcelo, F., Giovannangeli, C., Garestier, T.,

Hélène, C. (1992) Kinetics and thermodynamics of triple-helix formation: Effect of ionic strength and mismatches. *Biochemistry.* 31, 9269-9278.

Rice, M.C., Czymmek, K., and Kmiec, E.B. (2001) The potential of nucleic acid repair in functional genomics. *Nature Biotech.* 19, 321-326.

Riley, M., Maling, B., and Chamberlin, M.J. (1966) Physical and chemical characterization of two- and three-stranded adenine-thymine and adenine-uracil homopolymer complexes. *J. Mol. Biol.* 20, 359-389.

Rusling, D.A., Powers, V.E.C., Ranasinghe, R.T., Wang, Y., Osbourne, S.D., Brown, T. and Fox, K.R. (2005) Four base recognition by triplex-forming oligonucleotides at physiological pH. *Nucleic Acids Res.* 33, 3025-3032.

Rusling, D.A., Le Strat, L., Powers, V.E.C., Broughton-Head, V.J., Booth, J., Lack, O. Brown, T. and Fox, K.R. (2005) Combining nucleoside analogues to achieve recognition of oligopurine tracts by triplex-forming oligonucleotides at physiological pH. *FEBS Letts.* 579, 6616-6620.

Rustighi, A., Tessari, M.A., Vascotto, F., Sgarra R., Giancotti, V., and Manfioletti, G. (2002) A polypyrimidine/polypurine tract within the Hmga2 minimal promoter: a common feature of many growth related genes. *Biochemistry.* 41, 1229-1240.

Seidman, M.M., and Glazer, P.M. (2003) The potential for gene repair via triple helix formation. *J. Clin. Invest.* 112, 487-494.

Shindo, H., Torigoe, H., and Sarai, A. (1993) Thermodynamic and kinetic studies of DNA triplex formation of an oligohomopyrimidine and a matched duplex by filter binding assay. *Biochemistry.* 32, 8963-8969.

Shimizu, M., Konishi, A., Shimada, Y., Inoue, H., and Oshtsuka, E. (1992) Oligo(2'-*O*-methyl)ribonucleotides: effective probes for duplex DNA. *FEBS Letts.* 302, 155-158.

Singh, S.K., Nielsen, P., Koshkin, A.A., and Wengel, J. (1998) Locked nucleic acid: synthesis and high affinity nucleic acid recognition. *Chem. Commun.* 455-456.

Singleton, S.F and Dervan, P.B. (1992) Influence of pH on the equilibrium association constants for oligodeoxyribonucleotide-directed triple helix formation at single DNA sites. *Biochemistry.* 32, 4761-4765.

Singleton, S. F., and Dervan, P. B. (1993) Equilibrium association constants for oligonucleotide-directed triple helix formation at single DNA sites: linkage to cation valence and concentration. *Biochemistry.* 32, 13171-13179.

Singleton, S. F., and Dervan, P. B. (1994) Temperature dependence of the energetics of oligonucleotide-directed triple helix formation at a single DNA site. *J. Am. Chem. Soc.* 116, 10376-10382.

Singleton, S. F., and Dervan, P. B. (1995) Sequence composition effects on the energetics of triple helix formation by oligonucleotides containing a designed mimic of protonated cytosine. *J. Am. Chem. Soc.* 117, 10376-10382.

Soliva, R., Guimil-Garcia, R., Blas, J.R., Eritja, R., Asensio, J.L., Gonzalez, C., Luque, F.J., and Orozco, M. (2000) DNA-triplex stabilising properties of 8-aminoguanine. *Nucleic Acids Res.* 28, 4531-4539.

Sollogoub, M., Darby, R.A., Cuenod, B., Brown, T., and Fox, K.R. (2002) Stable DNA triple helix formation using oligonucleotides containing 2'-aminoethoxy, 5-propargylamino-U. *Biochemistry.* 41, 7224-7231.

Soto, A.M., Loo, J. and Marky, L.A. (2002) Energetic contribution for the formation of TAT/TAT, TAT/CGC+ and CGC+/CGC+ base triplet stacks. *J. Am. Chem. Soc.* 124, 14355-14363.

Spink, C.H., and Chaires, J.B. (1999) Effects of hydration, ion release, and excluded volume on the melting of triplex and duplex DNA. *Biochemistry.* 38, 496-508.

Staubli, A.B., and Dervan, P.B. (1994) Sequence specificity of the non natural pyrido[2,3-*d*]pyrimidine nucleoside in triple helix formation. *Nucleic Acids Res.*

22, 2637-2642.
St. Clair, A., Xiang, G., and Mclaughlin, L.W. (1998) Synthesis and triplex forming properties of an acyclic N7-glycosylated guanine nucleoside. *Nucleosides and Nucleotides.* 17, 925-937.
Steely, H.T., Gray, D.M., and Ratliff, L. (1986) CD of homoploymer DNA.RNA hybrid duplexes and triplexes containing A.T or A.U base pairs. *Nucleic Acids Res.* 14, 10071-10090.
Steffens, R., and Leumann,C.J. (1999) Synthesis and thermodynamic and biophysical properties of tricyclo-DNA. *J. Am. Chem. Soc.* 121, 3249–3255.
Stonehouse, T.J., and Fox, K.R. (1994) DNase I footprinting of triple helix formation at polypurine tracts by acridine-linked oligopyrimidines: stringency, structural changes and interaction with minor groove binding ligands. *Biochim. Biophys. Acta.* 1218, 322-330.
Strekowski, L., Hojjat, M., Wolinska, E., Parker, A.N., Paliakov, T., Tanious, F.A., and Wilson, D.W. (2005) New triple-helix DNA stabilising agents. *Biorg. Med. Chem. Lett.*15, 1097-1100.
Strobel, S.A., and Dervan, P. (1990) Site-specific cleavage of a yeast chromosome by oligonucleotide-directed triple-helix formation. *Science.* 249, 73-75.
Suck, D. (1994) DNA recognition by DNase I. *J Mol. Recognit.* 7, 65-70.
Sugimoto, N., Wu, P., Hara, H., and Kawamoto, Y. (2001) pH and cation effects on the properties of parallel pyrimidine motif triplexes. *Biochemistry.* 40, 9396-9405.
Sun, J-S., Mergny, J-L., Lavery, R., Montenay-Garestier, T., and Hélène, C. (1991) Triple helix structures: sequence dependence, flexibility and mismatch effects. *J. Biomol. Struct. Dyn.* 9, 411-424.
Sun, J-S., and Hélène, C. (1993) Oligonucleotide-directed triple helix formation. *Curr. Opin. Struct. Biol.* 3, 345-356.
Sun, B-W., Babu, R., Sørensen, M.D., Zakrzewska, K., Wengel, J. and Sun, J-S. (2004) Sequence and pH effects of LNA-containing triple helix-forming oligonucleotides: physical chemistry, biochemistry, and modelling studies. *Biochemistry*, 43, 4160-4169.
Svinarchuk, F., Bertrad, J.R., and Malvy, C. (1994) A short purine oligonucleotide forms a highly stable triple helix with the promoter of the murine c-pim-1 proto-oncogene. *Nucleic Acids Res.* 22, 3742-3747.
Takasugi, M., Guendouz, A., Chassignol, M., Decout, J.L. Lhomme, J., Thuong, N.T. and Helene, C. (1991) Sequence-specific photo-induced cross-linking of the two strands of double helical DNA by a psoralen covalently linked to a triple helix forming oligonucleotide. *Proc. Natl. Acad. Sci. USA.* 88, 5602-5606.
Tarköy, M., and Leumann, C.J. (1993) Synthesis and pairing properties of decanucleotides from (3´S,5´R)-2´-Deoxy-3´, 5´-ethano-β-*D*-ribofuranosyladenine and –thymine. *Angew. Chem. Intl. Ed. Engl.* 32, 1432.
Tarköy, M., Phipps, A.K., Schultz, P., and Feigon, J. (1998) Solution structure of an intramoleuclar DNA triplex linked by hexakis(ethylene glycol) units: d(AGAGAGAA-(EG)6-TTCTCTCT-(EG)6-TCTCTCTT). *Biochemistry. 37,* 5810-5819.
Thomas, T., and Thomas, T.J. (1993) Selectivity of polyamines in triplex DNA stabilization. *Biochemistry*, 32, 14068-14074.
Torigoe, H., Hari, Y., Sekiguchi, M., Obika, S., and Imanishi, T. (2001) 2´-*O*-,4´-*C*-methylene bridged nucleic acid modification promotes pyrimidine motif triplex DNA formation at physiological pH. *J. Biol. Chem.* 276, 2354-2360.
Torigoe, H. (2001) Thermodynamic and kinetic effects of N3'->P5' phosphoramidate modification on pyrimidine motif triplex DNA formation. Biochemistry. 40, 1063–1069.

Torigoe, H., Katayama, T., Obika, S., Maruyama, A., and Imanishi, T. (2005) Combination of poly(L-lysine)-graft-dextran copolymer and 2'-O,4'-C-methylene bridged nucleic acid (2',4'-BNA) modification synergistically stabilises pyrimidine motif triplex at neutral pH. *Nucleosides Nucleotides Nucleic Acids.* 24, 635-638.

Thuong, N.T., and Hélène, C. (1993) Sequence-specific recognition and modification of double-helical DNA by oligonucleotides. *Angew. Chem. Int. Ed. Engl.* 32, 666-690.

Tullius, T.D., Dombroski, B.A., Churchill, M.E., and Kam, L. (1997) Hydroxyl radical footprinting: a high resolution method for mapping protein-DNA contacts. *Mehtods Enzymol.* 155, 537-538.

Ushijima, K., Ishibashi, T., Yamakaw, H., Tsukahara, S., Takai, K., Maruyama, T., and Takaku, H. (1999) Inhibition of restriction endonuclease cleavage by triple helix formation with RNA and 2′-*O*-methyl RNA oligonucleotides containing 8-oxo-adenosine in place of cytidine. *Biochemistry.* 38, 6570-6575.

Van Craynest, N., Guianvarc'h, D., Peyron, C., and Benhida, R. (2004) Efficient synthesis of extended guanine analogues designed for recognition of an A.T inverted base pair in triple helix based-strategy. *Tett. Letts.* 45, 6243-6247.

Van Dyke, M.W., Hertzberg, R.P., Dervan, P.B. (1982) Map of distamycin, netropsin, and actinomycin binding sites on heterogeneous DNA: DNA cleavage-inhibition patterns with methidiumpropyl-EDTA.Fe(II). *Proc. Natl Acad. Sci. USA.* 79, 5470-5474.

Van Dyke, M.W., and Dervan, P.B. (1983) Methidiumpropyl-EDTA.Fe(II) and DNase I footprinting report different small molecule binding site sizes on DNA. *Nucleic Acids Res.* 11, 5555-5567.

Völker, J., and Klump, H.K. (1994) Electrostatic effects in DNA triple helices. Biochemistry. 33, 13502-13508.

Vasquez, K.M., Narayanan, L., and Glazer, P. (2000) Specific mutations induced by triplex-forming oligonucleotides in mice. *Science.* 290, 530-533.

Wang, Y., and Patel, D.J. (1995) Bulge defects in intramolecular pyrimidine.purine.pyrimidine DNA triplexes in solution. *Biochemistry.* 34, 5696-5704.

Wang, G., and Vasquez, K.M. (2003) Naturally occurring H-DNA-forming sequences are mutagenic in mammalian cells. *PNAS.* 101, 13448-13453.

Wang, Y., Rusling, D.A., Powers, V.E.C., Lack, O., Osbourne, S., Fox, K.R and Brown, T. (2005) Stable recognition of TA interruptions by triplex forming oligonucleotides containing a novel nucleoside. *Biochemistry.* 44, 5884-5892.

Wilson, W.D., Tanious, F.A., Mizan, S., Yao, S., Kieslyov, A.S., Zon, G., and Strekowski, L. (1993) DNA triple-helix specific intercaltors as antigene enhancers: unfused aromatic cations. *Biochemistry.* 32, 10614-10621.

Wittung, P., Nielsen, P., and Norden, B. (1997) Extended DNA-recognition repetoire of peptide nucleic acid (PNA): PNA-dsDNA triplex formed with cytosine-rich homopyrimidine PNA. *Biochemistry.* 36, 7973-7979.

Wu, P., Kawamoto, Y., Hara, H., and Sugimoto, N. (2002) Effect of divalent cations and cytosine protonation on thermodynamic properties of intermolecular DNA double and triple helices. *J. Inorganic. Biochem.* 91, 277-285.

Xiang, G., Soussou, W., and McLaughlin, L.W. (1994) A new pyrimidine nucleoside ($m^{5ox}C$) for the pH-independent recognition of G-C pairs by oligonucleotide-directed triplex formation. *J. Am. Chem. Soc.* 116, 11155-11156.

Xiang, G., Bogacki, R., and McLaughlin, L.W. (1996) Use of a pyrimidine nucleoside that functions as a bidentate hydrogen bond donor for the recognition of isolated or contiguous GC base pairs by oligonucleotide directed triplex formation. *Nucleic Acid Res.* 24, 1963-1970.

Xiang, G., and McLaughlin, L.W. (1998) A cytosine analogue cotaining a conformationally flexible acyclic linker for triplex formation at sites with contiguous GC base pairs. *Tetrahedron.* 54, 375-392.

Xodo, L.E., Manzini, G., Quadrifoglio, F., van der Marel, G.A., and Boom, J.H. (1991) Effect of 5-methylcytosine on the stability of triple-stranded DNA- a thermodynamic study. *Nucleic Acids Res.* 20, 5625-5631.

Xodo, E. L. (1995) Kinetic analysis of triple-helix formation by pyrimidine oligodeoxynucleotides and duplex DNA. *Eur. J. Biochem.* 228, 918-926.

Yoon, K., Hobbs, C.A., Koch, J., Sardaro, M., Kutny, R., and Weis, A.L. (1992) Elucidation of the sequence-specific third-strand recogntion of four Watson-Crick base pairs in a pyrimidine tripl-helix motif: T.AT, C.GC, T.CG and G.TA. *Proc. Natl. Acad. Sci.* 89, 3840-3844.

Young, S.L., Krawczyk, S.H., Matteucci, M.D., and Toole, J.J. (1991) Triple helix formation inhibits transcription elongation in vitro. *Proc. Natl. Acad. Sci. USA.* 88, 100023-10026.

Zain, R. and Sun, J-S. (2003) Do natural DNA triple-helical structures occur and function in vivo? *Cell. Mol. Life. Sci.* 60, 862-870.